UNIVERSIDAD DE TALCA
INSTITUTO DE QUIMICA DE RECURSOS NATURALES

CHANGES IN COMPOSITION AND BIOLOGICAL ACTIVITY OF THE PHENOLIC COMPOUNDS FROM *Ribes magellanicum* AND *Ribes punctatum* AFTER *in vitro* GASTROINTESTINAL DIGESTION AND COLONIC FERMENTATION

ALBERTO JAVIER BURGOS EDWARDS

TESIS PARA OPTAR AL GRADO DE:

DOCTOR EN CIENCIAS, MENCIÓN INVESTIGACIÓN Y DESARROLLO DE PRODUCTOS BIOACTIVOS

Director

Dr. Guillermo Schmeda Hirschmann

Talca, 2019

CONSTANCIA

La Dirección del Sistema de Bibliotecas a través de su unidad de procesos técnicos certifica que el autor del siguiente trabajo de titulación ha firmado su autorización para la reproducción en forma total o parcial e ilimitada del mismo.

Talca, 2019

Changes in composition and biological activity of the phenolic compounds from *Ribes magellanicum* and *Ribes punctatum* after *in vitro* gastrointestinal digestion and colonic fermentation

Cambios en la composición y actividad biológica de los compuestos fenólicos de *Ribes magellanicum* y *Ribes punctatum* posterior a la digestión gastrointestinal y fermentación colónica *in vitro*

Alberto Javier Burgos Edwards

Fecha inicio Tesis: Enero 2016

Fecha término Tesis: Octubre 2019

Director de Tesis:

Guillermo Schmeda Hirschmann,
Universidad de Talca, Instituto de Química de Recursos Naturales, Casilla 747, Talca, Chile.
Email: schmeda@utalca.cl

Integrantes de la comisión de Tesis:

1. Dr. Ramiro Araya Maturana, Universidad de Talca.

2. Dr. Sergio Wehinger Wehinger, Universidad de Talca.

3. Dr. Camilo López Alarcón, Pontificia Universidad Católica de Chile.

Acknowledgments

- To PIEI-QUIM-BIO program from Universidad de Talca for financial support.
- CONICYT for the doctoral grant PFCHA Doctorado Nacional 2015-21151561 (April 2015-January 2019).
- To my family for always being by my side along this path, despite the distance.
- To my best friend Laura Lascano for giving me her unconditional support, especially in the difficult times.
- Prof. Guillermo Schmeda-Hirschmann and Cristina Theoduloz, for sharing with me their knowledge, experiences and advices, allowing me to develop this work.
- To Mrs. Irene Manrriquez and Mr. Sergio Reyes for their teachings and support day by day.
- To my good friends and lab mates Daniel Mieres, Javier Antileo, Jean Paulo de Andrade, Verónica Olate, Samanta Thomas, Felipe Jimenez, Liudis Pino, Victoria Nina, and Sergio Reyes for their advice and help every time I needed them.
- To the entire Instituto de Quimica de Recursos Naturales, for their goodwill in helping me.
- I would like to thank Prof. Mar Larrosa and the members of the Nutrition, Microbiota and Health Group (Arantxa Fernández, Laura Martin, Natalia Moracho, Cristina Vitores, Goyi Montalvo, Beatriz Lucas and Jose García) from the Faculty of Biomedical Sciences of the European University of Madrid, for their help in the development of this Thesis.
- To my former Professors Esteban Ferro, Nelson Alvarenga, María Eugenia Flores, María Luisa Kennedy, and Javier Barúa, who encouraged me to follow this path.
- To Olga Coronel and all my dear friends in Asunción that supported me from the distance.
- To my dear friends in Talca Viviana Donoso, Carolina Ojeda, and Jefferson Romero.

Thank you very much.

General index

Figures index

Table Index

Glossary of abbreviations

ACN	Acetonitrile
AGS	Human gastric epithelial cells
amu	Atomic mass unit
APCI	Atmospheric pressure chemical ionization
APPI	Atmospheric pressure photoionization
BCFA	Branched-chain fatty acids
CH	Caffeoyl hexoside
3-CQA	3-caffeoylquinic acid
5-CQA	5-caffeoylquinic acid
CE	Catechin equivalents
3-CoQA	3-coumaroylquinic acid
CD	Crohn's disease
COX	Cyclooxygenase
CUPRAC	Cupric reducing antioxidant capacity
DAD	Diode array detector
DPPH	2,2-diphenyl-1-picrylhydrazyl
ESI	Electrospray ionization
FAO	Food and Agriculture Organization of the United Nations
FBS	Fetal bovine serum
FOS	Fructooligosaccharides
FQA	Feruloylquinic acid
FRAP	Ferric reducing antioxidant capacity
GAE	Gallic acid equivalents
GD-PEE	Gastric digested polyphenol-enriched extract
GID	Gastrointestinal digestion
g	Gram
GSH	Reduced glutathione
HAT	Hydrogen atom transfer
HCA	Hydroxycinnamic acids
h	hours
HPLC	High performance liquid chromatography
IBD	Inflammatory bowel diseases
ID-PEE	Intestinal digested polyphenol-enriched extract
IL	Interleukin
iNOS	Inducible nitric oxide synthase
L	Liter
LC	Liquid chromatography
M	Molar
MeOH	Methanol
µg	Microgram
mg	Milligram
min	Minute
µL	Microliter
mL	Milliliter
mM	Milimolar
MS	Mass spectrometry
m/z	Mass/charge
ng	Nanogram
nm	Nanometer
NO	Nitric oxide
NSAIDs	Non-steroidal anti-inflammatory drugs
ORAC	Oxygen radical absorbance capacity
PEE	Polyphenolic-enriched extract
PG	Prostaglandins
Rt	Retention time
rpm	Revolutions per minute
SC_{50}	Scavenging capacity 50 %
SCFA	Short-chain fatty acids
SEM	Standard error of the mean
SET	Single electron transfer
SD	Standard deviation
SPE	Solid phase extraction
TEAC	Trolox equivalent antioxidant capacity
TE	Trolox equivalents
TF	Total flavonoid content
TNF-α	Tumor necrosis factor alpha
TP	Total phenolic content
UC	Ulcerative colitis
UV	Ultraviolet
WHO	World health organization
µM	Micromolar

Abstract

The wild Chilean currants *Ribes magellanicum* and *Ribes punctatum* are a good source of polyphenolic compounds with interesting bioactivities in several *in vitro* models. The effect of simulated gastrointestinal digestion (GID) and *in vitro* colonic fermentation on phenolic content, composition and antioxidant capacity was determined. The inhibitory activity of the non-digested, digested, and fermented samples towards metabolic syndrome-associated enzymes (α-amylase, α-glucosidase, and lipase) was evaluated. The anti-inflammatory activities of the gastro-intestinal digested PEEs were assessed using differentiated human Caco-2 (clone C2BBe1) cells stimulated with interleukin 1β (IL-1β). The inhibitory effect of non-digested and digested PEEs towards human cyclooxygenase 1 (COX-1) and COX-2 and the gene expression of COX-2 and inducible nitric oxide synthase (iNOS) was determined. The potential prebiotic-like effect of the pre-digested PEEs was evaluated in a simulated colon model. Digested PEEs were submitted to a colonic fermentation with feces from healthy human donors. Samples were taken at 1, 4, 8 and 24 h of incubation, monitoring pH, ammonia, branched-chain fatty acids (BCFA), short-chain fatty acids (SCFA) and bacterial growth. FOS (fructooligosaccharides) and fecal slurry without treatments were positive and negative control, respectively. The total phenolic (TP) and flavonoid contents (TF) decreased by about 50 % at the end of the *in vitro* GID. Main anthocyanins and hydroxycinnamic acids were strongly affected by this process, with a loss of about 80 %. A decrease in the antioxidant activity was observed throughout the digestion steps, which was correlated with the reduction in the TP and TF content. After the *in vitro* GID of the samples, only the inhibition of α-glucosidase was preserved. The phenolic profiles of the fermented samples showed significant changes after 24 h incubation. Nine metabolites, derived from the microbial fermentation, were tentatively identified, including dihydrocaffeic acid, dihydrocaffeoyl-,

dihydroferuloylquinic acid, 1-(3,4-dihydroxyphenyl)-3-(2,4,6-trihydroxyphenyl)propan-2-ol (3,4-diHPP-2-ol), among others. The content of anthocyanins and hydroxycinnamic acids was most affected by simulated colonic conditions, with a loss of 71–92 % and 90–100 % after 24 h incubation, respectively. The highest antioxidant capacity values (ORAC) were reached after 8 h incubation. The inhibitory activity against the enzyme α-glucosidase was maintained after the fermentation process. The digested PEE from *R. punctatum* decreased the secretion of IL-8, IL-6, and TNF-α; whereas *R. magellanicum* reduced IL-6 and TNF-α in the Caco-2 cells ($p < 0.05$). Both digested extracts significantly down-regulated the mRNA expression of COX-2 and iNOS ($p < 0.05$). PEEs showed 60 % of inhibition towards COXs, with higher inhibition against COX-2. The PEEs from *R. punctatum* displayed better anti-inflammatory activity in all the experiments. Both *Ribes* species reduced ($p < 0.05$) both BCFA and SCFA at 24 h. *R. punctatum* promoted the growth ($p < 0.05$) of beneficial bacteria such as *Clostridium* cluster XIVa, and *Faecalibacterium prausnitzii*. A trend to increase *Akkermansia muciniphila* was observed. *R. magellanicum* increased ($p < 0.05$) *Clostridium* cluster XIVa population. Total bacteria, *Escherichia coli*, *Lactobacillus spp*. and *Bifidobacterium spp*. remained unaffected. Our results show that the simulated GID and colonic fermentation modified the polyphenolic composition, influencing their potential health-promoting properties of the studied currants. Polyphenols from *R. magellanicum* and *R. punctatum* might be useful against intestine inflammation and possibly modulate both, bacterial metabolism and selected gut beneficial bacteria under simulated conditions. Therefore, Chilean currants might be useful as supplements to maintain a healthy colon. However, further *in vivo* studies are needed to confirm their prebiotic-like and anti-inflammatory effects.

Chapter 1

Introduction

1.1. Phenolic compounds

1.1.1. Overview

Chemically, the phenolic compounds are organic substances with at least one aromatic ring holding one or more hydroxyl substituents. The term “polyphenols” is also used to refer to natural products with at least two phenolic rings, including conjugated derivatives such as glycosides and esters (Lattanzio, 2013). From a biosynthetic point of view, Quideau, Deffieux, Douat-Casassus, & Pouységu, (2011) suggested that the term “polyphenol” should be used to refer to secondary metabolites from plants, which derived exclusively from the shikimate phenylpropanoid and/or the polyketide pathway(s), containing more than one phenolic ring without functional groups with nitrogen in their most basic structure. These compounds are widely distributed in plants and are less common in fungi, bacteriae, and algae. Phenolics are synthesized to improve interaction with the environment, allowing a better adaptation to stress conditions (Lattanzio, 2013). Among the functions of phenolics in plants are: constitution of structural material (cell wall), attraction of pollinators, internal physiological regulation (chemical messengers), protection from sunlight through the absorption of harmful wavelengths (UV light), and protection from predators, pests and pathogens (Cheynier, Comte, Davies, Lattanzio, & Martens, 2013). Edible fruits and vegetables accumulate a high amount and variety of phenolics; their regular ingesta is recommended to reduce the risk of developing non-transmissible diseases, such as diabetes, inflammation, cardiovascular, and neurodegenerative diseases (Crozier, Jaganath, & Clifford, 2009; Del Rio et al., 2013;

Williamson, 2017). This association between polyphenols and health led to focus the attention on the analytical characterization of dietary polyphenol-rich sources and the evaluation of bioactivity through several *in vitro* assays (Kroon et al., 2004). However, the biological activity of the polyphenols before ingestion may not be representative of what occurs in the human organism, due to the compositional changes elicited by physiological conditions before the interaction with the biological target (Crozier et al., 2009; Kroon et al., 2004). The action mechanisms of polyphenols are not fully understood yet. This knowledge is necessary to achieve the maximum benefit of polyphenols consumption and to develop novel supplementations and dietary interventions for the prevention and treatment of the mentioned diseases. Since clinical studies are expensive, time-consuming, and contain ethical restrictions; the optimization and interpretation of *in vitro* experiments became necessary to elucidate possibles action mechanisms of polyphenols (Kroon et al., 2004).

1.1.2. Biosynthesis

The biosynthesis of phenolic compounds in plants is complex since it does not occur only through a single metabolic route. The phenylpropanoid pathway is responsible for the generation of an important group of phenolics (Figure 1). The name of this pathway refers to the common C6-C3 skeleton conserved in the end products of this route (Vermerris & Nicholson, 2008). The deamination reactions of phenylalanine and tyrosine originate cinnamic acid and *p*-coumaric acid, respectively. The last could also be formed through the hydroxylation of coumaric acid (Chouhan, Sharma, Zha, Guleria, & Koffas, 2017). This pathway ends with the formation of *p*-coumaroyl-Coenzyme A from *p*-coumaric acid. Further reactions (hydroxylation, reduction, methylation, etc) lead to other hydroxycinnamoyl-CoA esters, hydroxycinnamic acids, and other specific classes of compounds (Quideau et al., 2011; Vermerris & Nicholson, 2008). In fact, lignan/neolignan dimers $(C6\text{-}C3)_2$ and lignin polymers $(C6\text{-}C3)_n$ are synthesized from hydroxycinnamic acids, esters and

alcohols by means of oxidative coupling reactions (Dewick, 2002; Quideau et al., 2011). Cinnamic acid derivatives may also originate monophenolic acids with C6-C2 and C6-C1 skeletons through decarboxylation reactions (Quideau et al., 2011). Another important metabolic route is the shikimate pathway, which constitutes an alternative source of phenylalanine and tyrosine and is responsible for the generation of non-phenolic acids commonly found in nature such as quinic and shikimic acid (Dewick, 2002; Vermerris & Nicholson, 2008).

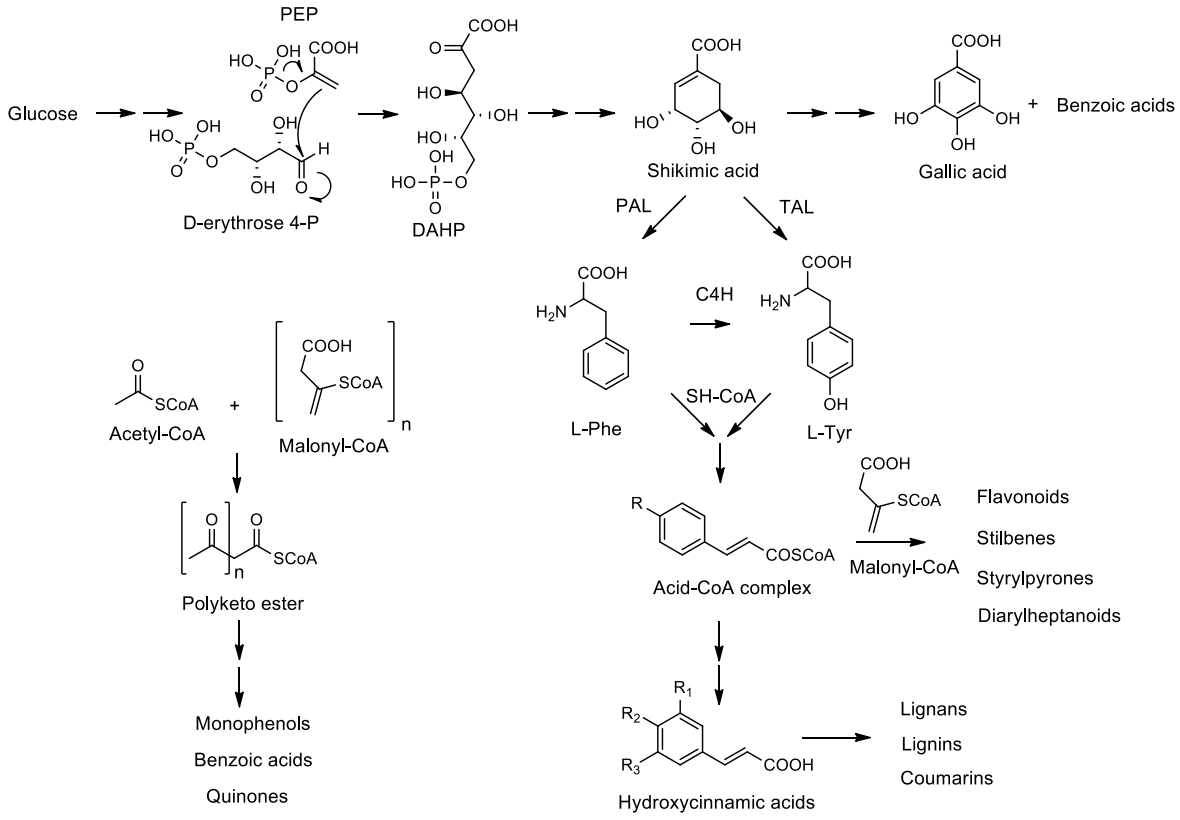

Figure 1. Main biosynthetic pathways of the most common phenolic compounds occurring in plants. Abbreviations are as follows: C4H: cinnamate 4-hydroxylase; D-erythrose 4-P: D-erythrose 4-phosphate; DAHP: D-arabino-heptulosonic acid 7-phosphate; CoA: coenzyme A; PAL: phenylalanine ammonia lyase; TAL: tyrosine ammonia lyase; PEP: Phosphoenolpyruvate. Source: Adapted from Chouhan et al. (2017) and Dewick, (2002).

The formation of polyketides from acetyl-CoA and malonyl-CoA and their posterior cyclization also generates aromatic structures; constituting the acetate-malonate pathway (Dewick, 2002). This

pathway is responsible for the synthesis of some quinones and phenolic acids, aldehydes, and phenols; but also, along with the shikimate pathway, originating flavonoids, stilbenes, diarylheptanoids and styrylpyrones (Chouhan et al., 2017; Dewick, 2002; Quideau et al., 2011).

1.1.3. Classification

A great diversity of phenolic structures can be found in plants, surpassing 8000 structures reported in the literature (Crozier et al., 2009; Del Rio et al., 2013). These compounds can be classified considering their basic carbon skeleton (Tsimogiannis & Oreopoulou, 2019). In addition, Crozier et al. (2009) proposed a categorization separating flavonoids and non-flavonoid due to the high amount of the members of the former group. Structural examples of each basic skeleton of non-flavonoid phenolics are shown in Figure 2. The simple phenols, so-called monophenols, are categorized as C6 since their basic structure is composed only by one aromatic ring; catechol, hydroquinone, and phloroglucinol are members of this group. Catechol and hydroquinone were reported in leaves of *Gaultheria* and *Vaccinium* species, respectively, the last was found as *O*-glycoside. The glucoside of phloroglucinol was reported in the peel of citrus fruits (Lattanzio, 2013). Benzoic acids and benzaldehyde, as well as their hydroxylated and/or methoxylated derivatives, integrate the C6-C1 category. They are found in fruits and vegetables as glucosides or as free aglycon. Important members of this group are salicylic acid, protocatechuic acid, gallic acid and vanillin (Tsimogiannis & Oreopoulou, 2019). The C6-C2 group encompasses phenylethanoids such as phenylacetic acid, acetophenone, and phenethyl alcohol. They can be found substituted mostly as either 3- or 4- monohydroxy and 3,4-dihydroxy. Although there is an exception, the homogentisic acid, which is substituted by hydroxyl, groups in carbon 2 and 5 (Tsimogiannis & Oreopoulou, 2019).

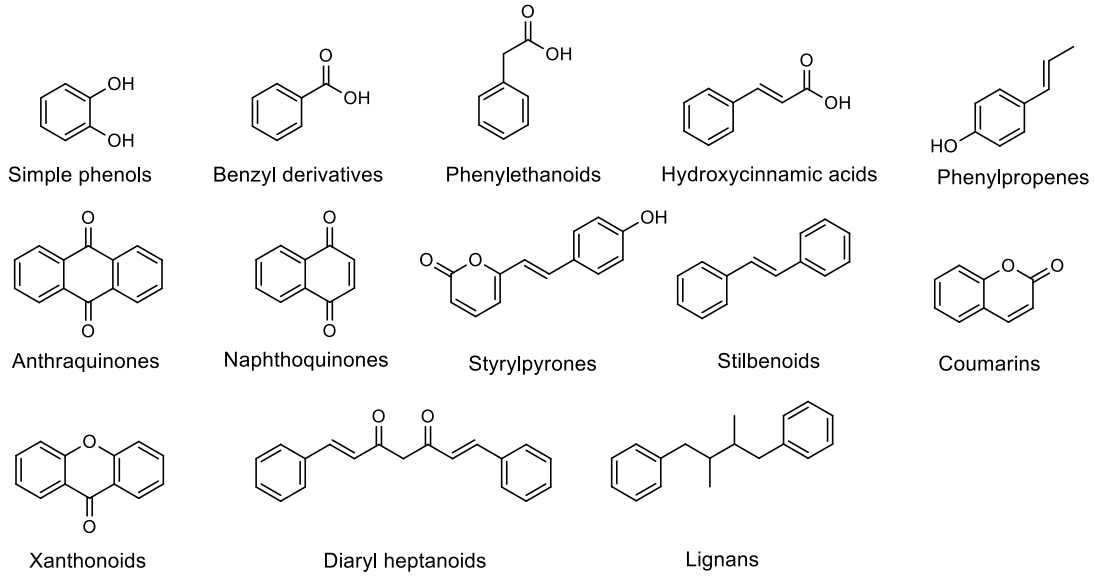

Figure 2. Basic structural skeletons of common non-flavonoids.

The hydroxycinnamic acids along with their less oxidized derivatives (cinnamic aldehydes and alcohols), coumarins, and phenylpropenes, belong to the C6-C3 category. Whose most widespread members in plants are the hydroxycinnamic acids. The most commonly found are *p*-cinnamic acid, caffeic, and ferulic acid. These metabolites usually form esters with quinic acid, tartaric acid, 3,4-dihydroxy phenyl lactic acid, among others. The cinnamic alcohols are also important since they are precursors of lignans and lignins (Tsimogiannis & Oreopoulou, 2019). The naphthoquinones are part of the C6-C4 category. They are natural pigments found in several families of plants (Lattanzio, 2013). Finally, the styrylpyrones are a restricted group of compounds, found in kava roots (*Piper methysticum*) with anxiolytic activity, the skeleton corresponds to a C6-C7 (Dewick, 2002).

Among the phenolics with two aromatic rings are the xanthonoids, which belong to the C6-C1-C6 category. They are not very widespread since they were reported in only 20 families of higher plants (Tsimogiannis & Oreopoulou, 2019). Stilbenoids and anthraquinones are members of the C6-

C2-C6 group, whose main representants are resveratrol and aloe-emodin, respectively. The diaryl heptanoids, whose basic skeleton belong to C6-C7-C6 category, were reported in *Curcuma longa* and have displayed interesting cardiovascular protective activities (Tsimogiannis & Oreopoulou, 2019).

Flavonoids comprise a family of polyphenols characterized by a 15 carbons skeleton, consisting of two phenyls connected by a bridge of three carbons forming a C6-C3-C6 basic structure (Figure 3). They are the most diverse and widespread group of phenolics in the plant kingdom (Crozier et al., 2009). These phenolics are further classified into the opened and closed bridge flavonoids, based on the nature of the heterocyclic ring. The closed heterocyclic ring may have 5- or 6- members (Tsimogiannis & Oreopoulou, 2019). These compounds are usually found as glycosides. Flavonols, flavones, flavan-3-ols, isoflavones, flavanones, and anthocyanidins compose the most abundant subclasses (Figure 3). The flavonoid skeleton (2-phenylchromane) is often substituted by hydroxy groups at 5-, 7-, 3'-, and 4'- positions and some of them might be methylated (Tsimogiannis & Oreopoulou, 2019). Flavonols, flavones, and isoflavones have a carbonyl in C4 and a 2,3 double bond in the heterocycle. Flavonols have an hydroxyl at the C3 position, while isoflavones have the B ring attached to C3 instead to C2 (Figure 3). Flavonols are often glycosylated at 3, 5, 7-, 4', 3', and 5', but the C3 is preferred. Kaempferol, quercetin, isorhamnetin, and myricetin *O*-glycosides are the most common flavonol glycosides (Del Rio et al., 2013). The *O*-glycosylation at C7' is the most common in flavones, but hydroxylated, methylated, *O*- and *C*- alkylated/glycosylated derivatives may occur. Flavones are not distributed widely but occur in celery, parsley, and citrus; while isoflavones are mainly found in the Fabaceae family (Del Rio et al., 2013). Flavanones bears the 4-carbonyl, but the 2,3 double bond is absent, originating a chiral center at C2, often with 2*S* configuration. Dihydroflavonols (flavanonols or 3-hydroxyflavanones) are their 3-hydroxy derivatives, bearing two chiral centers (C2 and C3); usually with 2*R*, 3*R* stereochemistry

(Tsimogiannis & Oreopoulou, 2019). The flavan-3-ol group only holds the hydroxyl in the C3 of the heterocycle, containing two chiral centers originating four stereoisomers. The configuration 2*R*, 3*S* is the basic and the 2*R*, 3*R* is known as "*epi*" derivatives. Among them, (+)-catechin and (-)-(*epi*)-catechin are widely found, while their enantiomers are rare (Crozier et al., 2009). Those monomers could be hydroxylated to form (*epi*)-gallocatechin, esterified with gallic acid, and/or coupled to produce oligomeric and polymeric proanthocyanidins. If the C ring bears another hydroxyl, the structure belongs to the leucoanthocyanidins group, formed by flavan-3,4-diols and flavan-4-ols (Tsimogiannis & Oreopoulou, 2019). In anthocyanidins, the heterocyclic C ring is forming a pyrylium cation; they usually have a hydroxyl in C3 conjugated with a sugar. These conjugates are called anthocyanins and may be found as esters of hydroxycinnamic and other organic acids such as acetic acid (Crozier et al., 2009).

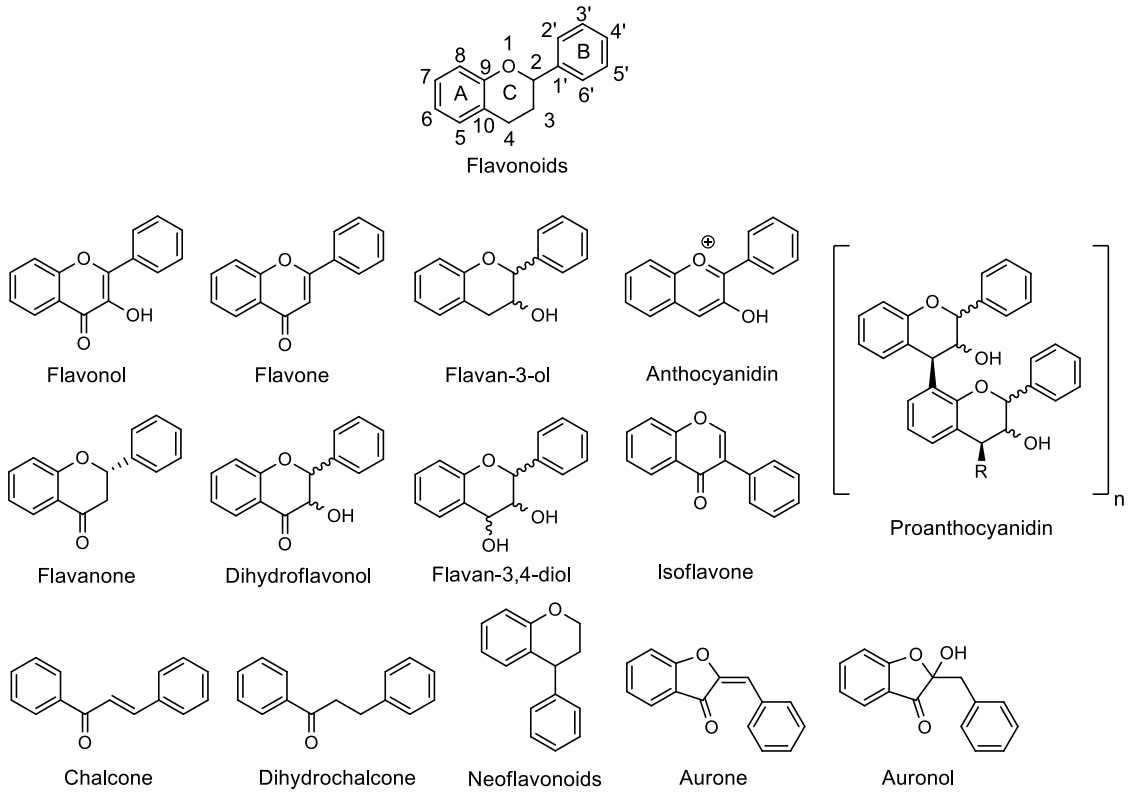

Figure 3. Basic structural skeletons of flavonoids. Adapted from Crozier et al. (2009).

The chalcones, aurones, and neoflavonoids are the less common subclasses of flavonoids. The chalcones are opened bridge flavonoids, characterized by the carbonyl next to the A-ring and the α, β unsaturation on the carbon bridge. They are intermediaries of the closed bridge flavonoids and dihydrochalcones, which lack the unsaturation in C2-C3 (Figure 3). The aurones form a heterocyclic ring of five members and the B ring is attached to C2, the hydroxyl-substituted derivatives are the auronols (Figure 3). The neoflavonoids characteristic skeleton is the 4-phenylchromane; however, the heterocycle may be unsaturated at C3-C4 and/or present a carbonyl (C2 or C3) leading to derivatives such as neoflavens and aryl coumarins (Tsimogiannis & Oreopoulou, 2019).

1.1.4. Metabolism

The phenolic profile of fruits and vegetables undergo several metabolic modifications after their ingestion (Figure 4). The biological activity of the resulting metabolites may not be the same as the parent compounds (Del Rio et al., 2013; Manach, Scalbert, Morand, Rémésy, & Jiménez, 2004). Before polyphenols become accessible for absorption, they are exposed to potential pH-dependent transformations such as hydrolysis, isomerization, and/or oxidation, as well as binding with biological and food-derived macromolecules (Alminger et al., 2014; D'Archivio, Filesi, Varì, Scazzocchio, & Masella, 2010). The first step of the digestion starts in the oral cavity, where mastication breaks the vegetal cells releasing the phytochemicals from cell compartments. The amylase enzyme from salivary secretion starts to breakdown the alimentary matrix, releasing the phytochemicals. Taking into account the short interaction time during this step, the influence of enzymatic action on phenolic compounds would be minimum (Hur, Lim, Decker, & McClements, 2011; Laurent, Besançon, & Caporiccio, 2007). During the gastric phase, pepsin digestion, the low pH (1.3-2.5) along with the mechanical movements release the phenolics from the alimentary matrix (Alminger et al., 2014; Bohn, 2014). It has been suggested that some phenolic acids and flavonoid aglycones could be absorbed in this step (Lafay et al., 2006; Manach et al., 2004). Once the chyme arrives at the duodenum, the pH reaches around 6.5 reaching 7.5 in the distal ileum (Minekus et al., 2014). This slightly alkaline environment may affect some phenolics, including anthocyanins, which are one of the least absorbed phenolic group with an uptake below 1 % (Bohn, 2014; Manach, Williamson, Morand, Scalbert, & Rémésy, 2005). In addition, some non-enzymatic hydrolysis of glycosides might occur (Bermúdez-Soto, Tomás-Barberán, & García-Conesa, 2007). The available fraction of phenolic compounds with an attached sugar (glucose, arabinose or xylose) is a potential substrate for endogenous human enzymes; while the rhamnosides reach the colon where are cleaved by the α-rhamnosidases from the human microbiota (Scalbert & Williamson,

2000). The lactase-phlorizin hydrolase (LPH) and other esterases in the brush border of the small intestine epithelial cells catalyze the hydrolysis of the glucosides, releasing the aglycon, which is absorbed by passive diffusion into the intestinal cells (Day et al., 2000; Del Rio et al., 2013; Manach et al., 2004). An alternative absorption of some flavonoid glycosides has been proposed, through the sodium-glucose-linked transporter 1 (SGLT1); after the intake, the cytosolic β-glucosidase (CBG) release the aglycon (Gee et al., 2000). However, this mechanism is still controversial since some studies could not confirm its participation (Bohn, 2014).

Aglycones may undergo phase II metabolism within the intestinal cell before the passage to the bloodstream, including sulphation, glucuronidation and/or methylation by the action of sulphotransferases (SULTs), uridine 5'-diphosphate glucuronosyltransferases (UGT) and catechol-*O*-methyltransferases (COMT), respectively (Del Rio et al., 2013). An efflux back into the lumen of the small intestine may occur through the ATP-binding cassette transporters, including multidrug resistance proteins (MRPs) and P-glycoprotein (Murakami & Takano, 2008). The unmodified fraction of phenolics and its metabolites reach the bloodstream through simple diffusion or by transporters such as MRP-3and the facilitated glucose transporter (GLUT2). The portal circulation carries them to the liver, where may undergo further phase II metabolism or return to the small intestine for bile excretion (Del Rio et al., 2013). Those non-absorbed compounds, usually polymeric proanthocyanidins, quinic acid esters, and flavonoid rhamnosides, reach the colon, where they are metabolized by the gut microbiota. The colonic microbial population submit polyphenols to hydrolysis, C-ring cleavage, and reduction reactions leading to new metabolites that can be reabsorbed through enterohepatic circulation, reaching the liver (Espín, González-Sarrías, & Tomás-Barberán, 2017).

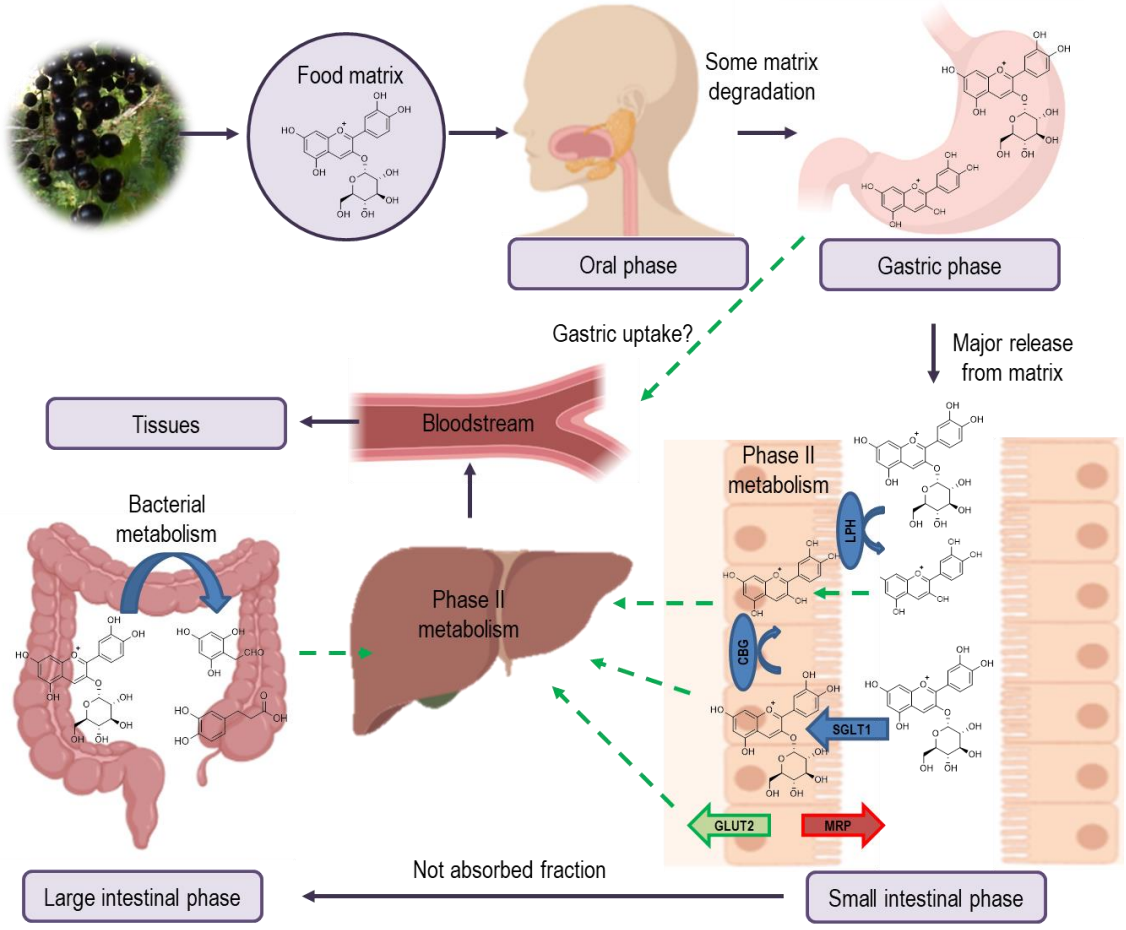

Figure 4. Overview of the metabolism of phenolic compounds. The scheme was adapted from Bohn, (2014) and the images were extracted from https://biorender.com. Abbreviations; LPH: lactase-phlorizin hydrolase; CBG: cytosolic β-glucosidase; SGLT1: sodium-glucose-linked transporter 1; GLUT2: facilitated glucose transporter 2; MRP: multidrug resistance proteins.

1.1.5. Biological effects

Numerous studies informed that a high polyphenol ingesta prevent complex diseases such as type-2 diabetes (Guo, Yang, Tan, Jiang, & Li, 2016), low grade inflammation (Bonaccio et al., 2017), cardiovascular diseases (Liu et al., 2017), neurodegenerative diseases (Barberger-Gateau et al., 2007), and cancer (Grosso et al., 2017). Given their antioxidant activity under *in vitro* conditions it was proposed that the health-related effects are a consequence of their capacity to quench harmful free radicals. On the other hand, this is not always transferable to the biological environment since

the effect depends on bioavailability and interaction with cellular targets (Williamson, 2017). The stability and bioavailability of these compounds varies greatly depending on their structure (Manach et al., 2004). In many cases, only the circulating metabolites of the original phenolics are detectable in the bloodstream (Williamson & Clifford, 2010). The complexity of their metabolism makes it difficult to elucidate the action mechanisms underlying health benefits of polyphenols consumption. Nevertheless, *in vitro* cell models and preclinical assays demonstrated to be useful, performing a major contribution to this area (Foito, McDougall, & Stewart, 2018).

The best-studied property of polyphenols is, without a doubt, their antioxidant capacity. Their phenolic structure allows them to reduce free radicals through the electron transference or donation of a hydrogen atom. The resultant phenoxyl radical is stable as a consequence of the delocalization of the charge within the aromatic ring, breaking the radical chain reactions (Losada-Barreiro & Bravo-Díaz, 2017). Also, they can form chelates with metals involved in free radical production such as iron and copper (Fraga, Galleano, Verstraeten, & Oteiza, 2010). The antioxidant potential through free radical scavenging and metal chelating capacity is probably intensified by cellular detoxifying mechanisms since polyphenols may also activate the nuclear factor erythroid-related factor (Nrf)-2, which induces the synthesis of detoxifying enzymes such as superoxide dismutase (SOD), catalase (CAT), glutathione peroxidase (GPx), and glutathione reductase (GR) (Zhang & Tsao, 2016).

Phenolic compounds may be involved in other cellular signaling processes, also related to oxidant species generation. The activation of the nuclear factor kappa B (NFκB) and/or mitogen-activated protein kinase (MAPK) signaling cascades, leads to the expression of pro-inflammatory mediators (cytokines) and enzymes (COX-2, iNOS) (Zhang & Tsao, 2016). These signals increase the migration of the immune cells to the stimulus, releasing free radicals potentially damaging the cells. The constant stimulation of these signals is associated with chronic inflammation and

carcinogenesis (Surh et al., 2001). There is substantial evidence that polyphenols disrupt this signaling cascade (Leyva-López, Gutierrez-Grijalva, Ambriz-Perez, & Heredia, 2016; Sangiovanni, Fumagalli, & Dell'Agli, 2017). This anti-inflammatory effect may also occur via direct inhibition of certain enzymes such as cyclooxygenases (Desai, Prickril, & Rasooly, 2018).

On the other hand, the plasmatic concentrations of phenolics and its metabolites are low, varying among 0 and 4 μmol/L after intake of 50 mg aglycone equivalents (Manach et al., 2005). This supports the suggestion that the gastrointestinal tract is the main target of the effects of polyphenols due to its high exposure (Halliwell, 2007). Therefore, the gastric and intestinal lining cells are most likely subjected to the mentioned protective effects against oxidative stress (Gorelik et al., 2005; Halliwell, 2007) and inflammation (Leyva-López et al., 2016). As they pass throughout the gastrointestinal tract the polyphenols could inhibit some key enzymes occurring in the intestinal lumen such as α-amylase, α-glucosidase, and lipase. This inhibition delays the absorption of monosaccharides and fatty acids after the meal, preventing postprandial hyperglycemia and hyperlipidemia (Boath, Grussu, Stewart, & McDougall, 2012; McDougall, Kulkarni, & Stewart, 2009). There is also evidence that polyphenols could avoid glucose absorption through the inhibition of the SGLT1 and/or GLUT2 transporters (Schulze et al., 2014; Williamson, 2013).

The influence of the colon on metabolism and health has been underestimated for years. Now it is recognized that the individuals' gut microbiota exerts a significant influence on health and human physiology (Verbeke et al., 2015). The composition of the microorganisms' resident in the colon is complex and encompasses beneficial and potentially harmful microbial communities. An imbalance among species (so-called dysbiosis) is associated with inflammatory diseases, diabetes, metabolic syndrome, and neurological diseases (Flint, Scott, Louis, & Duncan, 2012; Lynch & Pedersen, 2016). It has been suggested that polyphenols and gut microbiota interact reciprocally (Ozdal et al., 2016). Despite the extensive catabolism carried out by bacteria; polyphenols may inhibit potential

pathogens and promote beneficial strains (Duda-Chodak, Tarko, Satora, & Sroka, 2015; Tuohy, Conterno, Gasperotti, & Viola, 2012). Although further research in this area is required, the interaction among polyphenols and gut microbiota seems to play a key role in the health benefits related to polyphenol ingesta (Espín et al., 2017; Esposito et al., 2015).

Polyphenols may also act as prooxidants at high concentrations, high pH, and in the presence of transition metals (Procházková, Boušová, & Wilhelmová, 2011). The interaction of phenolics with free radicals leads to aroxil radicals formation; these species may react with oxygen to produce superoxide anion. Also, this process favors quinones accumulation, which may also react with DNA, forming adducts. Although polyphenols may act as transition metal chelators, they can also reduce them, contributing to the accumulation of hydroxyl radicals. A high concentration of these chemical species may induce cytotoxicity to the exposed cells (León-González, Auger, & Schini-Kerth, 2015). This process can take place in the gastrointestinal tract, where unabsorbed transition metal ions and polyphenols could reach considerable concentrations (Halliwell, 2008). On the other hand, it has been proposed that the cytotoxicity mediated by polyphenols occur through apoptosis promotion; which may be useful for cancer therapy through the employment of polyphenols sources as adjuvants or chemopreventive agents (León-González et al., 2015).

1.2. Currants and gooseberries (*Ribes* spp.)

The currants and gooseberries are shrubs whose berries are appreciated by their pleasant taste and healthy properties; the plant belongs to the genus *Ribes* L., from the family Grossulariaceae L. The natural occurrence of wild *Ribes* species are regions with cold winters and moderate summers, including the mountains of North, Central and South America as well as circumpolar regions (Hummer & Dale, 2010). The fruits of *Ribes* are very popular in European countries and some species are commercialized either fresh or processed; among the manufactured products are jams,

jellies, liqueurs, colorants, additives, and extracts for nutritional supplements (Hummer & Dale, 2010). According to the lasts official statistics from the food and agriculture organization (FAO) of the United Nations, the world's gross production value of currants ranged from 891 to 911million US$ approximately among 2014 and 2016; mostly cultivated in countries from Eastern Europe (FAOSTAT, 2018). Although in the present, the most economically important species are the European ones such as blackcurrant (*Ribes nigrum*), red currant (*Ribes rubrum*) and gooseberries (*Ribes grossularia*) (Brennan, Stewart, & Russell, 2008); the investigation of other less-known members of the *Ribes* genus may be interesting given the commercial potential of these fruits (Arena, Bernini, & Vater, 2007). In Chile, fifteen *Ribes* species have been identified, mainly represented by *Ribes magellanicum*, *Ribes punctatum*, and *Ribes cucullatum* (Figure 5). Their distribution range comprises from Coquimbo to Punta Arenas, with *R. punctatum* as the northernmost species; while *R. magellanicum* occurs in the southernmost zones (Bañados, Hojas, Patillo, & Gonzalez, 2002). In Chile and Argentina, they are commonly known as "parrillas" and/or "zarzaparrillas". They are wild-collected or cultivated in home gardens for consumption (Eyssartier, Ladio, & Lozada, 2009). The horticulture potential of these native species has been recognized, increasing the interest on their chemical characterization, shoot growth and fruiting for crops development and large scale production (Arena et al., 2007; Arena & Coronel, 2011; Arena & Pastur, 1995). Chile has become one of the most important exporters of berries with destination to the European Union (Mezzetti, 2013). At the local market, a higher demand for berries was observed in the last years, increasing the cultivation of currants, strawberries, and raspberries. Regarding currants, only the European species are harvested, especially *R. rubrum*, mainly for export; Argentina and Netherlands are the main destinies (McLeod et al., 2014). Despite that, efforts for the incorporation of the naturally occurring currants as a crop should be increased due to the possibility of their production out of season regarding Europe (Arena & Coronel, 2011).

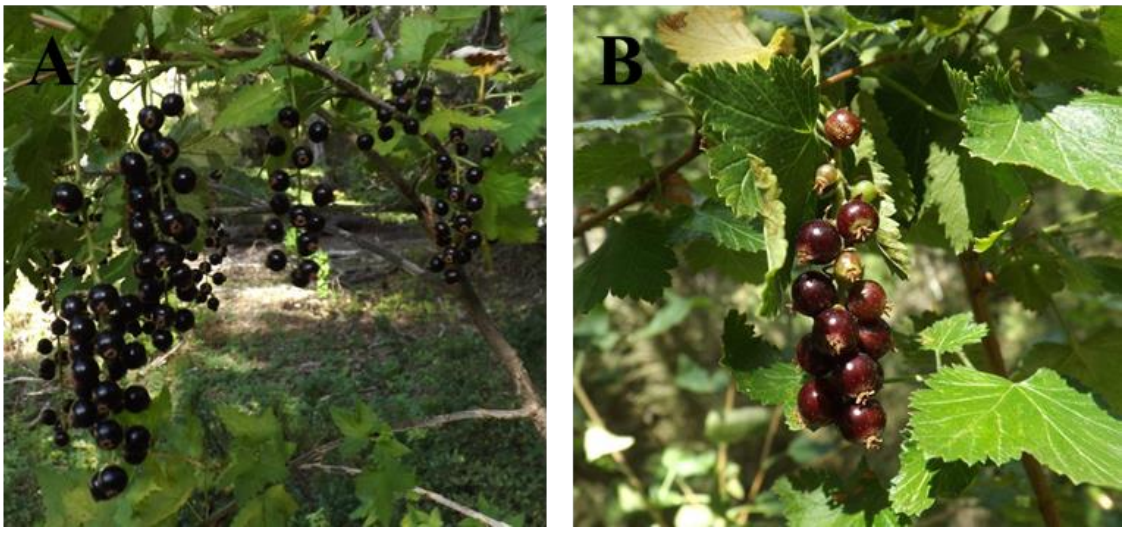

Figure 5. Ripe fruits of *R. magellanicum* (A), and *R. punctatum* (B).

The phenolic composition of the berries is important since it defines several properties of berries, including flavor, color, and possible health effects (Foito et al., 2018). Currants are a rich source of polyphenolic compounds, including rutinosides and glucosides of delphinidin and cyanidin, as the main anthocyanins; flavonols such as myricetin, quercetin and kaempferol; and flavan-3-ol monomers and oligomers (Beattie, Crozier, & Duthie, 2005; Gopalan et al., 2012). Blackcurrant (*R. nigrum*) is the best characterized, and its polyphenols have demonstrated to be potentially beneficial for health; not only by their antioxidant activity (Tabart et al., 2012), but also by their effects in several models against inflammation (Olejnik et al., 2016), type 2 diabetes (Esposito et al., 2015), cáncer (Bishayee et al., 2013), and the promotion of beneficial gut bacteria growth (Molan, Liu, & Plimmer, 2014). Regarding the Patagonian *Ribes* species, the composition of *R. magellanicum*, *R. punctatum*, *R. cucullatum*, and *R. trilobum* was described, showing profile similarities with the European *R. nigrum*. However, they differ in the higher amount and variety of hydroxycinnamic acids occurring in the South American species (Jiménez-Aspee, et al., 2016c; Ruiz et al., 2015, 2013; Theoduloz, Burgos-Edwards, Schmeda-Hirschmann, & Jiménez-Aspee, 2018). The current

information on the chemical profile of wild Chilean currants has been recently reviewed (Schmeda-Hirschmann, Jiménez-Aspee, Theoduloz & Ladio, 2019). The full composition of phenolics described in these fruits, separated by anthocyanins, hydroxycinnamic acids, and other flavonoids is shown in Table 1, Table 2, and Table 3, respectively. The antioxidant activities of these berries have been well characterized through *in vitro* experiments, showing promising results (Jiménez-Aspee et al., 2016c; Jiménez-Aspee et al., 2016b); however, these experiments are mainly focused on the effects of the PEEs before exposition to the digestion process, not taking into account its influence on their active constituents. No reports focusing on other bioactivities could be found in the literature.

Table 1. Anthocyanins reported in the literature for Patagonian *Ribes* species. Source: Schmeda-Hirschmann et al. (2019).

Compound	***R. cucullatum***	***R. magellanicum***	***R. punctatum***	***R. trilobum***
Cyanidin pentoside	Jiménez-Aspee et al., 2016c	Jiménez-Aspee et al., 2016c	Jiménez-Aspee et al., 2016c	Jiménez-Aspee et al., 2016c
Cyanidin glucoside	Jiménez-Aspee et al., 2016c; Ruiz et al., 2013	Jiménez-Aspee et al., 2016c; Ruiz et al., 2013	Jiménez-Aspee et al., 2016c	Jiménez-Aspee et al., 2016c
Cyanidin pentoside hexoside		Jiménez-Aspee et al., 2016c		
Cyanidin dihexoside 1 and 2		Jiménez-Aspee et al., 2016c		Jiménez-Aspee et al., 2016c
Cyanidin rutinoside	Jiménez-Aspee et al., 2016c; Ruiz et al., 2013	Jiménez-Aspee et al., 2016c; Ruiz et al., 2013	Jiménez-Aspee et al., 2016c	Jiménez-Aspee et al., 2016c
Cyanidin hexoside derivative		Jiménez-Aspee et al., 2016c		
Cyanidin malonyl hexoside 1 and 2		Jiménez-Aspee et al., 2016c		
Cyanidin hexoside succinate		Jiménez-Aspee et al., 2016c		
Delphinidin pentoside	Jiménez-Aspee et al., 2016c	Jiménez-Aspee et al., 2016c		Jiménez-Aspee et al., 2016c
Delphinidin glucoside	Jiménez-Aspee et al., 2016c; Ruiz et al., 2013	Jiménez-Aspee et al., 2016c; Ruiz et al., 2013	Jiménez-Aspee et al., 2016c	Jiménez-Aspee et al., 2016c
Delphinidin rutinoside	Jiménez-Aspee et al., 2016c; Ruiz et al., 2013	Jiménez-Aspee et al., 2016c; Ruiz et al., 2013	Jiménez-Aspee et al., 2016c	Jiménez-Aspee et al., 2016c
Delphindin dihexoside		Jiménez-Aspee et al., 2016c		
Delphinidin malonyl hexoside		Jiménez-Aspee et al., 2016c		
Petunidin hexoside			Jiménez-Aspee et al., 2016c	
Petunidin rhamnoside		Jiménez-Aspee et al., 2016c		
Petunidin malonyl hexoside		Jiménez-Aspee et al., 2016c		
Pelargonidin rutinoside		Jiménez-Aspee et al., 2016c		
Peonidin hexoside	Jiménez-Aspee et al., 2016c	Jiménez-Aspee et al., 2016c		
Peonidin rutinoside	Jiménez-Aspee et al., 2016c	Jiménez-Aspee et al., 2016c		
Petunidin rutinoside		Jiménez-Aspee et al., 2016c		
Malvidin rhamnose pentose		Jiménez-Aspee et al., 2016c	Jiménez-Aspee et al., 2016c	
Malvidin hexoside			Jiménez-Aspee et al., 2016 c	

Table 2. Hydroxycinnamic acids and other flavonoids informed in the literature for Patagonian currants (*Ribes spp*.). Source: Schmeda-Hirschmann et al. (2019).

Compound	***R. cucullatum***	***R. magellanicum***	***R. punctatum***	***R. trilobum***
Caffeoylquinic acid		Jiménez-Aspee et al., 2016c Ruiz et al., 2015		Jiménez-Aspee et al., 2016c
Caffeoyl hexoside 1		Jiménez-Aspee et al., 2016c	Jiménez-Aspee et al., 2016c	
3-*O*-caffeoylquinic acid	Jiménez-Aspee et al., 2016c Ruiz et al., 2015	Jiménez-Aspee et al., 2016c Ruiz et al., 2015	Jiménez-Aspee et al., 2016c	Jiménez-Aspee et al., 2016c
Caffeoyl hexoside 2	Jiménez-Aspee et al., 2016c	Jiménez-Aspee et al., 2016c	Jiménez-Aspee et al., 2016c	Jiménez-Aspee et al., 2016c
Caffeoyl hexoside 3	Jiménez-Aspee et al., 2016c Ruiz et al., 2015	Jiménez-Aspee et al., 2016c Ruiz et al., 2015	Jiménez-Aspee et al., 2016c	Jiménez-Aspee et al., 2016c
Caffeoyl hexoside 4			Jiménez-Aspee et al., 2016c	Jiménez-Aspee et al., 2016c
4-*O*-caffeoylquinic acid	Jiménez-Aspee et al., 2016c; Ruiz et al., 2015	Jiménez-Aspee et al., 2016c; Ruiz et al., 2015	Jiménez-Aspee et al., 2016c	Jiménez-Aspee et al., 2016c
3-*O*-feruloylquinic acid	Jiménez-Aspee et al., 2016c; Ruiz et al., 2015	Jiménez-Aspee et al., 2016c; Ruiz et al., 2015	Jiménez-Aspee et al., 2016c	Jiménez-Aspee et al., 2016c
5-*O*-feruloylquinic acid	Jiménez-Aspee et al., 2016c Ruiz et al., 2015	Ruiz et al., 2015	Jiménez-Aspee et al., 2016c	Jiménez-Aspee et al., 2016c
3-*p*-coumaroylquinic acid	Jiménez-Aspee et al., 2016c; Ruiz et al., 2015	Jiménez-Aspee et al., 2016c; Ruiz et al., 2015	Jiménez-Aspee et al., 2016c	Jiménez-Aspee et al., 2016c
5-*p*-coumaroylquinic acid	Ruiz et al., 2015	Jiménez-Aspee et al., 2016c; Ruiz et al., 2015		
Coumaric acid acetyldeoxy hexoside	Ruiz et al., 2015			
Synapoyl hexoside		Jiménez-Aspee et al., 2016c		

Table 3. Flavonoids reported in Patagonian currants (*Ribes spp*.). Source: Schmeda-Hirschmann et al. (2019).

Compound	***R. cucullatum***	***R. magellanicum***	***R. punctatum***	***R. trilobum***
Api pentoside			Jiménez-Aspee et al., 2016c	Jiménez-Aspee et al., 2016c
Api hexoside		Jiménez-Aspee et al., 2016c	Jiménez-Aspee et al., 2016c	Jiménez-Aspee et al., 2016c
K rhamnoside			Jiménez-Aspee et al., 2016c	
K hexoside		Jiménez-Aspee et al., 2016c	Jiménez-Aspee et al., 2016c	Jiménez-Aspee et al., 2016c
K hexoside	Jiménez-Aspee et al., 2016c	Jiménez-Aspee et al., 2016c	Jiménez-Aspee et al., 2016c	Jiménez-Aspee et al., 2016c
K rutinoside	Jiménez-Aspee et al., 2016c; Ruiz et al., 2015	Jiménez-Aspee et al., 2016c; Ruiz et al., 2015		Jiménez-Aspee et al., 2016c
K hexoside malonate	Jiménez-Aspee et al., 2016c	Jiménez-Aspee et al., 2016c	Jiménez-Aspee et al., 2016c	Jiménez-Aspee et al., 2016c
K-acetylhexoside		Ruiz et al., 2015		
Q pentoside	Jiménez-Aspee et al., 2016c; Ruiz et al., 2015	Jiménez-Aspee et al., 2016c;	Jiménez-Aspee et al., 2016c	Jiménez-Aspee et al., 2016c
Q rhamnoside		Jiménez-Aspee et al., 2016c	Jiménez-Aspee et al., 2016c	
Q hexoside	Jiménez-Aspee et al., 2016c; Ruiz et al., 2015	Jiménez-Aspee et al., 2016c; Ruiz et al., 2015	Jiménez-Aspee et al., 2016c	
Q-3-*O*-glucoside	Ruiz et al., 2015	Ruiz et al., 2015		
Q hexoside *as galactoside	Jiménez-Aspee et al., 2016c; * Ruiz et al., 2015	Jiménez-Aspee et al., 2016c; * Ruiz et al., 2015	Jiménez-Aspee et al., 2016c	Jiménez-Aspee et al., 2016c
Q dihexoside		Jiménez-Aspee et al., 2016c	Jiménez-Aspee et al., 2016c	Jiménez-Aspee et al., 2016c
Q rutinoside		Jiménez-Aspee et al., 2016c	Jiménez-Aspee et al., 2016c	
Q-3-rhamnoside-7-glucoside	Ruiz et al., 2015	Ruiz et al., 2015		
Q rutinoside (rutin)	Jiménez-Aspee et al., 2016c; Ruiz et al., 2015	Jiménez-Aspee et al., 2016c; Ruiz et al., 2015	Jiménez-Aspee et al., 2016c	Jiménez-Aspee et al., 2016c
Q dihexoside rhamnoside	Jiménez-Aspee et al., 2016c		Jiménez-Aspee et al., 2016c	Jiménez-Aspee et al., 2016c
Q-pentoside-rutinoside	Ruiz et al., 2015	Ruiz et al., 2015		
Q-acetylglucoside		Ruiz et al., 2015		
Isorhamnetin hexoside		Jiménez-Aspee et al., 2016c		Jiménez-Aspee et al., 2016c
Isorhamnetin rhamnoside		Jiménez-Aspee et al., 2016c		
Myr pentoside		Jiménez-Aspee et al., 2016c	Jiménez-Aspee et al., 2016c	Jiménez-Aspee et al., 2016c
Myr rhamnoside * as 3-*O*-	*Ruiz et al., 2015	Jiménez-Aspee et al., 2016c	Jiménez-Aspee et al., 2016c	Jiménez-Aspee et al., 2016c
Myr hexoside	Jiménez-Aspee et al., 2016c; Ruiz et al., 2015	Jiménez-Aspee et al., 2016c; Ruiz et al., 2015	Jiménez-Aspee et al., 2016c	
Myr rutinoside	Jiménez-Aspee et al., 2016c; Ruiz et al., 2015	Ruiz et al., 2015		
Myr hexoside acetate			Jiménez-Aspee et al., 2016c	

Table 3. (Continued)

Compound	***R. cucullatum***	***R. magellanicum***	***R. punctatum***	***R. trilobum***
Catechin/(*epi*)catechin hexoside		Jiménez-Aspee et al., 2016c	Jiménez-Aspee et al., 2016c	Jiménez-Aspee et al., 2016c
(*epi*)-catechin-(*epi*)-catechin (Procyanidin B)	Jiménez-Aspee et al., 2016c	Jiménez-Aspee et al., 2016c	Jiménez-Aspee et al., 2016c	

Abbreviations: Api: Apigenin; K: Kaempferol; M: Myricetin; Q: Quercetin.

1.3. *In vitro* methodologies for the evaluation of the digestion process

1.3.1. Overview

Human clinical studies are the best way to evaluate the effects of phytochemicals. However, they are not exempt from some limitations. These experiments often require a meticulous planning, organization of volunteers, specific technical resources, a lack of invasiveness, and they have some analytical constraints. All these factors lead to an important economic investment and high consumption of time (Cardoso, Afonso, Lourenço, Costa, & Nunes, 2015). Some authors pointed out the need for optimization of the *in vitro* experiments, taking into consideration the interaction of phytochemicals with the physiological environment after the ingesta (Guerra et al., 2012; Kroon et al., 2004). Over the past two decades, several *in vitro* digestion systems have been developed, simulating the stomach and small intestine conditions (Alminger et al., 2014; Guerra et al., 2012; Minekus et al., 2014). A generic scheme of the procedure is represented in Figure 6.

The fraction of a specific nutrient or phytochemical, released from the food matrix throughout the gastrointestinal tract available for absorption is known as bioaccessibility (Carbonell-Capella, Buniowska, Barba, Esteve, & Frígola, 2014). The *in vitro* digestion method has been widely used to predict bioaccessibility since it provides the possibility to consider the release of phytochemicals from the food matrix, their solubility, and their stability under digestive lumen conditions (Alminger et al., 2014; Carbonell-Capella et al., 2014). The main advantages of this methodology are the lower cost regarding *in vivo* methods; it allows the control of the experimental variables, enhancing reproducibility; specific mechanism of action at each step of the gastrointestinal digestion (GID) may be assessed as well as the digestion, absorption or transport effectiveness; it possibilities the screening of multiple samples; and is not restricted by ethical issues (Carbonell-Capella et al., 2014; Cardoso et al., 2015; Minekus et al., 2014). These models may also be

combined with human cell cultures to emulate the host responses more accurately, which also allow the study of the potential bioactivity on the cells lining the gastrointestinal tract (Guerra et al., 2012). In addition, colonic fermentation experiments may also be performed to the small intestinal fractions, to assess the influence of the large intestine conditions on phytochemicals and the impact of these compounds on the resident gut microbiota (Alminger et al., 2014; Carbonell-Capella et al., 2014).

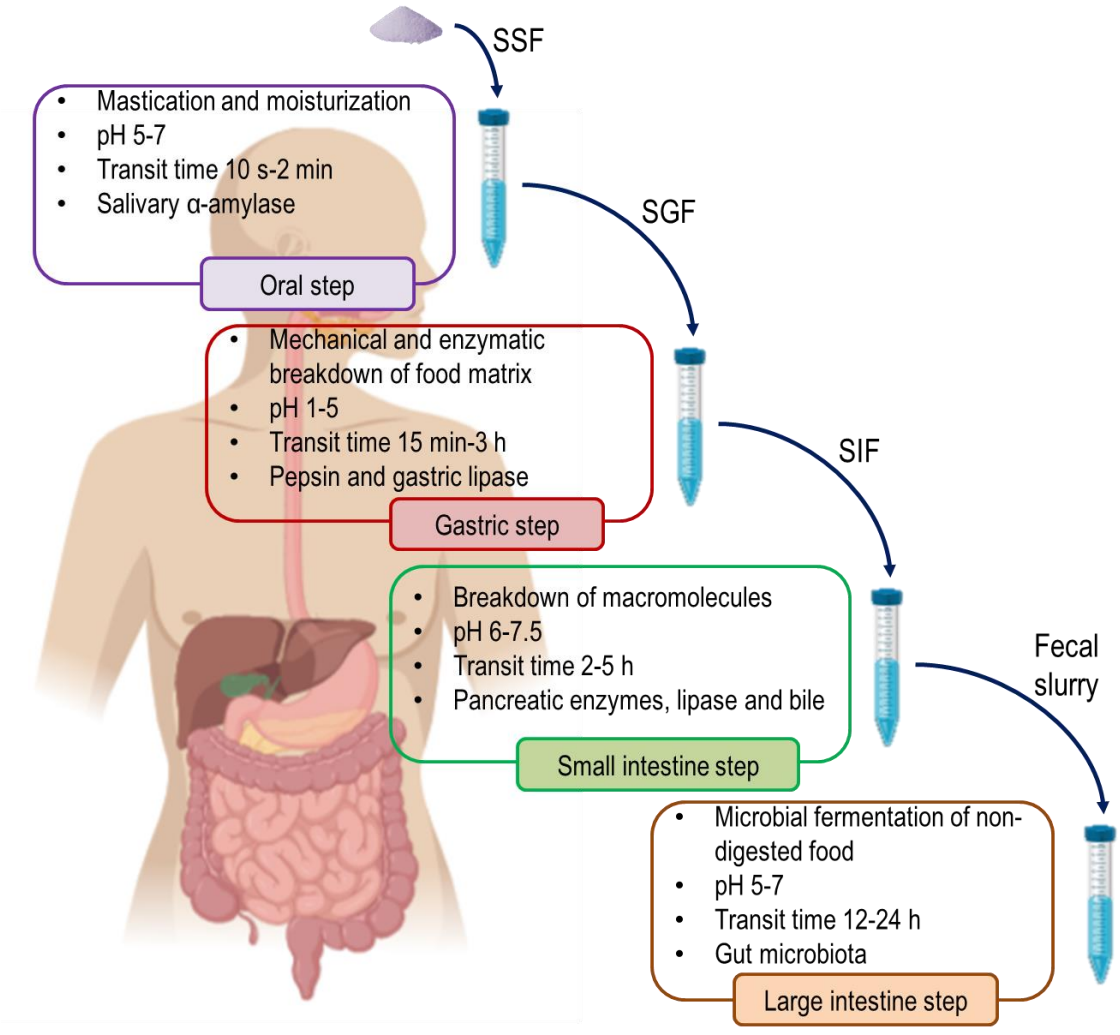

Figure 6. Scheme of physiological processes emulated with *in vitro* digestión. Adapted from Guerra et al. (2012). Abbreviations; SSF: Simulated salivary fluid; SGF: Simulated gastric fluid; SIF: Simulated intestinal fluid.

On the other hand, the *in vitro* simulations remain simplified regarding the *in vivo* digestion process. Some limitations are the absence of host response, simplified acting mechanical forces, poor simulation of gastric emptying, excessive attachment to healthy and average digestion, and the absence of homeostatic mechanisms (Carbonell-Capella et al., 2014; Cardoso et al., 2015; Guerra et al., 2012). Therefore, the results obtained from these experiments should be considered preliminary; although they are useful as supporting evidence to avoid preforming *in vivo* trials needlessly. It is necessary to further confirm them through *in vivo* approaches, first in aminal models and finally in human trials (Guerra et al., 2012).

1.3.2. Simulated gastric and intestinal digestion models

The simulated GID method is a useful technique that is commonly used to assess several parameters, such as structural changes analysis, bioaccessibility, and sample stability (Hur et al., 2011). Most studies are carried out in two major steps simulating gastric and small intestinal phases. Occasionally oral and large intestine phases might be coupled (Minekus et al., 2014). These simulations are performed incubating the samples with simulated biological fluids, for a determined time, based on *in vivo* data. Two models of *in vitro* digestion have been described in the literature: static and dynamic (Cardoso et al., 2015; Guerra et al., 2012).

The static models are composed of a set of sequential stages, each characterized by incubations at fixed parameters such as pH value, salts and enzyme concentrations, temperature (37 °C), and agitation for the duration of each digestion phase (Guerra et al., 2012). Each step is meant to emulate the oral cavity, the gastric environment, and small intestinal lumen, respectively. However, sometimes the oral phase is omitted due to the short time of interaction under *in vivo* conditions, especially if the sample does not contain complex carbohydrates (Minekus et al., 2014). The oral step comprises a previous homogenization of the sample and further incubation for 2 min at pH 6.8-

7.0 with a simulated salivary solution. This process reproduces the mastication and moisturization to form the bolus. The salivary solution is mostly α-amylase and electrolytes, based on human saliva composition (Minekus et al., 2014). The gastric phase consists of the incubation of the homogenized sample (or the oral processed sample) with the simulated gastric fluid, composed by pepsin, hydrochloric acid (HCl), electrolytes and water (Guerra et al., 2012). Only pepsin is used at this step since gastric lipolysis is too low compared to duodenal. The porcine-derived enzyme is mostly employed due to its low cost and its high homology (84 %) with the human pepsin (Minekus et al., 2014). The gastric step may last from 30 min to 2 hours, depending on the composition of the sample. Although it takes 3 or 4 h for the emptying of the stomach after a meal (Schulze, 2006), the adaptation of this parameter to the assessed food has been recommended for *in vitro* digestions, due to the transit time varies with the composition of the ingested food (Guerra et al., 2012; Hur et al., 2011). The pH in static models usually remains constant (pH 1-2). However, it is known that in healthy humans, this parameter increases from 1-2 to above 4.5 after food intake (Alminger et al., 2014). For a more realistic approach, this phase might be modified, through the addition of an additional step increasing the pH to simulate the buffering capacity of the food (Cardoso et al., 2015). After the gastric phase, the digested sample is mixed in proportion 1:1 with the simulated intestinal fluid, whose most important components are the pancreatic enzymes and the bile. The pancreatic juice is mainly composed of a complex mixture of proteases, amylases, and lipases (Guerra et al., 2012). For the simulation of this stage, individual enzymes are accepted to prepare the pancreatin solution. However, the use of a porcine-derived mixture of enzymes offer some advantages such as the low cost, the availability as well as the high reproducibility of the results obtained with them (Hur et al., 2011). Despite the duodenal pH is around 6.5, reaching 7.5 at the distal ileum, it has been suggested that incubation at pH 7.0 for 2 hours is enough to achieve the digestion (Hur et al., 2011; Minekus et al., 2014).

The dynamic models offer the closest approximation to the *in vivo* conditions since they also emulate the continuous changes of the digestion such as the transport of digested food, pH and enzyme variations during the process, as well as the peristaltic movement (Alminger et al., 2014). Some methods are mono-compartmental such as the dynamic gastric model (DGM) and the human gastric simulator (HGS). Both allow the feedback mechanism of acidification, the control of pepsin flow rate, and gastric emptying, but the last perform a more accurate reproduction of the peristaltic movements occurring in the stomach (Hoebler et al., 2002; Kong & Singh, 2010). The multi-compartmental models involve sophisticated equipment controlled by computers leading to an even closer approximation to *in vivo* conditions. For example, the TNO (Dutch Organization for Applied Scientific Research) gastrointestinal model 1(TIM-1) simulate the stomach, duodenal, jejunal, and ileal compartments; whereas other systems such as the proximal colon simulator TIM-2 coupled to TIM-1 and SHIME (Simulator of Human Intestinal Microbial Ecosystem) include the digestion from the stomach to the colon, allowing to assess the interaction of phytochemicals and other components with the gut microbiota (Alminger et al., 2014).

Despite the advantages of the dynamic models, the most widely employed method for phenolic compounds bioaccessibility is still the static *in vitro* digestion (Carbonell-Capella et al., 2014). The qualitative and quantitative analysis of the *in vitro* digested fractions of purified phenolics provides valuable information on their stability and degradation time (Bermúdez-Soto et al., 2007; Cerezo, Cuevas, Winterhalter, Garcia-Parrilla, & Troncoso, 2010; McDougall, Dobson, Smith, Blake, & Stewart, 2005). Similarly, its application to polyphenol-rich sources, such as freeze-dried fruits and enriched extracts, allows the monitoring of the compositional changes in their profile as well as assessing the variations in their potential bioactivity at each stage of digestion (Kamiloglu & Capanoglu, 2013; Lucas-Gonzalez et al., 2016; Olejnik et al., 2016; Tavares et al., 2012). To achieve a closer approximation to the physiological conditions, some researchers use this method as

a previous step for evaluating the biological activity of polyphenol sources (Li et al., 2015; Orqueda et al., 2017). Further, it is well known that the gut microbiota plays an important role in the metabolism of polyphenols and possibly in their mechanism of action. Therefore, the addition of the colonic stage is indispensable for their study (Alminger et al., 2014). In this sense, several studies combining the *in vitro* digestion with a simulated fermentation step were useful to identify potential polyphenol metabolites occurring *in vivo* and to elucidate the metabolic pathway followed by the phenolics occurring in the diet (Correa-Betanzo et al., 2014; Gullon et al., 2015; Juániz et al., 2017; Mosele, Macià, Romero, Motilva, & Rubió, 2015).

1.3.3. Simulated colonic fermentation models

As it was mentioned before, there is substantial evidence that changes in the gut microbiota composition of the host may influence health. Efforts have been focused on the discovery of prebiotic supplementation to increase the beneficial bacterial species such as *Lactobacillus*, *Bifidobacterium*, *Faecalibacterium*, and *Akkermansia muciniphila* (Espín et al., 2017). The catabolites of these bacteria are absorbable by the colonic cells influencing physiological processes at local and systemic levels. The difficulties inherent to the accessibility of the intestinal tract *in vivo* led to the design of *in vitro* methods using fecal inocula to evaluate the impact of diet components on the gut microbiota metabolism and composition (Verbeke et al., 2015).

Several *in vitro* colonic fermentation methods have been designed, all based on a single or multiple vessels inoculated with fecal microbiota, incubated at physiological pH (5-7) and temperature (37 °C), under anaerobic conditions. The inoculum employed to emulate the gut microbiota could be a pure culture, a defined mixture of microorganisms, or fecal material (Macfarlane & Macfarlane, 2007). The degree of complexity of these models raises along with the number of fermenter vessels operating simultaneously. This aims to simulate the proximal, transverse and distal regions of the

colon (Alminger et al., 2014). The simplest method to simulate the colonic environment is the batch culture fermentation model; which consists of the incubation of the inoculum in a selected medium under anaerobic conditions for a determined time, all carried out within closed systems without the further addition of nutrients (Payne, Zihler, Chassard, & Lacroix, 2012). The main advantages of this method are the low cost associated, lack of complexity, useful for the determination of metabolite profile produced by the microbiota, and for fast testing of substrates. On the other hand, this method is restricted to short-term studies due to problems inherent to the closed system. The long-term cultures in such conditions produce eventual depletion of substrates, drop of pH as a consequence of metabolism, and accumulation of toxic metabolites, leading to environmental selectivity and alterations in the microbial populations as well as their fermentation profiles (Moon, Li, Bang, & Han, 2016). The development of continuous *in vitro* fermentation models allowed overcoming this drawback. These are useful for long-term studies due to the constant addition of fresh growth medium restoring the nutrients; while preventing the accumulation of toxic products through replacement of the spent culture medium. As it was mentioned before, the TIM-2 simulates the proximal colon and is employed for microbial community focused-studies. However, it requires the coupling to the TIM-1 digestor to replicate the complete digestive tract. The SHIME model encompasses five sequential compartments, two destined to the replication of gastric and small intestine stages, while the rest mimics the proximal, transversal, and distal colon (Payne et al., 2012). Artificial colonic fermentation has some limitations such as the lack of major host functions, low reproducibility due to the high individual variations, and the microbiota cultured *in vitro* may not reflect the human colonic composition. Therefore, the conclusions obtained from the application of these methodologies should be complemented with *in vivo* studies to confirm them (Payne et al., 2012).

The role played by colonic bacteria in the metabolism of phenolic compounds, is no less important and requires deep research since their metabolites can reach significant concentrations in plasma; besides bacterial exposure to those compounds may also influence their composition (Espín et al., 2017). In this sense, the *in vitro* colonic models became the preferred method to study polyphenol-microbiota interactions (Alminger et al., 2014). It has been pointed out that addressing the metabolites of phenolic compounds through *in vitro* fermentation experiments may help to a better evaluation of the bioavailability of polyphenols in humans. These metabolites could also be used as markers to evaluate exposure to specific foods in epidemiologic studies (Dall'Asta et al., 2012). Despite the advantages of dynamic methodologies, the batch culture fermentation is a highly employed method to address polyphenol metabolites from common food sources, including such as blueberry, apple, green tea, black tea, coffee, black currant, strawberry, raspberry, among others (Brown et al., 2012; Dall'Asta et al., 2012). It is also a useful method to study the short-term influence of phenolic compounds on colonic bacterial metabolism and growth (Mills et al., 2015; Sánchez-Patán et al., 2012; Tzounis et al., 2008).

1.4. Analysis of phenolic compounds

1.4.1. Extraction

The extraction of polyphenols from fruits should be ideally carried out with fresh samples to avoid losses through degradation during storage. However, the freeze-drying process reduces the rate of degradation (Bohn, 2014). Further, the plant material is usually ground to obtain a fine powder. This process provokes cell wall disruption and enhances the surface area improving the yield of the extraction with solvents (Haminiuk, Maciel, Plata-Oviedo, & Peralta, 2012). The powder is then extracted with an appropriate solvent to solubilize the phenolics from the plant matrix. Acidified methanol or ethanol is the most commonly used, but the first one provides better yields (Ignat, Volf,

& Popa, 2011). Extractions with solvents have low selectivity often solubilizing other compounds, including sugars, organic acids, and proteins. Therefore, a subsequent purification procedure is required to improve the sensitivity (Ignat et al., 2011). Besides the extraction procedure, other external factors may influence the polyphenolic composition. The biosynthesis of phenolics in fruits and vegetables is highly dependent on growth conditions such as climate, soil, altitude, among others. These factors, along with ripening and stress may generate variations among samples (Bohn, 2014).

1.4.2. Samples pre-treatment

The solid-phase extraction (SPE) is a useful technique to purify or enrich phenolic extracts. In this method, phenolics are adsorbed into a solid sorbent. This retention allows the washout of the samples previous to the analyte elution. Some devices such as cartridges, columns, and syringes filled with several types of sorbents were developed, mostly C18-bonded silica (Ignat et al., 2011). SPE sorbents with C18 (reversed-phase) and ion-exchange fillings were successfully employed for polyphenol purification from fruits, vegetables, and even biological fluids; the elution was mostly performed with methanol, ethanol, or aqueous mixtures (Ignat et al., 2011; Vacek, Ulrichová, Klejdus, & Šimánek, 2010). The high chemical stability, selectivity towards aromatic compounds, and simplicity for re-utilization of styrene-divinylbenzene (Amberlite or XAD) resins led to its wide use for pre-purification purposes (Li, 2001). Differents XAD adsorbents are effective for this purpose, depending on the polarity of the analytes (Ignat et al., 2011; Li, 2001); in this sense for phenolic compounds from fruits, XAD-7 has given acceptable recovery percentages (Jiménez-Aspee et al., 2016b).

1.4.3. Phenolic profiling by HPLC-DAD and HPLC-ESI-MS/MS

High-Performance Liquid Chromatography (HPLC) is the most employed technique for the analysis of polyphenols from fruits. The separation of the mixture of phenolics is carried out, almost exclusively, in a reversed-phase C18 column coupled to a UV-Vis diode array detector (DAD) that registers the elution of the analytes. The mobile phase is usually composed of a binary solvent system, including acidified water (solvent A) and a polar organic solvent (solvent B). This system is a powerful analytical tool, providing valuable structural information on polyphenols, based on the retention time (Rt) and the UV-Vis absorption. The retention time gives information about the polarity of the molecule, due to the more polar compounds are less retained in a reversed-phase column. For instance, glycosyl groups decrease the retention time, whereas acylation increase the retention in the column. Similarly, the conjugations with the aromatic ring give particular UV-vis absorption spectra for each class of phenolics, making possible their distinction among sub-groups. For example, among flavonoids sub-groups, the anthocyanins show a UV-vis maximum absorption among 500-550 nm; while flavonols and flavones absorb between 300-380 nm (de Villiers, Venter, & Pasch, 2016; Haminiuk et al., 2012).

The diode array connected to a mass spectrometry detector (MS) became the most commonly used detection system for polyphenol characterization (de Villiers et al., 2016; Haminiuk et al., 2012). The coupling of the MS detector to the mentioned system requires an interface that vaporizes the eluent and generates the ions. In this sense, the electrospray ionization (ESI), atmospheric pressure chemical ionization (APCI), and atmospheric pressure photoionization (APPI) are suitable ionization sources for HPLC-MS analysis of polyphenol. The ESI source in negative ion mode showed higher sensitivity for this purpose, while positive ion mode gives improved sensitivity for anthocyanins due to the flavylium cation. The analytes are detected either in their protonated $[M+H]^+$ or deprotonated $[M–H]^–$ forms. This technique provides information on the molecular

weight and characteristic fragmentation patterns of each polyphenol, complementing the spectral information mentioned before, making it possible to build the phenolic profile through dereplication (de Villiers et al., 2016).

1.5. *In vitro* methods for biological activity evaluation

1.5.1. Antioxidant activity

Several methodologies *in vitro* have been developed to assessing the antioxidant capacity of foods. The oxygen radical absorbance capacity (ORAC) assays is one of the most employed methods for estimating the antioxidant capacity of consumed foods and beverages. This assay measures the ability of the phytochemicals to inactivate peroxyl radicals by hydrogen donation, through the monitoring of the fluorescence decay of a probe in the absence and presence of the tested compounds (López-Alarcón & Denicola, 2013). Other methods employing metal complexes, such as ferric reducing antioxidant power (FRAP) and cupric reducing antioxidant power (CUPRAC), are often used. These measure the ability of the sample to reduce cupric or ferric ions; this reduction is monitored by their absorbance. Evaluating the scavenging capacity towards stable free radicals, including $DPPH^{\bullet}$ (2,2-Diphenyl-1-picrylhydrazyl) and ABTS (2,2'-Azinobis-(3 ethylbenzothiazole-6-sulphonate) radical cation, $ABTS^{\bullet+}$) are also common techniques for assessing polyphenol-rich foods. Those are two free radicals, whose absorbance is registered after incubation with the samples, providing information about the amount of free radical consumed in a fixed incubation time. Although they are not representative of biological free radicals, these methods are widely used for screening antioxidant capacity of pure and complex samples (López-Alarcón & Denicola, 2013; Magalhães, Segundo, Reis, & Lima, 2008). Another methodology employing a physiologically relevant free radical is the superoxide anion ($O^{2\bullet-}$) scavenging method. In this assay, the reduction of nitroblue tetrazolium (NBT) into formazan is spectrophotometrically monitored. A competition

for superoxide anion among NBT and the sample occurs. The antioxidants decrease the rate of the reaction by scavenging the radical (Magalhães et al., 2008). This method has also been used for assessing the antioxidant capacity of polyphenolic sources (Cheel, Theoduloz, Rodríguez, Caligari, & Schmeda-Hirschmann, 2007). It has been recommended to employ several assays to measure antioxidant properties due to the different mechanisms involved in these reactions (López-Alarcón & Denicola, 2013; Tabart, Kevers, Pincemail, Defraigne, & Dommes, 2009).

Additionally to their radical scavenging potential, a cellular-based assay is essential to assess the antioxidant activity considering physiological conditions, due to the activity of the tested compound will be also dependent of lipophilicity, cellular uptake, and the ability to induce a cellular response (López-Alarcón & Denicola, 2013). The gastrointestinal lining cells are often exposed to a high concentration of food-derived compounds, including polyphenols (Halliwell, 2007). It was pointed out that the gastric epithelial cells might be a relevant target for polyphenols-mediated effects (Ávila, Theoduloz, López-Alarcón, Dorta, & Schmeda-Hirschmann, 2017). The human gastric adenocarcinoma cell line (AGS) consists of mucus-secreting epithelial cells that preserves several characteristics of normal gastric epithelial cells and good power of differentiation (Cheli & Baldi, 2011). This led to their use as a gastric epithelial cell model to assess polyphenol-rich extracts from fruits; in this assays, the tetrazolium salts (MTT) reduction is used for the assessment of the cell viability after exposure to an oxidant agent (Ávila et al., 2017; Jiménez-Aspee et al., 2016a; 2016c; Thomas-Valdés, Theoduloz, Jiménez-Aspee, Burgos-Edwards, & Schmeda-Hirschmann, 2018).

1.5.2. Inhibition of metabolic syndrome-related enzymes

The enzymes α-glucosidase, α-amylase, and lipase occurring in the small intestine lumen, play an important role in the absorption of glucose and fats, respectively. Currently, therapies with its inhibitors help to control glucose postprandial levels and obesity (Boath et al., 2012). Several *in*

vitro studies proposed that polyphenols from fruits may inhibit these enzymes (Boath et al., 2012; McDougall et al., 2009; Rubilar et al., 2011). Therefore, *in vitro* enzymatic inhibition assays were proposed to test these effects (Costamagna et al., 2016; McDougall et al., 2009; Tan, Chang, & Zhang, 2017). All are colorimetric methods, in the case of α-glucosidase and lipase, the enzyme is incubated along with the p-nitrophenyl derivative of the substrate with or without the sample, producing several degrees of coloration as a consequence of the enzymatic action. Regarding α-amylase, the reaction among the enzyme and its substrate takes place, and then the color reagent is added. These methods were employed by several authors to test polyphenol sources (Boath et al., 2012; Ercan & El, 2016; Li et al., 2015; Rubilar et al., 2011; Thomas-Valdés et al., 2018).

1.5.3. Anti-inflammatory activity

Polyphenols from fruit also demonstrated the capacity to inhibit pro-inflammatory enzymes such as COX-1 and COX-2 (Strugała, Gładkowski, Kucharska, Sokół-Łętowska, & Gabrielska, 2016). Although this activity might be determined by other colorimetric methods, the enzyme-linked immunosorbent assay (ELISA) provides reliable results due to its sensitivity and specificity, which constitutes a useful tool for screening inhibitors (Jiménez-Aspee et al., 2015). As it was mentioned, polyphenols exert anti-inflammatory effects through influencing cellular signaling cascades involved in pro-inflammatory responses (Desai et al., 2018; Leyva-López et al., 2016; Ribeiro, Freitas, Lima, & Fernandes, 2015). The Caco-2 cell model has been the most widely employed cell line to evaluate the anti-inflammatory activity of polyphenols for several reasons. The intestinal epithelial cells are exposed to higher quantities of polyphenols than other tissues, it emulates effectively the epithelial barrier functions of the small intestine, some clones are responsive to inflammatory stimulus, it allows to perform co-incubation experiments with immune cell lines (Biasi, Astegiano, Maina, Leonarduzzi, & Poli, 2011; Leonard, Collnot, & Lehr, 2010; Peterson & Mooseker, 1992). Despite these advantages, these experiments are also commonly performed with

immune cell lines such as monocytic leukemia cells (THP-1) or murine macrophages (RAW264.7) (Huebbe et al., 2012; Lyall et al., 2009). For the assay, an inflammatory stimulus is performed once the cells reach confluency, usually with IL-1β, lipopolysaccharides (LPS) or TNF-α. The polyphenolic extracts or purified fractions are generally incubated after the inflammatory stimulus. Then, the response to the stimulus is quantified through the determination of cytokines and/or pro-inflammatory enzymes by ELISA, quantitative polymerase chain reaction (qPCR), and/or western blot techniques (Jung, Kwak, & Hwang, 2014; Olejnik et al., 2016; Romier-Crouzet et al., 2009; Romier, Van De Walle, During, Larondelle, & Schneider, 2008).

1.5.4. Prebiotic activity

The prebiotics are non-digestible compounds that are metabolized by microorganisms in the gut, modulating the composition and/or activity of the microbiota, leading to a beneficial effect on the host (Bindels, Delzenne, Cani, & Walter, 2015). Polyphenols also present a prebiotic like effect since they modify the gut microbiota to favor the growth of some species (Espín et al., 2017). The evaluation of the prebiotic effect *in vitro* requires performing a colonic fermentation (static or dynamic) and the subtraction of aliquots at different time-points for the monitoring of bacterial species and metabolism. The measurement of pH, ammonia content, short-chain fatty acids (SCFAs) are indirect indicators of bacterial metabolism that can be measured by instrumental analysis, including potentiometry, conductimetry, and gas chromatography (Blachier et al., 2017; Verbeke et al., 2015; Yao, Muir, & Gibson, 2016). The sequencing of (16S) ribosomal RNA (rRNA) gene allows fastly and accurately identification of large intestinal bacteria. Currently, primers for 16S rRNA genes are available, making possible to quantify specific bacteria through qPCR. This technique is widely employed lately for monitoring bacterial composition from fecal samples (Flint et al., 2012). These methodologies along combined with *in vitro* fermentation experiments are useful for the evaluation of the prebiotic effect of polyphenols and other complex

polysaccharides from the diet (Cantu-Jungles et al., 2018; Kemperman et al., 2013; Sánchez-Patán et al., 2015, 2012; Sáyago-Ayerdi, Zamora-Gasga, & Venema, 2019).

Hypothesis

The phenolic composition of the native Chilean fruits *Ribes magellanicum* and *Ribes punctatum*, known as zarzaparrilla (so-called currants), are a rich source of polyphenols with a high antioxidant activity under *in vitro* conditions. However, the biochemical and physicochemical conditions of the human gastrointestinal tract may induce changes in the composition, altering the initial bioactivity. The *in vitro* digestion models simulate physiological conditions of the human gastrointestinal tract, becoming a useful alternative to evaluate such an influence on the food constituents. Based on the state of the art, we present the following hypothesis:

The simulated gastrointestinal digestion of the phenolic enriched extracts (PEEs) from the Chilean berries *Ribes magellanicum* and *Ribes punctatum* generate changes in their chemical composition. These variations in the phenolic profile alter their biological activity, influencing the nutraceutical potential of the mentioned fruits.

Objectives

1. General objective

To determine the polyphenolic profile of the Chilean currants (so-called zarzaparrillas), *Ribes magellanicum* and *Ribes punctatum*, after simulated gastrointestinal digestion; as well as the potential biological activity of non-digested and digested phenolic-enriched extracts (PEEs) through *in vitro* methods.

2. Specific objectives

1. To identify and quantify the major compounds occurring in the PEEs after *in vitro* gastrointestinal digestion, through spectroscopic and spectrometric methods.
2. To assess the antioxidant activity of each PEE, gastric-digested (GD-PEE) and intestinal digested (ID-PEE) fractions through *in vitro* assays.
3. To associate the composition of the PEE, GD-PEE, and ID-PEE from each fruit with their antioxidant activity.
4. To evaluate the cytoprotective effect of the extracts against the oxidative stress induced by hydrogen peroxide and methylglyoxal in a human gastric epithelial cell model (AGS cells).
5. To assess the changes in phenolic profile of PEEs under simulated colonic fermentation conditions.
6. To determine the inhibitory effect of each extract against digestive enzymes related to metabolic syndrome (α-amylase, α-glucosidase, and lipase).

7. To evaluate the activity of the ID-PEEs against intestinal inflammation; through measurement of inflammatory markers in an intestinal cell model (Caco-2 cells).

8. To determine the inhibitory activity of the non-digested and digested PEEs towards human cyclooxygenases (COX-1 and COX-2) enzymes related to inflammation.

9. To assess the potential influence of ID-PEEs on the growth of bacterial groups and their metabolism by means of batch-culture fermentation system with feces from healthy human donors.

Chapter 2

Materials and Methods

2.1. Reagents and solvents

The extraction of the plant samples was carried out employing technical grade solvents, previously purified by fractionated distillation. HPLC grade solvents were used for chromatographic analyses (HPLC-DAD and HPLC-MS).

- ABTS (2,20-azino-bis(3-ethylbenzothiazoline-6-sulfonic acid) diammonium salt), Trolox (6-hydroxy-2,5,7,8-tetramethylchro man-2-carboxylic acid), hemin chloride, potassium persulfate ($K_2S_2O_8$), sodium carbonate (Na_2CO_3), sodium bicarbonate (Na_2HCO_3), neocuproin, acetic acid, Iron (III) chloride hexahydrate ($FeCl_3x6H_2O$), calcium chloride dihydrate ($CaCl_2x2H_2O$), acetonitrile (ACN), methanol (MeOH), magnesium sulphate heptahydrate ($MgSO_4x7H_2O$), fluorescein sodium salt, vitamin K_1 (Phytomenadione), potassium sodium tartrate and formic acid were purchased from Merck (Darmstadt, Germany).
- (+)-Arabinogalactan from larch wood was purchased from TCI (Tokyo, Japan).
- Cyanidin-3-glucoside, cyanidin-3-rutinoside, 3-caffeoylquinic acid, quercetin-3-glucoside, querecetin-3-rutinoside, kaempferol-3-glucoside, (+)-catechin, and quercetin were purchased from Phytolab GmbH (Vestenbergsgreuth, Germany).
- Culture media F-12, antibiotics and fetal bovine serum (FBS) were from Invitrogen Corp (Grand Island, NY, USA).
- Ethyl acetate HPLC grade and acetic acid were from VWR chemicals (Fontenay-sous-Bois, France).

- GENbox anaerobic sachets were purchased from BioMérieux (Marcy L'Etoile, France).
- IL-1β was purchased from PeproTech, Inc. (Pepro Tech EC, Ltd., London, UK).
- Tween 80, sodium chloride (NaCl), potassium phosphate monobasic (KH_2PO_4), sodium hydroxide (NaOH) and yeast extract for prebiotic assays were purchased from Scharlau (Barcelona, Spain).
- Pepsin A was acquired from Biomol GmbH (Hamburg, Germany).
- 2,2′-azobis(2-methy-propionamidine) dihydrochloride (AAPH), acarbose, 2,2- diphenyl-1-picrylhydrazyl radical (DPPH), 3,5-dinitrosalicylic acid, hypoxanthine, 4-nitrophenyl-α-d-glucopyranoside, nitroblue tetrazolium salt (NBT), *p*-nitrophenyl palmitate, starch, Triton X-100, Folin-Ciocalteu reagent, TPTZ (2,4,6-tri(2-pyridyl)1,3,5-triazine), MTT (3-[4,5-dimethyl-2-thiazolyl]-2,5-diphenyl-2H-tetrazolium bromide), methylglyoxal (MGO), potassium chloride (KCl), catechin, gallic acid, aluminum trichloride ($AlCl_3$), L-cysteine hydrochloride, amberlite XAD-7 HP resin, pancreatin from porcine pancreas, lipase from porcine pancreas, porcine bile extract, α-amylase from porcine pancreas, amyloglucosidase from *Aspergillus niger*, α-glucosidase from *Saccharomyces cerevisiae*, bile salts for medium, penicillin (10,000 U/mL) and streptomycin (10 mg/mL) solutions, L-glutamine, human transferrin, sodium pyruvate, Dulbecco's Modified Eagle's Medium - high glucose (DMEM), fructooligosaccharide (FOS), trizma® maleate buffer, propionic acid, butyric acid, isobutyric acid, valeric acid, isovaleric acid, caproic acid, 2-ethylbutiric acid, and 4-methylvaleric acid were obtained from Sigma-Aldrich (St. Louis, MO).
- Orlistat was from Laboratorio Chile (Santiago, Chile).
- Fetal bovine serum for Caco-2 cells culture was acquired from Corning Mediatech, Inc. (Manassas, VA, USA).
- Peptone was from HIMEDIA (Mumbai, India).

- Phosphate buffered saline without calcium and magnesium (10x) was acquired from BioWhittaker® (Lonza, Verviers, Belgium).
- Pectin was purchased from MP Biomedicals (Illkirch, France).
- Resazurin sodium salt was acquired from ACROS Organics (New Jersey, USA).
- Sodium sulfate anhydrous was purchased from Labkem (Barcelona, Spain).
- BD BBL™ Trypticase™ Peptone for microbiota cultures was purchased from BD Biosciences (Sparks, MD, USA).
- Trypsin-EDTA (0.25 %) was purchased from Gibco (Thermo Fisher Scientific, Waltham, MA, USA).
- Ultrapure water was from a Barnsted EasyPure water system (Thermo Scientific, Marietta, OH).
- Yeast extract was obtained from OXOID (Hampshire, England).

2.2. Samples collection

The samples employed in this study consisted of ripe fruits of Chilean currants, collected from central-southern Chile during the summer months (January–February) of 2015 and 2016. *Ribes magellanicum* Poir. berries were from Laguna Verde, Parque Nacional Conguillío, located in the Araucanía region (38° 41'S; 71° 35'W); while *Ribes punctatum* Ruiz & Pav., fruits were collected from Las Trancas, located in the Ñuble region (36° 54'S; 71° 25'W). All samples were botanically identified by Dr. Patricio Peñailillo (Herbario de la Universidad de Talca). The collection places are shown in Figure 7.

Figure 7. Map of Chile showing the collection places of *Ribes* spp. fruits. A) Ñuble region, Las Trancas; B) Araucanía region, Parque Nacional Conguillio. Source: Google Maps.

2.3. Sample processing

2.3.1. Fruits extraction

Fruits were transported to the laboratory under refrigeration and immediately frozen at -20 °C for further extraction and analysis. Fruits were washed, homogenized in a blender (Thomas TH-501V; Thomas Elektrogeräte, Germany), lyophilized and extracted five times with MeOH/formic acid (99:1 v/v) in the dark. The extraction was assisted by sonication (15 min each time) using an Elma Transsonic 700/H bath (Singen, Germany) and it was performed in a homogenate:solvent ratio of 1:3 w/v. The solvent was completely removed from each sample under reduced pressure at 37 °C (Jiménez-Aspee et al., 2016b).

2.3.2. Phenolic-enriched extract (PEE) obtention

The obtained MeOH extract was enriched with Amberlite XAD-7-HP® resin according to a previously validated methodology for *R. magellanicum* phenolics (Jiménez-Aspee, et al., 2016b). The resin was pre-conditioned with a NaOH (0.1 M) solution for 2 h (two times). It was rinsed with water and neutralized with HCl (0.1 M) for 2 h. Then, it was washed with distilled water several times until reaching a neutral pH. The phenolic enrichment procedure was performed as follows; the freeze-dried MeOH extract was dissolved in water, filtered and mixed with Amberlite in a 1:5 (extract:Amberlite) ratio under constantly stirring for 40 min. The resin was filtered, washed with H_2O and the phenolic compounds were desorbed with MeOH. The eluents were combined and the solvent was eliminated by vacuum evaporation and subsequently freeze-dried to obtain the phenolic-enriched extract (PEE) for analysis.

2.4. *In vitro* gastrointestinal tract experiments

2.4.1. Simulated gastrointestinal digestion (GID)

The PEEs were submitted to a two-step *in vitro* digestion procedure following a previously described method (Cerezo et al., 2010; USP, 1995). The simulated gastric fluid (SGF) contained NaCl (0.2 % w/v), pepsin (0.32 % w/v), HCl (0.7 % v/v) and ultrapure water (pH 1.2). The simulated intestinal fluid (SIF) was composed of K_2HPO_4, NaOH, pancreatin (1 % w/v) and ultrapure water (pH 7.5). Trizma-maleate buffer (0.2 M, pH 6.8) was used to dissolve amyloglucosidase (120 mg/mL) and α-amylase (120 mg/mL), while PBS buffer (pH 7.5) was employed for lipase (0.6 % w/v) and bile extract (1.6 % w/v) solution. The PEE extracts were digested at 37 °C, protected from light with constant shaking (180 rpm) as follows; each PEE (0.5 g) was treated with 28.7 mL of SGF (pH 1.2) for 30 min, and the pH was adjusted to 4.5 ± 0.2.

Then, 0.15 mL of amyloglucosidase solution were added and further incubated. After 30 min the pH was adjusted to 6.9 ± 0.2 for the addition of α-amylase solution and incubated for 45 min. At the end of the incubation, the mixture was centrifuged (10 min, 3000 rpm, 4 °C). A portion of the supernatant was frozen at 80 °C for subsequent analyses. The remaining portion of the gastric digested sample was mixed with 28.7 mL of SIF (pH 7.5) and further incubated for 30 min. Then, 3.61 mL of a lipase and bile extract solution was added and incubated for 30 min. The intestinal digested samples were centrifuged (10 min, 3000 rpm, 4 °C) and the supernatant was frozen at 80 °C for subsequent analyses. Polyphenols were recovered from gastric and intestinal digested samples through solid-phase extraction (SPE), using HF Bond Elut C18 cartridges (Agilent Technologies, Santa Clara, CA). Cartridges were pre-conditioned with 18 mL of MeOH, MeOH-H_2O (1:1 v/v) and distilled water. Samples were loaded onto the cartridges, washed with distilled water in order to eliminate polar digestion residues, and the phenolics were subsequently desorbed with MeOH. The procedure was performed three times, combining the extracts, and the solvent was evaporated and lyophilized. This yielded the polyphenol-enriched extract after *in vitro* gastric digestion (GD-PEE) and the polyphenol-enriched extract after *in vitro* intestinal digestion (ID-PEE).

2.4.2. Simulated colonic fermentation conditions

2.4.2.1. Growth medium

One liter of growth medium contained the following ingredients: 2 g of peptone, 2 g of yeast extract, 2 g of arabinogalactan, 2 g of pectin, 0.5 g of bile salts, 0.5 g of L-cysteine, 0.1 g of NaCl, 0.04 g of K_2HPO_4, 0.04g of KH_2PO_4, 2 g of $NaHCO_3$, 0.01 g of $MgSO_4x7H_2O$, 0.01 g of $CaCl_2x6H_2O$, 0.05 g of hemin chloride, 10 µL of vitamin K_1, 2 mL of Tween 80 and 1 mg of

resazurin sodium salt. The medium pH was adjusted to 7.4 ± 0.1 and it was sterilized at 121 °C for 15 min at 1 atm of pressure before the experiment.

2.4.2.2. Fecal slurry

After consent of the Ethical Committee of the Universidad de Talca, fresh fecal samples were collected from two male healthy volunteers (27 years old), normal weight (BMI between 18.5-24.9 kg/m^2), without previous intestinal diseases or consumption of antibiotics for the previous 6 months and a polyphenol restrictive diet for 2 days before the donation. Samples were collected in sterile jars and processed within 2 hours from the collection. The fecal slurry was prepared in sterile Falcon tubes, by mixing 5 g of fresh feces with 50 mL of sterile PBS buffer (pH 7.4, conc.: 10 % w/v) for 5 min in a vortex. Then, the mixture was centrifuged at 4000 rpm for 10 min, taking an aliquot of 9 mL of supernatant for the fermentation vessels.

2.4.2.3. *In vitro* colonic fermentation procedure

The *in vitro* fermentation was carried out as previously reported (Dall'Asta et al., 2012), with several modifications. Briefly, each fermentation vessel contained 9 mL of fecal slurry, 61 mL of growth medium and 20 mL of filtered PEE solution reaching a final volume of 90 mL. The vessel containing the fermentation mixture was sealed with a septum and air was displaced by nitrogen stream to generate the anaerobic condition. Samples were incubated at 37 °C in the dark under constant shaking (60 rpm). After 8 h and 24 h of incubation, the fermented samples were processed. First, samples were centrifuged at 4000 rpm for 20 min. Then, the supernatants were filtered through 0.22 µm PVDF filters and the filtrate was stored at -80 °C. One control was prepared following the same procedure without the addition of PEEs. Two independent experiments were carried out for each sample. For polyphenol recovery, fermented samples and controls were defrosted and the extraction procedure described in the previous section 3.2 (Jiménez-Aspee et al.,

2016b) was followed. This procedure yielded the polyphenol-enriched extracts after 8 and 24 hours of *in vitro* colonic fermentation.

2.5. Chromatographic analyses

2.5.1. HPLC-DAD analyses of GID samples

The HPLC system used for the analyses of the PEE, GD-PEE and ID-PEE was from Shimadzu (Shimadzu Corporation, Kyoto, Japan) with an LC-20AT pump, SPD-M20A UV diode array detector and CTO-20AC column oven, and Labsolution software. The analyses were performed with a MultoHigh 100 RP-18 column, 5 µm, 250 x 4.6 mm, (CS-Chromatographie Service GmbH, Langerwehe, Germany) maintained at 30 °C, using a linear gradient solvent system consisting of H_2O-formic acid-ACN (87:5:3, v/v/v, solvent A) and H_2O-formic acid-ACN (40:5:50, v/v/v, solvent B), following a previously described method (Jiménez-Aspee et al., 2016c). The compounds were monitored at 280, 320 and 520 nm. Spectra from 200 to 600 nm were recorded for peak characterization. Quantification of anthocyanins and HCAs was carried out by HPLC-DAD employing external calibration curves prepared with pure standards. Six-point calibration curves were performed employing cyanidin-3-glucoside (12.5–400 µg/mL, r = 0.9995), cyanidin-3-rutinoside (12.5–600 µg/mL, r = 0.9957) and 3- caffeoylquinic acid (10–1000 µg/mL, r = 0.9999). The samples were injected at 10 mg/mL and the peak areas were determined at 520 nm for anthocyanins and at 320 nm for HCAs. The peak areas were quantified with the corresponding calibration curve and results were expressed as mg equivalents of the corresponding standard per g of PEE.

2.5.2. HPLC-DAD analyses of fermented samples

A Shimadzu chromatograph (Shimadzu Corporation, Kyoto, Japan) equipped with an LC-20AT pump, SPD-M20A UV diode array detector, and CTO-20AC column oven, with Lab solution software was employed. The analyses were performed with a Inertsil ODS-4 column, 5 μm, 250 × 4.6 mm, (GL Sciences Inc., Tokyo, Japan) maintained at 30 °C, using a linear gradient solvent system consisting of H2O-formic acid-acetonitrile (ACN) (87:5:3, v/v/v, solvent A) and H2O-formic acid-ACN (40:5:50, v/v/v, solvent B). The initial composition was 6 % B, at min 70 the gradient composition changed to 50 % B; it reached 100 % B from min 75 to 78, returning to the initial composition at min 82, keeping the conditions until min 90 for column equilibration. The flow rate was 0.5 mL/min and the injected volume was 20 μL. The compounds were monitored at 280, 320 and 520 nm. Spectra from 200 to 600 nm were recorded for peak characterization. Quantification of main anthocyanins and hydroxycinnamic acids (HCAs) was performed by HPLC-DAD by means of external calibration curves prepared with pure standards. Five point calibration curves were built employing cyanidin-3-glucoside (12.5–750 μg/mL, r = 0.9967), cyanidin-3-rutinoside (12.5–750 μg/mL, r = 0.9963) and 3-caffeoylquinic acid (5–750 μg/mL, r = 0.9997). Samples were injected at 10 mg/mL in triplicate and the peak areas were determined at 520 nm for anthocyanins and 320 nm for HCAs. The peak areas were quantified with their respective calibration curve and results were expressed as mg equivalents of the corresponding standard/g of PEE.

2.5.3. Identification by HPLC-ESI-MS/MS^n

Mass spectra were obtained with an HPLC HP1100 (Agilent Technologies Inc., Santa Clara, CA) liquid chromatography system connected through a split to an Esquire 4000 Ion Trap LC/MS system (Bruker Daltoniks, Germany). Mass spectra were measured by full-scan between m/z 20 and

2200. Mass spectrometry data were acquired in the positive ion mode for anthocyanins and in the negative mode for all other phenolic compounds. The nebulizer gas was nitrogen at 27.5 psi, 350 °C and at a flow rate of 8 L/min. The mass spectrometric conditions were: electrospray needle, 4000 V; end plate offset, 500 V; skimmer 1, 56.0 V; skimmer 2, 6.0 V; capillary exit offset, 84 V; and capillary exit, 140.6 V. Collision-induced dissociation (CID) spectra were obtained with a fragmentation amplitude of 1.00 V (MS/MS) using helium as the collisioner gas. The compounds were tentatively identified by comparison of the retention time, UV and MS fragmentations patterns with literature.

2.6. Total flavonoid (TF) and total phenolic (TP) content

The TP content was quantified spectrophotometrically by the Folin-Ciocalteau method and TF was measured by the $AlCl_3$ method, as previously reported (Jiménez-Aspee et al., 2016c). Briefly, stock solutions of PEE, GD-PEE, and ID-PEE were dissolved in MeOH (0.33–1.0 mg/mL). For TP, each extract was filtered and diluted to 25 mL. The Folin–Ciocalteu reagent (0.2 mL) was added to 1 mL of extract, incubating for 5 min at room temperature. Then, 1 mL of Na_2CO_3 solution (20 % w/v) was added, diluting the mixture to 25 mL with water. After 60 min of incubation, the absorbance was measured at 725 nm. The TP values were presented as g of gallic acid equivalent (GAE)/100 g of sample. For the total flavonoid (TF) determination, 250 µL of each sample was added to 1.25 mL of water. A volume of 75 µL of 5 % $NaNO_2$ solution was added to the mixture, letting stand at room temperature for 5 min. Then a 10 % $AlCl_3x6H_2O$ solution (150 µL) was added. After 5 min, 500 µL of 1 M NaOH and 275 µL of distilled water were added to the mixture. The absorbance was read immediately at 510 nm. Each sample was assayed in triplicate and results were expressed as catechin equivalents (CE)/100 g sample.

2.7. Antioxidant activity

2.7.1. Discoloration of the DPPH radical

The free radical scavenging activity of the PEE, GD-PEE, and ID-PEE was determined by the discoloration of the free radical DPPH (20 µg/mL) as previously described (Jiménez-Aspee et al., 2016c). Samples were dissolved in MeOH (300 µg/mL) and were used to perform serial dilutions of 100, 33, 11 and 3 µg/mL in 96-well plates. Catechin was employed as a reference compound and MeOH as the negative control. An aliquot of 100 µL of the sample was mixed with 200 µL of the DPPH solution, incubated at room temperature for 5 min. Absorbance was measured at 515 nm in a universal microplate reader (Biotek Instruments Inc., ELx 800, Winooski, VT). The results are expressed as the amount of sample that is able to scavenge the DPPH radical by 50 % (SC_{50}, µg/mL). Samples were evaluated in triplicate.

2.7.2. Ferric reducing antioxidant power (FRAP)

The FRAP values were obtained employing a previously reported method (Jiménez-Aspee et al., 2016c). A mixture of acetate buffer (300 mM; pH 3.6), TPTZ 10 mM, and $FeCl_3$ 20 mM in a 10:1:1 (v/v/v) ratio was employed as working solution. The samples were dissolved in MeOH to final concentrations of 30–150 µg/mL. An aliquot of 150 µL of each sample concentration was mixed with 2.85 mL of the FRAP working solution at 37°C. The mixture was placed in the dark for 30 min. The absorbance was read at 593 nm in a Genesys 10UV (Thermo Spectronic, Rochester, NY). A standard curve was constructed with Trolox (9-63 mmol). Samples were assayed in triplicate and results are expressed as mmol Trolox equivalents (TE) per g of sample.

2.7.3. Trolox equivalent antioxidant capacity (TEAC)

The ABTS radical scavenging capacity of the PEEs and digestion products were determined as described (Jiménez-Aspee et al., 2016c). An aliquot of 5 mL of ABTS (7.47 mM) was mixed with 88 μL of potassium persulfate (140 mM) to generate the $ABTS^{\cdot+}$ radical. The solution was stored in the dark for 16 h and then diluted with MeOH reaching an absorbance of 0.700 ± 0.005 at 734 nm. Determinations were carried out by mixing the $ABTS^{\cdot+}$ radical solution with fresh Trolox solution (1 mmol/L) or samples at 4 different concentrations (50–300 μg/mL). After 6 min, the absorbance was measured at 734 nm. A curve was plotted for each sample and a correlation coefficient (*r*) with a 95 % confidence limit was established. Results were expressed as mM TE/g sample.

2.7.4. Cupric-reducing antioxidant power (CUPRAC)

The CUPRAC assay was performed as previously described (Jiménez-Aspee et al., 2016c). Briefly, 150 μL of samples (or standard) dissolved in MeOH (150 μg/mL) and diluted with 0.95 mL of H_2O. This was added to a mixture containing 1 mL of each: $CuCl_2$ (0.01 M), neocuproine (7.5 mM) and ammonium acetate buffer (1 M, pH 7.0). After 30 min, absorbance was read at 450 nm. Samples were assayed in triplicate. Trolox (36-210 μmol) was employed as the reference compound. Results were expressed as mmol TE/g sample.

2.7.5. Superoxide anion scavenging capacity

The superoxide anion scavenging capacity was carried out according to Cheel et al. (2007) . In this assay, the enzyme xanthine oxidase was used to generate the superoxide anion. Sodium phosphate buffer (50 mM, pH 7.5) was employed to dissolve hypoxanthine (2.0 mM), NBT (1 mM) and xanthine (1.2 U/mL). These reactants were mixed with the sample (or standard) and the absorbance was monitored every 20 s during 4-5 min. The samples were evaluated in triplicate at 1–50 μg/mL

and absorbances were read at 560 nm. Catechin was used as the reference compound. The results are expressed as SC_{50} (µg/mL).

2.7.6. Oxygen radical absorbance capacity (ORAC)

The ORAC value for the samples was determined as previously described by Ou, Hampsch-Woodill, & Prior. (2001), with slight modifications. Briefly, all reagents and samples were dissolved in phosphate buffer (75 mM, pH 7.4). A six-point calibration curve was carried out using Trolox (0–50 µM) as an external standard. Black-wall 96-well plates (Thermo Fischer Scientific, Pittsburgh, PA, USA) were employed. Each well contained 150 µL fluorescein (83 nM) and 25 µL of standard, sample (10 µg/mL) or phosphate buffer (blank). After a pre-incubation at 37 °C for 30 min, 25 µL of AAPH solution (19 mM) was added to each well. The fluorescence decline (λ_{em} = 515 nm; λ_{ex} = 493 nm) was measured every min during 90 min in a microplate reader (Synergy HTX, Biotek Instruments Inc., VT, USA). The ORAC values were calculated by means of a linear regression between the area under the curve (AUC) and Trolox concentration. The results were expressed as µmol of Trolox equivalents (TE) per gram of sample (µmol TE/g).

2.7.7. Cell-based assays

Human gastric adenocarcinoma AGS cells (ATCC CRL-1739) were employed as a model of the gastric epithelium. The medium employed for cell culture was Ham F-12, supplemented with 1 mM L-glutamine, 1.5 g/L sodium bicarbonate, 10 % fetal bovine serum (FBS), 100 IU/mL penicillin and 100 µg/mL streptomycin. Cells were plated as monolayers at a density of 2.5 $x10^4$ cells/mL, in a humidified incubator with 5 % CO_2 in air at 37°C.

2.7.7.1. Cytotoxicity assay

The assay was performed in 96-well plates. The PEEs were dissolved in culture medium without FBS and were added to the confluent cultures of AGS cells, incubating for 24 h at concentrations ranging from 0 to 250 µg/mL. Untreated cells were employed as controls. Cell viability was determined at the end of the incubation through the MTT reduction assay (Jiménez-Aspee et al., 2016c).

2.7.7.2. Cytoprotection of the extracts against H_2O_2 and MGO

The confluent cultures of AGS cells were treated overnight with two concentrations (31.25 and 62.5 µg/mL) of PEE, GD-PEE, and ID-PEE. PEEs were dissolved in medium supplemented with 2 % FBS and antibiotics (100 IU/mL penicillin and 100 µg/mL streptomycin); while digested extracts were previously dissolved in dimethyl sulfoxide (DMSO). The concentration of DMSO in dissolved samples did not exceed 0.5 % (v/v). The culture medium was removed by vacuum aspiration after the incubation and the stress was induced with 10 mM H_2O_2 or 15 mM methylglyoxal (MGO) for 2 h. The H_2O_2 and MGO solutions were freshly prepared using medium without FBS. Viability (negative) controls consisted of cells treated only with the 2 % FBS and antibiotics. Cells treated with H_2O_2 or MGO served as damage controls. Cell viability was determined through the MTT reduction assay (Cheli & Baldi, 2011; Jiménez-Aspee et al., 2016a). Two independent experiments were performed and concentrations were tested in quintuplicate. Results were expressed as the percentage of viability respect with the negative control.

2.8. Inhibitory effect on metabolic syndrome-associated enzymes

2.8.1. α-amylase inhibition assay

The α-amylase inhibition assay was carried out as described by Tan, Chang, & Zhang. (2017) with slight modifications. Briefly, 100 µL of the sample (5.0–25.0 µg/mL) were co-incubated with 100 µL of 1 % starch for 5 min at 37 °C, and 100 µL of α-amylase solution (8 U/mL) was added and incubated for a further 20 min. At the end of the incubation, 200 µL of the color reagent (prepared by mixing 20 mL of 96 mM 3,5-dinitrosalicylic acid with 8 mL of 5.31 M sodium potassium tartrate in 2 M NaOH and 12 mL of distilled water), was added and incubated for 15 min in boiling water. Then, 40 µL of this mixture was diluted with 210 µL of water and absorbance was measured in a microplate reader at 550 nm. Acarbose was included as a positive control. Samples were assayed in quadruplicate and results were expressed as the amount of sample that was able to inhibit the enzyme by 50 % (IC_{50}, µg sample/mL ± SD).

2.8.2. α-glucosidase inhibition assay

The α-glucosidase inhibition assay was carried out as described by Costamagna et al. (2016) with slight modifications. Briefly, the reaction mixture contained 20 µL of sodium phosphate buffer (200 mM, pH 6.6), 120 µL of the sample (0.01–10.0 µg sample/mL) prepared in the same buffer and 20 µL of a solution of α-glucosidase (0.25 U/L). After 15 min pre-incubation at 37 °C, the reaction was started by adding 20 µL of *p*-nitrophenyl-α-D-glucopyranoside (5 mM) into the wells. The reaction was further incubated for 15 min at 37 °C. Then, absorbance was measured at 415 nm in a microplate reader (Biotek ELx801). Samples were assayed in triplicate. Results were expressed as IC_{50} values (µg sample/mL ± SD). Acarbose was included as a positive control.

2.8.3. Lipase inhibition assay

This assay was carried out according to McDougall et al. (2009), with slight modifications. Porcine pancreatic lipase type II was re-suspended in ultrapure water at 20 mg/mL. The enzyme solution was centrifuged at 13,000 rpm at 4 °C for 10 min, and the supernatant was recovered for the assay. The substrate *p*-nitrophenyl palmitate (*p*NPP, 0.08 % w/v) was prepared in 5 mM sodium acetate buffer (pH 5.0) containing 1 % Triton X-100. This solution was heated in boiling water for 2 min for a better dissolution and cooled down to room temperature. Samples were dissolved in 10 µL of DMSO, and the final concentration was adjusted with ultrapure water. The same vehicle was used in the enzyme control. The assay mixture was 400 µL of 100 mM Tris buffer (pH 8.2), 50 µL of the sample (50–25 µg/mL), 150 µL of lipase and 450 µL of substrate solution. The mixture was incubated for 2 h at 37 °C and the absorbance was read at 400 nm. All samples were assayed in quadruplicate. Orlistat was used as the reference compound (Costamagna et al., 2016). Results are expressed as IC_{50} values (µg sample/mL ± SD).

2.9. Anti-inflammatory activity

2.9.1. Cell-based assays

Caco-2 cells clone C2BBe1 (ATCC CRL-2102) were grown as monolayers in low bicarbonate (1.5g/L) DMEM medium supplemented with 2 mM L-glutamine, 1 mM sodium pyruvate, 10 µg/mL transferrin, 10 % heat-inactivated fetal bovine serum (FBS), 100 IU/mL penicillin and 100 µg/mL streptomycin. Cells were maintained in a humidified incubator at 37 °C in a 5 % CO2. The medium was renewed every two days and the cells were sub-cultured every week at a split ratio of 1 to 20 by trypsinization (0.25 % trypsin-EDTA). Cells were plated at a density of $6.0x10^4$ cells/cm^2 for the subsequent experiments.

2.9.1.1. Cytotoxicity assay

The cytotoxicity of the ID-PEEs was determined employing the dimethylthiazol diphenyl tetrazolium bromide (MTT) reduction assay (van Meerloo, Kaspers, & Cloos, 2011). After 21 days of cell differentiation in 96-well plates, cells were treated with the ID-PEE samples previously dissolved in dimethyl sulfoxide (DMSO), at concentrations ranging from 0 to 500 µg/mL. The concentration of DMSO in cell medium did not exceeded 0.5 %, v/v. Medium with 0.5 % of DMSO was used for controls. After 24 h incubation, the treatments were removed and each well was washed twice with sterile phosphate saline buffer (PBS). Then, MTT solution (1 mg/mL) was added to each well and incubated for 1 h. The MTT solution was removed and DMSO was added to dissolve the formazan salt. The absorbance at 570 and 690 nm (for sample and background, respectively) were measured with a microplate reader (SPECTROstar® Nano, Offenburg, Germany). The results were expressed as a percentage of viability compared to the untreated controls. Each treatment was performed in quintuplicate with two independent experiments.

2.9.1.2. Inflammatory stimulation and treatment conditions

Caco-2 cells were grown on 24-well plates, forming a fully differentiated monolayer after 21 days in culture. First, cells were incubated during 4 h with the ID-PEE from *R. magellanicum* and *R. punctatum* at final concentrations of 500, 250, 125 and 62.5 µg/mL. At the end of the incubation, cells were stimulated with IL-1β (10 ng/mL) for 24 h. Stimulated cells without the extracts were employed as inflammation controls (positive), while those without any treatment were employed as negative controls. After incubation, the culture media were transferred to sterile microtubes and the cells were lysed with 200 µL of TRI Reagent® solution (Thermo Fischer Scientific, MA, USA). Culture media, as well as cell lysates, were stored at −80 °C until analysis for no more than 3 weeks. Three biological replicates were performed.

2.9.1.3. Quantification of pro-inflammatory cytokines

The release of IL-8, IL-6, and TNF-α into the cell medium was measured, using ABTS ELISA Development Kits (Pepro Tech EC, Ltd., London, UK) following the manufacturer instructions. Samples were diluted 1:2 for IL-8 determinations. Three independent experiments were performed, assessing each sample in duplicate.

2.9.1.4. Pro-inflammatory gene expression by quantitative PCR

Total RNA from Caco-2 cells was isolated with TRI reagent® solution (ThermoFisher Scientific, MA, USA) according to the manufacturer instructions. The purity and concentrations of isolated RNAs were verified with a Nanodrop (Thermo Fisher Scientific, Waltham, MA, USA). The cDNAs were synthesized from 1 µg of RNA with the PrimeScript RT Master Mix Kit (Takara Bio, Otsu, Japan). The qPCR was performed with 25 ng of cDNA in a 10 µL reaction mixture, with Perfecta SYBR Green SuperMix (Quantabio, Beverly, MA). Sequence of primer pairs are detailed in Table 4. The quantitative PCRs thermal conditions were at 94 °C during 10 min for initial denaturation, followed by 15 s at 94 °C, and 60 s at 62 °C to complete 40 PCR cycles. Each cDNA sample was amplified in triplicate in a BioRad CFX96 System (BioRad, Hercules, CA, USA). The relative quantification of mRNA level was determined by means of the $2^{-\Delta\Delta Ct}$ method, using the constitutive glyceraldehyde 3-phosphate dehydrogenase (GADPH) gene expression levels.

Table 4. Primers employed for quantitative PCR analysis.

Primer	Forward	Reverse
iNOS	5'-CGG TGC TGT ATT TCC TTA CGA GGC GAA-3'	5'-GGT GCT GTC TGT TAG GAG GTC AAG TAA-3'
GADPH	5'-GAA GGT GAA GGT CGG AGT-3'	5'-GAA GAT GGT GATGGG ATT TC-3'
COX-2	5'-TCC TTG CTG TTC CCA CCC ATG-3'	5'-CAT CAT CAG ACC AGG CAC CAG-3'

iNOS, inducible NO synthase; GADPH, glyceraldehyde 3-phosphate dehydrogenase; COX-2, cyclooxygenase 2.

2.9.2. COX-1 and COX-2 enzymes inhibition assay

The inhibitory capacity of undigested and digested PEEs towards COX-1 and COX-2 was assessed using a Human COX Inhibitor Screening Assay Kit (Cayman Chemical, Ann Arbor, MI, USA), following the manufacturer protocol. The PEE, GD-PEEs, and ID-PEE from both *Ribes* species were evaluated at 250 and 25 μg/mL, while indomethacin was employed as a positive control. Briefly, the extracts were incubated with COX-1 or COX-2 for 10 min, followed by the addition of arachidonic acid. After 2 min, HCl (1 M) was added to stop the reaction. Finally, PGE_2 was determined by means of ELISA. The absorbance was measured at 405 nm on a plate reader (Biotek ELx801). The experiments were carried out by duplicate.

2.10. Prebiotic effect measurement

2.10.1. Pre-reduced sterile bacterial growth medium

The fermentation medium was prepared according to Tzounis et al. (2008). The pH of the medium was adjusted to 7.0 ± 0.1 and it was then sterilized at 121 °C for 15 min, at 1 atm. Finally, the oxygen was displaced from the medium by overnight incubation (16-18 h) within an anaerobic chamber (Baker Ruskinn Concept 4000, Bridgend, UK), full-filled with a gaseous mixture of N_2 and H_2 (90:10). Similarly, the PBS (0.1 M, pH 7.2) for fecal slurry preparations was supplemented with resazurin (1 mg/L) and L-cysteine (0.5 g/L) and was incubated overnight to ensure pre-reduced environment.

2.10.2. *In vitro* batch-culture incubations of GID-extracts with human microbiota

Fresh fecal materials were obtained from three healthy male donors (30-39 years old). The procedure was approved by the Clinical Research Ethical Committee of Comunidad de Madrid

(Reference number 07/694487.9/17). The volunteers declared the absence of intestinal diseases or antibiotics treatment for the previous 6 months. Samples were collected in sterile containers and transported to the lab in anaerobic jars provided with gas generation sachets. The fecal material was processed within 2 hours from the collection. Fecal suspensions (1:10, w/v) were prepared separately, by mixing 5 g of feces with 50 mL of pre-reduced PBS. The suspensions were homogenized manually within stomacher® bags (Seward Limited, West Sussex, UK) for 3 min and then filtered, resulting in fecal slurries from each donor. The ID-PEEs were separately dissolved in pre-reduced PBS and sterilized through 0.22 µm syringe filters. FOS was dissolved in pre-reduced PBS and sterilized by autoclave.

The fermentation experiments were conducted in sterile Falcon tubes containing the ID-PEE, the pre-reduced medium (pH 7.0) and the fecal slurry. The ID-PEE of each berry was incubated at 40, 80 and 160 µg/mL. Doses were chosen assuming 60-240 mg of polyphenols arriving within chyme at the colon, in a volume of 1.5 L (Bazzocco, Mattila, Guyot, Renard, & Aura, 2008). These concentrations are easily reached *in vivo* at the terminal ileum (Brown et al., 2014). FOS (1 %, w/v) and fecal slurry without sample were employed as a positive and negative control, respectively. The mixtures were incubated at 37 °C under anaerobic conditions and aliquots of 3 mL were collected at 1, 4, 8 and 24 h for analyses. Each aliquot was further centrifuged (15 min, 5000 rpm, 4 ºC), taking the supernatant for pH, ammonium and SCFA determination while the pellet was used for bacterial DNA extractions. Supernatants as well as pellets were stored at -80 ºC until analysis. Three independent experiments were conducted and incubations for each donor were carried out in duplicate.

2.10.3. Determination of pH, and ammonia content

The pH of the obtained supernatants at each time-point was measured using a basic 20+ Crison pH meter (Hach Lange, Barcelona, Spain) following a methodology previously described (Dai & Karring, 2014). The ammonia content was determined employing a high-performance ammonia selective ion electrode (Orion™, ThermoFisher Scientific, Waltham, MA, USA), as previously described (Moreno-Pérez et al., 2018). Briefly, 300 µL of each supernatant was diluted in MilliQ water (1:10, v/v), alkalized with 30 µL of NaOH (1 M) and immediately measured. The ammonia content was calculated by means of a standard curve, built with serial dilutions of ammonium chloride (0.1 M) following the electrode manufacturer's instructions. The results were expressed as parts per million (ppm).

2.10.4. Short-chain fatty acids and branched-chain fatty acids

SCFA and BCFA were extracted following a previously described method (García-Villalba et al., 2012), with some modifications. First, an aliquot of each supernatant was mixed with an equal volume of phosphoric acid (1 %, v/v). Second, 300 µL of the sample was spiked with 20 µL of 4-methylvaleric acid (100 mM) employed as a recovery standard. Third, the mixture was extracted with 300 µL of ethyl acetate, homogenized with vortex for 1 min and centrifuged (3 min, 10000 rpm), transferring the upper phases to a new Eppendorf tube. This procedure was repeated three times. Finally, anhydrous sodium sulfate was added to remove water traces. The samples were vortexed, centrifuged and transferred to GC-vials for analyses. Analyses were carried out with an Agilent GC System 7820A chromatograph equipped with a DBWax 121-7037LT column and an Agilent Series MSD 5975 detector (Agilent Technologies, Inc. Santa Clara, CA, USA). Injection volume was 1 µL of sample or standard for each analysis. The data was acquired by selective ion monitoring (SIM). The target and qualifier ions are detailed in Table 5**.** SCFA and BCFA

quantification was performed by means of an eight-point external calibration curve (0.015 to 2 mM) with reference standards. 2-ethylbutiric acid was used as the internal standard.

Table 5. Mass of the target and qualifier ions employed for the identification and quantification of short-chain fatty acids (SCFA).

SCFA	Target ion (m/z)	Qualifier ions (m/z)
Acetic acid	43	45; 60
Propionic acid	74	73; 57
Butyric acid	73	60
Isobutyric acid	73	88
Valeric acid	73	60
Isovaleric acid	87	60
Caproic acid	87	60; 73
2-Ethylbutiric acid	88	73; 87
4-Methylvaleric acid	73	74; 60

2.10.5. Bacterial groups quantification

2.10.5.1. Bacterial DNA Extraction

The bacterial DNA was extracted from the pellets obtained after centrifugation of 3 mL of each fermented sample. The E.Z.N.A.® Stool DNA Kit (Omega Biotek, Norcross, GA, USA) and a bead-beating homogenizer (Bullet Blender Storm, Next Advance, Troy, NY, USA) were employed for the extractions. The concentration and purity of bacterial DNA were determined with a NanoDrop equipment (ThermoFisher Scientific, Waltham, MA, USA).

2.10.5.2. Quantitative PCR Analysis

Quantitative PCR (qPCR) analysis was carried out for monitoring the abundance of the following bacteria: *Clostridium cluster* XIVa (Matsuki et al., 2002), *Bifidobacterium spp.* (Delroisse et al., 2008), *Lactobacillus spp*. (Vigsnæs, Holck, Meyer, & Licht, 2011), *F. prausnitzii* (Son et al., 2015), *A. muciniphila* (Collado, Derrien, Isolauri, De Vos, & Salminen, 2007), *E. coli* (Bressa et al., 2017)

and total bacteria (Ott, Musfeldt, Ullmann, Hampe, & Schreiber, 2004). Primers sequences, concentrations and annealing temperature are detailed in Table 6.

A CFX Connect™ Real-Time PCR Detection System (BioRad, Barcelona, Spain) was employed for bacterial quantification, using SYBR Green I chemistry (BioRad, Barcelona, Spain) as a fluorescence probe. The analyses were performed in 20 µL reactions including one microliter (10 ng) of DNA template and 200-500 nM of primers. Cycling parameters were as follows: 95 ºC during 10 min, then 40 cycles at 95 ºC for 15 s, 1 min at the established annealing temperature and 72 ºC for 45 s. Afterwards, melting curve analysis were performed, measuring fluorescence while the temperature increased from 50 ºC to 95 ºC. Bacterial populations were quantified through standard curves built with serial dilutions of DNA from a known number of bacteria, corresponding to each species cultivated under anaerobic conditions. Absolute quantification of each bacterial taxa was performed by the standard-curve (SC) method using the formula DNA (copy) = 6.02 × 10^{23}(copy/mol) × DNA amount (g)/ DNA length (dp) × 660 (g/mol/dp). The genome sizes used were 5.44, 3.09, 2.70, 2.43, 5.13, 1.99, and 5.44 Mbp (base pairs) for *E. coli*, *F. prautznii*, *A. muciniphila, Bifidobacterium spp., Clostridium spp.,* and *Lactobacillus spp.*, and total bacteria, respectively. Results are represented as Log_{10} of absolute bacterial number.

Table 6. Sequence, annealing temperature, and concentration of primers.

Target	Primers sequence		Annealing temperature (ºC)	Concentration (nM)	Reference
	Reverse	Forward			
Clostridium cluster XIVa	5'-AGT TTY ATT CTT GCG AAC G-3'	5'-CGG TAC CTG ACT AAG AAG C-3'	61	500	Matsuki et al. (2002)
Bifidobacterium spp.	5'-CCC CAC ATC CAG CAT CCA-3'	5'-CGC GTC YGG TGT GAA A-3'	58	300	Delroisse et al. (2008)
Lactobacillus spp.	5'-CAC CGC TAC ACA TGG AG-3'	5'-AGC AGT AGG GAA TCT TCC A-3'	61	200	Vigsnæs et al. (2011)
Faecalibacterium prautznii	5'-GTC GCA GGA TGT CAA GAC-3'	5'-CCC TTC AGT GCC GCA GT-3'	48	500	Son et al. (2015)
Akkermansia muciniphila	5'-CCT TGC GGT TGG CTT CAG AT-3'	5'-CAG CAC GTG AAG GTG GGG AC-3'	49	500	Collado et al. (2007)
Escherichia coli	5'-CTT TGG TCT TGC GAC GTT AT-3'	5'-AGA AGC TTG CTC TTT GCT GA-3'	55	250	Bressa et al. (2017)
Total bacteria 27F/518R	5'-ATT ACC GCG GCT GCT GG-3'	5'-GAG TTT GAT CMT GGC TCA G-3'	61	200	Ott et al. (2004)

2.11. Statistical analysis

Statistically significant differences within each species before and after *in vitro* GID were determined by one-way analysis of variance (ANOVA) followed by Tukey's multiple comparison test ($p < 0.05$); employing the SPSS 14.0 software (IBM, Armonk, NY). Pearson's correlation coefficient was used to determine the relationships among variables. For the analysis of *in vitro* colonic fermentation samples, the one-way analysis of variance (ANOVA) followed by Tukey's multiple comparison test ($p < 0.05$) was also employed. The Student's t-test was performed for

comparison among Caco-2 cell treatments with the inflamed control, using the Statistical Package for Social Sciences for Windows software, version 22.0 (SPSS Inc., Chicago, IL, USA). All data were expressed as the mean ± SD. Regarding prebiotic assays, significant differences among non-treated control and treatments were assessed employing the Student's t-test. Results were expressed as the mean ± SEM. The statistical analyses were performed with the Statistical Package for Social Sciences for Windows software, version 22.0 (SPSS Inc., Chicago, IL, USA) and the graphics were constructed with GraphPad Prism® version 7.0 (San Diego, CA). Statistical significance was established at $p < 0.05$ for all employed analyses.

Chapter 3

Qualitative and quantitative changes in polyphenol composition and bioactivity of *Ribes magellanicum* and *R. punctatum* after *in vitro* gastrointestinal digestion

Results are presented following the articles published as the product of the experimental work. Therefore, the enumeration of the identified compounds is individual for each chapter. With the exception of cell-based assays and ORAC; the data presented in Chapter 3 was prepared as a manuscript, published in Food Chemistry. Burgos-Edwards, A., Jiménez-Aspee, F., Thomas-Valdés, S., Schmeda-Hirschmann, G., and Theoduloz, C. (2017). Qualitative and quantitative changes in polyphenol composition and bioactivity of *Ribes magellanicum* and *R. punctatum* after *in vitro* gastrointestinal digestion. *Food Chemistry*, 237, 1073–1082.

3.1. Introduction

The consumption of small fruits and berries is considered to be part of a healthy diet, due to their high content in polyphenols and vitamin C (WHO, 2003). It has been demonstrated that polyphenols, especially flavonols, anthocyanins, proanthocyanidins and phenolic acids, might prevent several illnesses, such as cardiovascular, inflammatory and neurological diseases, as well as certain types of cancer (Gopalan et al., 2012).

Among berries, the currants (*Ribes spp*.) are considered to be a good source of polyphenolic compounds (Beattie et al., 2005). In South America, wild *Ribes* species can be found in southern Chile and Argentina and are appreciated by their pleasant taste and sweet flavor. They are

commonly known as ‘‘zarzaparrilla” or ‘‘parrilla” and are consumed fresh or processed as jams and preserves (Arena & Coronel, 2011). The most abundant species occurring in Chile are *Ribes magellanicum*, *Ribes punctatum* and *Ribes cucullatum* (Bañados, Hojas, Patillo, & Gonzalez, 2002). The polyphenolic profiles have been described, showing a complex mixture of phenolic compounds. The main anthocyanins are cyanidin-3-glucoside and cyanidin-3-rutinoside, while delphinidin and peonidin derivatives were also detected as minor constituents (Jiménez-Aspee et al., 2016c; Ruiz et al., 2013). In addition, caffeic, ferulic and coumaric acid derivatives were found as major hydroxycinnamic acids (HCA). For flavonoids, the flavonols quercetin and kaempferol derivatives were also described (Jiménez-Aspee et al., 2016b; 2016c; Ruiz et al., 2015).

Ruiz et al. (2013) reported a comparative antioxidant study on berries collected in Chilean Patagonia, by means of the TEAC assay. In this report, *Ribes spp*. showed the highest antioxidant capacity, similar to that exhibited by the northern hemisphere species *Ribes nigrum*. The same trend was observed by these authors in another study including several Chilean Patagonian berries by means of the CUPRAC method (Ruiz et al., 2015). A recent study reported the antioxidant activity of several *Ribes* species, including *R. magellanicum*, *R. punctatum*, *R. cucullatum* and *R. trilobum*. The best results were shown by *R. magellanicum* and *R. punctatum* by means of the DPPH discoloration, CUPRAC and FRAP assays (Jiménez-Aspee et al., 2016c). In addition, both species showed significant cytoprotective effect against oxidative and dicarbonyl-induced stress in human gastric epithelial AGS cells (Jiménez-Aspee et al., 2016c).

The high polyphenol content of currants has also been associated with the capacity to inhibit digestive enzymes associated with the metabolic syndrome. A recent review on several prospective cohort studies concluded that increasing the consumption of berries by 17 g/day reduces the risk of developing type 2 diabetes by 5 % (Guo et al., 2016). The inhibition of α-amylase, α-glucosidase and lipase enzymes by berries was reported (Boath et al., 2012). Rubilar et al. (2011) described the

inhibition of α-amylase and α-glucosidase by the polyphenols present in the Chilean berries *Ugni molinae* (murta) and *Aristotelia chilensis* (maqui). In a murine model of type-2 diabetes, the anthocyanins from *A. chilensis* improved fasting glucose levels and glucose tolerance in obese mice fed on a high-fat diet (Rojo et al., 2012). It has been proposed that the consumption of berries may delay the breakdown of oligosaccharides, disaccharides and triglycerides, thus decreasing the absorption of glucose and fat (Rubilar et al., 2011).

Most studies on biological activity of food plants are based on crude extracts, sometimes enriched in a group of constituents such as phenolics. While in a first research step, those studies offer valuable information on the chemical identity and bioactivity of the food plant constituents, much less is known on the stability and biological effects of polyphenols after digestion. A powerful tool is the use of *in vitro* gastrointestinal digestion (GID) models to simulate the steps occurring in the human digestion process. These models represent a good alternative to animal and human studies because they are devoid of ethical issues, faster and less expensive than *in vivo* methods (Minekus et al., 2014). Simulated or *in vitro* digestion is usually carried out in two steps. First, a mixture of pepsin-HCl mimics gastric digestion, followed by a treatment with pancreatin, lipase and bile salts simulating intestinal digestion (Cerezo et al., 2010). The stability of polyphenols and their biological activity can be assessed before and after *in vitro* digestion by HPLC-DAD-MS/MS and selective bioassays, respectively. This allows the determination of changes in content and eventually the identification of new products resulting from digestion. A recent study showed the variations in composition and antioxidant potential of maqui berry (*A. chilensis*) after *in vitro* GID (Lucas-Gonzalez et al., 2016). The simulated GID of *Ribes nigrum* extracts dose-dependently reduced ROS and oxidative DNA damage in Caco-2 cells (Olejnik et al., 2016).

The aim of our study was to assess the changes in the phenolic composition and its effect on antioxidant activity and the inhibition of metabolic syndrome-associated enzymes (α-amylase, α-

glucosidase and lipase) of the Chilean currants *Ribes magellanicum* and *R. punctatum*, before and after *in vitro* GID. To the best of our knowledge, this report is the first study evaluating the effect of simulated GID on the polyphenol composition and antioxidant activity of South American *Ribes* species.

3.2. Results and discussion

In recent years, *in vitro* (simulated) digestion models for different foods have been used to disclose changes in composition, bioactivity and bioavailability of different kind of components (Hur et al., 2011). The polyphenolic-enriched extracts (PEEs) of two Chilean currants (*R. magellanicum* and *R. punctatum*) were assessed for polyphenol composition, antioxidant activity, and inhibition of metabolic syndrome-associated enzymes before and after simulated GID. Three PEEs of both species were studied, namely: the non-digested PEE, the PEE after gastric digestion (GD-PEE) and the PEE after intestinal digestion (ID-PEE).

3.2.1. Tentative identification of polyphenols from *R. magellanicum* and *R. punctatum* by HPLC-DAD-MS/MS^n

The phenolic profiles of the non-digested and digested PEEs were compared by HPLC-DAD at 280 nm (Figure 8 and Figure 9), showing similar patterns in both species, mainly constituted by anthocyanins, hydroxycinnamic acids (HCAs) and flavonols, in agreement with previous reports (Table 7 and Table 8) (Jiménez-Aspee et al., 2016c). In addition, in the present study, 10 flavan-3-ol derivatives, 4 HCAs, 2 anthocyanins and 23 flavonols were tentatively identified for the first time in Chilean *R. magellanicum* and *R. punctatum*. These differences with our previous report might be due to population variations, environmental conditions and collection places of the fruits.

3.2.1.1. Anthocyanins

Anthocyanins were tentatively identified by means of HPLC-ESI-MS/MS^+ analysis. Two main peaks and four minor compounds, all with λ_{max} of 520 nm, were detected. The peaks **3**, **4** and **6**, with $[M+H]^+$ ions at *m/z* 449, 595 and 477 amu, respectively, showed an MS^2 base peak at m/z 287, in accordance with cyanidin derivatives. The main compounds were identified as cyanidin-3-glucoside (**3**) and cyanidin-3-rutinoside (**4**), and their identities were confirmed by comparison with the respective standards. Compound **6** showed a non-defined neutral loss of 190 amu and it was assigned as cyanidin derivative. The peaks **1** and **2** showed the neutral loss of 162 amu, characteristic of a hexoside, leading to the MS^2 base peak ions at *m/z* 317 and 303, being attributable to petunidin and delphinidin cores, respectively. The compounds were assigned as petunidin hexoside (**1**) and delphinidin hexoside (**2**). One malvidin rhamnoside derivative (**5**) was tentatively identified, based on the consecutive neutral losses of the fragments of 146 amu according to rhamnose and the non-defined fragment of 156 amu, leading to the malvidin ion at *m/z* 331. The characterization of the anthocyanins from Chilean currants PEEs and simulated digestion samples is summarized in Table 7.

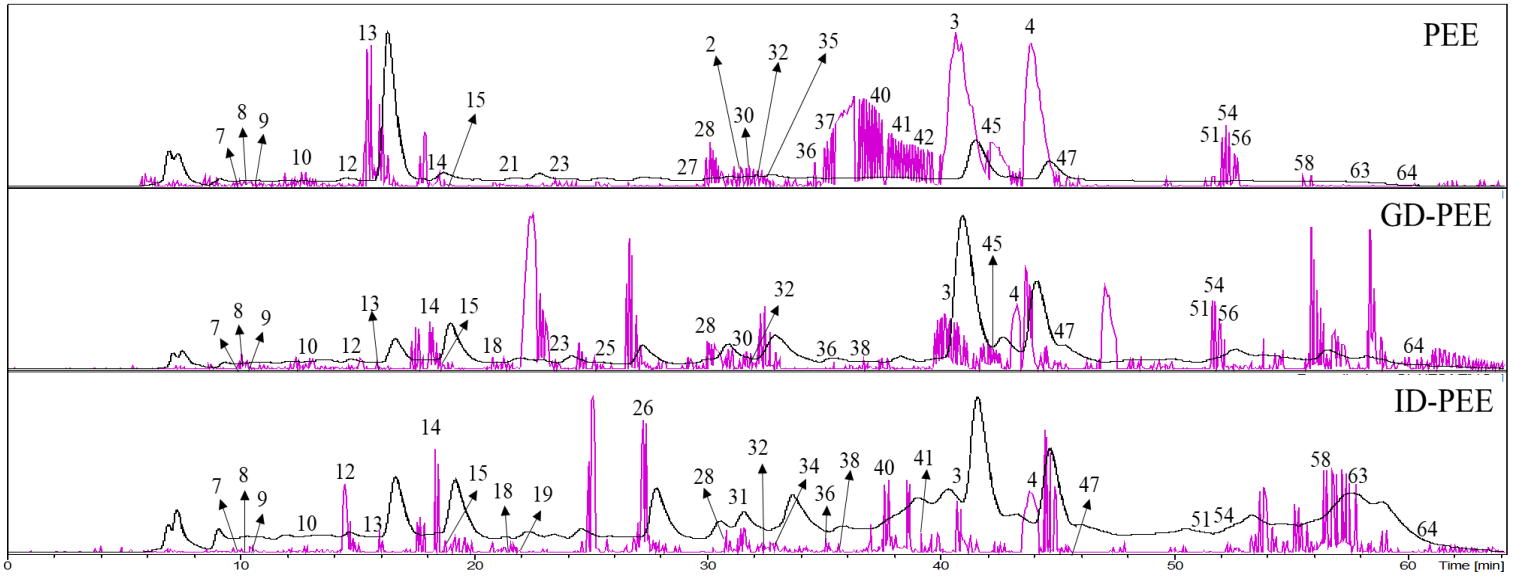

Figure 8. HPLC-DAD chromatograms at 280 nm (black) and total ion chromatograms in the negative ionization mode (pink) of *R. magellanicum* polyphenolic-enriched extract (PEE), after gastric digestion (GD-PEE) and after intestinal (ID-PEE) digestion.

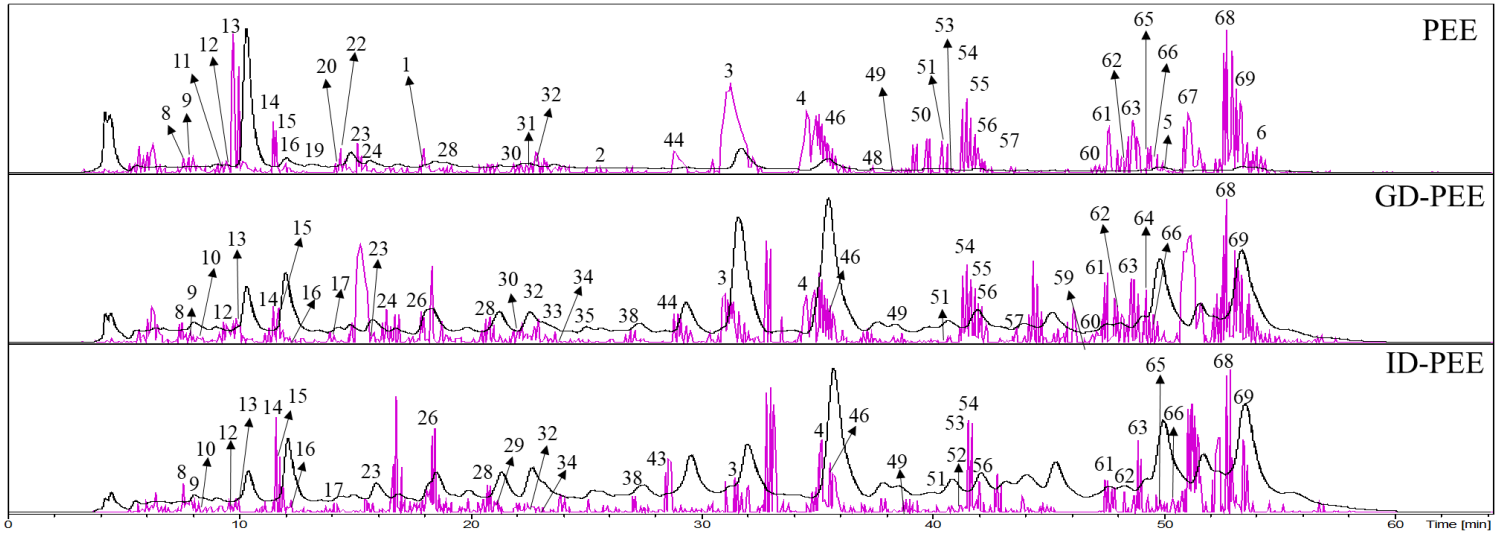

Figure 9. HPLC-DAD chromatograms at 280 nm (black) and total ion chromatograms in the negative ionization mode (pink) of *R. punctatum* polyphenolic-enriched extract (PEE), after gastric digestion (GD-PEE) and after intestinal (ID-PEE) digestion.

Table 7. Tentative identification of anthocyanins in undigested and digested *R. magellanicum* (*Rm*) and *R. punctatum* (*Rp*) PEE by HPLC-ESI-MS/MS$^+$.

Peak	Rt (min)	UV/Vis max	$[M+H]^+$	MS/MS (m/z)	Tentative identification	*Rm*	*Rp*
1	19.2		481	317(100)	Petunidin hexoside		X
2	25.9	523,340,276,247	465	303(100)	Delphinidin hexoside	X	X
3	30.8-32.5	516,280,247	449	287(100)	Cyanidin-3-glucoside[a]	X	X
4	33.5-36.2	517,284,247	595	449(81), 287(100)	Cyanidin-3-rutinoside[a]	X	X
5	50.2-51.8	517,348,267sh,247	633	487(37), 331(100)	Malvidin rhamnoside derivative		X
6	53.5-54.5		477	287(100)	Cyanidin derivative		X

[a] Identity confirmed with standards.

3.2.1.2. Other phenolics

The HPLC-ESI-MS/MS$^-$ analysis allowed the detection of monomers and oligomers of proanthocyanidins. The fragmentation of peaks **9**, **12**, **15**, **16**, and **24** led to a base peak ion at *m/z* 289, characteristic of (*epi*)-catechin units. Compounds **9**, **12** and **16** showed an $[M-H]^-$ at 593 amu, with a neutral loss of 168 amu leading to an MS^2 base peak at *m/z* 425, suggesting an (*epi*)-gallocatechin core (Lin, Sun, Chen, Monagas, & Harnly, 2014). Compounds **15** and **24**, showed an $[M-H]^-$ at *m/z* 577, with a neutral loss of 152 amu leading to an MS^2 base peak at *m/z* 425, suggesting an (*epi*)-catechin core (Lin et al., 2014). Thus, compounds **9**, **12** and **16** were assigned as (*epi*)-catechin-(*epi*)-gallocatechin isomers and compounds **15** and **24** as (*epi*)-catechin-(*epi*)-catechin isomers. On the other hand, the fragmentation of the compounds **7**, **8**, **10** and **25** led to a base peak at *m/z* 305, compatible with (*epi*)-gallocatechin cores. The neutral loss of 168 amu in compounds **8** and **25** indicated a bonded (*epi*)-gallocatechin unit. Thus, these compounds were assigned as (*epi*)-gallocatechin dimer isomers. Compounds **7** and **10**, showed an $[M-H]^-$ peak at *m/z* 913 and were assigned as (*epi*)-gallocatechin trimer isomers. Compound **18** showed an $[M-H]^-$ peak at *m/z* 305, leading to an MS^2 base peak at m/z 221, in agreement with an (*epi*)-gallocatechin unit (Lin et al., 2014). Compound **23** showed an $[M-H]^-$ peak at *m/z* 289, leading to an MS^2 base peak at *m/z* 245, in agreement with an (*epi*)-catechin unit (Lin et al., 2014).

A group of HCAs was also detected in both *Ribes* species PEEs as well as in the digestion fractions, and tentatively identified following the hierarchical scheme reported by Clifford et al. (2003). Compound **11** showed a parent ion at *m/z* 515, with an MS^2 peak at m/z 341 and an MS^3 at *m/z* 179, corresponding to a dicaffeoylquinic acid. Compound **20** also showed a parent ion at *m/z* 515, with an MS^2 peak at *m/z* 353 and an MS^3 at *m/z* 191. The characteristic fragmentation was in agreement with a 3,5-dicaffeoylquinic acid (Clifford et al., 2003). The main compound **13** showed a parent ion at *m/z* 353 with an MS^2 base peak at *m/z* 191 and a secondary peak at *m/z* 179, compatible with 3-caffeoylquinic acid (Clifford et al., 2003; Jiménez-Aspee et al., 2016c). Compounds **19** and **26** showed a parent ion at *m/z* 353. While compound **19** presented an MS^2 base peak at *m/z* 191, compound **26** showed a fragmentation at *m/z* 173. The identities were tentatively assigned as caffeoylquinic acid isomer and 4-caffeoylquinic acid. Coumaroylquinic (**22**) and feruloylquinic acid (**28**) were also found, based on the parent ions of *m/z* 337 and 368, leading to MS^2 base peaks of *m/z* 163 and 161, respectively. In addition, two compounds (**45** and **47**) with parent ions at *m/z* 335 amu were also detected. Both of them showed an MS^2 fragmentation at base peak *m/z* 161 with secondary ions at *m/z* 179, in accordance with caffeoyl derivatives. The compounds were assigned as caffeoyl derivatives 1 and 2. Peaks **14**, **30**, **33** and **38** showed a neutral loss of 162 amu leading to base peak ions at *m/z* 179, 179, 181 and 177, respectively. The compounds were tentatively identified as caffeoylhexoside 1 (**14**), caffeoylhexoside 2 (**30**), dihydrocaffeoylhexoside (**33**) and caffeoylhexoside 3 (**38**). The MS of compound **21** showed a parent ion at *m/z* 163, leading to a MS^2 base peak ion at *m/z* 119, compatible with *p*-coumaric acid.

Finally, flavonols and flavanols derivatives were also detected, constituting the most variated group of phenolic compounds present in the PEEs. Twelve compounds were tentatively identified as kaempferol derivatives following the MS^2 base peak at *m/z* 285 and UV profiles. Compounds **29**, **35**, **41**, **63** and **68** were assigned as kaempferol hexosides, due to the neutral loss of 162 amu.

Compounds **43**, **50**, **55** and **67** presented a neutral loss of 204 amu and were tentatively identified as kaempferol acetylhexosides. Compound 53 showed an $[M-H]^-$ at *m/z* 593 with a neutral loss of 308 amu, compatible with kaempferol rutinoside. Compounds **32** and **44** were assigned as kaempferol derivatives due to the unidentified neutral loss of 181 amu. Fourteen compounds were tentatively identified as quercetin derivatives due to the presence of an MS^2 ion at m/z 301 and their UV profiles. The compounds presented the neutral loss of a rhamnose and a hexose (**27**, **42** and **49**), two hexosides (**34**), acetylhexoside (**58**), rutinoside (**31**, **36** and **52**) and hexoside (**37**, **40**, **48**, **54**, **66** and **69**), as reported in Table 8. In addition, several myricetin derivatives were found by detection of the base peak ion at m/z 317 and the neutral loss of hexose and rhamnose (**51**), hexose (**56**), pentose (**57**), acetylhexose (**60**) and rhamnose (**61** and **64**). Compounds **39** and **62** showed an MS^2 base peak ion at m/z 315 and 301, with neutral losses of 294 and 146 amu, respectively. Compounds were in agreement with isorhamnetin hexoside pentoside (**39**) and rhamnoside (**62**). Four dihydroquercetin derivatives were tentatively identified based on the MS^2 base peak at m/z 303 and their UV spectra. Compound **17** showed a neutral loss of 162 amu, while compounds **46**, **59** and **65** showed a neutral loss of 132 amu, respectively. The tentative identities of the compounds are presented in Table 8.

Table 8. Tentative identification of flavonoids and hydroxycinamic acids in non-digested and digested *R. magellanicum* (*Rm*) and *R. punctatum* (*Rp*) by HPLC-ESI-MS/MS^{-}.

Peak	Rt (min)	UV/vis max	$[M-H]^-$	MS/MS (*m/z*)	Tentative identification	*Rm*	*Rp*
7	7.2		913	745(44), 727(100), 305(10)	(*epi*)-GC-(*epi*)-GC-(*epi*)-GC trimer 1	X	
8	7.3-7.5		609	483(66), 441(100), 423(89), 305(25)	(*epi*)-GC-(*epi*)-GC dimer	X	X
9	7.3-7.6		593	467(71), 425(100), 289(38)	(*epi*)-C-(*epi*)-GC dimer 1	X	X
10	8.6		913	745(86), 727(100), 305(3)	(*epi*)-GC-(*epi*)-GC-(*epi*)-GC trimer 2	X	X
11	9.1		515	353(50), 341(100), 179(46)	Dicaffeoyl quinic acid 1		X
12	9.4-9.6		593	467(42), 425(100), 289(20)	(*epi*)-C-(*epi*)-GC dimer 2	X	X
13	9.8-10.3	324, 284sh, 247	353	191(100), 179(45)	3-caffeoylquinic acid[a,b]	X	X
14	11.5	330, 298sh, 248	341	179(100)	Caffeoyl hexoside 1	X	X
15	11.7-12.1		577	451(74), 425(100), 289(26)	(*epi*)-C-(*epi*)-C dimer 1	X	X
16	11.9		595	467(52), 425.2(100), 289.3(12)	(*epi*)-C-(*epi*)-GC dimer 3		X
17	13.8		465	303(100), 285(13)	Dihydroquercetin hexoside		X
18	13.9-14.1	279, 247	305	261(65), 221(100), 179(59)	(*epi*)-gallocatechin	X	
19	14.1		353	191(100), 179(47)	Caffeoylquinic acid 2	X	X
20	14.2		515	353(100), 191(24)	3,5-dicaffeoylquinic acid[b]		X
21	14.3		163	119(100)	*p*-coumaric acid	X	
22	14.4		337	191(8), 163(100)	Coumaroyl quinic acid 1		X
23	15.7	279, 247	289	245(100), 205(31)	(*epi*)-catechin	X	X
24	16.0	280, 247	577	451(60), 425(100), 289(23)	(*epi*)-C-(*epi*)C dimer 2		X
25	16.3		609	441(100), 305(32)	(*epi*)-GC-(*epi*)-GC dimer 2	X	
26	17.9-18.1	325,291sh,247	353	179(52), 173(100)	4-caffeoylquinic acid[b]	X	X
27	20.6		609	447(19), 301(100)	Quercetin hexoside rhamnoside 1	X	
28	20.8-21.2		367	193(8), 161(100), 135(13)	Feruloyl quinic acid	X	X
29	21.4		447	285(100)	Kaempferol hexoside 1		X
30	22.1	324, 287sh, 247	341	179(100)	Caffeoyl hexoside 2	X	X
31	22.1		609	301(100)	Quercetin rutinoside 1	X	X
32	22.8		465	303(23), 285(100)	Kaempferol derivative	X	X
33	22.8-23.0		343	181(100), 179(26)	Dihydrocaffeoyl hexoside		X
34	23.7		625	463(100), 301(13)	Quercetin dihexoside	X	X
35	24.2		447	285(100)	Kaempferol hexoside 2	X	X
36	24.2		609	301(100)	Quercetin rutinoside 2	X	
37	25.8		465	337(42), 301(100)	Quercetin hexoside 1	X	
38	27.2	321, 287sh, 247	341	177 (100)	Caffeoyl hexoside 3	X	X

Table 8. (Continued)

39	27.7		609	315(40), 301(100)	Isorhamnetin pentoside hexoside	X	
40	28.2		463	301(100)	Quercetin hexoside 2	X	
41	28.3		447	285(100)	Kaempferol hexoside 3	X	
42	28.4		609	447(54), 301(100)	Quercetin hexoside rhamnoside 2		X
43	28.6		489	285(100)	Kaempferol acetyl hexoside 1		X
44	29.0		465	285(100), 151(29)	Kaempferol derivative 2	X	
45	32.3		335	179(10), 161(100)	Caffeoyl derivative 1		X
46	34.7-35.2		435	303 (100), 285(74), 151(37)	Dihydroquercetin pentoside 1	X	
47	35.0		335	179(9), 161(100)	Caffeoyl derivative 2		X
48	35.2		463	301(100)	Quercetin hexoside 3		X
49	38.5-38.7		609	447(100), 301(21)	Quercetin hexoside rhamnoside 3		X
50	41.5-41.6		489	285(100)	Kaempferol acetyl hexoside 2	X	X
51	40.6		625	463 (92), 317(100)	Myricetin hexoside rhamnoside		X
52	40.7	348, 270, 247	609	301(100)	Quercetin rutinoside 3		X
53	41.2-41.8		593	285(100)	Kaempferol rutinoside	X	X
54	41.3-41.7		463	301(100)	Quercetin hexoside 4		X
55	41.5-41.6		489	285(100)	Kaempferol acetyl hexoside 3	X	X
56	41.5-41.7		479	317(100)	Myricetin hexoside		X
57	43.5-43.6		449	317(72), 285(100)	Myricetin pentoside	X	
58	46.4		505	301(100)	Quercetin acetyl hexoside		X
59	46.6	279, 247	437	303(100), 285(27)	Dihydroquercetin pentoside 2		X
60	47.2-47.9		521	479 (28), 317 (100)	Myricetin acetyl hexoside		X
61	47.6-47.8		463	316(100)	Myricetin rhamnoside 1		X
62	48.6-49.0		463	315(93), 301(100)	Isorhamnetin rhamnoside	X	X
63	48.7-49.6		447	285(100)	Kaempferol hexoside 4	X	X
64	48.8		463	316.2(100)	Myricetin rhamnoside 2		X
65	49.3		437	303(100), 285(16)	Dihydroquercetin pentoside 3		X
66	49.5-51.1		463	301(100)	Quercetin hexoside 5		X
67	50.9		489	429(44), 285(100)	Kaempferol acetyl hexoside 4		X
68	52.7	352, 268, 247	447	285(100)	Kaempferol hexoside 5		X
69	52.8-53.6	352, 266, 246	463	301(100)	Quercetin hexoside 6	X	

[a]Identity confirmed with standards;[b] according to the hierarchical scheme of Clifford et al. (2003). Abbreviations; C: catechin; GC: gallocatechin.

3.2.2. Effect of simulated gastrointestinal digestion (GID) on phenolic content and composition

The simulated GID of both *R. magellanicum* and *R. punctatum* PEEs led to qualitative and quantitative differences with respect to the PEEs (Figure 8 and Figure 9). Although not all the phenolics identified could be quantified, decreases in the signals were expected due to the degradation of compounds upon the effect of digestive enzymes and pH (Bergmann, Rogoll, Scheppach, Melcher, & Richling, 2009). This has been reported in several fruits and foods subjected to simulated digestion (Mosele et al., 2015; Nderitu, Dykes, Awika, Minnaar, & Duodu, 2013; Olejnik et al., 2016).

After the gastric digestion step, all anthocyanins detected in the positive ion mode decreased the intensity of their signals. As depicted in Figure 8 and Figure 9, the peaks assigned as compounds **3** and **4** showed a reduction in both species following the gastric digestion. The same trend was observed after the intestinal digestion. In order to quantify these changes, an external calibration curve was prepared using commercial standards of cyanidin-3-glucoside (**3**) and cyanidin-3-rutinoside (**4**). In both species, the quantified anthocyanins decreased their concentration compared to the PEE ($p < 0.05$) (Table 9). In *R. magellanicum*, after gastric digestion, compound **3** decreased by 82.6 % and compound 4 by 80.1 %. In *R. punctatum*, the losses were 73.5 % and 69.4 % for compounds **3** and **4**, respectively. These results are different from those reported in other anthocyanin-rich berries, such as chokeberry (Bermúdez-Soto et al., 2007), blueberry (Correa-Betanzo et al., 2014) and blackberry (Tavares et al., 2012), with high recovery percentages after gastric digestion. These authors attribute the high stability and recovery of anthocyanins to the acidic pH of the gastric solution. However, this low pH condition is related more to the human fasting state rather than the physiological pH of the stomach measured after food intake (Alminger

et al., 2014). The changes of gastric pH after ingestion were taken into account in our dynamic digestion model that contemplates a gradual increase of pH; unlike the above cited reports that can be considered as static *in vitro* studies, with no changes of pH during the gastric digestion (Alminger et al., 2014; Reboul et al., 2006). This might explain the differences in the anthocyanin recovery percentages, where the increase of pH during the gastric digestion favors anthocyanin degradation.

Table 9. Concentrations of main anthocyanins and hydroxycinnamic acids, expressed as mg of anthocyanin or 3-caffeoylquinic acid equivalents, in Chilean *Ribes magellanicum* and *R. punctatum* PEEs, before and after *in vitro* gastric digestion (GD-PEE) and intestinal digestion (ID-PEE), per g of sample.

Samples	Anthocyanins				HCA			
	Cyanidin-3-glucoside	% var.	Cyanidin-3-rutinoside	% var.	3-CQA	% var.	CH-1	% var.
R. magellanicum								
PEE	20.70 ± 0.28^{a}		9.06 ± 0.13^{a}		83.32 ± 0.94^{a}		4.60 ± 0.02^{a}	
GD-PEE	3.61 ± 0.16^{b}	-82.6	1.80 ± 0.09^{b}	-80.1	0.77 ± 0.03^{b}	-99.1	1.45 ± 0.08^{b}	-68.5
ID-PEE	2.08 ± 0.10^{c}	-90.0	1.35 ± 0.05^{c}	-85.1	1.40 ± 0.06^{b}	-98.3	1.58 ± 0.07^{b}	-65.6
R. punctatum								
PEE	12.93 ± 0.40^{d}		3.53 ± 0.11^{d}		83.59 ± 0.35^{d}		6.27 ± 0.35^{d}	
GD-PEE	3.43 ± 0.16^{e}	-73.5	1.08 ± 0.04^{e}	-69.4	0.99 ± 0.05^{e}	-98.8	2.07 ± 0.15^{e}	-66.9
ID-PEE	1.60 ± 0.12^{f}	-87.6	0.65 ± 0.03^{f}	-81.6	1.84 ± 0.08^{f}	-97.8	2.95 ± 0.01^{f}	-53.0

3-CQA-1: 3-caffeoylquinic acid; CH-1: caffeoyl hexoside 1.
Data are expressed as mean values ± SD; n =3; % var.: percentage of variation with respect to the undigested PEE.
Different letters (a-f) in the same column show significant differences among each determination, according to Tukey's test ($p < 0.05$).

In *R. magellanicum*, after intestinal digestion, compound **3** decreased by 90.0 % and compound **4** by 85.1 %. In *R. punctatum*, the losses were 87.6 % and 81.6 % for compounds **3** and **4**, respectively. The content of anthocyanins in *R. nigrum* after intestinal digestion, was reported by Olejnik et al. (2016), showing also an important reduction (54.5–59.6 %).

This drastic decrease in the anthocyanin content could be explained due to their poor stability at pH higher than 4.5. Under these conditions, the flavylium cation structure is lost, leading to the chalcone form at slightly alkaline conditions (pH 7.5) (Nielsen, Haren, Magnussen, Dragsted, & Rasmussen, 2003). However, the degradation products of anthocyanins were not detected by our HPLC-MS/MS^n analyses of the ID-PEEs.

After the gastric digestion phase, the total ion chromatogram detected in the negative ion mode showed a clear decrease in the intensity of the signals of compounds **13**, **40**, **41** and **42** (Figure 8 and Figure 9). On the other hand, the intensity of the minor signals seems to be apparently increased due to a proportional change with respect to the main signals. The UV profiles demonstrated a real increase in the proportion of compounds eluting between 50–60 min. This effect was more evident after the intestinal digestion step (Figure 8 and Figure 9). In order to quantify these changes, an external calibration curve was prepared using a commercial standard of 3-caffeoylquinic acid. Other compounds were not quantified because of the poor chromatographic resolution observed after the digestion process (Figure 8 and Figure 9). In both species, the quantified HCAs, 3-caffeoylquinic acid (3-CQA, **13**) and caffeoyl hexoside 1 (CH-1, **14**), decreased their concentration compared to the PEE after the gastric step ($p < 0.05$; Table 9). In *R. magellanicum*, after gastric digestion, compound **13** decreased by 99.1 % and compound **14** by 68.5 %, respectively. In *R. punctatum*, the losses were 98.8 % and 66.9 % for compounds **13** and **14**, respectively. In *R. magellanicum*, after intestinal digestion, compound **13** decreased by 98.3 % and compound **14** by 65.6 %, but these

changes were not statistically significant (Table 9). In *R. punctatum*, the losses were 97.8 % and 53.0 % for compounds **13** and **14**, respectively. Previous studies reported the low stability of phenolic acids under gastric digestion (Kamiloglu & Capanoglu, 2013). A reduction in the content of HCAs (47.0 %), flavanols (27.0 %) and flavonols (19.8 %) after *in vitro* GID of *R. nigrum* PEE has also been reported (Olejnik et al., 2016). Interestingly, when comparing the content of compound **13** in the GD-PEE with the ID-PEE of both *R. magellanicum* and *R. punctatum*, an increase was observed (Table 9). Nevertheless, this increment was not statistically significant. This effect has been explained by Bermúdez-Soto et al. (2007), due to isomerization reactions among the HCAs under the simulated intestinal conditions.

3.2.3. Changes in total phenolics (TP) and total flavonoid (TF) content before and after simulated digestion process

After *in vitro* gastric digestion the TP content of *R. magellanicum* did not change significantly, whereas in *R. punctatum* it decreased by 13.7 % ($p < 0.05$; Table 10). In both species the TP content decreased by around 50 % after the simulated intestinal digestion ($p < 0.05$). These results are in accordance with data reported for blueberry and blackberry, in which the TP content after gastric digestion were 94 % and 93 % compared to the non-digested samples, respectively (Correa-Betanzo et al., 2014; Tavares et al., 2012). Our results show an apparent high stability of polyphenols in the gastric step, but not after the intestinal stage. However, as depicted in the HPLC-DAD-MS/MS profiles (Figure 8 and Figure 9), several changes can be observed, indicating that the simulated digestion induced chemical transformations in the PEEs (Bermúdez-Soto et al., 2007).

A decrease of 11.6 % in the TF content was observed in both species after gastric digestion. After the simulated intestinal digestion, the TF content of *R. magellanicum* was reduced by 46.2 %, while in *R. punctatum* it decreased by 34.1 % ($p < 0.05$). Bergmann et al. (2009) suggested that the

alkaline pH of the intestinal digestion might explain the decrease in the TP content. Mosele et al. (2015) also reported a decrease of about 60 % in the polyphenol content of pomegranate juice after the duodenal phase. A reduction of about 80 % in the TP and TF content of maqui berry after *in vitro* GID has also been reported (Lucas-Gonzalez et al., 2016).

Table 10. Yields of extraction, total phenolic (TP) and total flavonoid (TF) content and their recovery percentages (% rec.) from Chilean *R. magellanicum* and *R. punctatum* phenolic-enriched extracts (PEE), before and after *in vitro* gastric (GD-PEE) and intestinal digestion (ID-PEE).

Samples	% MeOH	% PEE	TP (g GAE/100 g extract)	% rec.	TF (g CE/100 g extract)	% rec.
R. magellanicum						
PEE	9.8	3.1	39.2 ± 0.3^{a}		17.3 ± 0.2^{a}	
GD-PEE			39.5 ± 0.1^{a}	101.0	15.2 ± 0.3^{b}	87.9
ID-PEE			18.7 ± 0.1^{b}	47.8	9.3 ± 0.0^{c}	53.8
R. punctatum						
PEE	25.0	2.9	47.5 ± 0.9^{c}		21.4 ± 0.2^{d}	
GD-PEE			41.0 ± 0.5^{d}	86.3	19.0 ± 0.2^{e}	88.8
ID-PEE			20.3 ± 0.2^{e}	42.7	14.1 ± 0.3^{f}	65.9

% rec.: percentage of recovery with respect to the undigested PEE.
Different letters (a-f) in the same column show significant differences among each determination, according to Tukey's test ($p < 0.05$).

3.2.4. Changes in antioxidant activity after simulated digestion process

Different chemical-based methodologies have been developed to determine the antioxidant capacity of fruits and food plants. These assays are based on different strategies providing different information about the interaction between radicals and samples.

A review of the chemical aspects of antioxidant assays pointed out that for a correct evaluation of the antioxidant properties of natural products, a single *in vitro* chemical method is not enough and should be complemented with other strategies (López-Alarcón & Denicola, 2013). In the present work, we evaluated the antioxidant activity of the samples using six different *in vitro* assays, addressing the two main mechanisms involved in the neutralization of free radicals by antioxidants; hydrogen atom transfer reaction (HAT) and single electron transfer reaction (SET). Different radicals/ions were tested due to the dominating mechanism depends on the chemical species involved in the raction (Prior, Wu, & Schaich, 2005). The antioxidant activity is tightly associated with the polyphenol content and composition; in line with the trend observed for the antioxidant effect of *R. magellanicum* and *R. punctatum* PEEs submitted to *in vitro* GID (Table 11).

DPPH, FRAP, TEAC, CUPRAC, and superoxide anion scavenging assays showed a loss of the antioxidant activity throughout the simulated GID ($p < 0.05$) for *R. magellanicum* (Table 11). A similar trend was observed in the samples of *R. punctatum* with the exception of FRAP and the superoxide anion scavenging assays. In these determinations, the antioxidant activity increased slightly but significantly after the gastric digestion phase ($p < 0.05$, Table 11). Lucas-Gonzalez et al., (2016) working with Chilean maqui berry reported that the simulated GID significantly affected the antioxidant capacities of the extracts, with higher or lower values depending on the assay. In the FRAP assay with the digested and non-digested PEEs from *R. punctatum*, our results are in agreement with those obtained by Lucas-Gonzalez et al. (2016) and Gullon et al. (2015). These

authors observed an increase of the antioxidant activity after the gastric step. Regarding the TEAC assay, Olejnik et al. (2016) reported a decrease in the antioxidant capacity after simulated GID in *R. nigrum*, in line with our results.

Regarding ORAC, the results are summarized in Table 11. The undigested PEE of *R. magellanicum* and *R. punctatum* showed ORAC values of 22.09 and 17.01 μmol TE/g fresh fruit, respectively (data were converted for comparison purposes); in line with the reported for *Ribes spp*. fruits, whose ORAC values rank from 17 to 116 μmol TE/g fresh fruit (Moyer, Hummer, Finn, Frei, & Wrolstad, 2002). The ORAC values significantly increased ($p < 0.05$) throughout the *in vitro* GID of Chilean currants (Table 11). The highest activity was observed at the gastric step. At the intestinal phase, occurred a significant decrease ($p < 0.05$) with respect to the gastric level; still, the ORAC values in the ID-PEEs remained significantly higher ($p < 0.05$) than the non-digested PEEs. A similar trend was observed for winemaking (seeds and stem) byproducts extracts (Jara-Palacios, Gonçalves, Hernanz, & Heredia, 2018) as well as for black beans extracts (Soriano Sancho, Pavan, & Pastore, 2015); which reported a marked increased in the ORAC values throughout *in vitro* GID. These authors also informed a diminution in the DPPH (Jara-Palacios et al., 2018) and ABTS radical scavenging capacity (Soriano Sancho et al., 2015) during the *in vitro* GID process, in agreement with our results. For gooseberries (*Ribes uva-crispa*), the ORAC values were not affected by the *in vitro* digestion, in any of the two tested varieties; however, the authors also reported a lack of correlation of ORAC with the other antioxidant assays (Chiang, Kadouh, & Zhou, 2013). Tabart, Kevers, Pincemail, Defraigne, & Dommes (2009) evaluated several pure phenolic compounds through differents antioxidant *in vitro* methods. They reported a good correlation among the data obtained by DPPH, TEAC, and superoxide anion scavenging capacity assays; however, ORAC data showed a poor correlation with the mentioned assays, in agreement with our results. The ORAC method considers the complete reaction of the antioxidants with a free radical,

unlike the other mentioned assays, explaining the observed differences among methods (Tabart et al., 2009). In *Ribes* samples, ORAC increased after gastric digestion, possibly due to the relative stability of the flavonoids in both species. Flavonoids (different from anthocyanins) are less affected by the digestion conditions than other polyphenols, increasing their relative proportion after *in vitro* GID (Jara-Palacios et al., 2018; Tagliazucchi, Verzelloni, Bertolini, & Conte, 2010).

Table 11. Antioxidant activity of Chilean *R. magellanicum* and *R. punctatum* PEEs, before and after *in vitro* gastric (GD-PEE) and intestinal digestion (ID-PEE).

Samples	DPPH SC_{50} (µg extract/mL)	$O_2^{\bullet}$ scavenging SC_{50} (µg/mL)	FRAP (mmol TE/g extract)	TEAC (µmol TE/g extract)	CUPRAC (mmol TE/g extract)	ORAC (µmol TE/g extract)
R. magellanicum						
PEE	6.32 ± 0.11^{a}	3.07 ± 0.09^{a}	7.69 ± 0.05^{a}	4610.36 ± 35.71^{a}	6.16 ± 0.20^{a}	2008.37 ± 186.13^{a}
GD-PEE	8.85 ± 0.18^{b}	5.56 ± 0.30^{b}	2.16 ± 0.06^{b}	2706.24 ± 20.72^{b}	3.49 ± 0.08^{b}	5387.17 ± 219.85^{b}
ID-PEE	10.88 ± 0.18^{c}	13.27 ± 0.45^{c}	1.51 ± 0.01^{c}	2214.77 ± 16.95^{c}	2.53 ± 0.04^{c}	4113.74 ± 110.20^{c}
R. punctatum						
PEE	3.38 ± 0.10^{d}	3.63 ± 0.15^{d}	5.38 ± 0.06^{d}	4881.24 ± 86.63^{d}	6.62 ± 0.18^{d}	1418.02 ± 40.43^{d}
GD-PEE	6.50 ± 0.15^{e}	2.96 ± 0.09^{e}	5.58 ± 0.09^{e}	3562.14 ± 27.33^{e}	4.79 ± 0.13^{e}	6212.21 ± 228.28^{e}
ID-PEE	10.36 ± 0.19^{f}	4.43 ± 0.24^{f}	2.00 ± 0.02^{f}	2256.87 ± 19.23^{f}	3.15 ± 0.08^{f}	4584.55 ± 244.65^{c}
Catechin*	11.41 ± 1.60	8.67 ± 0.10	5.40 ± 0.09	n.d.	13.42 ± 0.33	n.d.

*reference compound. Data are expressed as means ± SD, n = 3.

TE: Trolox equivalents; MeOH: methanol extract; PEE: phenolic enriched extract; GAE: gallic acid equivalents; CE: catechin equivalents; n. d.: not determined.

Different letters (a-f) in the same column show significant differences among each determination, according to Tukey's test ($p < 0.05$).

3.2.5. Inhibition of metabolic syndrome-associated enzymes before and after the simulated digestion process

The non-digested PEEs from *R. magellanicum* and *R. punctatum* were able to inhibit α-amylase with IC_{50} values of 21.7 and 20.1 µg PEE/mL, respectively. However, the inhibitory activity was lost after the simulated GID (Table 12). Digested and nondigested PEEs of *R. magellanicum* were inactive towards lipase. On the other hand, the PEE from *R. punctatum* was able to inhibit lipase with an IC_{50} value of 41.0 µg PEE/mL, but this activity was lost after GID. In other studies, the inhibitory activity of the PEEs was maintained after *in vitro* digestion, although with lower values. The activity of a PEE obtained from the pulp from an Argentinean *Solanum betaceum* sample towards α-amylase and lipase decreased after simulated GID by 50.0 % and 8.5 %, respectively (Orqueda et al., 2017). In another study with chickpeas, the inhibitory activity towards α-amylase and lipase was evaluated before and after simulated digestion. The inhibition diminished by 15.2 % for α-amylase and 7.2 % for lipase after the digestion process (Ercan & El, 2016).

The PEE, GD-PEE and ID-PEE from *R. magellanicum* and *R. punctatum* inhibited α-glucosidase (Table 12). Interestingly, after the gastric digestion phase the IC_{50} values showed an increase, indicating a loss of inhibitory activity in both species. However, after the *in vitro* intestinal digestion, this activity was significantly recovered by 37.5 % ($p < 0.05$). Orqueda et al. (2017) found that at the end of the GID, the inhibitory activity of *S. betaceum* towards α-glucosidase was lost by 58.2 %. A reduction of 7.2 % in the inhibitory effect against this enzyme was reported after the digestion process of a chickpea sample (Ercan & El, 2016). On the other hand, Li et al. (2015) described that the inhibitory activity of *Choerospondias axillaris* towards α-glucosidase remained almost unchanged during simulated GID. Overall, our results are in accordance with those reported

in the literature. The GID process seems to affect the inhibitory effects of polyphenols towards these metabolic syndrome-associated enzymes.

Table 12. Effect of Chilean *R. magellanicum* and *R. punctatum* PEEs, before and after *in vitro* gastric digestion (GD-PEE) and intestinal digestion (ID-PEE) towards metabolic syndrome-associated enzymes.

Samples	α-amylase (IC_{50}, µg/mL)	α-glucosidase (IC_{50}, µg/mL)	Lipase (IC_{50}, µg/mL)
R. magellanicum			
PEE	21.65 ± 0.54	0.38 ± 0.00[a]	> 100
GD-PEE	> 100	1.36 ± 0.02[b]	> 100
ID-PEE	> 100	0.85 ± 0.02[c]	> 100
R. punctatum			
PEE	20.07 ± 1.72	0.31 ± 0.01[d]	41.0 ± 1.2
GD-PEE	> 100	1.92 ± 0.19[e]	> 100
ID-PEE	> 100	1.54 ± 0.05[f]	> 100
Acarbose*	28.48 ± 0.29	120.86 ± 1.99	
Orlistat*	-	-	0.04 ± 0.01

*reference compounds; Data are expressed as means ± SD, n = 3-6. Different letters (a-f) in the same column show significant differences among each determination, according to Tukey's test ($p < 0.05$).

3.2.6. Cytoprotective effect of Chilean currants PEEs against oxidative and dicarbonyl stress

In this experiment, the AGS cells were chosen as a model to emulate the gastric epithelium, based on two main reasons: their response to oxidative stress seems to be comparable to non-tumor cells response, and the gastric epithelium exposure to polyphenols before absorption under physiological conditions (Cheli & Baldi, 2011; Theoduloz et al., 2018). None of the extracts showed cytotoxicity towards AGS cells among 0 and 125 μg/mL. Based on the mentioned, we set the treatments at 62.50 and 31.25 μg/mL for the cytoprotection assays. Hydrogen peroxide (H_2O_2) and methylglyoxal (MGO) induced a significant decline ($p < 0.05$) in the viability of the AGS cells, which decreased by 24 % and 27 %, respectively, and were considered as damage controls for further comparisons (Figure 10 and Figure 11). The most abundant compound in the PEEs was 3-CQA, thus it was assessed as a reference compound. No significant differences ($p < 0.05$) were observed among the cells previously treated with 3-CQA (65 μg/mL) and the H_2O_2 or MGO controls. The cells pre-treated with the PEE and GD-PEE of *R. magellanicum* attenuated significantly ($p < 0.05$) the damage occasioned by the two stressors at 62.50 and 31.25 μg/mL compared to the damaged controls (Figure 10). Cells treated with the two doses of ID-PEE showed a significantly ($p < 0.05$) higher viability compared to the MGO control, however, no protective effect was observed against H_2O_2 (Figure 10). Regarding *R. punctatum*, the cells pre-treated with the PEE and GD-PEE showed higher viability ($p < 0.05$) than both damaged controls at all tested doses; suggesting a protective effect against the harm induced by H_2O_2 and MGO (Figure 11). The ID-PEE of *R. punctatum* did not induce significant ($p < 0.05$) changes among the pre-treated cells and the damage controls (Figure 11). The cytoprotection of AGS cells against the stress induced by H_2O_2 and MGO was described for the PEEs and fractions of *R. magellanicum* and *R. punctatum* from different collection places, in agreement with our results (Jiménez-Aspee et al., 2016b; 2016c). Only the ID-PEE of *R.*

magellanicum was able to protect AGS cells against MGO; this might be due to its higher anthocyanin content relative to *R. punctatum* ID-PEE. In addition, Jiménez-Aspee et al. (2016c) informed that the anthocyanin fraction of *R. magellanicum* may induce protective mechanisms in AGS cells against MGO induced stress.

Polyphenols may exert antioxidant effects thorugh direct interaction with ROS and also indirectly by the induction of endogenous protective mechanisms (Jiménez-Aspee et al., 2016a). Our experimental conditions involved a pre-incubation overnight and aspiration of the extracts before the addition of stressor agents in order to measure only the ability to induce cell protective mechanisms. In general, the PEEs of both currants induced higher cytoprotection than the digested fractions, in line with the observed loss of phenolic compounds throughout the simulated digestion process. Theoduloz et al. (2018) reported that the detoxifying enzymes superoxide dismutase (SOD), catalase (CAT), glutathione peroxidase (GSH-Px), and glutathione reductase (GSH-R) may be increased after pre-treatment with *R. magellanicum* and *R. punctatum* PEEs; whose activity seem to be related to the anthocyanins content in *R. magellanicum* and to the co-pigments in *R. punctatum*. The induction of intracellular protective mechanisms was also reported for *Ribes nigrum* (blackcurrant), whose extracts enhanced the activity of endogenous antioxidant enzymes, such as SOD, CAT, and GSH-Px in fibroblasts from lung tissue (MRC-5 cells) (Jia, Li, Diao, & Kong, 2014). Both stressor agents considered in this experiment are potentially harmful under physiological conditions. Hydrogen peroxide may lead to the generation of highly reactive species via Fenton's and Haber–Weiss reactions, including hydroxyl radical and superoxide radical (Losada-Barreiro & Bravo-Díaz, 2017; Valko et al., 2007). While, the MGO is a very reactive dicarbonyl compound, produced as a consequence of the glycolysis process and it is an important precursor of advanced glycation end-products (AGEs), which are associated with pathologies such as aging, neurodegenerative diseases, and diabetes (Allaman, Bélanger, & Magistretti, 2015). Thus,

our results suggest that polyphenols from *R. magellanicum* and *R. punctatum* may be able to exert a protective role on the gastric epithelium, most likely through the increase of detoxifying enzymes (Theoduloz et al., 2018). Although this effect is influenced by the digestion conditions, the activity seems to be maintained for both species during the gastric step and partially maintained under intestinal conditions for *R. magellanicum.*

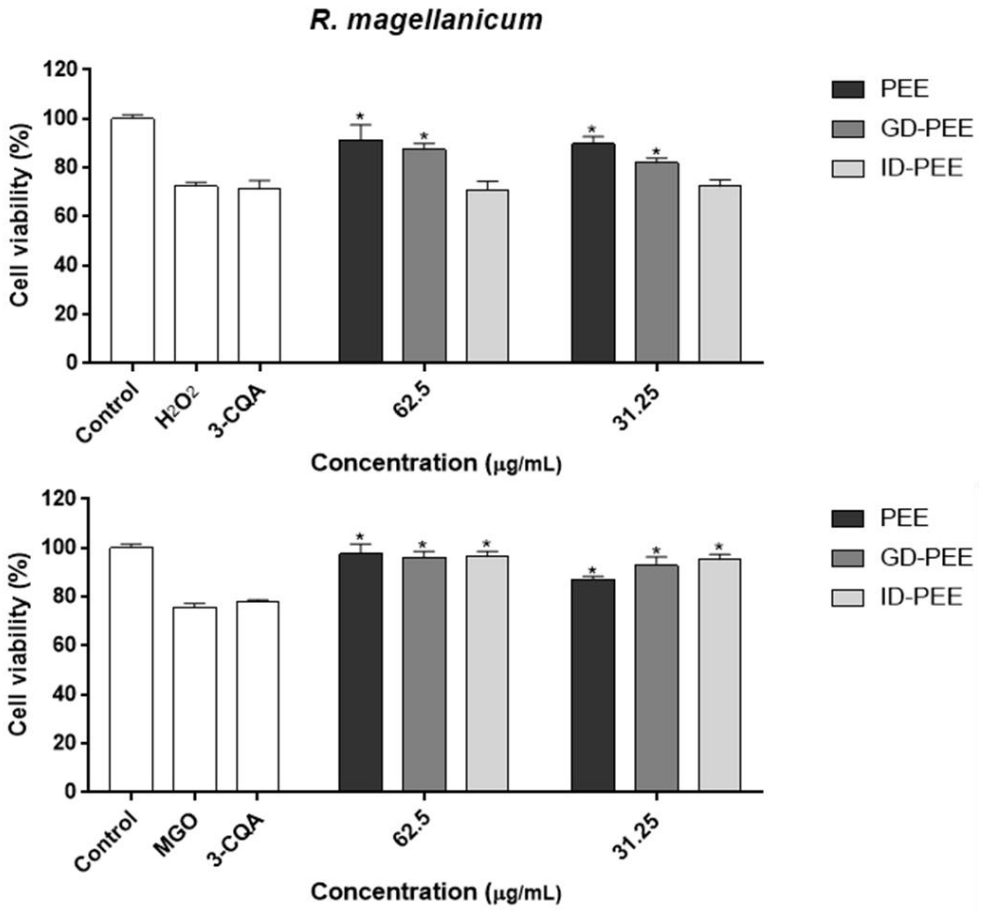

Figure 10. Protective effect of *Ribes magellanicum* PEEs, throughout *in vitro* digestion, on human AGS cells against the stress induced by H_2O_2 and MGO, respectively. Results are expressed as means ± SD (n = 5).

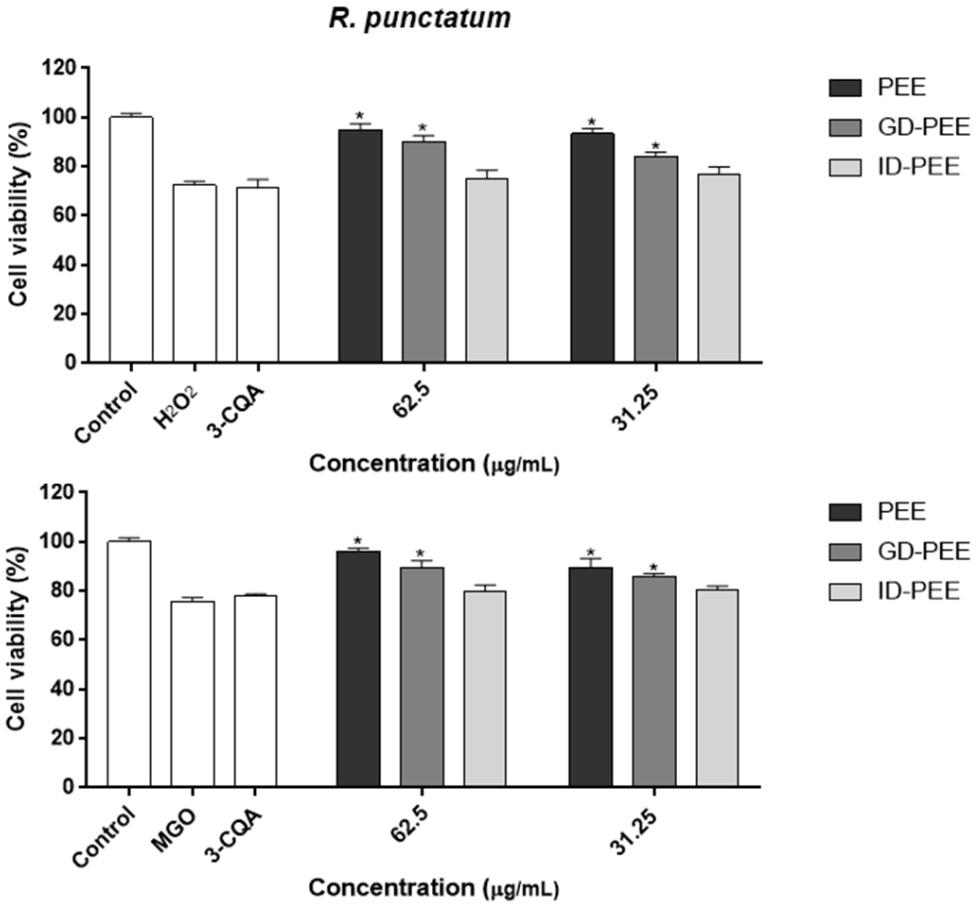

Figure 11. Protective effect of *Ribes punctatum* PEEs, before and after *in vitro* digestion, on human AGS cells against stress induced by H_2O_2 and MGO. Results are expressed as means ± SD (n = 5).

3.2.7. Statistical correlations

The Pearson's coefficient indicated significant correlations ($p < 0.05$) between the phenolic content of the two *Ribes* species and the antioxidant activity after the *in vitro* digestion (Table 13). The activity showed a better correlation with TF, suggesting that this phenolic group is a major contributor to the antioxidant activity of these fruits. On the other hand, an inverse correlation ($p < 0.05$) was observed among the HCA content and the ORAC values (Table 13). The HCA reduction after GID led to an increased relative proportion of flavonoids in the samples, possibly explaining the observed correlation. Flavonoids, especially flavan-3-ols usually show a high contribution to the ORAC values (Tabart et al., 2009). Overall, these results confirm that the modifications in the polyphenol content and composition resulting from the GID process lead to a deleterious effect in the antioxidant capacity of the studied samples. This finding is in agreement with previous reports, showing a loss of the antioxidant activity due to the reduction in the total phenolic content.

Huang, Sun, Lou, Li, & Ye (2014) showed correlations between the total phenolic and total anthocyanin content with the loss of antioxidant activity in Chinese bayberry fruits, determined by the FRAP, ABTS, DPPH and ORAC assays, after simulated GID. In a similar way, the decrease in the total phenolic and total flavonoid content was statistically correlated with the reduction of antioxidant activity in maqui berries following the *in vitro* oral, gastric and intestinal digestion steps (Lucas-Gonzalez et al., 2016).

Table 13. Pearson's correlation coefficient values among the content of the main phenolic groups occurring in Chilean currants and the antioxidant activity.

Antioxidant assay	*R. magellanicum*			*R. punctatum*		
	TP	TF	HCA	TP	TF	HCA
Cytoprotection H_2O_2	0.909**	0.914**	0.535	0.955**	0.953**	0.693*
Cytoprotection MGO	0.034	0.063	0.235	0.938**	0.933**	0.762*
DPPH	-0.817**	-0.929**	-0.895**	-0.977**	-0.986**	-0.821**
FRAP	0.576	0.756*	0.994**	0.952**	0.928**	0.441
CUPRAC	0.697*	0.851**	0.962**	0.948**	0.967**	0.871**
TEAC	0.649	0.813**	0.979**	0.963**	0.977**	0.858**
Superoxide anion	-0.967**	-0.997**	-0.683*	-0.750*	-0.691*	-0.064
ORAC	-0.127	-0.362	-0.926**	-0.422	-0.484	-0.946**

Abbreviations: TP: Total phenolics; TF: total flavonoids; HCA: hydroxycinnamic acids (sum of quantified HCAs; CH-1 and 3-CQA); *: $p < 0.05$; **: $p < 0.01$.

Chapter 4

Colonic fermentation of polyphenols from Chilean currants (*Ribes spp.*) and its effect on antioxidant capacity and metabolic syndrome-associated enzymes

The enumeration of the compounds identified in this chapter is independent of the employed for other chapters of this work. The results presented in Chapter 4 were published in Food Chemistry. Burgos-Edwards, A., Jiménez-Aspee, F., Theoduloz, C. & Schmeda-Hirschmann, G. (2018). Colonic fermentation of polyphenols from Chilean currants (*Ribes* spp.) and its effect on antioxidant capacity and metabolic syndrome-associated enzymes. *Food Chemistry*, 258, 144-155.

4.1. Introduction

Colonic microbiota is responsible for the biotransformation of polyphenolic structures into low-molecular-weight phenolic metabolites that may be associated with the health beneficial properties of polyphenol-rich foods, rather than the parent compounds (Cardona, Andrés-Lacueva, Tulipani, Tinahones, & Queipo-Ortuño, 2013). The interaction between food polyphenols and gut microbiota is reciprocal, with biotransformations of the precursor compounds by the microbes, as well as the modulation of the microbiota by the polyphenols and their metabolites (Ozdal et al., 2016). In a broad sense, the main reactions involved in microbial transformation of polyphenols in the gut include hydrolysis, ring cleavage and reductions (Espín et al., 2017). Studies with single groups of food polyphenols allowed to disclose the sequences in microbial transformation and the identity of the resulting metabolites of: anthocyanins (Aura et al., 2005), caffeic acid and its esters (Gonthier et al., 2006), chlorogenic acid (Ludwig, de Peña, Concepción, & Alan, 2013; Tomas-Barberan et al.,

2014) and flavonoids (Labib, Hummel, Richling, Humpf, & Schreier, 2006; Rechner et al., 2004), among others. Reports on the stability of polyphenols showed relevant changes in their profiles generated by colonic microbiota, as shown for cranberry and grape seed polyphenols (Sánchez-Patán et al., 2015), wild blueberry (Correa-Betanzo et al., 2014), cardoon (Juániz et al., 2017), black tea and red wine (Gross et al., 2010), mate tea (Gómez-Juaristi, Martínez-López, Sarria, Bravo, & Mateos, 2018) and cupuassu fruit (Barros, García-Villalba, Tomás-Barberán, & Genovese, 2016), among others.

Several dietary intervention studies suggest that the consumption of polyphenol-rich foods have a protective effect towards chronic noncommunicable diseases, including type-2 diabetes, cardiovascular diseases and certain types of cancer (Del Rio, Borges, & Crozier, 2010). However, polyphenols from diet undergo extensive structural modifications throughout the gastrointestinal tract. Before the excretion, a considerable amount of polyphenols reaches the colon, where they are accumulated. The colonic bacterial populations generate catabolites from the parent compounds, which can be absorbed and enter into enterohepatic circulation. In fact, the gut microbiota-derived metabolites were found in plasma and tissues at higher concentrations than the precursors (Espín et al., 2017). Therefore, the characterization of the metabolites produced by colonic bacteria is relevant for fully understand the scope of health benefits of polyphenols.

Currants (*Ribes spp*.) are a group of berries appreciated by their pleasant flavor and high polyphenol content (Gopalan et al., 2012). In Chile they are known as “zarzaparrilla” and are consumed fresh or processed in jams or syrups (Arena & Coronel, 2011). The currants *Ribes magellanicum* and *Ribes punctatum* are the most abundant wild species in Chile (Bañados et al., 2002). Several polyphenols have been described in both species, as well as their antioxidant capacity and cytoprotective effect towards oxidative and dicarbonyl-induced stress in human gastric AGS cells (Jiménez-Aspee et al., 2016b; 2016c). In addition, the polyphenols from these *Ribes* species inhibit α-glucosidase before

and after *in vitro* gastrointestinal digestion, suggesting a potential role preventing postprandial hyperglycemia (Burgos-Edwards, Jiménez-Aspee, Thomas-Valdés, Schmeda-Hirschmann, & Theoduloz, 2017).

Several changes have been described in the polyphenolic profile of Chilean berries after simulated gastrointestinal digestion (Burgos-Edwards et al., 2017; Lucas-Gonzalez et al., 2016; Thomas-Valdés et al., 2018). However, there is no information on the effect of colonic fermentation on the polyphenols from these fruits. Taking into account the above mentioned information, we hypothesize that colonic fermentation of polyphenols from *R. magellanicum* and *R. punctatum* will undergo relevant changes in their content, composition and bioactivity. The aim of this study was to assess the changes in the phenolic profile of *R. magellanicum* and *R. puctatum* under simulated colonic fermentation and their implication in the antioxidant capacity as well as the inhibition of metabolic syndrome-associated enzymes.

4.2. Results and discussion

The PEE from the native Chilean currants *R. magellanicum* and *R. punctatum* were investigated for changes in chemical content, composition and bioactivity, as a consequence of *in vitro* colonic fermentation. The w/w percent yield of the PEE from 100 g of fresh fruits was 1.1 % and 1.2 % for *R. magellanicum* and *R. punctatum* respectively.

4.2.1. Chemical characterization of native phenolics in the PEE and their metabolites after *in vitro* colonic fermentation

A comparison of the PEEs phenolic profiles was carried out including the starting PEEs (t = 0 h) and samples taken at different incubation times (t = 8 and t = 24 h). The polyphenols occurring in PEEs and the metabolites originated from the colonic fermentation were tentatively identified by

HPLC-DAD-MS/MS^{n}. The compounds were identified by interpretation of the MS and UV data, comparison with literature and reference compounds when available. A blank was used for comparison with the fermented samples, to discard polyphenols from sources other than PEEs and/or bacterial metabolism. The results are summarized in Table 14. The HPLC chromatograms showing the compounds identified in *R. magellanicum* and *R. punctatum* samples during fermentation are shown in Figure 12 and Figure 13, respectively.

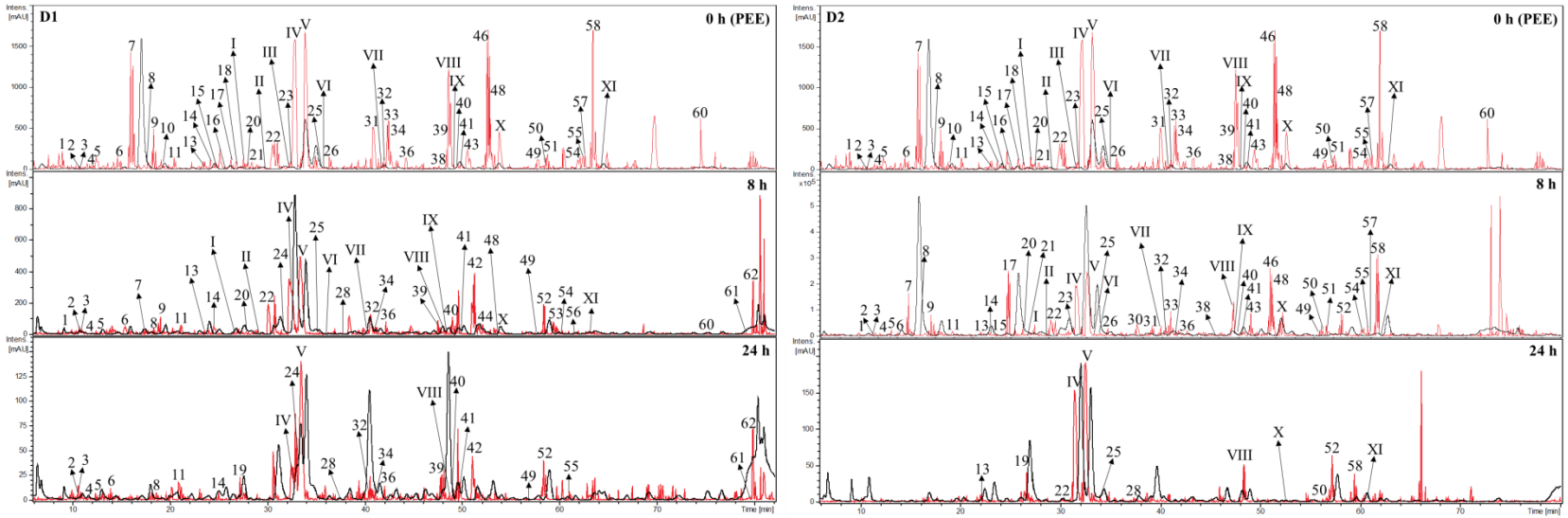

Figure 12. HPLC-DAD chromatograms at 280 nm (black) and total ion chromatograms in the negative ionization mode (red) of *Ribes magellanicum* after colonic fermentation with donor 1 (D1) and donor 2 (D2) samples, at time-points 0h, 8h and 24h.

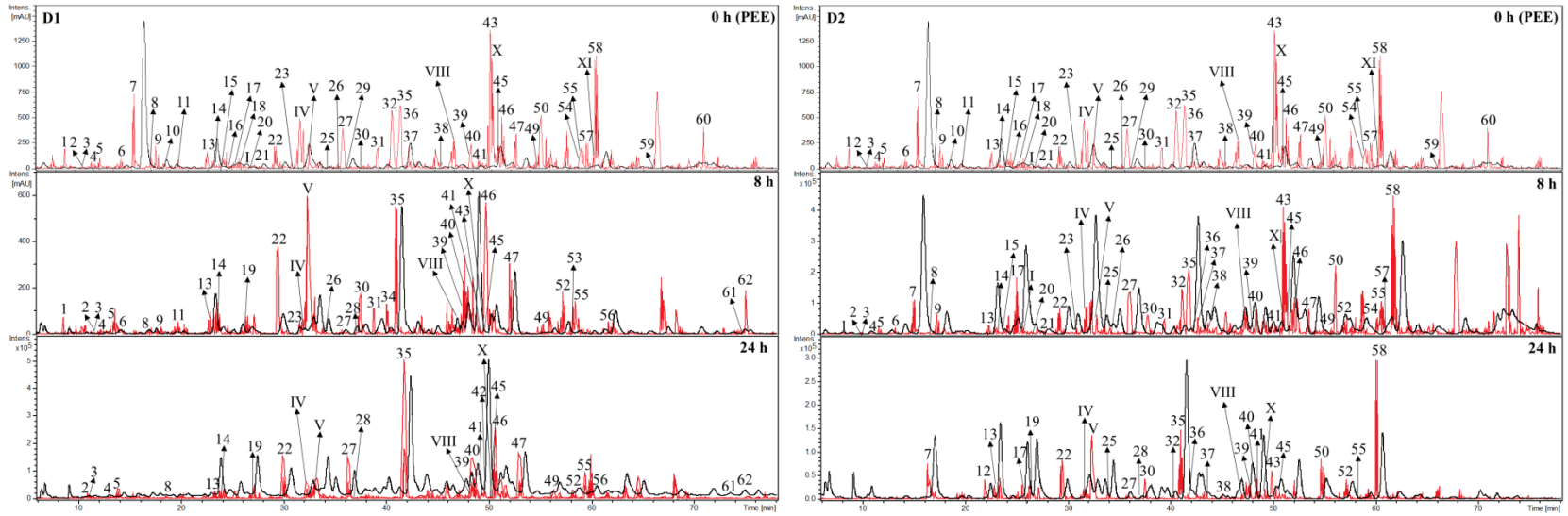

Figure 13. HPLC-DAD chromatograms at 280 nm (black) and total ion chromatograms in the negative ionization mode (red) of *Ribes punctatum* after colonic fermentation with donor 1 (D1) and donor 2 (D2) samples, at time-points 0h, 8h and 24h.

4.2.1.1. Anthocyanins

The HPLC-ESI-MS/MS analyses in the positive ion mode allowed the tentative identification of 11 anthocyanins in the PEEs, listed with roman numerals in Table 14. The compounds **III**-**VIII** and **XI** showed an intense fragment ion at *m/z* 287 amu, indicating a cyanidin core. The compound **III**, showing neutral losses of rhamnose (146 amu) and hexosylpentose (294 amu) was assigned as cyanidin rhamosyl hexoside pentoside. The compounds **IV** and **V** presented the neutral loss of one hexose (162 amu) and a rutinose unit (308 amu), being assigned as cyanidin hexoside and cyanidin rutinoside, respectively. The identity of both compounds was confirmed by comparison with commercial standards of cyanidin-3-O-glucoside and cyanidin-3-O-rutinoside. The compound **VI** was tentatively identified as cyanidin acetylpentoside hexoside, based on the acetylpentoside (174 amu) and hexose (162 amu) neutral loss. Compounds **VII** and **VIII** have a common neutral loss of hexoside formate (190 amu), with an additional rhamnose (146 amu) loss in compound **VII**. The anthocyanins were tentatively identified as cyanidin rhamnosyl hexoside formate and cyanidin hexoside formate, respectively. The compound **XI** showed neutral loss of malonylhexose (248 amu) and was assigned as cyanidin malonylhexoside. The compounds **I**, **II** and **X** presented a MS/MS base peak at *m/z* 303 amu, in agreement with delphinidin. The neutral loss of hexose (162 amu), rutinose (308 amu) and malonyl hexose (248 amu) allowed the tentative identification of the compounds as delphinidin hexoside (**I**), delphinidin rutinoside (**II**) and delphinidin malonyl hexoside (**X**), respectively. The compound **IX** showed a MS^2 base peak at *m/z* 331 amu, in agreement with malvidin. The characteristic losses of rhamnose (146 amu) and C-glycosidic hexose (156 amu) allow the tentative identification as malvidin-C-hexoside rhamnoside, in agreement with literature (Vukics & Guttman, 2010). Anthocyanins **III** and **VI** were found for the first time in *R. magellanicum*, and **X** and **XI** in *R. punctatum*.

4.2.1.2. Flavan-3-ol derivatives

Nine flavan-3-ol derivatives were detected (Table 14). The compounds **1**, **2** and **5** show a common pseudomolecular ion at *m/z* 609 amu, with a neutral loss of 168 amu leading to the base peak ion at *m/z* 441 amu, in agreement with an (*epi*)-gallocatechin unit as well as an ion at *m/z* 305, suggesting an additional (*epi*)-gallocatechin unit. Compounds **1**, **2** and **5** were assigned as isomeric (*epi*)-gallocatechin-(*epi*)-gallocatechin dimers (Lin et al., 2014). Peaks **3**, **4** and **6** showed a parent ion at *m/z* 593 amu. In compounds **3** and **6**, the fragment ion at *m/z* 289 amu was detected, compatible with (*epi*)-catechin. The neutral loss of 168 amu suggests an additional (*epi*)-gallocatechin unit. The compound **4** showed a neutral loss of the A-ring in the (*epi*)-catechin unit (126 amu), leading to the fragment ion at *m/z* 467 amu. The ion at *m/z* 305 amu indicates an additional (*epi*)-gallocatechin unit (Lin et al., 2014). Thus, compounds **3**, **4** and **6** were tentatively identified as isomeric (*epi*)-catechin-(*epi*)-gallocatechin dimers. The compound **8** showed a MS^2 base peak at *m/z* 289 amu, in agreement with (*epi*)-catechin. The neutral loss of 152 amu, suggest a retro Diels-Alder fission of a second catechin unit (Lin et al., 2014), allowing its assignation as an (*epi*)-catechin dimer. Compounds **11** and **14** presented molecular ions at *m/z* 305 and 289, respectively, suggesting flavan-3-ol monomers. Compound **11** presented MS^2 ions at *m/z* 261, 221 and 179, compatible with (*epi*)-gallocatechin, while compound **14** showed MS^2 ions at m/z 245 and 205, in agreement with (+)-catechin (Lin et al., 2014). Identity of compound **11** was confirmed by comparison with (+)-catechin standard. Thus, compound **11** and **14** were assigned as (+)-catechin and (*epi*)-gallocatechin, respectively.

4.2.1.3. Hydroxycinnamic acids

Hydroxycinnamic acids (HCAs) were tentatively identified following the hierarchical scheme proposed by Clifford et al. (2003). The compounds **7**, **17** and **18** showed the same pseudomolecular

ion at *m/z* 353 with product ions at *m/z* 191, 179 and/or 173, assigned as 3-, 4-, and 5-caffeoylquinic acid, respectively. The identity of 3-caffeoylquinic acid was confirmed by comparison with a standard. The compound **44** was assigned as dicaffeoylquinic acid, based on the neutral loss of a caffeoyl moiety (162 amu), leading to intense MS^2 fragments at *m/z* 353 and 173 amu, in agreement with caffeoylquinic acid (Clifford et al., 2003).

The compounds **13**, **25** and **29** showed a pseudomolecular ion at *m/z* 337 amu with fragment ions at *m/z* 191, 163 and/or 173, compatible with coumaroylquinic acids, assigned as 3-, 4- and 5-coumaroylquinic acid, respectively (Clifford et al., 2003). The compounds **20**, **22** and **30** showed $[M-H]^-$ ion at *m/z* 367 amu, with a neutral loss of quinic acid (174 amu), leading to a product ion at *m/z* 193, in agreement with feruloylquinic acid. Following the hierarchical scheme of Clifford et al. (2003), compound **20** was identified as 3-feruloylquinic acid, while compounds **22** and **30** were assigned as feruloylquinic acid 2 and 3, respectively. HCAs hexosides were also detected. The compounds **9**, **15**, **23** and **26** showed the $[M-H]^-$ ion at *m/z* 341 with a neutral loss of hexose (162 amu), yielding an intense fragment ion at *m/z* 179, compatible with caffeic acid. Therefore, compounds **9**, **15**, **23** and **26** were tentatively identified as caffeoyl hexoside 1, 2, 3 and 4, respectively. The compound **31** was assigned as a caffeoyl derivative due to its UV profile and the MS^2 fragment ion at *m/z* 179, compatible with caffeic acid. Compounds **10** and **16** showed a molecular ion at *m/z* 325, with a neutral loss of hexose (162 amu), leading to a base peak at *m/z* 163, in agreement with coumaric acid, assigned as coumaroyl hexosides 1 and 2, respectively. Both compounds are reported for the first time in these species. The compound **21** was assigned as sinapoyl hexoside, due to the neutral loss of hexose (162 amu) leading to the product ion at *m/z* 223, compatible with sinapic acid.

4.2.1.4. Flavonoids

Most phenolic occurring in the PEEs of the studied *Ribes* species are flavonoids (Table 14). Six quercetin derivatives (compounds **32**, **33**, **40**, **46**, **50** and **55**) were assigned on the basis of the MS/MS fragment at *m/z* 301 and they differ in the number and identity of the sugar moieties. The observed neutral losses of 324 amu (dihexoside), 308 amu (rutinose), 162 amu (hexose), 204 amu (acetylhexose) and 146 amu (rhamnose) allowed the assignments of compound **32** as quercetin dihexoside, **33** and **40** as quercetin hexoside rhamnoside and quercetin-3-rutinoside, respectively, **46** as quercetin-3-glucoside, **50** as quercetin acetylhexoside, and **55** as quercetin rhamnoside. The identities of compounds **40** and **46** were confirmed by comparison with standards. Four compounds were tentatively identified as myricetin derivatives due to the MS^2 base peak at *m/z* 317 and UV profiles. Myricetin rutinoside (**34**), myricetin hexoside (**36**), myricetin acetylhexoside (**38**) and myricetin rhamnoside (**39**) were assigned according with the observed neutral losses of rutinose, hexose, acetylhexose and rhamnose, respectively. Five kaempferol derivatives were identified, based on the MS^2 ion at *m/z* 285 amu and their UV profiles. The compound **48** showed two successive losses of 162 amu and was assigned as kaempferol dihexoside. The compound **49** was tentatively identified as kaempferol rutinoside by the neutral loss of rutinose; while compound **54** showing the neutral loss of a hexose was identified as kaempferol-3-glucoside. The identity of compound **54** was confirmed by comparison with a commercial standard. Compound **58** and **60** showed the neutral loss of acetylhexose and rhamnose and were assigned as kaempferol acetylhexoside and kaempferol rhamnoside, respectively. Compounds **51** and **59** were in agreement with isorhamnetin derivatives, due to the observed MS/MS base peak at *m/z* 315. The neutral loss of an hexose and a rhamnose allowed their tentative identification as isorhamnetin hexoside (**51**) and isorhamnetin rhamnoside (**59**), respectively.

Three flavones were tentatively identified, based on their MS and UV profiles. The compound **41** showed a $[M-H]^-$ ion at *m/z* 431 and a fragment ion at *m/z* 311 after a neutral loss of 120 amu and was assigned as (iso)-vitexin (apigenin-C-hexoside) (Vukics & Guttman, 2010). The UV profile and the MS/MS product ions at *m/z* 285 and 241 of compound **43** were compatible with a luteolin derivative. The neutral loss of a hexose allowed identification of **43** as luteolin hexoside. Compounds **41** and **43** are reported for the first time in these species. The compound **57**, with a MS/MS base peak at *m/z* 269 and a neutral loss of a hexose (162 amu) was assigned as apigenin hexoside.

Four dihydroflavonols and two dihydroflavones were assigned, based on their MS and UV profiles. The compounds **27**, **35**, **37** and **47** showed fragment ions at *m/z* 303 and 285, compatible with dihydroquercetin derivatives. The neutral loss of one hexose, one pentose, one acetylhexose and one pentose allowed the tentative identification as dihydroquercetin hexose (**27**), dihydroquercetin pentoside 1 (**35**), dihydroquercetin acetylhexoside (**37**) and dihydroquercetin pentoside 2 (**47**), respectively. Fragment ions at *m/z* 287 and 269 were detected in compound **45**, compatible with a dihydrokaempferol derivative. These compounds were the main qualitative difference between both species, being only detected in *R. punctatum*. Due to the neutral loss of a pentose, it was tentatively assigned as dihydrokaempferol pentoside. The UV profile and the fragment ions at *m/z* 301, 285 and 125 of compound **52** were compatible with hesperetin. The compound also showed a neutral loss of rutinose, leading to its tentative identification as hesperetin rutinoside (**52**).

Table 14. Flavonoids and HCAs detected in *R. magellanicum* and *R. punctatum* PEEs and fermented samples by means of HPLC-ESI-MS/MS.

Peak	Rt (min)	$[M+H]^+$/ $[M-H]^-$	UV max	MS/MS	Tentative Identification
	Anthocyanins				
I	27.5-27.8	465.2		303.1(100)	Delphinidin hexoside
II	28.6	611.2	521,275	465.0(56), 303.1(100)	Delphinidin rutinoside
III	30.9	727.4		581.1(51), 287.1(100)	Cyanidin rhamnosyl hexoside pentoside
IV	32.8	449.0	516,279	287.1(100)	Cyanidin-3-glucoside[a]
V	33.5	595.2	517,280	449.1(62), 287.1(100)	Cyanidin-3-rutinoside[a]
VI	36.1	623.3		449.1(7), 287.1(100)	Cyanidin acetylpentoside hexoside
VII	38.9	623.4		477.1(100), 287.1(99)	Cyanidin rhamnosyl hexoside formate
VIII	48.7-49.0	477.3	517,277	287.1(100)	Cyanidin hexoside formate
IX	50.1	633.5		487.1(19), 331.2(100)	Malvidin-C-hexoside rhamnoside
X	53.5-53.7	551.6		465.1(89), 303.1(100)	Delphinidin malonyl hexoside
XI	62.8	535.3		287.1(100)	Cyanidin malonyl hexoside
	Other polyphenols				
1	6.7-6.8	609.1		441.1(100), 305.1(33)	(*epi*)-gallocatechin-(*epi*)-gallocatechin dimer 1
2	7.8	609.2		441.1(100), 305.2(40)	(*epi*)-gallocatechin-(*epi*)-gallocatechin dimer 2
3	8.1	593.5		425.1(100), 289.4(13)	(*epi*)-catechin-(*epi*)-gallocatechin dimer 1
4	10.9	593.2		467.0(100), 423.2(93), 305.1(39)	(*epi*)-catechin-(*epi*)-gallocatechin dimer 2
5	11.8	609.5		441.0(100), 305.0(34)	(*epi*)-gallocatechin-(*epi*)-gallocatechin dimer 3
6	14.1	593.1		424.9(100), 288.9(25)	(*epi*)-catechin-(*epi*)-gallocatechin dimer 3
7	16.5	352.9	324, 296sh	190.9(100), 179.1(35)	3-caffeoylquinic acid[a]
8	17.2	577.3		425.2(100), 289.4(29)	(*epi*)-catechin dimer
9	17.7-18.1	341.1	329, 296sh	178.9(100)	Caffeoyl hexoside 1
10	18.9	325.3	310, 282sh	162.9(100)	Coumaroyl hexoside 1
11	19.5	305.8		260.7(47), 220.6(100), 178.8(93)	(*epi*)-gallocatechin
12	21.0	356.3		172.5(100)	Dihydrocaffeoylquinic acid
13	23.1	337.4	310, 290sh	162.9(100)	3-coumaroylquinic acid[b]
14	23.7	289.7		244.9(100), 205.1(27)	(+)-catechin[a]
15	24.2-24.4	341.7		178.8(100)	Caffeoyl hexoside 2
16	25.5	325.7	313, 280sh	162.9(100)	Coumaroyl hexoside 2
17	25.9	353.9		173.1(100)	4-caffeoylquinic acid[b]
18	26.3	353.7		190.9(100), 178.7(12)	5-caffeoylquinic acid[b]

Table 14. (Continued)

19	26.9-27.2	369.7		336.9(100), 194.9(18)	Dihydroferuloylquinic acid
20	27.5	367.6		192.9(100)	3-feruloylquinic acid[b]
21	28.0	385.6		222.9(100)	Sinapoyl hexoside
22	30.2	367.3	324,293sh	192.9(10), 160.9(100)	Feruloylquinic acid 2
23	32.7-33.0	341.1		178.9(100)	Caffeoyl hexoside 3
24	33.2	291.1		246.7(100), 205.0(3), 167.1(3)	3,4-diHPP-2-ol
25	35.5	337.4		172.8(100), 162.4(7)	4-coumaroylquinic acid[b]
26	36.4	340.5	324, 285sh	176.9(100)	Caffeoyl hexoside 4
27	37.6	465.1	338sh, 289	302.9(11), 284.9(100)	Dihydroquercetin hexoside
28	37.8	181.4		136.3(100), 121.2(75)	Dihydrocaffeic acid
29	37.9	337.2		190.9(100), 163.0(6)	5-coumaroylquinic acid[b]
30	38.6	367.2		160.9(100), 192.8(4)	Feruloylquinic acid 3
31	40.0-40.8	335.1	328, 274	178.9(11), 160.9(100)	Caffeoyl derivative
32	40.6-41.3	625.7		300.8(100)	Quercetin dihexoside
33	42.3-43.1	463.2	350, 266	300.9(100)	Quercetin rutinoside
34	42.4	625.4	351, 267	316.0(100)	Myricetin rutinoside
35	43.4	435.1	338, 289	302.9(80), 285.0(100)	Dihydroquercetin pentoside 1
36	44.3	479.4		316.7(100)	Myricetin hexoside
37	44.3	507.4		303.0(8), 285.0(100)	Dihydroquercetin acetylhexoside
38	47.7-49.3	521.7		315.9(100)	Myricetin acetyl hexoside
39	50.0-50.8	463.8	350, 269	316.1(100)	Myricetin rhamnoside
40	50.1	609.7	353, 266	300.8(100)	Quercetin-3-rutinoside[a]
41	50.5	431.9		311.1(100)	(iso)-vitexin
42	51.2	519.4		336.9(100), 180.5(11)	Di-dihydrocaffeoylquinic acid 1
43	52.9	447.2	347, 265	284.9(100) , 241(3)	Luteolin hexoside
44	53.5	515.5	324, 297sh	352.8(100), 172.4(13)	Dicaffeoylquinic acid
45	53.6	419.9		286.8(19), 268.9(100)	Dihydrokaempferol pentoside
46	54.1	463.2	351, 268	300.9(100)	Quercetin-3-glucoside[a]
47	54.7	435.1		302.9(100), 285.3(24)	Dihydroquercetin pentoside 2
48	56.2	609.0		446.8(100), 284.9(37)	Kaempferol dihexoside
49	57.4	593.0		284.8(100)	Kaempferol rutinoside
50	58.1	505.4		300.8(100)	Quercetin acetylhexoside
51	58.3	477.9		314.9(100)	Isorhamnetin hexoside
52	58.5	609.3	334sh, 283	300.9(100)	Herperetin rutinoside
53	59.3	519.2		336.9(100), 180.7(16)	Di-dihydrocaffeoylquinic acid 2
54	61.3	448.6	347,265sh	284.9(100)	Kaempferol-3-glucoside

Table 14. (Continued)

55	61.6	447.7		300.8(100)	Quercetin rhamnoside
56	61.8	501.1		337.1(100), 173.0(35)	Dihydrocaffeoyl-coumaroylquinic acid
57	63.1	431.6	337, 267	268.9(100)	Apigenin hexoside
58	63.9	489.2	347, 266	284.9(100)	Kaempferol acetyl hexoside
59	69.9	461.1		432.9(52), 314.9(100), 300.9(52)	Isorhamnetin rhamnoside
60	71.9-73.8	431.3	341, 266	284.8(100)	Kaempferol rhamnoside
61	75.2-76.4	301.0	370, 262	206.9(37), 178.5(100), 150.5(52)	Quercetin
62	75.5-77.0	285.0	347, 266	284.7(100), 240.6(21), 198.5(13), 174.4(17)	Luteolin

[a]Confirmed by comparison of their retention times with commercial standards; [b]according hierarchical scheme suggested by Clifford et al., (2003).

4.2.1.5. Biotransformation of polyphenols during *in vitro* colonic fermentation

After the incubation of the PEEs under simulated human colonic conditions, nine additional compounds were detected by HPLC-DADMS/MS at t = 8 and t = 24 h (Table 15). Six dihydro-HCAs were identified, including five dihydrocaffeic acid- and one dihydroferulic acid derivative. The compound **12** with a pseudomolecular ion at *m/z* 355, showed a neutral loss of dihydrocaffeic acid (181 amu) leading to the MS/MS base peak at *m/z* 173, in agreement with quinic acid. Thus, the compound was assigned as dihydrocaffeoylquinic acid. Compound **28** was tentatively identified as dihydrocaffeic acid, based on its $[M-H]^-$ ion at *m/z* 181, and a MS/MS base peak at *m/z* 137. The compounds **42** and **53** presented a MS/MS fragment at *m/z* 181, compatible with dihydrocaffeic acid and a neutral loss of 182 amu, in agreement with a second dihydrocaffeic acid unit. Compounds **42** and **53** were tentatively identified as di-dihydrocaffeoylquinic acid 1 and 2, respectively. The compound **56** was assigned as dihydrocaffeoyl-coumaroylquinic acid, based on the neutral loss of a dihydrocaffeoyl unit (164 amu) and fragments ions at *m/z* 337 and 173, in agreement with coumaroylquinic acid and quinic acid, respectively. Compound **19** showed a pseudomolecular ion at *m/z* 369. The compound was tentatively identified as dihydroferuloylquinic acid, due to the neutral loss of a quinoyl moiety (174 amu) and the MS/MS product ion at *m/z* 195, in agreement with dihydroferulic acid. The compound **24** showed a pseudomolecular ion at *m/z* 291 and product ions at *m/z* 247, 205, and 167, in agreement with 1-(3,4-dihydroxyphenyl)-3-(2,4,6-trihydroxyphenyl)propan-2-ol (3,4-diHPP-2-ol) (Kutschera, Engst, Blaut, & Braune, 2011). Compound **61** was identified as quercetin, based on its molecular ion at *m/z* 301 and the MS/MS fragments at *m/z* 207, 179 and 151, confirmed by comparison with a commercial standard. The compound **62**, with a molecular ion at *m/z* 285 and MS/MS fragment ions at *m/z* 241, 199 and 175 was identified as luteolin (Schmidt, 2016).

Our results suggest that compounds: dihydrocaffeoylquinic acid (**12**), dihydroferuloylquinic acid (**19**), 3,4-diHPP-2-ol (**24**), dihydrocaffeic acid (**28**), di-dihydrocaffeoylquinic acids (**42** and **53**), dihydrocaffeoyl-coumaroylquinic acid (**56**), quercetin (**61**) and luteolin (**62**), are metabolites resulting from the incubation of *Ribes* polyphenols with human fecal microbiota, since they were not present in the nonfermented PEE (Table 15). The hydrogenation of the double bond in the aliphatic chain of HCAs derivatives is a typical reduction reaction catalyzed by gut microbes (Espín et al., 2017). Subsequent ester bond hydrolysis reactions of **12**, **42**, **53** and **56** by bacterial esterases can explain the presence of dihydrocaffeic acid (**28**) (Tomas-Barberan et al., 2014). Nevertheless, it needs to be considered that the ring fission of luteolin can also lead to compound **28** (Juániz et al., 2017). In the same way, the appearance of dihydrocaffeic acid (**28**) was detected after 5, 6 and 24 h of *in vitro* fermentation of coffee, black tea, green tea, apple juice, blueberry and cranberry (Dall'Asta et al., 2012; Sánchez-Patán et al., 2015). The dehydroxilation products of dyhydrocaffeic acid (**28**) [3-(phenyl)-propionic acid and 3-(4′-hydroxyphenyl)-propionic acid], were reported as end catabolites of the *in vitro* gastrointestinal digestion and colonic fermentation of *Ribes nigrum* (Brown et al., 2012). Our results show a similar metabolic pathway; however, these end catabolites were not detected in our samples. Similar variations in rate and extent of metabolism were previously observed, with different end products between donors, suggesting that individual variations in gut microbiota composition might influence the formation of catabolites (Ludwig et al., 2013). In addition, the high initial content of HCA esters could delay their degradation rate (Rechner et al., 2004). Flavan-3-ols, which are also present in our samples, may generate changes in bacterial composition, influencing the rate and extent of the catabolism of HCAs (Cueva et al., 2013; Marín, Miguélez, Villar, & Lombó, 2015).

Dihydrocaffeoylquinic acid (**12**) was observed after 24 h in *R. punctatum* only in donor 2 (Table 15). A similar observation was reported by Juániz et al. (2017), were this metabolite was only

detected after 24 h fermentation of *Cynara cadunculus*. Dihydroferuloylquinic acid (**19**) appeared at t = 24 h in the PEE from *R. magellanicum* fermented with samples from both donors. In *R. punctatum*, the same compound was detected at t = 8 and t = 24 h for donor 1, and only at t = 24 h for donor 2. The same compounds have been reported as colonic metabolites after the ingestion of yerba mate infusions in humans (Gómez-Juaristi et al., 2018).

Compounds **42**, **53** and **56** were not detected in the PEEs from both species (t = 0 h) (Table 15). Compound **42** appeared in *R. magellanicum* at t = 8 and t = 24 h only in donor 1, while for *R. punctatum*, this compound was found only at t = 24 h in donor 1. Compound **53** was present in both species at t = 8 h only in donor 1, and was not detected at t = 24 h. Compound **56** was detected only in donor 1, in *R. magellanicum* at t = 8 h and in *R. punctatum* at t = 8 and t = 24 h. Compounds **42** and **53** detected in fermented PEEs of *R. magellanicum* are likely formed by hydrogenation of dicaffeoylquinic acid (**44**). On the other hand, since compound **44** was not found in the non-fermented PEE of *R. punctatum* (Table 15), compounds **42** and **53** might be formed by the reduction of HCAs double bond and subsequent trans-esterification reactions. Isomerization reactions in CQAs and di-CQAs were reported under similar conditions (Juániz et al., 2017; Rechner et al., 2004; Tomás-Barberán et al., 2014). This can also explain the formation of dihydrocaffeoyl-coumaroylquinic acid (**56**). To the best of our knowledge, compounds **42**, **53** and **56** are reported here for the first time as potential colonic metabolites.

Compound **24** was detected only in the fermentation of *R. magellanicum* PEE at t = 8 and t = 24 h in donor 1. The presence of this compound suggests its formation through a C-ring fission reaction of (+)-catechin, as previously described (Kutschera et al., 2011). The same metabolite was observed in caecum, colon and feces from mice fed with polyphenol extract from cupuassu (*Theobroma grandiflorum*) (Barros et al., 2016).

Quercetin (**61**) and luteolin (**62**) were detected at t = 8 and t = 24 h of incubation of both *Ribes*, but only with donor 1 samples. These compounds were likely formed by deglycosilation from quercetin hexosides (**32**, **33**, **40**, **46**, and **55**) and luteolin hexoside (**43**). The deglycosilation reactions might be catalyzed by the hydrolases (rhamnosidases and glucosidases) present in colonic bacteria (Espín et al., 2017). The release of flavonoid aglycons by colonic bacteria has been previously described (Juániz et al., 2017; Rechner et al., 2004).

Table 15. Native polyphenols and metabolites detected after *in vitro* colonic fermentation of Chilean currants (*R. magellanicum* and *R. punctatum*).

Peak	Rt (min)	Native phenolics and metabolites	*R. magellanicum*					*R. punctatum*				
			Time									
			0h	Donor 1		Donor 2		0h	Donor 1		Donor 2	
			(PEE)	8h	24h	8h	24h	(PEE)	8h	24h	8h	24h
		Anthocyanins										
I	27.5-27.8	Delphinidin hexoside	X	X	-	X	-	X	-	-	X	-
II	28.6	Delphinidin rutinoside	X	X	-	X	-	-	-	-	-	-
III	30.9	Cyanidin rhamnosyl hexoside pentoside	X	-	-	-	-	-	-	-	-	-
IV	32.8	Cyanidin-3-glucoside[a]	X	X	X	X	X	X	X	X	X	X
V	33.5	Cyanidin-3-rutinoside[a]	X	X	X	X	X	X	X	X	X	X
VI	36.1	Cyanidin acetylpentoside hexoside	X	X	-	X	-	-	-	-	-	-
VII	38.9	Cyanidin rhamnosyl hexoside formate	X	X	-	X	-	-	-	-	-	-
VIII	48.7-49.0	Cyanidin hexoside formate	X	X	X	X	X	X	X	X	X	X
IX	49.8	Malvidin-C-hexoside rhamnoside	X	X	-	X	-	-	-	-	-	-
X	53.5-53.7	Delphinidin malonyl hexoside	X	X	-	X	X	X	X	X	X	X
XI	62.8	Cyanidin malonyl hexoside	X	X	-	X	X	X	-	-	-	-
		Other polyphenols										
1	6.7-6.8	(*epi*)-gallocatechin-(*epi*)-gallocatechin dimer 1	X	X	-	X	-	X	X	-	X	-
2	7.8	(*epi*)-gallocatechin-(*epi*)-gallocatechin dimer 2	X	X	X	X	-	X	X	X	X	-
3	8.1	(*epi*)-catechin-(*epi*)-gallocatechin dimer 1	X	X	X	X	-	X	X	X	X	-
4	10.9	(*epi*)-catechin-(*epi*)-gallocatechin dimer 2	X	X	X	X	-	X	X	X	X	-
5	11.8	(*epi*)-gallocatechin-(*epi*)-gallocatechin dimer 3	X	X	X	X	-	X	X	X	X	-
6	14.1	(*epi*)-catechin-(*epi*)-gallocatechin dimer 3	X	X	X	X	-	X	X	-	X	-
7	16.5	3-caffeoylquinic acid[a]	X	X	-	X	-	X	-	-	X	X
8	17.2	(*epi*)-catechin dimer	X	X	X	X	-	X	X	X	X	-
9	17.7-18.1	Caffeoyl hexoside 1	X	X	-	X	-	X	X	-	X	-
10	18.9	Coumaroyl hexoside 1	X	-	-	-	-	X	-	-	-	-
11	19.5	(*epi*)-gallocatechin	X	X	X	X	-	X	X	-	-	-
12	21.0	Dihydrocaffeoylquinic acid	-	-	-	-	-	-	-	-	-	X
13	23.1	3-coumaroylquinic acid[b]	X	X	-	X	X	X	X	X	X	X
14	23.7	(+)-catechin[a]	X	X	X	X	-	X	X	X	X	-

Table 15. (Continued)

15	24.2-24.4	Caffeoyl hexoside 2	X	-	-	X	-	X	-	-	X	-
16	25.5	Coumaroyl hexoside 2	X	-	-	-	-	X	-	-	-	-
17	25.9	4-caffeoylquinic acid[b]	X	-	-	X	-	X	-	-	X	X
18	26.3	5-caffeoylquinic acid[b]	X	-	-	-	-	X	-	-	-	-
19	26.9-27.2	Dihydroferuloylquinic acid	-	-	X	-	X	-	X	X	-	X
20	27.5	3-feruloylquinic acid[b]	X	X	-	X	-	X	-	-	X	-
21	28.0	Sinapoyl hexoside	X	-	-	X	-	X	-	-	X	-
22	30.2	Feruloylquinic acid 2	X	X	-	X	X	X	X	X	X	X
23	32.7-33.0	Caffeoyl hexoside 3	X	-	-	X	-	X	X	-	X	-
24	33.2	3,4-diHPP-2-ol	-	X	X	-	-	-	-	-	-	-
25	35.5	4-coumaroylquinic acid[b]	X	-	-	X	X	X	-	-	X	X
26	36.4	Caffeoyl hexoside 4	X	X	-	X	-	X	X	-	X	-
27	37.6	Dihydroquercetin hexoside	-	-	-	-	-	X	X	X	X	X
28	37.8	Dihydrocaffeic acid	-	X	X	-	X	-	X	X	-	X
29	37.9	5-coumaroylquinic acid[b]	X	-	-	-	-	X	-	-	-	-
30	38.6	Feruloylquinic acid 3	X	X	-	X	-	X	X	-	X	X
31	40.0-40.8	Caffeoyl derivative	X	X	-	X	-	X	X	-	X	-
32	40.6-41.3	Quercetin dihexoside	X	X	X	X	-	X	-	-	X	X
33	42.3-43.1	Quercetin rutinoside	X	-	-	X	-	-	-	-	-	-
34	42.4	Myricetin rutinoside	X	X	X	X	-	-	X	-	-	-
35	43.4	Dihydroquercetin pentoside 1	-	-	-	-	-	X	X	X	X	X
36	44.3	Myricetin hexoside	X	X	X	X	-	X	-	-	X	X
37	44.3	Dihydroquercetin acetylhexoside	-	-	-	-	-	X	-	-	X	X
38	47.7-49.3	Myricetin acetyl hexoside	X	-	-	X	-	X	-	-	X	X
39	50.0-50.8	Myricetin rhamnoside	X	X	X	-	-	X	X	X	X	X
40	50.1	Quercetin-3-rutinoside[a]	X	X	X	X	-	X	X	X	X	X
41	50.5	(iso)-vitexin	X	X	X	X	-	X	X	X	X	X
42	51.2	Di-dihydrocaffeoylquinic acid 1	-	X	X	-	-	-	-	X	-	-
43	52.9	Luteolin hexoside	X	-	-	X	-	X	X	-	X	X
44	53.5	Dicaffeoylquinic acid	-	X	-	-	-	-	-	-	-	-
45	53.6	Dihydrokaempferol pentoside	-	-	-	-	-	X	X	X	X	X
46	54.1	Quercetin-3-glucoside[a]	X	-	-	X	-	X	X	X	X	-
47	54.6	Dihydroquercetin pentoside 2	-	-	-	-	-	X	X	X	X	-
48	56.2	Kaempferol dihexoside	X	X	-	X	-	-	-	-	-	-
49	57.4	Kaempferol rutinoside	X	X	X	X	-	X	X	X	X	-
50	58.1	Quercetin acetylhexoside	X	-	-	X	X	X	-	-	X	X

Table 15. (Continued)

51	58.3	Isorhamnetin hexoside	X	-	-	X	-	-	-	-	-	-
52	58.5	Herperetin rutinoside	-	X	X	X	X	-	X	X	X	X
53	59.3	Di-dihydrocaffeoylquinic acid 2	-	X	-	-	-	-	X	-	-	-
54	61.3	Kaempferol-3-glucoside	X	-	-	X	-	X	-	-	X	-
55	61.6	Quercetin rhamnoside	X	-	-	X	-	X	X	X	X	X
56	61.8	Dihydrocaffeoyl-coumaroylquinic acid	-	X	-	-	-	-	X	X	-	-
57	63.1	Apigenin hexoside	X	-	-	X	-	X	-	-	X	-
58	63.9	Kaempferol acetyl hexoside	X	-	-	X	X	X	-	-	X	X
59	69.9	Isorhamnetin rhamnoside	-	-	-	-	-	X	-	-	-	-
60	71.9-73.8	Kaempferol rhamnoside	X	X	-	-	-	X	-	-	-	-
61	75.2-76.4	Quercetin	-	X	X	-	-	-	X	X	-	-
62	75.5-77.0	Luteolin	-	X	X	-	-	-	X	X	-	-

-: Not detected

4.2.2. Quantitative changes in main precursors by colonic fermentation

Hydroxycinnamic acids (HCAs) and anthocyanins were the major compounds found in the PEEs before fermentation. Therefore, both groups of compounds were quantified at t = 0, t = 8 and t = 24 h. The total HCAs content in the non-fermented PEE was 78.64 mg 3-caffeoylquinic acid equivalents (3-CQA eq)/g in *R. magellanicum* and 88.03 mg 3-CQA eq/g in *R. punctatum*. The total anthocyanin content was 34.43 and 15.96 mg/g PEE in *R. magellanicum* and *R. punctatum*, respectively. Several flavonol and dihydroflavonol conjugates were detected, but their close retention time did not allow their quantification (Figure 12 and Figure 13). These results are summarized in Table 16.

The simulated human colonic conditions elicited clear changes in the phenolic profile of both *Ribes* species, when comparing the PEE profiles at t = 0, t = 8 and t = 24 h (Figure 12 and Figure 13). In both species, the HCAs were the most affected compounds by the colonic biotransformation. A similar observation was reported by Ludwig et al. (2013), who described a significant decrease in the HCA content within 4 h of *in vitro* colonic fermentation of polyphenols from coffee. In our study, a decrease in the total HCA content was observed at t = 8 h, with a loss of 76 % (donor 1) and 98 % (donor 2) for *R. magellanicum*, and a loss of 80 % (donor 1) and 99 % (donor 2) for *R. punctatum*. The most affected compound was 3-CQA (**7**), with recoveries between 0 % (donor 1) and 17 % (donor 2). Regarding donor 1, feruloylquinic acid 2 (FQA2, **22**) showed a recovery of 20 % in *R. magellanicum* and 7 % in *R. punctatum*. These recovery values were higher when compared to the other HCAs quantified. In donor 2, an increase in the FQA2 content was observed after 8 h incubation, with 64 % in *R. magellanicum* and 32 % in *R. punctatum*, suggesting its biosynthesis during the fermentation process. The observed increase in FQA2 (**22**) content at t = 8 h compared to t = 0, is compatible with the isomerization reactions reported for HCA esters favored by the pH of the *in vitro* fermentation (Rechner et al., 2004; Tomás-Barberán et al., 2014).

The decrease in total HCA content was higher after 24 h of fecal incubation, with losses of 90–100 % for both species. In particular, compound **13** was less affected, showing recoveries of 9 % in *R. magellanicum* and 27 % in *R. punctatum*, for donor 2. In the samples from donor 1, compound **13** was not detected in *R. magellanicum*, while in *R. punctatum* was recovered by 6.4 %. The differences in the catabolic rate might be explained by the variations in colonic microbiota composition (Rechner et al., 2004; Ludwig et al., 2013). At the end of the experiment, the total HCA recovery was higher in *R. punctatum* (1–8 %) than in *R. magellanicum* (less than 1 %).

Regarding the anthocyanin content, cyanidin-3-glucoside (**IV**) was the main compound in both species, followed by cyanidin-3-rutinoside (**V**) and cyanidin hexoside formate (**VIII**) (Table 16). A high decline in the total anthocyanin content was observed after 8 h of colonic fermentation, with losses of 68 % (donor 2) and 74 % (donor 1) in *R. magellanicum*; and losses of 64 % (donor 2) and 90 % (donor 1) in *R. punctatum*. The recoveries of anthocyanins in the samples incubated with fecal material from donor 2 were slightly higher than those treated with material from donor 1, similar to HCAs (Table 16). Cyanidin hexoside formate (**VIII**) was almost completely biotransformed, yielding amounts below the quantification limit.

After 24 h incubation, the total anthocyanin content was lost by 85 % (donor 2) and 92 % (donor 1) in *R. magellanicum*; and lost by 71 % (donor 2) and 85 % (donor 1) in *R. punctatum*. Cyanidin-3-glucoside was the most affected anthocyanin, with a degradation of 92–97 %. Cyanidin-3-rutinoside and cyanidin hexoside formate showed higher stability, with recoveries of 14–22 % and 16–27 %, respectively. In *R. punctatum* fermented with donor 1 samples, an increment of 27 % in the cyanidin hexoside formate content was observed at t = 24 h, compared to t = 8 h.

The decrease in the anthocyanin content was associated with the instability of the flavylium cation in the fermentation medium, as well as by the bacterial metabolism (Aura et al., 2005; Del Rio et

al., 2010). Cyanidin-3-glucoside was degraded faster than the other quantified anthocyanins, in agreement with the faster rate of deglycosilation by bacterial glucosidases compared to rhamnosidases (Aura et al., 2005). In addition, the metabolism of di- and tri-saccharides is much slower than mono-saccharides (Marín et al., 2015). Cyanidin hexoside formate (**VIII**) showed higher stability compared to cyanidin-3-glucoside. Correa-Betanzo et al. (2014) observed that acetylated anthocyanins were transformed in a lesser extent by colonic microbiota, due to a higher stability given by the formyl residue. The increase in the content of cyanidin hexoside formate at t = 24 compared to t = 8 h can be explained by the esterification reactions with formic acid, as observed in HCAs. No anthocyanin derived metabolite was found at the end of the experiment, despite their high degradation rate. A possible explanation could be the overlapping of the signals by other metabolites. This fact was previously observed by Aura et al. (2005), and was attributed to the capacity of the fecal matrix to bind flavonoids and their metabolites. The slower rate and minor extent of degradation in the quantified native anthocyanins by donor 2, may be attributed to the individual variations in the colonic microbiota of the donors (Gross et al., 2010; Ludwig et al., 2013). The slower degradation rate of phenolic compounds may contribute to increase their bioavailability, due to a greater chance to be absorbed (Marín et al., 2015).

Table 16. Time-related quantitative modifications in main phenolic compounds (mg of compound/g PEE) of Chilean currants during *in vitro* fermentation.

Compound	*Ribes magellanicum*					*Ribes punctatum*				
	0 hours (PEE)	8 hours		24 hours		0 hours (PEE)	8 hours		24 hours	
		D1	D2	D1	D2		D1	D2	D1	D2
HCAs										
3-CQA	69.33±1.11	-	13.45±0.04	-	-	65.65±0.89	-	8.15±0.59	-	2.58±0.04
CH-1	3.96±0.02	0.45±0.01	1.62±0.01	-	-	4.56±0.01	-	1.56±0.03	-	-
3-CoQA	2.60±0.01	0.39±0.01	0.71±0.00	-	0.23±0.00	11.70±0.22	0.46±0.03	2.46±0.17	0.75±0.04	3.22±0.05
FQA 2	1.74±0.04	0.36±0.00	2.86±0.02	-	-	3.27±0.18	0.24±0.02	4.33±0.31	0.16±0.00	0.92±0.03
Caffeoyl derivative	1.01±0.01	-	0.54±0.00	-	-	2.85±0.2	0.13±0.01	1.59±0.02	-	-
Anthocyanins										
Cyanidin-3-glucoside	20.72±0.04	5.10±0.03	6.48±0.11	0.71±0.00	2.05±0.02	8.69±0.01	0.65±0.04	2.62±0.13	0.74±0.01	1.51±0.02
Cyanidin-3-rutinoside	10.09±0.03	2.83±0.02	3.43±0.03	1.42±0.01	2.10±0.01	4.49±0.01	0.95±0.00	1.74±0.03	0.97±0.00	1.82±0.01
Cyanidin hexoside formate	3.62±0.05	0.95±0.02	1.05±0.02	0.59±0.00	0.94±0.02	2.78±0.01	-	1.41±0.02	0.76±0.01	1.28±0.01

Data are expressed as mean ± SD, n = 3. D1: donor 1; D2: donor 2.
3-CQA: 3-caffeoylquinic acid; CH: caffeoyl hexoside; 3-CoQA: 3-*p*-coumaroylquinic acid; HCA: hydroxycinnamic acid; FQA: feruloylquinic acid;
-: below quantification limit.
*The content of Cyanidin hexoside formate and HCAs are expressed as mg cyanidin-3-glucoside equivalents/g PEE and 3-caffeoylquinic acid equivalents/g PEE, respectively.

4.2.3. Effect of simulated colonic fermentation on the antioxidant capacity

The role of free radicals in the development of several colonic pathologies has been proposed (Zuo et al., 2017). Antioxidants derived from diet can act as scavengers, helping to prevent cell and tissue damage. Phenolic compounds may help to protect the gastrointestinal tract against oxidative damage before entering the systemic circulation (Halliwell, 2007). This feature is particularly important in the large intestine, as it is constantly being challenged by diet-derived oxidants, mutagens and carcinogens as well as by endogenously generated ROS (Ames, 1983; Tudek & Speina, 2012). Therefore, the presence of fermented metabolites with antioxidant capacity could help to maintain a reduced redox state, especially in the mucosal cells (Jaganath, Mullen, Lean, Edwards, & Crozier, 2009).

The antioxidant capacity of the non-fermented and fermented PEEs was determined by means of the ORAC assay. This method is extensively used to assess the chain-breaking antioxidant capacity at physiological pH (Ou et al., 2001). As shown in Table 17, the PEEs of *R. magellanicum* and *R. punctatum* showed ORAC values of 2008.37 and 2616.69 µmol TE/g PEE, respectively. Tabart et al. (2012) reported that *Ribes nigrum* fruits showed an ORAC value of 34.5 µmol TE/g of fresh fruit. In our samples, ORAC values of *R. punctatum* and *R. magellanicum* equate to 22.09 and 31.39 µmol TE/g fresh fruit, respectively.

After 8 h of colonic fermentation, a significant increase ($p < 0.05$) in the ORAC value was observed, between 3141 and 3442 µmol TE/g for *R. magellanicum* and 3027–3268 µmol TE/g for *R. punctatum* for donor 1 and 2, respectively. This effect has been associated with a higher antioxidant capacity of the metabolites derived from colonic fermentation of HCAs. In addition, the increased stabilities of the flavonol, flavan-3-ol and dihydroflavonol derivatives contribute to higher values in the ORAC assay (Gómez-Ruiz, Leake, & Ames, 2007; Tabart et al., 2009).

After 24 h, the *R. punctatum* fermented PEE showed ORAC values between 3148 and 3221 µmol TE/g for donor 1 and 2, respectively, which can be attributed to the content of dihydroflavonols derivatives. On the other hand, *R. magellanicum* presented a significant decrease in the ORAC values after 24 h fermentation ($p < 0.05$), with values of 1587–1880 µmol TE/g for donor 1 and 2, respectively. These results were not significantly different than those obtained for the non fermented PEE. Interestingly, the effect of colonic fermentation in the ORAC values of the PEEs showed no significant differences between both donors.

4.2.4. Effect of simulated colonic fermentation on the inhibition of metabolic syndrome-associated enzymes

The enzymes α-amylase, α-glucosidase and pancreatic lipase occur in the small intestine lumen and are responsible for the breakdown of carbohydrates and lipids, respectively. The inhibition of these enzymes delays the absorption of monosaccharides and fatty acids, which is recognized as an important strategy for treating postprandial hyperglycemia and obesity (McDougall et al., 2009). The non-fermented PEEs inhibited the enzyme α-amylase (Table 17). The IC_{50} values were 21.65 and 20.07 µg/mL for *R. magellanicum* and *R. punctatum*, respectively. This inhibitory activity was completely lost after colonic fermentation (t = 8 and t = 24 h, Table 17). In a similar way, the inhibitory activity of the PEEs against α-amylase was lost after simulated gastric and intestinal digestion (Burgos-Edwards et al., 2017). The PEEs and fermentation products from both species were inactive towards pancreatic lipase (data not shown).

The non-fermented PEE from *R. magellanicum* inhibited α-glucosidase with an IC_{50} value of 0.38 µg /mL (Table 17). After 8 h fermentation, a significant decrease in the inhibitory activity against α-glucosidase was observed ($p < 0.05$), with IC_{50} values of 2.80 and 10.79 µg/ mL, for donor 1 and 2, respectively. After 24 h incubation, the inhibitory activity of *R. magellanicum* PEE showed IC_{50}

values of 8.96 and 31.30 µg/mL for donor 1 and 2, respectively. On the other hand, the non-fermented PEE of *R. punctatum* inhibited α-glucosidase with an IC_{50} value of 0.31 µg/mL (Table 17). After 8 h fermentation, a decrease in the inhibitory activity was observed, showing IC_{50} values of 10.25 and 11.21 µg/mL for donor 1 and 2, respectively. Interestingly, the inhibitory activity was recovered after 24 h fermentation, showing IC_{50} values of 3.94 and 7.13 µg PEE/mL for donor 1 and 2, respectively. Significant differences ($p < 0.05$) between donors were observed in the inhibitory effect against α-glucosidase of both fermented *Ribes* PEEs (Table 17). Samples from donor 1 were significantly more active in both species, in agreement with the major degradation of HCAs observed in these samples. The polyphenols, biotransformed by the gut microbiota, can reach again the small intestine via enterohepatic circulation helping in the control of postprandial glycemia (Espín et al., 2017). Esposito et al. (2015) reported that a *Ribes nigrum* extract reversed high blood glucose concentration in diet-induced obese mice, but only when the gut microbiome was intact. The results of this study showed that the integrity of the gut microbiome was essential to prevent glucose intolerance in mice. The authors fed the animals with an antibiotic cocktail to deplete all commensal bacteria. These antibiotic-treated mice showed a 45 % increase in the baseline blood glucose vs. controls, or animals treated with a black currant supplementation. Moreover, the antibiotic-treated animals showed high peak blood glucose values despite being fed with the black currant rich diet. The authors observed that the integrity of the gut microbioma was crucial for the protective effect of black currant anthocyanins against obesity and insulin resistance. The effect of polyphenols in the control of postprandial glycaemia has been associated with the inhibition of α-amylase and α-glucosidase, and the inhibition of the SGLT-1 cotransporter (Na^+/Glucose) in the intestinal lumen (Schulze et al., 2014). In a study carried out with male and postmenopausal female volunteers, a *R. nigrum* anthocyanin-rich beverage decreased postprandial glucose, insulin and incretin concentrations, suggesting a health promoting role against metabolic syndrome (Castro-Acosta et al., 2016).

In summary, our results suggest that fermented polyphenols from *R. magellanicum* and *R. punctatum* might contribute to the prevention of high-blood glucose levels. Indeed, this is a first approach in the understanding of the potential health benefits of these wild currants; however, further *in vivo* experiments must be carried out to confirm this effect.

Table 17. Oxygen radical absorbance capacity and effect of Chilean *R. magellanicum* and *R. punctatum* PEEs, before and after *in vitro* fermentation, towards metabolic syndrome-associated enzymes.

Samples		**α-amylase (IC_{50}, µg/mL)**	**α-glucosidase (IC_{50}, µg/mL)**	**Lipase (IC_{50}, µg/mL)**	**ORAC (µmol TE/g extract)**
R. magellanicum					
Time (h)					
0 PEE		21.65 ± 0.54	0.38 ± 0.00[a]	Inactive	2008.37±186.13[a]
8	D1	Inactive	2.8 ± 0.04[b]	Inactive	3442.50±147.34[b]
8	D2	Inactive	10.79 ± 0.30[c]	Inactive	3141.96±105.67[b]
24	D1	Inactive	8.96 ± 0.57[c]	Inactive	1880.48±8.56[a,c]
24	D2	Inactive	31.30 ± 1.54[d]	Inactive	1587.23±128.41[c]
R. punctatum					
Time (h)					
0 PEE		20.07 ± 1.72	0.31 ± 0.01[a]	Inactive	2616.69±176.49[a]
8	D1	Inactive	10.25 ± 0.27[b]	Inactive	3027.53±39.78[b]
8	D2	Inactive	11.21 ± 0.22[c]	Inactive	3268.26±138.47[b]
24	D1	Inactive	3.94 ± 0.21[d]	Inactive	3148.58±72.86[b]
24	D2	Inactive	7.13 ± 0.23[e]	Inactive	3221.35±40.09[b]
Orlistat*		n. d.	n. d.	0.37 ± 0.01	n. d.
Acarbose*		28.5 ± 0.3	120.9 ± 2.0	n. d.	n. d.

*reference compound. Data are expressed as means ± SD, n = 3.

TE: Trolox equivalents; PEE: phenolic enriched extract; n. d.: not determined. D1: donor 1; D2: donor 2.

Different letters (a-e) in the same column show significant differences among each determination, according to Tukey's test ($p < 0.05$).

Chapter 5

Anti-inflammatory effect of polyphenols from Chilean currants (*Ribes magellanicum* and *R. punctatum*) after *in vitro* gastrointestinal digestion on Caco-2 cells

The content of this chapter was prepared as a manuscript, published in Journal of Functional Foods. Burgos-Edwards, A., Martín-Pérez, L., Jiménez-Aspee, F., Theoduloz, C., Schmeda-Hirschmann, G., & Larrosa, M. (2019). Anti-inflammatory effect of polyphenols from Chilean currants (*Ribes magellanicum* and *R. punctatum*) after *in vitro* gastrointestinal digestion on Caco-2 cells. *Journal of Functional Foods*, 59, 329–336.

5.1. Introduction

Inflammatory bowel diseases (IBD) are chronic conditions including Crohn's disease (CD) and ulcerative colitis (UC). These illnesses are associated with a dysregulation of the immune response against the resident microbiota and are characterized by epithelial injuries and immune cell infiltration (Sartor, 2006). The populations from North American and European countries are the most affected by IBD; however, the prevalence and incidence in industrialized countries from Asia, the Middle East, Africa, and South America is increasing. This raise is associated with environmental and genetic factors, as well as to the diet (Kaplan & Ng, 2017).

The IBD treatment is focused on the control of the inflammatory and immune responses, and often involves long-term administration of nonsteroidal anti-inflammatory drugs (NSAIDs) and corticosteroids. The long-term use of these drugs results in a latent risk of side effects, lack of

response to the treatment and recurrence of the disease (Biasi et al., 2011). Pro-inflammatory cytokines such as interleukin 1 (IL-1), interleukin-6 (IL-6), and tumor necrosis factor alpha (TNF-α) are overexpressed in the intestinal mucosa from patients with IBD and seem to play an important role in its etiology and pathogenesis. In addition, the enzymes cyclooxygenase-2 (COX-2) and inducible nitric oxide synthase (iNOS) are overexpressed in the injured tissues, releasing prostaglandin E_2 (PGE_2) and nitric oxide (NO), respectively, which are directly linked to cancer development (Surh et al., 2001). The regulation of cytokines levels through diet-derived compounds might be helpful in the prevention and/or as a coadjuvant treatment. In this sense, polyphenols are good candidates due to the increasing evidence of their modulating capacity of the acute and chronic inflammatory status in humans (Leyva-López et al., 2016).

Fruits from *Ribes* species (currants), largely cultivated and commercialized, are important sources of polyphenols and antioxidants, thus, there is a growing interest in these berries as a potential source of functional ingredients (Gopalan et al., 2012). Studies focused on the anti-inflammatory activity of currant extracts have been mainly performed with *Ribes nigrum* (blackcurrant). The juice of blackcurrant, white currant (*Ribes sativum*), and gooseberry (*Ribes hirtellum*) modulate COX-2 expression levels in prostatic adenocarcinoma cells (PC-3) through the NF-kB pathway (Boivin, Blanchette, Barrette, Moghrabi, & Béliveau, 2007). Lyall et al. (2009) reported a decrease of TNF-α and IL-6 in human monocytes (THP-1). Huebbe et al. (2012) showed a reduction of mRNA levels of TNF-α, IL-1β, and iNOS in murine macrophages (RAW264.7) as a consequence of the pre-treatment with blackcurrant extract. Similar results were obtained in a Caco-2/ RAW264.7 co-cultured cell model, in which a reduction of IL-1α and IL-1β, COX-2 and iNOS was observed (Olejnik et al., 2016). In addition, a decreased COX-2 expression was observed in rats fed with anthocyaninrich black currant skin extracts (Bishayee et al., 2013).

The Chilean currants *R. magellanicum* and *R. punctatum* are also rich in polyphenols with some reported health-beneficial bioactivities. The polyphenolic-enriched extracts (PEEs) contain high amounts of hydroxycinnamic acids, dihydroflanovols, flavonols, and anthocyanins, with high antioxidant capacity and cytoprotective activity against oxidative stress (Jiménez-Aspee et al., 2016b; 2016c). The cytoprotection occurs by means of the induction of the antioxidant enzymes catalase, superoxide dismutase, glutathione peroxidase and reductase (Theoduloz et al., 2018). In addition, the PEE from *R. magellanicum* and *R. punctatum*, submitted to *in vitro* gastrointestinal digestion, showed inhibitory activity against α-glucosidase, thus indicating a potential role in the prevention of postprandial hyperglycemia (Burgos-Edwards et al., 2017). Among Chilean berries, extracts from maqui (*Aristotelia chilensis*), calafate (*Beberis microphylla*) (Reyes-Farias et al., 2015) and white strawberry (Molinett, Nuñez, Moya-León, & Zúñiga-Hernández, 2015) have been assayed as anti-inflammatory agents with promising results. However, no studies on Chilean currants could be found in literature so far.

Most *in vitro* studies have been conducted with crude extracts. However, the gastrointestinal environment affects the stability of polyphenols, generating qualitative and quantitative changes in the phenolic profile (Burgos-Edwards et al., 2017; Olejnik et al., 2016). In a previous study we isolated the main anthocyanins in both Chilean currants, which were unequivocally identified as cyanidin-3-glucoside and cyanidin-3-rutinoside. In addition, 3-caffeoylquinic acid and caffeoyl hexoside were the main hydroxycinnamic acid derivatives in the PEEs (Burgos-Edwards et al., 2017; Jiménez-Aspee et al., 2016c). Other compounds occurring in *R. magellanicum* and *R. punctatum* PEE include flavonoid glycosides based on the flavonols myricetin, quercetin and kaempferol. Proanthocyanidin monomers and oligomers were identified in both Chilean currant species. The content of the main compounds after intestinal digestion decreased roughly by 90 % for cyanidin-3-glucoside and 80 % for the corresponding rutinoside. This effect was more

pronounced for the hydroxycinnamic acid derivatives, with losses of nearly 98 % for 3-caffeoylquinic acid and about 50-65 % for caffeoyl hexoside (Burgos-Edwards et al., 2017). The *in vitro* digestion models became a useful alternative to simulate the influence of the human digestion process on food constituents. The absence of invasive methods and/or experimental animals, the low cost, and the fast results turned them into a widely employed procedure for these purposes (Minekus et al., 2014). In addition, polyphenol extracts submitted to *in vitro* gastrointestinal digestion (GID) show comparable bioactivity to that observed in *in vivo* studies (Brown et al., 2014). After GID, the intestinal tissue is often exposed to higher concentrations of polyphenols, unlike other tissues which require previous absorption of these metabolites (Biasi et al., 2011). The Caco-2 cell model has been widely used to emulate the epithelial barrier functions, and the C2BBe1 clone presents a homogeneous morphology forming a polarized monolayer with the apical brush border comparable to that of the human colon cells. In addition, this clone is responsive to inflammatory stimuli (Leonard et al., 2010).

The aim of our study was to assess the anti-inflammatory activity of the PEEs from *R. magellanicum* and *R. punctatum*, after *in vitro* gastrointestinal digestion in a Caco-2 cell inflammation model. The levels of pro-inflammatory cytokines (IL-6, TNF-α) and the pro-angiogenic chemokine IL-8, the expression of iNOS and COX-2, as well as the inhibitory activity against COX-1 and COX-2 were determined.

5.2. Results and discussion

In the present work, we investigated the effect of digested *Ribes* PEEs on intestinal inflammatory parameters using a Caco-2 cell model. For this purpose, gene expression of the inflammatory enzymes COX-2 and iNOS, the secretion of cytokines and chemokines (TNF-α, IL-6 and IL-8), and the inhibitory effects towards COX-1 and COX-2 enzymes was measured.

5.2.1. Cytotoxicity of the intestinal digested polyphenol-enriched extract (ID-PEE) from Chilean currants on intestinal Caco-2 cells

The cytotoxicity of the ID-PEEs was assessed to avoid death interference and to establish the concentrations to be used during the subsequent experiments. Cell proliferation was assessed by means of the MTT reduction assay after the incubation with each ID-PEE for 24 h. The extracts were devoid of toxicity towards Caco-2 cells (data not shown). In agreement with our results, the PEEs from *R. magellanicum* and *R. punctatum* were not toxic towards human gastric epithelial cells (AGS) at concentrations up to 500 µg/mL (Jiménez-Aspee et al., 2016c). Taking into account our results, the maximum concentration was set at 500 µg/mL for the subsequent experiments. The employed concentrations correspond to 93.5 and 101.5 µg gallic acid equivalents (GAE)/mL for *R. magellanicum* and *R. punctatum*, respectively (Burgos-Edwards et al., 2017). The concentration used are in agreement with physiologically relevant doses, since after the consumption of a polyphenol rich source, these compounds reach the intestinal level at concentrations of several hundreds of micromole per liter (Manach et al., 2004).

5.2.2. Effect of ID-PEE from Chilean *Ribes* species on IL-8, IL-6, and TNF-α release

The clone C2BBe1 from Caco-2 cell line was chosen to emulate the human intestinal epithelium due to its capability to develop a more homogeneous brush border than the parental cells (Peterson & Mooseker, 1992). Moreover, they can reproduce the physiopathology of the inflamed intestinal mucosa (Leonard et al., 2010).

Under our experimental conditions, the IL-1β (10 ng/mL) induced the secretion of IL-8, IL-6 and TNF-α by the Caco-2 cell monolayer, similar to the observations of Leonard et al. (2010). Without the IL-1β stimulus, the cells secreted background levels of IL-8, TNF-α, and IL-6 of about 20, 30,

and 35 pg/mL, respectively. The treatment for 24 h with IL-1β significantly raised ($p < 0.05$) the concentration of TNF-α and IL-6 by almost three-fold, while IL-8 levels were increased by almost 30 times, compared to the untreated cells (Figure 14).

The pre-treatment of Caco-2 cells with the ID-PEE from *R. magellanicum* did not significantly reduce the secretion of IL-8 in response to the IL-1β stimulation, compared to the inflamed controls (Figure 14). Interestingly, the pre-treatment of Caco-2 cells with the ID-PEE from *R. punctatum* significantly decreased by 32 % and 23 % the IL-8 levels at 500 and 250 µg/mL, respectively. The observed differences between both species might be related to their polyphenol content and composition. Several flavonoids can inhibit IL-8 over-secretion in IL-1β-stimulated Caco-2 cells (Romier et al., 2008). In this sense, the total flavonoid content was higher in the ID-PEE of *R. punctatum*, whereas *R. magellanicum* ID-PEE presented higher anthocyanin content (Burgos-Edwards et al., 2017). In addition, the ID-PEE of *R. punctatum* showed the presence of several dihydroquercetin (taxifolin) derivatives that were not found in the *R. magellanicum* samples (Burgos-Edwards et al., 2017). In murine bone marrow and LPS-stimulated dendritic cells, dihydroquercetin-3-glucoside inhibited the production of cytokines and NO (Kim, Choi, Lee, & Lee, 2008). Moreover, the structurally related flavanone dihydrokaempferol decreased the IL-8 production in a keratinocyte cell line (Venditti et al., 2013). Hence, dihydroquercetin derivatives from *R. punctatum* might contribute to the observed IL-8 reduction in cells treated with the ID-PEE.

It is noteworthy that not all polyphenol extracts show the same inhibitory effects towards the IL-8 secretion in Caco-2 cells. For example, Romier-Crouzet et al. (2009) evaluated polyphenol-enriched extracts from pomegranate, oak, grape seed, sugar cane, cocoa and mangosteen on the over-secretion of IL-8 levels. The authors reported that the best effect was found in pomegranate and oak, a moderate effect was found for sugar cane and grape seed, while cocoa and mangosteen were devoid of activity. In the same intestinal model, the polyphenol-rich extracts of cranberry bean

(*Phaseolus vulgaris*) reduced IL-8 levels at all tested doses, reaching complete inhibition at the highest concentration (Chen et al., 2017). A few *in vitro* studies on the effect of berries on the IL-8 secretion at the intestinal level could be found. Most of the studies were assessed at the gastric level using human gastric epithelial adenocarcinoma (AGS) cells. Blackberry (*Rubus fruticosus*), raspberry (*Rubus idaeus*), wild strawberry (*Fragaria vesca*), and strawberry (*Fragaria* × *ananassa*) decreased the high levels of IL-8 in AGS cells (Sangiovanni et al., 2017). The pre-treatment of a Caco-2/Raw264.7 model with a *Ribes nigrum* extract, submitted to simulated gastrointestinal digestion, reduced the IL-8 mRNA expression by 54 % (Olejnik et al., 2016). In comparison, the ID-PEE of *R. punctatum* showed slightly less inhibition on the secretion of this chemokine, probably due to the lower doses employed in our experiments. Similarly, phenolic compounds from *Aronia melanocarpa* submitted to GID decreased the secretion of IL-8 in a Caco-2/endothelial co-culture model (Wu et al., 2018). Our work is the first report addressing the IL-8 modulation by polyphenols from Chilean currants.

The expression of the IL-8 chemokine is found to be up-regulated in the colonic mucosa of patients with active UC and CD (Sartor, 2006). The rise of IL-8 during inflammation plays an important role in the chemotaxis and activation of immune cells, such as neutrophils, monocytes, and eosinophils. These cells produce free radicals in response to the stimulus, triggering oxidative stress and even cancer if the inflammation persists (Ribeiro et al., 2015). In addition, it has been reported that the overexpression of IL-8 increases the rate of colon cancer cell migration and invasion. This chemokine is also involved in angiogenesis, which is associated with tumorigenesis and growth, as well as resistance to chemotherapeutics drugs (Ning et al., 2011). Thus, naturally-occurring compounds from fruits might serve as IL-8 regulators, helping to control active inflammatory-related diseases. In this sense, our results suggest that *R. punctatum* fruits might be a good source of bioactive polyphenols potentially useful to prevent IL-8 over-secretion.

Cytokines are considered as biomarkers of chronic inflammation-related diseases, including IBD. TNF-α and IL-6 are the most well-studied cytokines and constitute drug targets in the treatment of chronic inflammation. These cytokines are over-secreted by inflamed tissues and are found in higher levels in patients suffering this type of illness (Leyva-López et al., 2016).

We observed that the treatments with digested polyphenols from the two Chilean currants were able to significantly decrease the secretion of IL-6 and TNF-α in Caco-2 cells. The levels of TNF-α in medium from cells incubated with ID-PEEs were lower than that of the positive inflammation control (Figure 14). The inhibition percentages ranged from 51 to 85 % for *R. magellanicum* and 79 to 89 % for *R. punctatum* at the different concentrations assayed. Similarly, the IL-6 concentrations were significantly lower in cells treated with ID-PEE of *R. magellanicum*. At 250 µg/mL, a reduction of 70 % was observed, whereas at 500 µg/ mL, the IL-6 levels were similar to the negative control (Figure 14). In a similar way, the digested extract of *R. punctatum* significantly prevented, in a dose-dependent manner, the production of IL-6 at three of the four tested concentrations. At 500 and 250 µg/mL, the concentration of IL-6 in the cell media was maintained close to the negative control, while at 125 µg/mL, it was reduced by 67 % compared to the inflammation control (Figure 14). These results are in agreement with those observed for the European relative *R. nigrum* in several inflammation models. Both, the undigested and the *in vitro* gastrointestinal digested extracts of *R. nigrum*, decreased the IL-6 and TNF-α mRNA levels, in an inflamed Caco-2/RAW264.7 co-cultured cell model (Olejnik et al., 2016). Huebbe et al. (2012) observed the same reduction in the mRNA levels of TNF-α employing only RAW264.7 cells, after the pre-incubation with a *R. nigrum* polyphenol-rich juice. Furthermore, the anthocyanin-rich extract from *R. nigrum* fruits reduced the secretion of TNF-α and IL-6 in LPS-stimulated acute monocytic leukemia (THP-1) cells, suggesting that anthocyanins are mainly responsible for this activity (Lyall et al., 2009).

Although both Chilean currants decreased IL-6 and TNF-α secretion, *R. punctatum* was the most active. Thus, as we pointed out above, the regulation of these cytokines might also be associated with the high content and variety of flavonoids occurring in *R. punctatum* (Burgos-Edwards et al., 2017). In agreement with our results, Olejnik et al. (2016) suggested that anthocyanins might have only a partial contribution to the inflammation-preventive effect of *R. nigrum* extracts. Flavonoids in general, and particularly quercetin and its derivatives, have been well characterized as TNF-α and IL-6 suppressors (Ribeiro et al., 2015). In addition, dihydroquercetin-3-glucoside showed inhibition of TNF-α production in bone marrow and splenic dendritic cells (Kim et al., 2008).

The regulation of the pro-inflammatory cytokine TNF-α by Chilean native fruit extracts have been previously reported. In LPS-stimulated RAW264.7 cells pre-treated with maqui and calafate extracts a reduction in the gene expression of TNF-α was observed (Reyes-Farias et al., 2015). In addition, rats fed with white strawberries (*Fragaria chiloensis*) showed a decreased gene expression of TNF-α, IL-6, and IL-1β in the liver, as well as lower serum concentrations of these cytokines compared to the controls (Molinett et al., 2015).

Several studies propose the implication of the inflammatory mediators TNF-α and IL-6 in the pathogenesis of IBD. During inflammation, the intestinal resident cells release cytokines. Both TNF-α, and IL-6 stimulate the production of adhesion molecules and endothelial activation, as well as binding and recruitment of polymorphonuclear cells and monocytes to the inflammatory focus (Sartor, 2006). The constant infiltration of immune cells and the release of oxidant species generate lesions to the tissue (Ribeiro et al., 2015). TNF-α induces the synthesis of IL-6, other cytokines and eicosanoids. IL-6 mediates the change of the inflammatory status, from acute to a chronic condition. In addition, it has been reported that IL-6 is produced by several types of cancer cells (Leyva-López et al., 2016). Therefore, the selective inhibitors of IL-6 and TNF-α are effective in the control of active IBD (Biasi et al., 2011; Leyva-López et al., 2016). The polyphenols from Chilean currants *R.*

magellanicum and especially *R. punctatum* seem to down-regulate cytokine and chemokine secretion in an intestinal cell model of inflammation, at physiologically relevant doses even after simulated intestinal digestion.

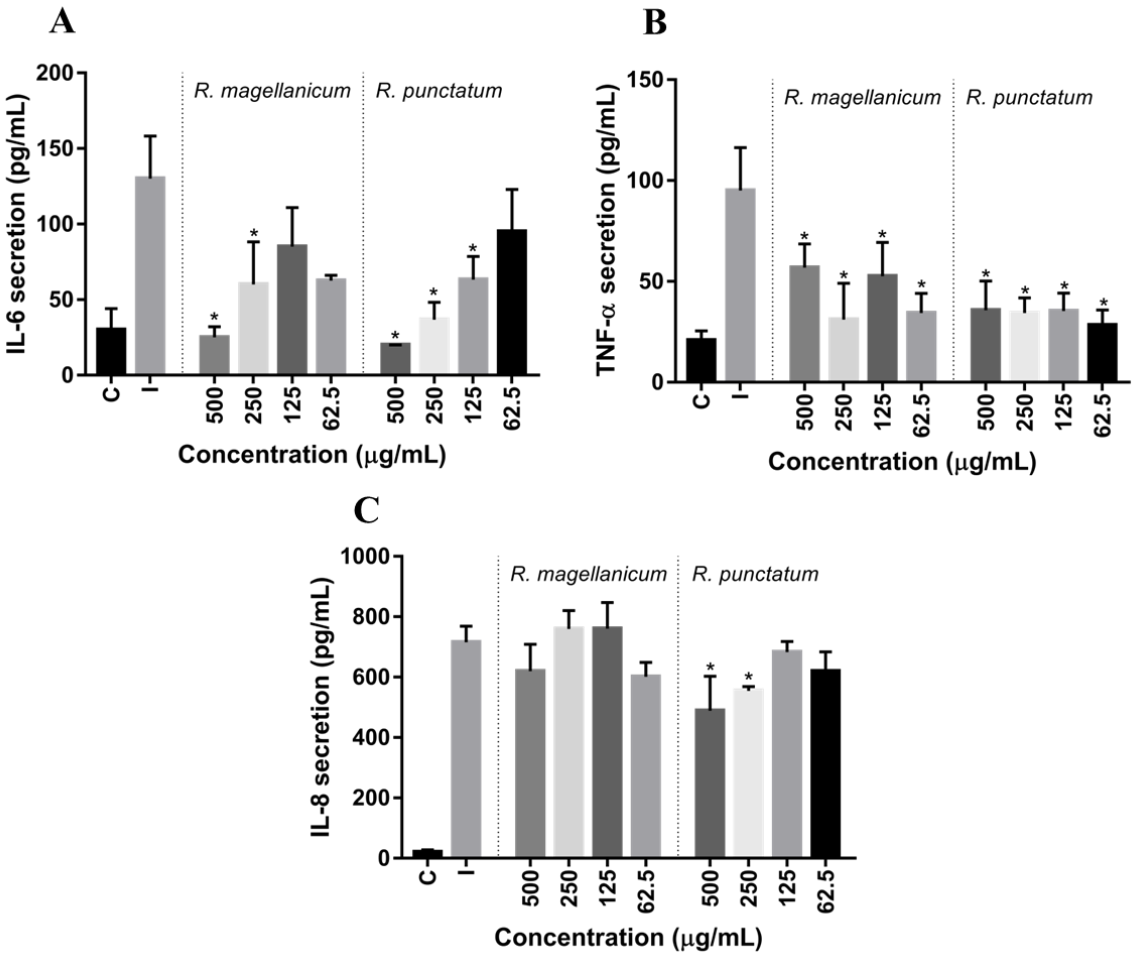

Figure 14. Effect of intestinal-digested polyphenol-enriched extracts (ID-PEE) from *R. magellanicum* and *R. punctatum* on the secretion of cytokines and chemokines A) IL-8; B) TNF-α; and C) IL-6 in intestinal Caco-2 cells stimulated with interleukin-1β (IL-1β). Letters C and I, means negative and inflammation controls, respectively. The results were expressed as means ± SD (n = 3). The symbol (*) on the bars show significant differences of each treatment compared to the inflammation control (Student's t test; $p < 0.05$).

5.2.3. Effect of the digested PEEs on COX-2 and iNOS expression in Caco-2 cells

The enzymes COX-2 and iNOS are over-expressed in inflammatory disorders, and IBDs are not an exception. The characteristic cytokine over-production occurring in active IBDs induces the activation of signaling pathways with transcription of enzymes, including iNOS and COX-2 (Leyva-López et al., 2016). These enzymes are responsible for the synthesis of prostaglandins (PGs) and nitric oxide (NO), respectively. Both are considered to be potent pro-inflammatory mediators with involvement in the pathogenesis of several types of cancer (Surh et al., 2001).

The results of the treatments with ID-PEE from each Chilean currant on the gene expression of COX-2 and iNOS in Caco-2 C2BBe1 cells are shown in Figure 15. The ID-PEE of *R. magellanicum* decreased by 63 % and 88 % the mRNA expression of COX-2 at 250 and 500 µg/mL, respectively ($p < 0.05$). Similarly, the iNOS mRNA expression was downregulated by 43 % and 58 % at 250 and 500 µg/mL, respectively, compared to the inflammation control (Figure 15). The ID-PEE of *R. punctatum* showed higher reductions in the mRNA expressions of the mentioned enzymes compared to the ID-PEE from *R. magellanicum*. The ID-PEE from *R. punctatum* significantly decreased the COX-2 gene expression at all tested concentrations, reaching a complete inhibition at 500 µg/mL. The iNOS mRNA levels were also significantly reduced after the treatments at 500, 250, and 125 µg/mL (Figure 15).

The anti-inflammatory activity of *R. nigrum* (black currant) is the most well characterized among *Ribes* species, including the COX-2 and iNOS gene expression. The gastro-intestinally digested extract from *R. nigrum* decreased the mRNA levels of COX-2 and iNOS by 44 % and 15 %, respectively, in a Caco-2/RAW264.7 co-cultured model (Olejnik et al., 2016). The treatment with black currants also down-regulated the mRNA levels of iNOS in LPS-induced RAW 264.7 murine macrophages (Huebbe et al., 2012). Boivin et al. (2007) observed that *R. nigrum*, *R. sativum* and *R.*

hirtellum inhibited the expression of COX-2 by 43 %, 49 %, and 83 %, respectively, in prostatic adenocarcinoma cells (PC-3), while *R. rubrum* did not show any anti-inflammatory activity. In addition, the anthocyanin-rich extract of *R. nigrum* also decreased the up-regulated levels of COX-2 expression at hepatic level in rats (Bishayee et al., 2013). It has been reported that cyanidin-3-glucoside and cyanidin-3-rutinoside down-regulate iNOS and COX-2 gene expression (Jung et al., 2014). Cyanidin-3-glucoside and cyanidin-3-rutinoside are the main anthocyanins occurring in the studied *R. magellanicum* and *R. punctatum* fruits. However, the digested extract of *R. punctatum* showed more activity than *R. magellanicum*, despite having a slight less anthocyanin content (Burgos-Edwards et al., 2017). This differential activity could be associated to the higher flavonoid content of *R. punctatum*, contributing to the anti-inflammatory effect.

Regarding other Chilean berries, few *in vitro* studies have been focused on the expression of these pro-inflammatory enzymes. It was reported that maqui polyphenolic extracts reduced the expression of COX-2 and iNOS, as well as PGE_2 and NO release in RAW264.7 macrophages (Schreckinger, Wang, Yousef, Lila, & Gonzalez de Mejia, 2010). These results were supported by Céspedes-Acuña et al. (2018), who observed that different varieties of maqui berry inhibit COX-2 and iNOS gene expression in the same cell line. It has been reported that calafate berry also decreases iNOS gene expression in RAW264.7 cells (Reyes-Farias et al., 2015). However, none of these reports considered the influence of the GID on the content and composition of the polyphenols.

COX-2 is over-expressed in inflamed tissues, where this enzyme is responsible for the synthesis of PGE_2. This eicosanoid enhances metastatic potential of cancer cells by decreasing apoptosis, promoting cell proliferation and angiogenesis (Desai et al., 2018). As previously mentioned, iNOS is also expressed as a response to inflammation, producing NO. Although low levels of NO have important physiological functions, its over-production may become harmful. NO is involved in the generation of powerful oxidant reactive nitrogen species with cytotoxic effects as well as tumor

progression through angiogenesis (Soufli, Toumi, Rafa, & Touil-Boukoffa, 2016; Surh et al., 2001). High levels of nitrite/nitrate have been found in the lumen of the colon of IBD patients and in those within the active phase of UC and CD (Soufli et al., 2016). Therefore, the excessive COX-2 and iNOS expression has been associated with the pathogenesis of IBD and may lead to tumor development. Our results suggest that the polyphenols from the studied Chilean currants, after GID, are able to reduce the expression of these pro-inflammatory genes in an *in vitro* intestinal inflammation cell model.

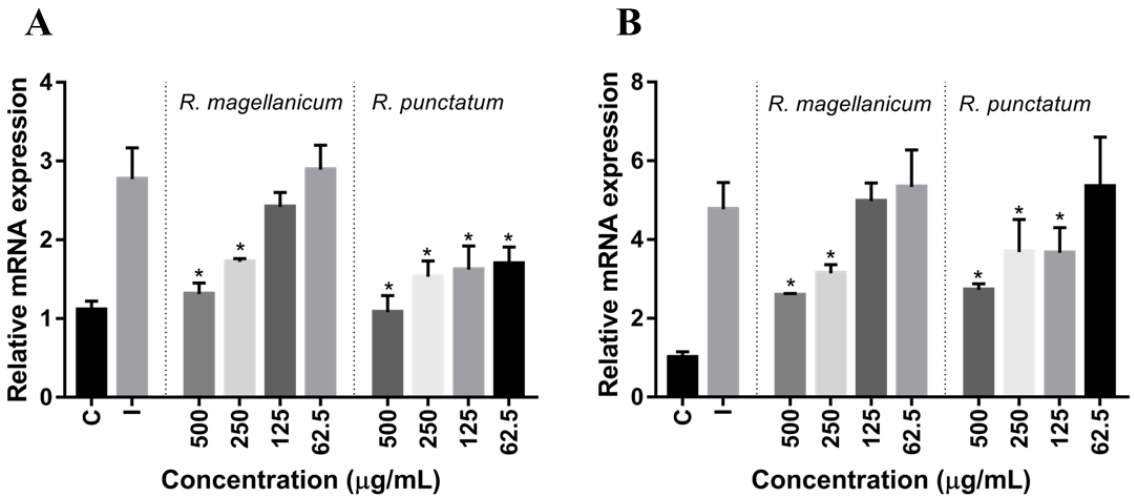

Figure 15. Effect of the intestinal-digested polyphenol-enriched extracts (ID-PEE) from *R. magellanicum* and *R. punctatum* on the relative mRNA expression of A) COX-2; and B) iNOS in intestinal Caco-2 cells stimulated with interleukin 1β (IL-1β). Letters C and I, means negative and inflammation controls, respectively. The results were expressed as means ± SD (n = 3). The symbol (*) on the bars show significant differences of each treatment compared to the inflammation control (Student's t test; $p < 0.05$).

5.2.4. Inhibitory activity of Chilean currants digested extracts towards COX-1 and COX-2

Desai et al. (2018) proposed that polyphenols might prevent inflammation and cancer by means of the inhibition of cyclooxygenases (COX). COX-1 is a constitutive enzyme expressed along the gastrointestinal tract (GI); while COX-2 is and inducible enzyme expressed only in inflammatory

conditions in the GI (Desai et al., 2018). In the present work, the inhibitory capacity of the non-digested and digested PEEs from *R. magellanicum* and *R. punctatum* towards COX-1 and COX-2 was assessed.

The inhibition percentages, induced by *R. magellanicum* and *R. punctatum* PEEs, towards COX-1 and COX-2 are shown in Table 18. The PEEs from both species inhibited COX-1 in the range of 80-89 %, while the inhibition of COX-2 was in the range of 89-99 %. After the gastric step, the inhibition of COX-1 was in the range of 78-89 %, and for COX- 2 64-97 %. The PEE obtained after the intestinal digestion inhibited COX-1 by 77-89 %, while the inhibition of COX-2 was in the range of 59-99 %. These results point out that the inhibitory effect of the polyphenols from *R. magellanicum* and *R. punctatum* withstand the simulated digestion process. In line with the results described above, the PEE of *R. puntatum* was the most active. The inhibitory activity was slightly higher than that reported for a *R. nigrum* extract at 40 µg/mL, which inhibited by 78 and 71 % COX-1 and COX-2, respectively (Strugała et al., 2016). The inhibition towards COX-2 decreased after the simulated digestion in both PEEs at 25 µg/mL, mainly after the intestinal step. The highest reduction was observed for *R. magellanicum*, possibly due to the flavonoid loss resulting from the simulated digestion. The PEE from *R. magellanicum* shows a higher content of anthocyanins than the PEE from *R. punctatum*. These compounds are more sensitive to the pH changes occurring in the digestion, being more affected than other polyphenols (Burgos-Edwards et al., 2017).

The non-steroidal anti-inflammatory drugs (NSAIDs) are COX inhibitors usually prescribed to ameliorate pain and inflammation in patients. Under our experimental conditions, the positive control indomethacin showed IC_{50} values of 0.08 and 0.01 µg/mL, for COX-1 and COX-2, respectively. However, indomethacin is not devoid of adverse effects such as dyspepsia, esophagitis, among others (Leyva-López et al., 2016). The PEEs from both Chilean currants show *in vitro* anti-inflammatory effect, with sustained activity despite the simulated GID process. Our

results suggest that polyphenols from *R. magellanicum* and *R. punctatum* might be helpful in ameliorating IBDs. However, further *in vivo* studies are needed to corroborate these effects.

Table 18. Percentage of inhibition of the PEEs from *Ribes magellanicum* and *R. punctatum* towards human COX-1 and COX-2.

Samples	Inhibition of COX-1 (%)		Inhibition of COX-2 (%)	
	250 µg/mL	25 µg/mL	250 µg/mL	25 µg/mL
R. magellanicum				
PEE	80.33 ± 0.45	88.45 ± 0.00	97.90 ± 0.20	89.12 ± 0.35
GD-PEE	80.89 ± 0.00	77.89 ± 2.32	97.14 ± 0.28	64.31 ± 0.58
ID-PEE	80.44 ± 0.95	88.69 ± 1.10	88.63 ± 1.56	59.16 ± 6.71
R. punctatum				
PEE	80.22 ± 3.03	81.21 ± 0.46	98.9.3 ± 0.00	94.22 ± 0.42
GD-PEE	79.12 ± 2.19	88.80 ± 1.27	96.41 ± 0.17	77.37 ± 3.82
ID-PEE	78.90 ± 1.88	76.50 ± 1.52	98.86 ± 1.07	75.33 ± 2.19
Indometacin*	IC_{50} = 0.08 ± 0.01 µg/mL		IC_{50} = 0.01 ± 0.00 µg/mL	

PEE: phenolic-enriched extract; PEE-GD: gastric digested phenolic-enriched extract; ID-PEE: intestinal digested phenolic-enriched extract; COX-1: cyclooxygenase 1; COX-2: cyclooxygenase 2; *reference compound.

Chapter 6

Prebiotic effect of *in vitro* gastrointestinal digested polyphenolic enriched extracts of Chilean currants (*Ribes magellanicum* and *Ribes punctatum*)

The information contained in this chapter was formatted as a manuscript and submitted to Food Research International. The article is currently under revision.

6.1. Introduction

The human gut microbiota is a group of commensal microorganisms, comprising bacteria, fungi, viruses, and protozoa that inhabit the intestinal tract. It contributes to maintain normal physiology through defense against pathogens, synthesis of vitamins, amino acids, and metabolites (Singh et al., 2017). Diet influences gut microbiota (De Filippo et al., 2010). A high intake of digestible saccharides, animal-derived fats and proteins, together with a low intake of diet fiber (so-called "Western diet") decrease the presence of health-promoting species in gut microbiota such as: *Faecalibacterium prausnitzii*, *Akkermansia muciniphila*, *Lactobacillus spp*., *Bifidobacterium spp*., *Clostridium* cluster XIVa; as well as bacterial diversity (Healey, Murphy, Brough, Butts, & Coad, 2017; Tuohy et al., 2012). Western diet also decreases the generation of beneficial metabolites, for instance short-chain fatty acids (SCFA) (Tan et al., 2014; Verbeke et al., 2015), increase toxic fermentation products and produces a gut microbiota enrichment of potentially detrimental bacteria (Blachier et al., 2017; Windey, De Preter, & Verbeke, 2012). The tight diet-microbiota relation and its implication in health, encourage the investigation of bioactive components in food as a novel therapeutic approach.

Polyphenols are naturally occurring compounds with a wide range of health-promoting properties. These compounds may modulate the bacterial communities in the gut (Duda-Chodak et al., 2015; Tuohy et al., 2012). Individual polyphenols such as 3-caffeoylquinic acid (3-CQA), 5-caffeoylquinic acid (5-CQA), quercetin-rutinoside and genistin display bifidogenic effects (Mayta-Apaza et al., 2018). Anthocyanins and flavan-3-ol monomers promote *Bifidobacterium* and *Lactobacillus* abundance (Hidalgo et al., 2012; Tzounis et al., 2008); while flavan-3-ol and 5-CQA increase the butyrate-producer group *Clostridium coccoides–Eubacterium rectale* (Mills et al., 2015; Tzounis et al., 2008). As expected, polyphenol-rich extracts seem to modulate the microbiota. The extent of the effect and the strains involved depends on the polyphenolic profile of the source. Among berries, blueberry (Vendrame et al., 2011) and blackcurrants (Molan et al., 2014) promote the growth of *Lactobacillus* and *Bifidobacterium* species in healthy humans. The last one also inhibits potential *Clostridium pathogenic* species. Cranberry supplementation to obese mice led to higher abundance of *A. muciniphila* population, which is associated with beneficial metabolic effects (Anhê et al., 2015).

The Chilean currants *Ribes magellanicum* and *Ribes punctatum* are a rich source of hydroxycinnamic acids (HCA), flavonols, dihydroflavonols, and anthocyanins (Jiménez-Aspee et al., 2016b). Therefore, these berries may be a good candidate for prebiotic supplementation.

In addition, these fruits exhibit interesting bioactivities. Their polyphenolic-enriched extracts (PEEs) show antioxidant activity through several *in vitro* methods, maintaining or increasing them throughout gastrointestinal digestion (Burgos-Edwards et al., 2017) or under simulated colonic conditions (Burgos-Edwards, Jiménez-Aspee, Theoduloz, & Schmeda-Hirschmann, 2018), respectively. The PEEs are cytoprotective against stress induced by oxygen peroxide and methylglyoxal (Jiménez-Aspee et al., 2016b; 2016c), by increasing the detoxifying enzymes such as catalase, superoxide dismutase, glutathione peroxidase and reductase (Theoduloz et al., 2018).

The polyphenol profile undergoes considerable modifications during the gastrointestinal tract (Burgos-Edwards et al., 2017). Therefore it is recommended to take into account its influence. In this sense, the *in vitro* digestion model is a valid tool, allowing the consideration of such impact on polyphenols before the assessment of their bioactivity (Brown et al., 2014).

To date, the effect of *in vitro* colonic fermentation on the polyphenols from Chilean currants and its impact on its bioactivity have been described (Burgos-Edwards et al., 2018). However, no information could be found about the influence of their polyphenols on gut bacteria. Therefore, this study aimed to assess the potential impact of gastrointestinal digested PEEs from *R. magellanicum* and *R. punctatum*, on the growth of bacterial groups as well as the pH, ammonia content and SCFA formation, by means of batch-culture fermentation system with feces from healthy human donors.

6.2. Results and discussion

The polyphenolic-enriched extracts (PEEs) from two Chilean currants (*R. magellanicum* and *R. punctatum*) were assessed for prebiotic activity through the measurement of the pH, ammonia, branched chain fatty acids (BCFA), short chain fatty acids (SCFA), and six colonic bacterial taxa during a simulated colonic fermentation for 24 h.

6.2.1. pH and ammonia variations throughout *in vitro* fermentation

Fecal pH and ammonia content are parameters associated with colon health. Both are considered indirect indicators of bacterial fermentation and metabolites production (Yao et al., 2016). Therefore, we monitored both parameters at four time-points (1, 4, 8, and 24 h) along the *in vitro* fermentation experiments. FOS treatments significantly decreased ($p < 0.05$) the pH of the medium at 4, 8 and 24 h after exposure respect to the non-treated control (Figure 16). Other authors reported similar results (Cantu-Jungles et al., 2018; Stewart, Timm, & Slavin, 2008) in which the pH drop

was attributed to the SCFA generated from FOS fermentation, leading to a more acidic environment. The pH of the samples treated with Chilean currants ID-PEEs and the non-treated control showed no significant ($p < 0.05$) differences (Figure 16). In the same way, fecal pH remained unaffected after cranberry supplementation to healthy adults (Rodríguez-Morató, Matthan, Liu, de la Torre, & Chen, 2018). However, a reduced fecal pH was observed after dietary intervention with black currant (*Ribes nigrum*) commercial extracts in healthy subjects (Molan et al., 2014). Changes in fecal pH after consumption of berries are probably due to their insoluble fiber content rather than their polyphenols (Jakobsdottir, Nilsson, Blanco, Sterner, & Nyman, 2014). The maintenance of a low pH may be beneficial; however, in a neoplasic colon, this might contribute to carcinogenesis (Blachier et al., 2017).

Regarding the ammonia content, samples with the ID-PEEs and the non-treated control showed no significant ($p < 0.05$) differences (Figure 16). Other polyphenol sources influenced this parameter with divergent results. Ammonia production remained unchanged after 24 h of fermentation with mango peel extracts in a TNO (Toegepast-Natuurwetenschappelijk Onderzoek) *in vitro* model of the colon (TIM-2), increasing it among 48 and 72 h (Sáyago-Ayerdi et al., 2019). Cranberry and grape seed polyphenols also increased ammonium production in a dynamic gastrointestinal simulator, the so-called SHIME (Sánchez-Patán et al., 2015). On the other hand, orange juice (Duque, Monteiro, Tallarico Adorno, Sakamoto, & Sivieri, 2016), black tea and red wine grape extracts (Kemperman et al., 2013) reduced its formation, also in a SHIME model. FOS treatment attenuated significantly ($p < 0.05$) the ammonia increment among 4 and 24 h of incubation (Figure 16). In our study, FOS as non-digestible carbohydrate may act as carbon source, delaying ammonia accumulation from protein fermentation (Verbeke et al., 2015; Windey et al., 2012). The catabolism of proteins by bacteria leads to potentially harmful metabolites, including ammonium, amines, cresols, indoles, and phenols (Blachier et al., 2017; Yao et al., 2016). In fact, the excessive protein

fermentation is associated with the pathogenesis of IBD and colorectal carcinogenesis (Windey et al., 2012). Therefore, the modulation of protein fermentation through dietary supplementation might be useful to prevent the excessive accumulation of its metabolites.

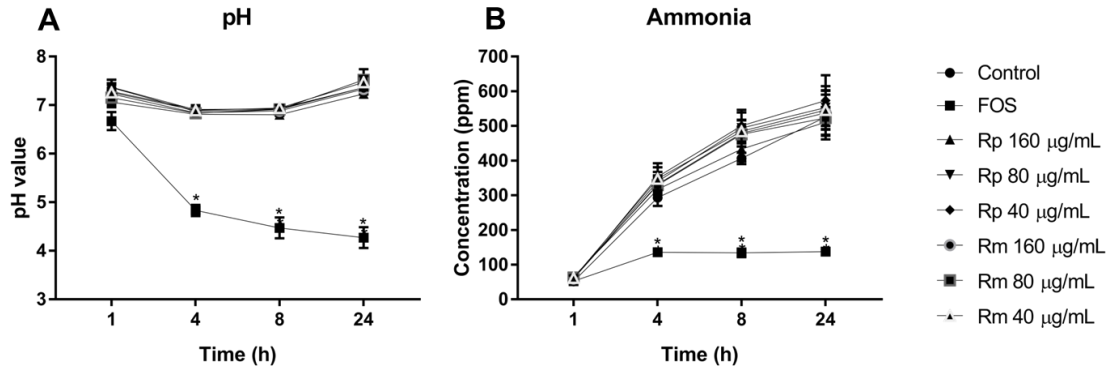

Figure 16. pH and ammonia variations during *in vitro* colonic fermentation of *Ribes punctatum* (Rp) and *R. magellanicum* (Rm) at 40, 80 and 160 µg/mL. The results are expressed as mean ± SEM (n = 3).The symbol (*) point out significant differences ($p < 0.05$) among control and samples, by the Student's t-test.

6.2.2. Branched-chain fatty acids (BCFA) production

BCFA are considered specific markers of protein fermentation as they are produced exclusively from amino acids (Windey et al., 2012; Yao et al., 2016). Therefore, we monitored variations in isobutyric and isovaleric acids and the total sum (Total BCFA) throughout the fermentation experiment (Figure 17). FOS decreased total BCFA by 75-96 % compared to the negative control. These reductions were significant ($p < 0.05$) after 8 and 24 h; supporting the potential displacement of amino acids, as a carbon source by FOS, as we observed for ammonia (Verbeke et al., 2015; Windey et al., 2012). Among currants, *R. magellanicum* dose-dependently decreased total BCFA ($p < 0.05$) at 24 h respect to the non-treated control (Figure 17); with reductions by 45 % and 52 % at 80 and 160 µg/mL, respectively. *R. punctatum* treatments showed the same trend in total BCFA, but only the diminution by 37 % of isobutyric acid was significant ($p < 0.05$), after 24 h of incubation at 160 µg/mL. Extracts-induced changes in bacterial BCFA production have been previously

informed. Pre-digested mango peel extract reduced isobutyric acid after 24 h of incubation within a TIM-2 model, in agreement with our results (Sáyago-Ayerdi et al., 2019). Cranberry and grape seed polyphenolic extracts did not elicit any changes in BCFA within SHIME (Sánchez-Patán et al., 2015). Additionally, in a study with rats fed with fiber enriched with polyphenol-rich extracts, it was informed that neither strawberry, blackcurrant or chokeberry supplementations were able to alter isobutyric and isovaleric acids in caecum (Kosmala, Zduńczyk, Karlińska, & Juśkiewicz, 2014).

Although BCFA and ammonia are produced by protein fermentation (Yao et al., 2016), only the first ones were reduced by ID-PEEs under our experimental conditions. These data suggest a potential influence of Chilean currants polyphenols on protein fermentation by human colonic bacteria. The fact that ammonia production was not altered could be due to the alternative formation of ammonia by urea hydrolysis; meanwhile, the measured BCFA derive exclusively from valine and leucine (Blachier et al., 2017; Windey et al., 2012).

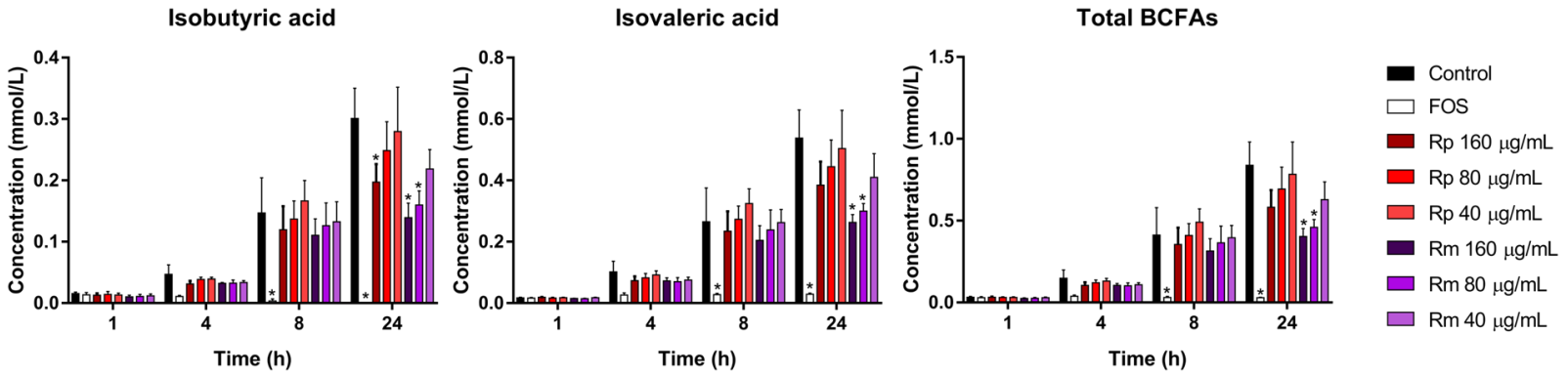

Figure 17. Branched-chain fatty acids (BCFA) formation during simulated colonic fermentation with the intestinal digested polyphenols from *R. punctatum* (Rp) and *R. magellanicum* (Rm) at 40, 80 and 160 µg/mL. The results are shown as mean ± SEM (n = 3). Significant differences ($p < 0.05$) in Student's t-test between treatments and control are indicated (*) in the graphics.

6.2.3. Short chain fatty acids (SCFA) analyses

SCFA are major end products from carbohydrates fermentation by the gut microbiota (Verbeke et al., 2015). Polyphenols from natural sources may regulate this metabolic process (Tuohy et al., 2012). We assessed the potential impact of *R. punctatum* and *R. magellanicum* polyphenols on SCFA production, monitoring SCFA for 24 h at four time-points (Figure 18). In fecal samples, acetic, propionic and butyric acids account for 95 % of the measured SCFAs, in a proportion of approximately 60:20:20, respectively (Flint, Scott, Louis, & Duncan, 2012; Tan et al., 2014; Verbeke et al., 2015). Under our experimental conditions, the main SCFA reached 94 %, in a molar ratio of approximately 57:19:18 (acetic, propionic and butyric acid) in the control, in line with the previously observed.

Among treatments, FOS increased significantly ($p < 0.05$) the acetic acid content between 4 and 8 h relative to the control (Figure 18). Propionic acid remained unaffected during eight hours, decreasing ($p < 0.05$) after 24 h, whereas butyric acid was higher ($p < 0.05$) in FOS samples at all time-points. However, valeric acid decreased ($p < 0.05$) in FOS treatments between 4 and 24 h. Although FOS increased ($p < 0.05$) caproic acid during the first hour, it was reduced ($p < 0.05$) after 8 and 24 h. The total SCFA significantly increased ($p < 0.05$) with FOS. These results are in agreement with the reported for FOS, yielding acetate and butyrate predominantly over other SCFA (Cantu-Jungles et al., 2018; Stewart et al., 2008). The ID-PEEs did not produce significant changes ($p < 0.05$) in total SCFA. However, the extracts decreased individual SCFA (except for acetic acid) mostly at the final stage of the incubation. ID-PEEs did not induce significant changes ($p < 0.05$) in acetic acid content compared with the control (Figure 18). Propionic and butyric acid decreased ($p < 0.05$) after ID-PEE treatments at 24 h. Reductions account for 22 % in both acids with *R. punctatum* (160 µg/mL); while *R. magellanicum* (160 and 80 µg/mL) reduced propionic acid by 34-46 % and butyric acid by 22-42 %. The valeric acid content decreased ($p < 0.05$) by 40 % and 19-25 % at 4

and 24 h, respectively, with *R. punctatum*. All treatments with *R. magellanicum* affected the valeric acid content, decreasing it by 40 % and 19-38 % after 4 and 24 h of incubation, respectively. Caproic acid was also significantly affected ($p < 0.05$) by ID-PEEs, decreasing by 67 % after eight hours. Past 24 h, *R. punctatum* inhibited its production ($p < 0.05$) by 75-88 % and *R. magellanicum* by 88 %.

Similar effects were reported for red wine grape extract, which reduced butyric acid (Kemperman et al., 2013); pre-digested mango peel, decreasing caproic and butyric acids (Sáyago-Ayerdi et al., 2019); and apple extracts, reducing the sum of acetic, propionic and butyric acids (Bazzocco et al., 2008), employing *in vitro* fermentation methods. On the other hand, cranberry and grape seed polyphenols did not influence SCFA in SHIME (Sánchez-Patán et al., 2015); while black tea raised acetic acid production (Kemperman et al., 2013) and orange juices increased acetic, propionic and butyric acids (Duque et al., 2016). Kosmala et al. (2014) measured SCFA production in rat caecum after the administration of fibers/polyphenol-rich extracts combinations. They reported a decrease in samples with proanthocyanidin-rich extracts, including black currant and chokeberry. In addition, isolated proanthocyanidins reduced SCFA under *in vitro* conditions (Bazzocco et al., 2008). We described the polyphenolic profile of *R. punctatum* and *R. magellanicum* ID-PEEs in a previous work, reporting proanthocyanidin monomers and oligomers in both extracts (Burgos-Edwards et al., 2017). They might be contributing to the observed SCFA inhibition.

SCFA may act as an energy source, anti-inflammatory, antitumorigenic, gut integrity promoters, and antimicrobial against pathogens (Tan et al., 2014; Verbeke et al., 2015; Windey et al., 2012). Thus, high SCFA generation may be involved in the beneficial effects of prebiotics (Tan et al., 2014). On the other hand, Tuohy et al. (2012) suggested that the *in vitro* inhibition of SCFA by polyphenols might be beneficial under *in vivo* conditions. Such inhibition may prolong SCFA

production until the distal colon, preventing the increase of potentially harmful proteolysis-derived metabolites.

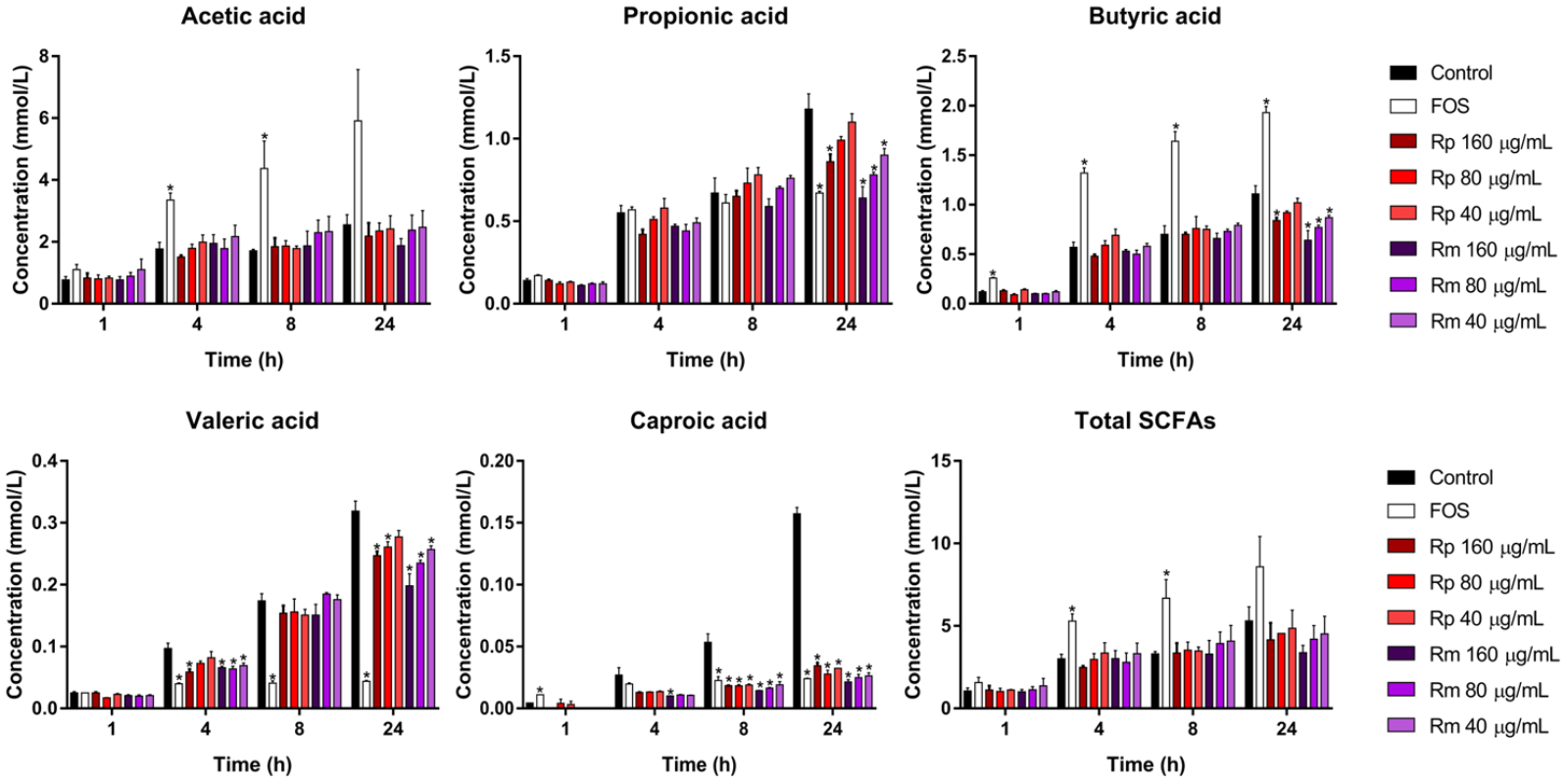

Figure 18. Production of short chain fatty acids (SCFA), after simulated colonic fermentation with the intestinal digested polyphenols from *R. punctatum* (Rp) and *R. magellanicum* (Rm) at 40, 80 and 160 µg/mL. Results are depicted as mean ± SEM (n = 3). Significant differences ($p < 0.05$) in Student's t-test between treatments and control are indicated (*) in the graphics.

6.2.4. Changes in bacterial populations by Chilean currants digested extracts

The influence of *Ribes* ID-PEEs on human microbiota *in vitro* was investigated by qPCR analyses, addressing total bacteria, three phylogenetic groups, and three specific bacteria. Changes in bacterial abundance elicited by *R. punctatum* and *R. magellanicum* are shown in Figure 19 and Figure 20, respectively.

Low counts of *Clostridium* cluster XIVa (*Clostridium coccoides* group) bacteria have been associated with a higher risk of IBD and colorectal cancer. Thus, their selective regulation through diet is considered as a novel strategy to achieve immunomodulation, maintaining colonic health (Cantu-Jungles et al., 2018; Healey et al., 2017). The ID-PEE of *R. punctatum* promoted a significant ($p < 0.05$) growth in this bacterial group at 160 µg/mL, reaching 0.2 log units over the control (Figure 19). The mentioned occurred at 1 h, without significant differences ($p < 0.05$) at other time-points. *R. magellanicum* ID-PEE augmented ($p < 0.05$) *Clostridium* XIVa cluster population by 0.2-0.26 log units during the first hour of incubation (Figure 20). However, these increments were not maintained. Similarly to Chilean currants, tart cherries polyphenolic-rich extract increased *Clostridium* XIVa cluster growth during *in vitro* fermentation with a SHIME model. The authors attributed the activity to the main components 3-CQA and 5-CQA (Mayta-Apaza et al., 2018). In addition, pure 5-CQA promoted the growth of *Clostridium coccoides-Eubacterium rectale* group (Mills et al., 2015). We detected both mentioned HCA esters in *R. punctatum* and *R. magellanicum* (Burgos-Edwards et al., 2017). Thus, the possible contribution of these HCA to the growth of the *Clostridium* cluster XIVa bacteria should be considered. The duration of the effect is also in agreement with the rapid degradation of these HCA under fermentation conditions (Burgos-Edwards et al., 2018). The flavan-3-ols from both ID-PEE (Burgos-Edwards et al., 2017), might also participate in the growth-promotion of this bacteria, considering that stimulation of *C. coccoides-E. rectale* group by flavan-3-ols was previously

observed *in vitro* (Tzounis et al., 2008). FOS showed an initial increment ($p < 0.05$) of 0.22 log units on this bacterial group; no changes were observed at the middle time-points, decreasing ($p < 0.05$) 0.34 log units after 24 h. Other authors have also observed a decrease in the members of this cluster during *in vitro* incubation with FOS, supporting our results (Cantu-Jungles et al., 2018; Mills et al., 2015).

Among other important members of a healthy gut microbial community are *Lactobacillus* and *Bifidobacterium* species. These bacteria are able to reduce the incidence and severity of intestinal inflammation diseases, to improve gut barrier, to maintain low LPS levels and to prevent colorectal cancer (Duda-Chodak et al., 2015; Healey et al., 2017; Singh et al., 2017). It is relevant to discover growth-promoters of these species as an alternative therapy for the above mentioned conditions. FOS significantly increased ($p < 0.05$) *Bifidobacterium spp.* and *Lactobacillus spp.* populations by 0.99 and 1.70 log units, respectively, at 24 h after exposure (Figure 19). The potential effect of ID-PEE from *R. punctatum* on both bacteria was assessed, without significant changes ($p < 0.05$) during 24 h (Figure 19). Samples treated with *R. magellanicum* did not show a growth-promoter effect ($p < 0.05$) of the mentioned species either (Figure 20). In agreement with our results, wine polyphenols extract, rich in quercetin, flavan-3-ols and anthocyanins, did not affect these bacterial groups under *in vitro* conditions (Sánchez-Patán et al., 2012). In fecal samples from healthy volunteers, cranberry powder did not alter the abundance of *Bifidobacterium* or *Lactobacillus* species either (Rodríguez-Morató et al., 2018). On the other hand, blueberry (*Vaccinium angustifolium*) drink promoted the growth of both mentioned bacteria after six-week consumption in human (Vendrame et al., 2011). These growth-promoter effects were also observed after administration of black currants commercial powders to healthy humans (Molan et al., 2014). Both *Bifidobacterium* and *Lactobacillus* species are increased by anthocyanins *in vitro* (Hidalgo et al., 2012), supporting their possible involvement in berries prebiotic-like activity. The loss of

anthocyanins during simulated GID might explain the absence of growth-promoter effect in ID-PEEs (Burgos-Edwards et al., 2017). Further, polyphenols from *R. punctatum* and *R. magellanicum* are catabolized by the microbiota during *in vitro* fermentation, generating quercetin and luteolin aglycons as metabolites (Burgos-Edwards et al., 2018). It has been reported that flavonoid aglycons, such as quercetin may inhibit the growth of gut bacteria, including *Lactobacillus* and *Bifidobacterium* species (Duda-Chodak et al., 2015).

The butyrate-producing bacterium *Faecalibacterium prausnitzii* is considered an important member of the health colonic community (Flint et al., 2012). Reduced abundance was reported in IBD and obese patients (Healey et al., 2017; Singh et al., 2017). We monitored the effect of the ID-PEEs on *F. prausnitzii* abundance during 24 h, contrasting to the non-treated control. FOS and *R. punctatum* did not produce significant variations ($p < 0.05$) in *F. prausnitzii* population during the first four hours of incubation (Figure 19). After 8 h, *R. punctatum* (160 µg/mL) and FOS increased *F. prausnitzii* population by 0.36 and 0.40 log units, respectively. This growth-promoter effect was maintained ($p < 0.05$) until 24 h, increasing 0.34 log units over control for *R. punctatum* (160 µg/mL) and 0.4 log units for FOS. On the other hand, *R. magellanicum* did not induce significant variations ($p < 0.05$) within 24 h of incubation (Figure 20). Similar results were informed for high-fat diet fed mice, whose gut microbiota was enriched in *Faecalibacterium* species after the administration of Lingonberry (*Vaccinium vitis-idaea* L.) extract; which was linked to reduced inflammation markers (Heyman-Lindén et al., 2016). On the other hand, Mayta-Apaza et al. (2018) informed a decrease in the relative abundance of *Faecalibacterium spp.* after administration of polyphenol-rich tart cherry (*Prunus cerasus*) juice to healthy humans. Our results suggest that *R. punctatum* might promote the growth of the health-promotor bacterium *F. prausnitzii*. This is the first study addressing the effect of polyphenols from *Ribes* species on the mentioned bacteria.

The mucin-degrader bacterium *Akkermansia muciniphila* is also considered a member of the healthy microbiota since its low abundance is associated with obesity, psoriatic arthritis, and IBD (Flint et al., 2012; Singh et al., 2017); therefore, it was addressed in this study. FOS did not significantly changed ($p < 0.05$) bacterial abundance; in fact, the population decreased after 24 h compared to the control. Neither *R. punctatum* nor *R. magellanicum* produced a significant increase ($p < 0.05$) in the population of *Akkermansia muciniphila*, although there was a tendency to increase with *R. punctatum* treatment. Increments showed dose-dependency, and the highest dose increased *A. muciniphila* by 0.2, 0.39, 0.43, and 0.27 log units at 1, 4, 8, and 24 h, respectively (Figure 19). This trend was not observed for *R. magellanicum* samples. This bacterium increased after treatments with polyphenols from black tea and red wine grape extracts within SHIME (Kemperman et al., 2013). Lingonberries also promoted its growth in high-fat diet mice after 11 weeks of administration (Heyman-Lindén et al., 2016). Cranberry consumption did not affect *A. muciniphila* populations in healthy subjects (Rodríguez-Morató et al., 2018); however, its polyphenol-rich extract administrated to mice not only increased *A. muciniphila* populations, it was associated with improved metabolism of glucose and lipids as well as anti-inflammatory effects (Anhê et al., 2015). We observed a dose-dependent trend to increase *A. muciniphila* abundance after *R. punctatum* treatments. The differences among individuals' initial microbiota might have influenced the global data making it difficult to find significant differences. This effect was observed before by other authors. They proposed to classify volunteers based on basal microbiota to avoid wrong interpretations of results (Healey et al., 2017; Mayta-Apaza et al., 2018).

The last monitored bacterium in this study was *Escherichia coli*, whose proliferation inside the colon is associated with higher risk of IBD, unlike the other assessed bacteria (Duda-Chodak et al., 2015; Singh et al., 2017). FOS decreased significantly ($p < 0.05$) its abundance by 1.15 log units at 24 h (Figure 19); whereas *R. punctatum* and *R. magellanicum* did not produce significant changes

($p < 0.05$) compared to the control (Figure 19 and Figure 20). Cranberry and grape seed extracts reduced members of the *Enterobacteriaceae* family within SHIME (Sánchez-Patán et al., 2015). Tzounis et al. (2008) reported that *in vitro* incubation of (+)-catechin at 150 mg/L increases the growth of *E. coli*. We did not observe that effect in Chilean currants, probably due to its low proportion within the extracts (Burgos-Edwards et al., 2017).

Overall, our data agree with a possible healthy modulation of the gut microbiota by the Chilean currants. Both species showed similar growth-promoter influence on *Clostridium* cluster XIVa. *R. punctatum* was the most beneficial, enhancing *F. prausnitzii*, and possibly *A. muciniphila*. As far as we know, this is the first work focused on the prebiotic-like effect of Chilean berries. Although these data needs to be further confirmed with *in vivo* experiments, these fruits might be helpful as a coadjuvant for the treatment and prevention of colonic diseases.

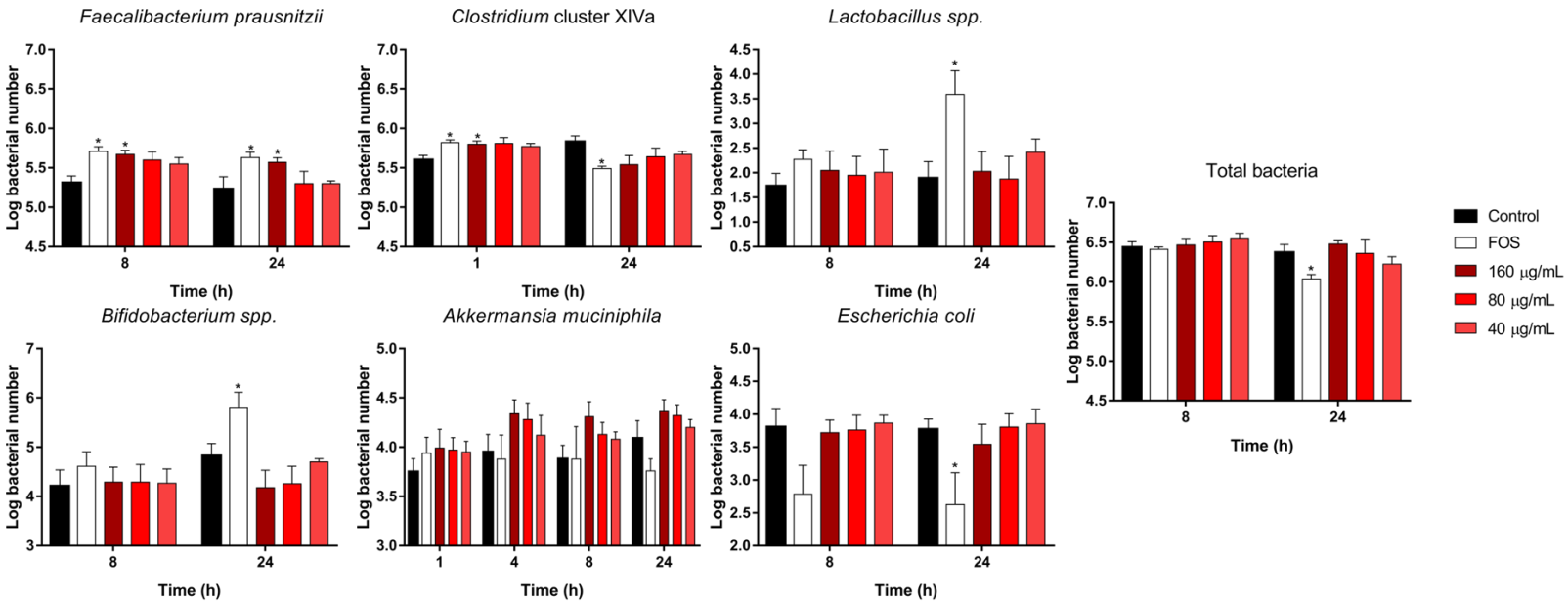

Figure 19. Influence of polyphenols from *R. punctatum* on the human bacterial composition during the simulated colonic fermentation. Results are expressed as Log_{10} bacterial number ± SEM. Statistical significance (Student's t-test, $p < 0.05$) between control and treatments are indicated (*) in the graphics.

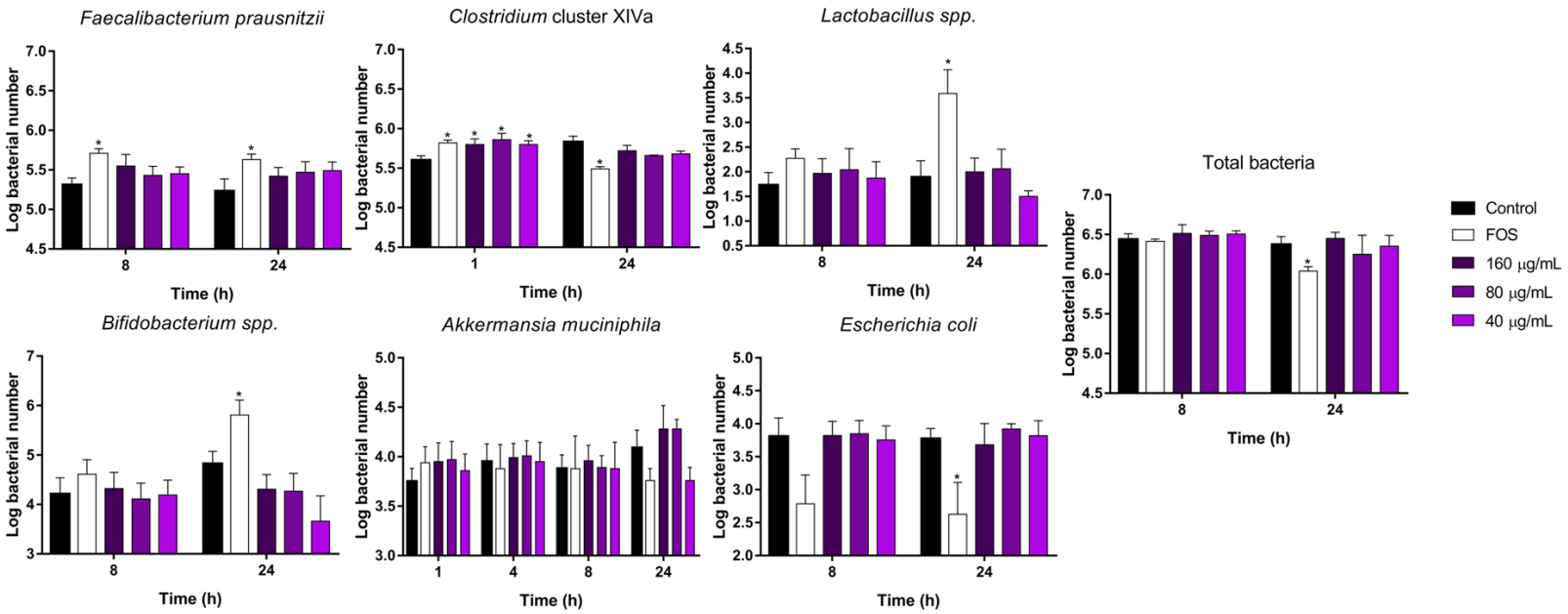

Figure 20. Changes in abundance of human colonic bacteria elicited by *R. magellanicum* polyphenols along time, during the *in vitro* fermentation. Results are expressed as Log_{10} bacterial number ± SEM. Statistical differences ($p < 0.05$) by Student's t-test respect to the control are pointed out (*).

Chapter 7

Conclusions

- The *in vitro* GID and colonic fermentation affected the phenolic composition of the South American currants *R. magellanicum* and *R. punctatum* and their potential bioactivity.
- Hydroxycinnamic acids and anthocyanins underwent drastic degradation, resulting in low recovery percentages after simulated GID. These compounds were also the most affected by simulated colonic conditions, with significant losses after 24 h incubation.
- Nine metabolites, derived from the microbial fermentation were tentatively identified by spectroscopic and spectrometric means, including dihydrocaffeic acid, dihydrocaffeoyl-, dihydroferuloylquinic acid, 1-(3,4-dihydroxyphenyl)-3-(2,4,6-trihydroxyphenyl)propan-2-ol (3,4-diHPP-2-ol), among others. The tentatively identified metabolites provide new insights in the biotransformation of polyphenols by the human gut microbiota.
- The changes in the phenolic content (HCA, TP, and TF) during *in vitro* digestion were significantly correlated with the loss of antioxidant activity observed in the cytoprotection, DPPH, TEAC, superoxide anion and CUPRAC assays.
- The modifications of the phenolic profile during *in vitro* digestion and fermentation changed the antioxidant effect of the PEEs, maintaining or even increasing their antioxidant capacity compared to the non-digested PEE, thus potentially preventing oxidative damage in the gastrointestinal tract.
- The inhibition of α-glucosidase by the non-digested, digested and fermented PEEs might contribute to control the postprandial glycaemia.

- The *in vitro* digested polyphenol-enriched extracts from *R. magellanicum* and *R. punctatum* showed anti-inflammatory properties on an intestinal inflammation model (IL-1β-stimulated Caco-2 C2BBe1 cells).
- The digested extracts decreased the secretion of the cytokines IL-6 and TNF-α, and the chemokine IL-8. A difference was observed between both species, in terms of their capacity to inhibit the IL-8 secretion. This might be associated to the high content of total flavonoids in the ID-PEE from *R. punctatum*, in particular with the presence of dihydroquercetin derivatives.
- The digested extracts from both species downregulated the gene expression of the pro-inflammatory enzymes COX-2 and iNOS. In addition, the non-digested and digested PEEs from both Ribes species inhibited human COX-1 and COX-2 *in vitro*.
- *R. punctatum* might promote the growth of beneficial bacteria, including *Clostridium* cluster XIVa, *F. prausnitzii*, and possibly *A. muciniphila*; while *R. magellanicum* may enhance *Clostridium* cluster XIVa growth.

Our results are a first approach to understand the stability and bioactivity of the polyphenols from the Chilean *Ribes* species. Their intake may be beneficial for small intestinal and colonic health since they demonstrated potential anti-inflammatory properties at physiologically relevant doses. Both are a rich source of potential regulators of bacterial metabolism, preventing toxic metabolites accumulation. However, further *in vivo* studies are needed to confirm these observations. Although we performed a complete simulation of the gastrointestinal tract, it should be taken into account the implicit limitations of the *in vitro* methodologies. Therefore, further *in vivo* experiments are needed to confirm these findings, considering this work as a first step to fully understand the stability of the polyphenols from

these South American wild currants as well as to validate the potential antioxidant, metabolic regulatory, anti-inflammatory, and prebiotic-like effect of these native fruits.

References

Allaman, I., Bélanger, M., & Magistretti, P. J. (2015). Methylglyoxal, the dark side of glycolysis. *Frontiers in Neuroscience*, 9, 23. https://doi.org/10.3389/fnins.2015.00023.

Alminger, M., Aura, A. M., Bohn, T., Dufour, C., El, S. N., Gomes, A., Karakaya, S., Martínez-Cuesta, M. C., McDougall, G. J., Requena, T., & Santos, C. N. (2014). *In vitro* models for studying secondary plant metabolite digestion and bioaccessibility. *Comprehensive Reviews in Food Science and Food Safety*, 13, 413–436. https://doi.org/10.1111/1541-4337.12081.

Ames, B. N. (1983). Dietary carcinogens and anticarcinogens. Oxygen radicals and degenerative diseases. *Science*, 221, 1256–1264. https://doi.org/10.3109/15563658408992561.

Anhê, F. F., Roy, D., Pilon, G., Dudonné, S., Matamoros, S., Varin, T. V., Garofalo, C., Moine, Q., Desjardins, Y., Levy, E., & Marette, A. (2015). A polyphenol-rich cranberry extract protects from diet induced obesity, insulin resistance and intestinal inflammation in association with increased *Akkermansia* spp. population in the gut microbiota of mice. *Gut,* 64, 872–883. https://doi.org/10.1136/gutjnl-2014-307142.

Arena, M. E., Bernini, M., & Vater, G. (2007). Growth and fruiting of *Ribes magellanicum* in Tierra del Fuego, Argentina. *New Zealand Journal of Crop and Horticultural Science*, 35(1), 61–66. https://doi.org/10.1080/01140670709510168.

Arena, M. E., & Coronel, L. J. (2011). Fruit growth and chemical properties of *Ribes magellanicum* "parrilla". *Scientia Horticulturae*, 127(3), 325–329. https://doi.org/10.1016/j.scienta.2010.10.026.

Arena, M. E., & Pastur, G. J. M. (1995). *In vitro* propagation of *Ribes magellanicum* Poiret. *Scientia Horticulturae*, 62(1–2), 139–144. https://doi.org/10.1016/0304-4238(94)00747-4.

Aura, A. M., Martin-López, P., O'Leary, K. A., Williamson, G., Oksman-Caldentey, K. M., Poutanen, K., & Santos-Buelga, C. (2005). *In vitro* metabolism of anthocyanins by human gut microflora. *European Journal of Nutrition*, 44(3), 133–142. https://doi.org/10.1007/s00394-004-0502-2.

Ávila, F., Theoduloz, C., López-Alarcón, C., Dorta, E., & Schmeda-Hirschmann, G. (2017). Cytoprotective mechanisms mediated by polyphenols from Chilean native berries against free radical-induced damage on AGS cells. *Oxidative Medicine and Cellular Longevity*, 2017, 9808520. https://doi.org/10.1155/2017/9808520.

Bañados, M. P., Hojas, C., Patillo, C., & Gonzalez, J. (2002). Geographical distribution of native *Ribes* species present in the herbarium of Chile. *Acta Horticulturae*, 585, 103–106. https://doi.org/10.17660/ActaHortic.2002.585.13.

Barberger-Gateau, P., Raffaitin, C., Letenneur, L., Berr, C., Tzourio, C., Dartigues, J. F., & Alpérovitch, A. (2007). Dietary patterns and risk of dementia: the Three-City cohort study. *Neurology*, 69(20), 1921–1930. https://doi.org/10.1212/01.wnl.0000278116.37320.52.

Barros, H. R. de M., García-Villalba, R., Tomás-Barberán, F. A., & Genovese, M. I. (2016). Evaluation of the distribution and metabolism of polyphenols derived from cupuassu (*Theobroma grandiflorum*) in mice gastrointestinal tract by UPLC-ESI-QTOF. *Journal of Functional Foods*, 22, 477–489. https://doi.org/10.1016/j.jff.2016.02.009.

Bazzocco, S., Mattila, I., Guyot, S., Renard, C. M. G. C., & Aura, A. M. (2008). Factors affecting the conversion of apple polyphenols to phenolic acids and fruit matrix to short-chain fatty acids by human faecal microbiota *in vitro*. *European Journal of Nutrition*, 47(8), 442–452. https://doi.org/10.1007/s00394-008-0747-2.

Beattie, J., Crozier, A., & Duthie, G. (2005). Potential health benefits of berries. *Current Nutrition & Food Science,* 1(1), 71–86. https://doi.org/10.2174/1573401052953294.

Bergmann, H., Rogoll, D., Scheppach, W., Melcher, R., & Richling, E. (2009). The Ussing type chamber model to study the intestinal transport and modulation of specific tight-junction genes using a colonic cell line. *Molecular Nutrition and Food Research*, 53(10), 1211–1225. https://doi.org/10.1002/mnfr.200800498.

Bermúdez-Soto, M. J., Tomás-Barberán, F. A., & García-Conesa, M. T. (2007). Stability of polyphenols in chokeberry (*Aronia melanocarpa*) subjected to *in vitro* gastric and pancreatic digestion. *Food Chemistry*, 102, 865–874. https://doi.org/10.1016/j.foodchem.2006.06.025.

Biasi, F., Astegiano, M., Maina, M., Leonarduzzi, G., & Poli, G. (2011). Polyphenol supplementation as a complementary medicinal approach to treating inflammatory bowel disease. *Current Medicinal Chemistry*, 18, 4851–4865. https://doi.org/10.2174/092986711797535263.

Bindels, L. B., Delzenne, N. M., Cani, P. D., & Walter, J. (2015). Towards a more comprehensive concept for prebiotics. *Nature Reviews. Gastroenterology & Hepatology*, 12(5), 303–310. https://doi.org/10.1038/nrgastro.2015.47.

Bishayee, A., Thoppil, R. J., Mandal, A., Darvesh, A. S., Ohanyan, V., Meszaros, J. G., Háznagy-Radnai, E., Hohmann, J., & Bhatia, D. (2013). Black currant phytoconstituents exert chemoprevention of diethylnitrosamine-initiated hepatocarcinogenesis by suppression of the inflammatory response. *Molecular Carcinogenesis*, 52(4), 304–317. https://doi.org/10.1002/mc.21860.

Blachier, F., Beaumont, M., Andriamihaja, M., Davila, A. M., Lan, A., Grauso, M., Armand, L., Benamouzig, R., & Tomé, D. (2017). Changes in the luminal environment of the colonic epithelial

cells and physiopathological consequences. *The American journal of pathology*, 187(3), 476-486. https://doi.org/10.1016/j.ajpath.2016.11.015.

Boath, A. S., Grussu, D., Stewart, D., & McDougall, G. J. (2012). Berry Polyphenols Inhibit Digestive Enzymes: a Source of Potential Health Benefits?. *Food Digestion*, 3(1-3), 1-7. https://doi.org/10.1007/s13228-012-0022-0.

Bohn, T. (2014). Dietary factors affecting polyphenol bioavailability. *Nutrition Reviews*, 72(7), 429–452. https://doi.org/10.1111/nure.12114.

Boivin, D., Blanchette, M., Barrette, S., Moghrabi, A., & Béliveau, R. (2007). Inhibition of cancer cell proliferation and suppression of TNF-induced activation of NFκB by edible berry juice. *Anticancer Research*, 27(2), 937–948.

Bonaccio, M., Pounis, G., Cerletti, C., Donati, M. B., Iacoviello, L., & de Gaetano, G. (2017). Mediterranean diet, dietary polyphenols and low grade inflammation: results from the MOLI-SANI study. *British Journal of Clinical Pharmacology*, 83(1), 107–113. https://doi.org/10.1111/bcp.12924.

Brennan, R., Stewart, D., & Russell, J. (2008). Developments and progress in *Ribes* breeding. *Acta Horticulturae*, 777, 49–55. https://doi.org/10.17660/ActaHortic.2008.777.3.

Bressa, C., Bailén-Andrino, M., Pérez-Santiago, J., González-Soltero, R., Pérez, M., Montalvo-Lominchar, M. G., Maté-Muñoz, J. L., Domínguez, R., Moreno, D., & Larrosa, M. (2017). Differences in gut microbiota profile between women with active lifestyle and sedentary women. *PLoS ONE*, 12(2), e0171352. https://doi.org/10.1371/journal.pone.0171352.

Brown, E. M., Nitecki, S., Pereira-Caro, G., Mcdougall, G. J., Stewart, D., Rowland, I., Crozier, A., & Gill, C. I. R. (2014). Comparison of *in vivo* and *in vitro* digestion on polyphenol composition in lingonberries: Potential impact on colonic health. *BioFactors*, 40(6), 611–623. https://doi.org/10.1002/biof.1173.

Brown, E. M., Mcdougall, G. J., Stewart, D., Pereira-Caro, G., González-Barrio, R., Allsopp, P., Magee, P., Crozier, A., Rowland, I., & Gill, C. I. R. (2012). Persistence of anticancer activity in berry extracts after simulated gastrointestinal digestion and colonic fermentation. *PLoS One*, 7(11), e49740. https://doi.org/10.1371/journal.pone.0049740.

Burgos-Edwards, A., Jiménez-Aspee, F., Theoduloz, C., & Schmeda-Hirschmann, G. (2018). Colonic fermentation of polyphenols from Chilean currants (*Ribes* spp.) and its effect on antioxidant capacity and metabolic syndrome-associated enzymes. *Food Chemistry*, 258, 144–155. https://doi.org/10.1016/j.foodchem.2018.03.053.

Burgos-Edwards, A., Jiménez-Aspee, F., Thomas-Valdés, S., Schmeda-Hirschmann, G., & Theoduloz, C. (2017). Qualitative and quantitative changes in polyphenol composition and bioactivity of *Ribes magellanicum* and *R . punctatum* after *in vitro* gastrointestinal digestion. *Food Chemistry*, 237, 1073–1082. https://doi.org/10.1016/j.foodchem.2017.06.060.

Cantu-Jungles, T. M., Ruthes, A. C., El-Hindawy, M., Moreno, R. B., Zhang, X., Cordeiro, L. M. C., Hamaker, B., R., & Iacomini, M. (2018). *In vitro* fermentation of *Cookeina speciosa* glucans stimulates the growth of the butyrogenic *Clostridium* cluster XIVa in a targeted way. *Carbohydrate Polymers*, 183, 219–229. https://doi.org/10.1016/j.carbpol.2017.12.020.

Carbonell-Capella, J. M., Buniowska, M., Barba, F. J., Esteve, M. J., & Frígola, A. (2014). Analytical methods for determining bioavailability and bioaccessibility of bioactive compounds

from fruits and vegetables: A review. *Comprehensive Reviews in Food Science and Food Safety*, 13(2), 155–171. https://doi.org/10.1111/1541-4337.12049.

Cardona, F., Andrés-Lacueva, C., Tulipani, S., Tinahones, F. J., & Queipo-Ortuño, M. I. (2013). Benefits of polyphenols on gut microbiota and implications in human health. *Journal of Nutritional Biochemistry*, 24(8), 1415–1422. https://doi.org/10.1016/j.jnutbio.2013.05.001.

Cardoso, C., Afonso, C., Lourenço, H., Costa, S., & Nunes, M. L. (2015). Bioaccessibility assessment methodologies and their consequences for the risk-benefit evaluation of food. *Trends in Food Science and Technology*, 41(1), 5–23. https://doi.org/10.1016/j.tifs.2014.08.008.

Castro-Acosta, M. L., Smith, L., Miller, R. J., McCarthy, D. I., Farrimond, J. A., & Hall, W. L. (2016). Drinks containing anthocyanin-rich blackcurrant extract decrease postprandial blood glucose, insulin and incretin concentrations. *Journal of Nutritional Biochemistry*, 38, 154–161. https://doi.org/10.1016/j.jnutbio.2016.09.002.

Cerezo, A. B., Cuevas, E., Winterhalter, P., Garcia-Parrilla, M. C., & Troncoso, A. M. (2010). Isolation, identification, and antioxidant activity of anthocyanin compounds in Camarosa strawberry. *Food Chemistry*, 123(3), 574–582. https://doi.org/10.1016/j.foodchem.2010.04.073.

Céspedes-Acuña, C. L., Xiao, J., Wei, Z.-J., Chen, L., Bastias, J. M., Avila Acevedo, J. G., Alarcón-Enos, J., Werner-Navarrete, E., & Kubo, I. (2018). Antioxidant and anti-inflammatory effects of extracts from maqui berry *Aristotelia chilensis* in human colon cancer cells. *Journal of Berry Research*, 8(4), 275-296. https://doi.org/10.3233/JBR-180356.

Cheel, J., Theoduloz, C., Rodríguez, J. A., Caligari, P. D. S., & Schmeda-Hirschmann, G. (2007). Free radical scavenging activity and phenolic content in achenes and thalamus from *Fragaria*

chiloensis ssp. *chiloensis*, *F. vesca* and *F. x ananassa cv*. Chandler. *Food Chemistry*, 102(1), 36–44. https://doi.org/10.1016/j.foodchem.2006.04.036.

Cheli, F., & Baldi, A. (2011). Nutrition-based health: cell-based bioassays for food antioxidant activity evaluation. *Journal of Food Science*, 76(9), 197–205. https://doi.org/10.1111/j.1750-3841.2011.02411.x.

Chen, P. X., Zhang, H., Marcone, M. F., Pauls, K. P., Liu, R., Tang, Y., Zhang, B., Renaud, J. B., & Tsao, R. (2017). Anti-inflammatory effects of phenolic-rich cranberry bean (*Phaseolus vulgaris* L.) extracts and enhanced cellular antioxidant enzyme activities in Caco-2 cells. *Journal of Functional Foods*, 38, 675–685. https://doi.org/10.1016/j.jff.2016.12.027.

Cheynier, V., Comte, G., Davies, K. M., Lattanzio, V., & Martens, S. (2013). Plant phenolics: recent advances on their biosynthesis, genetics, and ecophysiology. *Plant Physiology and Biochemistry*, 72, 1–20. https://doi.org/10.1016/j.plaphy.2013.05.009.

Chiang, C., Kadouh, H., & Zhou, K. (2013). Phenolic compounds and antioxidant properties of gooseberry as affected by *in vitro* digestion. *LWT - Food Science and Technology*, 51, 417–422. https://doi.org/10.1016/j.lwt.2012.11.014.

Chouhan, S., Sharma, K., Zha, J., Guleria, S., & Koffas, M. A. G. (2017). Recent advances in the recombinant biosynthesis of polyphenols. *Frontiers in Microbiology*, 8, 2259. https://doi.org/10.3389/fmicb.2017.02259.

Clifford, M. N., Johnston, K. L., Knight, S., & Kuhnert, N. (2003). Hierarchical scheme for LC-MS^n identification of chlorogenic acids. *Journal of Agricultural and Food Chemistry*, 51(10), 2900–2911. https://doi.org/10.1021/jf026187q.

Collado, M. C., Derrien, M., Isolauri, E., De Vos, W. M., & Salminen, S. (2007). Intestinal integrity and *Akkermansia muciniphila*, a mucin-degrading member of the intestinal microbiota present in infants, adults, and the elderly. *Applied and Environmental Microbiology*, 73(23), 7767–7770. https://doi.org/10.1128/AEM.01477-07.

Correa-Betanzo, J., Allen-Vercoe, E., McDonald, J., Schroeter, K., Corredig, M., & Paliyath, G. (2014). Stability and biological activity of wild blueberry (*Vaccinium angustifolium*) polyphenols during simulated *in vitro* gastrointestinal digestion. *Food Chemistry*, 165, 522–531. https://doi.org/10.1016/j.foodchem.2014.05.135.

Costamagna, M. S., Zampini, I. C., Alberto, M. R., Cuello, S., Torres, S., Pérez, J., Quispe, C., Schmeda-Hirschmann, G., & Isla, M. I. (2016). Polyphenols rich fraction from *Geoffroea decorticans* fruits flour affects key enzymes involved in metabolic syndrome, oxidative stress and inflammatory process. *Food Chemistry*, 190, 392–402. https://doi.org/10.1016/j.foodchem.2015.05.068.

Crozier, A., Jaganath, I. B., & Clifford, M. N. (2009). Dietary phenolics: Chemistry, bioavailability and effects on health. *Natural Product Reports*, 26, 1001–1043. https://doi.org/10.1039/b802662a.

Cueva, C., Sánchez-Patán, F., Monagas, M., Walton, G. E., Gibson, G. R., Martín-Álvarez, P. J., Bartolomé, B., & Moreno-Arribas, M. V. (2013). *In vitro* fermentation of grape seed flavan-3-ol fractions by human faecal microbiota: changes in microbial groups and phenolic metabolites. *FEMS Microbiology Ecology*, 83(3), 792–805. https://doi.org/10.1111/1574-6941.12037.

Dai, X., & Karring, H. (2014). A determination and comparison of urease activity in feces and fresh manure from pig and cattle in relation to ammonia production and pH changes. *PLoS ONE*, 9(11), e110402. https://doi.org/10.1371/journal.pone.0110402.

Dall'Asta, M., Calani, L., Tedeschi, M., Jechiu, L., Brighenti, F., & Del Rio, D. (2012). Identification of microbial metabolites derived from *in vitro* fecal fermentation of different polyphenolic food sources. *Nutrition*, 28, 197–203. https://doi.org/10.1016/j.nut.2011.06.005.

D'Archivio, M., Filesi, C., Varì, R., Scazzocchio, B., & Masella, R. (2010). Bioavailability of the polyphenols: Status and controversies. *International Journal of Molecular Sciences*, 11(4), 1321–1342. https://doi.org/10.3390/ijms11041321.

Day, A. J., Cañada, F. J., Díaz, J. C., Kroon, P. A., Mclauchlan, R., Faulds, C. B., Plumb, G. W., Morgan, M. R., & Williamson, G. (2000). Dietary flavonoid and isoflavone glycosides are hydrolysed by the lactase site of lactase phlorizin hydrolase. *FEBS Letters*, 468, 166–170. https://doi.org/10.1016/s0014-5793(00)01211-4.

Del Rio, D., Borges, G., & Crozier, A. (2010). Berry flavonoids and phenolics: Bioavailability and evidence of protective effects. *British Journal of Nutrition*, 104, S67–S90. https://doi.org/10.1017/S0007114510003958.

Del Rio, D., Rodriguez-Mateos, A., Spencer, J. P. E., Tognolini, M., Borges, G., & Crozier, A. (2013). Dietary (poly) phenolics in human health: structures, bioavailability, and evidence of protective effects against chronic diseases. *Antioxidants & Redox Signaling*, 18(14), 1818–1892. https://doi.org/10.1089/ars.2012.4581.

Delroisse, J. M., Boulvin, A. L., Parmentier, I., Dauphin, R. D., Vandenbol, M., & Portetelle, D. (2008). Quantification of *Bifidobacterium* spp. and *Lactobacillus* spp. in rat fecal samples by real-time PCR. *Microbiological Research*, 163(6), 663–670. https://doi.org/10.1016/j.micres.2006.09.004.

Desai, S. J., Prickril, B., & Rasooly, A. (2018). Mechanisms of phytonutrient modulation of cyclooxygenase-2 (COX-2) and inflammation related to cancer. *Nutrition and Cancer*, 70(3), 350–375. https://doi.org/10.1080/01635581.2018.1446091.

De Filippo, C., Cavalieri, D., Di Paola, M., Ramazzotti, M., Poullet, J. B., Massart, S., Collini, S., Pieraccini, G., & Lionetti, P. (2010). Impact of diet in shaping gut microbiota revealed by a comparative study in children from Europe and rural Africa. *Proceedings of the National Academy of Sciences of the United States of America*, 107(33), 14691-14696; https://doi.org/10.1073/pnas.1005963107.

de Villiers, A., Venter, P., & Pasch, H. (2016). Recent advances and trends in the liquid-chromatography–mass spectrometry analysis of flavonoids. *Journal of Chromatography A*, 1430, 16–78. https://doi.org/10.1016/j.chroma.2015.11.077.

Dewick, P. M. (2002). Medicinal Natural Products: A Biosynthetic Approach (Second). New York: John Wiley & Sons, Ltd.

Duda-Chodak, A., Tarko, T., Satora, P., & Sroka, P. (2015). Interaction of dietary compounds, especially polyphenols, with the intestinal microbiota: a review. *European Journal of Nutrition*, 54(3), 325-341. https://doi.org/10.1016/10.1007/s00394-015-0852-y.

Duque, A. L. R. F., Monteiro, M., Tallarico Adorno, M. A., Sakamoto, I. K., & Sivieri, K. (2016). An exploratory study on the influence of orange juice on gut microbiota using a dynamic colonic model. *Food Research International*, 84, 160–169. https://doi.org/10.1016/j.foodres.2016.03.028.

Ercan, P., & El, S. N. (2016). Inhibitory effects of chickpea and *Tribulus terrestris* on lipase, α-amylase and α-glucosidase. *Food Chemistry*, 205, 163–169. https://doi.org/10.1016/j.foodchem.2016.03.012.

Espín, J. C., González-Sarrías, A., & Tomás-Barberán, F. A. (2017). The gut microbiota: A key factor in the therapeutic effects of (poly)phenols. *Biochemical Pharmacology*, 139, 82–93. https://doi.org/10.1016/j.bcp.2017.04.033.

Esposito, D., Damsud, T., Wilson, M., Grace, M. H., Strauch, R., Li, X., Lila, M. A., & Komarnytsky, S. (2015). Black currant anthocyanins attenuate weight gain and improve glucose metabolism in diet-induced obese mice with intact, but not disrupted, gut microbiome. *Journal of Agricultural and Food Chemistry*, 63(27), 6172–6180. https://doi.org/10.1021/acs.jafc.5b00963.

Eyssartier, C., Ladio, A. H., & Lozada, M. (2009). Uso de plantas medicinales cultivadas en una comunidad semi-rural de la estepa patagónica. *Boletín Latinoamericano y Del Caribe de Plantas Medicinales y Aromáticas*, 8(2), 77–85.

FAOSTAT. (2018). Value of Agricultural Production. Retrieved July 27, 2019, from Food and Agriculture Organization of the United Nations (FAO) website: http://www.fao.org/faostat/es/#data/QV.

Flint, H. J., Scott, K. P., Louis, P., & Duncan, S. H. (2012). The role of the gut microbiota in nutrition and health. *Gastroenterology & Hepatology*, 9, 577–589. https://doi.org/10.1038/nrgastro.2012.156.

Foito, A., McDougall, G. J., & Stewart, D. (2018). Evidence for health benefits of berries. *Annual Plant Reviews*, 1, 1–43. https://doi.org/10.1002/9781119312994.apr0600.

Fraga, C. G., Galleano, M., Verstraeten, S. V., & Oteiza, P. I. (2010). Basic biochemical mechanisms behind the health benefits of polyphenols. *Molecular Aspects of Medicine*, 31(6), 435–445. https://doi.org/10.1016/j.mam.2010.09.006.

García-Villalba, R., Giménez-Bastida, J. A., García-Conesa, M. T., Tomás-Barberán, F. A., Carlos Espín, J., & Larrosa, M. (2012). Alternative method for gas chromatography-mass spectrometry analysis of short-chain fatty acids in faecal samples. *Journal of Separation Science*, 35(15), 1906–1913. https://doi.org/10.1002/jssc.201101121.

Gee, J. M., Dupont, M. S., Day, A. J., Plumb, G. W., Williamson, G., & Johnson, I. T. (2000). Intestinal transport of quercetin glycosides in rats involves both deglycosylation and interaction with the hexose transport pathway. *The Journal of Nutrition*, 130(11), 2765–2771. https://doi.org/10.1093/jn/130.11.2765.

Gómez-Juaristi, M., Martínez-López, S., Sarria, B., Bravo, L., & Mateos, R. (2018). Absorption and metabolism of yerba mate phenolic compounds in humans. *Food Chemistry*, 240, 1028–1038. https://doi.org/10.1016/j.foodchem.2017.08.003.

Gómez-Ruiz, J. Á., Leake, D. S., & Ames, J. M. (2007). *In vitro* antioxidant activity of coffee compounds and their metabolites. *Journal of Agricultural and Food Chemistry*, 55(17), 6962–6969. https://doi.org/10.1021/jf0710985.

Gonthier, M. P., Rémésy, C., Scalbert, A., Cheynier, V., Souquet, J. M., Poutanen, K., & Aura, A. M. (2006). Microbial metabolism of caffeic acid and its esters chlorogenic and caftaric acids by human faecal microbiota *in vitro*. *Biomedicine and Pharmacotherapy*, 60(9), 536–540. https://doi.org/10.1016/j.biopha.2006.07.084.

Gopalan, A., Reuben, S. C., Ahmed, S., Darvesh, A. S., Hohmann, J., & Bishayee, A. (2012). The health benefits of blackcurrants. *Food and Function*, 3(8), 795–809. https://doi.org/10.1039/c2fo30058c.

Gorelik, S., Lapidot, T., Shaham, I., Granit, R., Ligumsky, M., Kohen, R., & Kanner, J. (2005). Lipid peroxidation and coupled vitamin oxidation in simulated and human gastric fluid inhibited by dietary polyphenols: health implications. *Journal of Agricultural and Food Chemistry*, 53(9), 3397–3402. https://doi.org/10.1021/jf040401o.

Gross, G., Jacobs, D. M., Peters, S., Possemiers, S., Van Duynhoven, J., Vaughan, E. E., & Van De Wiele, T. (2010). *In vitro* bioconversion of polyphenols from black tea and red wine/grape juice by human intestinal microbiota displays strong interindividual variability. *Journal of Agricultural and Food Chemistry*, 58(18), 10236–10246. https://doi.org/10.1021/jf101475m.

Grosso, G., Godos, J., Lamuela-Raventos, R., Ray, S., Micek, A., Pajak, A., Sciacca, S., D'Orazio, N., Del Rio, D., & Galvano, F. (2017). A comprehensive meta-analysis on dietary flavonoid and lignan intake and cancer risk: Level of evidence and limitations. *Molecular Nutrition and Food Research*, 61(4), 1600930. https://doi.org/10.1002/mnfr.201600930.

Guerra, A., Etienne-Mesmin, L., Livrelli, V., Denis, S., Blanquet-Diot, S., & Alric, M. (2012). Relevance and challenges in modeling human gastric and small intestinal digestion. *Trends in Biotechnology*, 30(11), 591–600. https://doi.org/10.1016/j.tibtech.2012.08.001.

Gullon, B., Pintado, M. E., Barber, X., Fernández-López, J., Pérez-Álvarez, J. A., & Viuda-Martos, M. (2015). Bioaccessibility, changes in the antioxidant potential and colonic fermentation of date pits and apple bagasse flours obtained from co-products during simulated *in vitro* gastrointestinal digestion. *Food Research International*, 78, 169–176. https://doi.org/10.1016/j.foodres.2015.10.021.

Guo, X., Yang, B., Tan, J., Jiang, J., Li, D. (2016). Associations of dietary intakes of anthocyanins and berry fruits with risk of type 2 diabetes mellitus: a systematic review and meta-analysis of

prospective cohort studies. *European Journal of Clinical Nutrition*, 70(12), 1360-1367. https://doi.org/10.1016/10.1038/ejcn.2016.142.

Halliwell, B. (2007). Dietary polyphenols: Good, bad, or indifferent for your health?. *Cardiovascular Research*, 73(2), 341–347. https://doi.org/10.1016/j.cardiores.2006.10.004.

Halliwell, B. (2008). Are polyphenols antioxidants or pro-oxidants? What do we learn from cell culture and *in vivo* studies?. *Archives of Biochemistry and Biophysics*, 476(2), 107–112. https://doi.org/10.1016/j.abb.2008.01.028.

Haminiuk, C. W. I., Maciel, G. M., Plata-Oviedo, M. S. V., & Peralta, R. M. (2012). Phenolic compounds in fruits - an overview. *International Journal of Food Science and Technology*, 47(10), 2023–2044. https://doi.org/10.1111/j.1365-2621.2012.03067.x.

Healey, G. R., Murphy, R., Brough, L., Butts, C. A., & Coad, J. (2017). Interindividual variability in gut microbiota and host response to dietary interventions. *Nutrition reviews*, 75(12), 1059-1080. https://doi.org/10.1093/nutrit/nux062.

Heyman-Lindén, L., Kotowska, D., Sand, E., Bjursell, M., Plaza, M., Turner, C., Holm, C., Fåk, F., & Berger, K. (2016). Lingonberries alter the gut microbiota and prevent low-grade inflammation in high-fat diet fed mice. *Food & Nutrition Research*, 60, 29993. https://doi.org/10.3402/fnr.v60.29993.

Hidalgo, M., Oruna-Concha, M. J., Kolida, S., Walton, G. E., Kallithraka, S., Spencer, J. P., & de Pascual-Teresa, S. (2012). Metabolism of anthocyanins by human gut microflora and their influence on gut bacterial growth. *Journal of Agricultural and Food Chemistry*, 60(15), 3882-90. https://doi.org/10.1080/10.1021/jf3002153.

Hoebler, C., Lecannu, G., Belleville, C., Devaux, M., Popineau, Y., & Barry, J. (2002). Development of an *in vitro* system simulating bucco-gastric digestion to assess the physical and chemical changes of food. *International Journal of Food Sciences and Nutrition*, 53(5), 389–402. https://doi.org/10.1080/0963748021000044732.

Huang, H., Sun, Y., Lou, S., Li, H., & Ye, X. (2014). *In vitro* digestion combined with cellular assay to determine the antioxidant activity in Chinese bayberry (*Myrica rubra* Sieb. et Zucc.) fruits: A comparison with traditional methods. *Food Chemistry*, 146, 363–370. https://doi.org/10.1016/j.foodchem.2013.09.071.

Huebbe, P., Giller, K., de Pascual-Teresa, S., Arkenau, A., Adolphi, B., Portius, S., Arkenau, C. N., & Rimbach, G. (2012). Effects of blackcurrant-based juice on atherosclerosis-related biomarkers in cultured macrophages and in human subjects after consumption of a high-energy meal. *British Journal of Nutrition*, 108(2), 234–244. https://doi.org/10.1017/S0007114511005642.

Hummer, K. E., & Dale, A. (2010). Horticulture of *Ribes*. *Forest Pathology*, 40, 251–263. https://doi.org/10.1111/j.1439-0329.2010.00657.x.

Hur, S. J., Lim, B. O., Decker, E. A., & McClements, D. J. (2011). *In vitro* human digestion models for food applications. *Food Chemistry*, 125, 1–12. https://doi.org/10.1016/j.foodchem.2010.08.036.

Ignat, I., Volf, I., & Popa, V. I. (2011). A critical review of methods for characterisation of polyphenolic compounds in fruits and vegetables, *Food Chemistry*, 126, 1821–1835. https://doi.org/10.1016/10.1016/j.foodchem.2010.12.026.

Jaganath, I. B., Mullen, W., Lean, M. E. J., Edwards, C. A., & Crozier, A. (2009). *In vitro* catabolism of rutin by human fecal bacteria and the antioxidant capacity of its catabolites. *Free*

Radical Biology and Medicine, 47(8), 1180–1189. https://doi.org/10.1016/j.freeradbiomed.2009.07.031.

Jakobsdottir, G., Nilsson, U., Blanco, N., Sterner, O., & Nyman, M. (2014). Effects of soluble and insoluble fractions from bilberries, black currants, and raspberries on short-chain fatty acid formation, anthocyanin excretion, and cholesterol in rats. *Journal of Agricultural and Food Chemistry*, 62, 4359–4368. https://doi.org/10.1021/jf5007566.

Jara-Palacios, J. M., Gonçalves, S., Hernanz, D., Heredia, F. J., & Romano, A. (2018). Effects of *in vitro* gastrointestinal digestion on phenolic compounds and antioxidant activity of different white winemaking byproducts extracts. *Food Research International*, 109, 433–439. https://doi.org/10.1016/j.foodres.2018.04.060.

Jia, N., Li, T., Diao, X., & Kong, B. (2014). Protective effects of black currant (*Ribes nigrum* L.) extract on hydrogen peroxide-induced damage in lung fibroblast MRC-5 cells in relation to the antioxidant activity. *Journal of Functional Foods*, 11, 142–151. https://doi.org/10.1016/j.jff.2014.09.011.

Jiménez-Aspee, F., Alberto, M. R., Quispe, C., Caramantin Soriano, M., Theoduloz, C., Zampini, I. C., Isla, M. I., & Schmeda-Hirschmann, G. (2015). Anti-inflammatory activity of copao (*Eulychnia acida* Phil., Cactaceae) fruits. *Plant Foods for Human Nutrition*, 70(2), 135–140. https://doi.org/10.1007/s11130-015-0468-7.

Jiménez-Aspee, F., Theoduloz, C., Ávila, F., Thomas-Valdés, S., Mardones, C., von Baer, D., & Schmeda-Hirschmann, G. (2016a). The Chilean wild raspberry (*Rubus geoides* Sm.) increases intracellular GSH content and protects against H_2O_2 and methylglyoxal-induced damage in AGS cells. *Food Chemistry*, 194, 908–919. https://doi.org/10.1016/j.foodchem.2015.08.117.

Jiménez-Aspee, F., Thomas-Valdés, S., Schulz, A., Ladio, A., Theoduloz, C., & Schmeda-Hirschmann, G. (2016b). Antioxidant activity and phenolic profiles of the wild currant *Ribes magellanicum* from Chilean and Argentinean Patagonia. *Food Science and Nutrition*, 4(4), 595–610. https://doi.org/10.1002/fsn3.323.

Jiménez-Aspee, F., Theoduloz, C., Vieira, M.N., Rodriguez-Werner, M.A., Schmalfuss, E., Winterhalter, P., & Schmeda-Hirschmann, G. (2016c). Phenolics from the Patagonian currants *Ribes spp*.: isolation, characterization and cytoprotective effect in AGS cells. *Journal of Functional Foods* 26, 11–26. https://doi.org/10.1016/j.jff.2016.06.036.

Juániz, I., Ludwig, I. A., Bresciani, L., Dall'Asta, M., Mena, P., Del Rio, D., Cid, C., & de Peña, M. P. (2017). Bioaccessibility of (poly)phenolic compounds of raw and cooked cardoon (*Cynara cardunculus* L.) after simulated gastrointestinal digestion and fermentation by human colonic microbiota. *Journal of Functional Foods*, 32, 195–207. https://doi.org/10.1016/j.jff.2017.02.033.

Jung, H., Kwak, H.-K., & Hwang, T. (2014). Antioxidant and antiinflammatory activities of cyanidin-3-glucoside and cyanidin-3-rutinoside in hydrogen peroxide and lipopolysaccharide-treated RAW264.7 cells. *Food Science and Biotechnology*, 23(6), 2053–2062. https://doi.org/10.1007/s10068-014-0279-x.

Kamiloglu, S., & Capanoglu, E. (2013). Investigating the *in vitro* bioaccessibility of polyphenols in fresh and sun-dried figs (*Ficus carica* L.). *International Journal of Food Science and Technology*, 48(12), 2621–2629. https://doi.org/10.1111/ijfs.12258.

Kaplan, G. G., & Ng, S. C. (2017). Understanding and preventing the global increase of inflammatory bowel disease. *Gastroenterology*, 152(2), 313–321. https://doi.org/10.1053/j.gastro.2016.10.020.

Kemperman, R. A., Gross, G., Mondot, S., Possemiers, S., Marzorati, M., Van de Wiele, T., Doré, J., & Vaughan, E. E. (2013). Impact of polyphenols from black tea and red wine/grape juice on a gut model microbiome. *Food Research International*, 53, 659–669. https://doi.org/10.1016/j.foodres.2013.01.034.

Kim, Y. J., Choi, S. E., Lee, M. W., & Lee, C. S. (2008). Taxifolin glycoside inhibits dendritic cell responses stimulated by lipopolysaccharide and lipoteichoic acid. *Journal of Pharmacy and Pharmacology*, 60(11), 1465–1472. https://doi.org/10.1211/jpp.60.11.0007.

Kong, F., & Singh, R. P. (2010). A human gastric simulator (HGS) to study food digestion in human stomach. *Journal of Food Science*, 75(9), E627–E635. https://doi.org/10.1111/j.1750-3841.2010.01856.x.

Kosmala, M., Zduńczyk, Z., Karlińska, E., & Juśkiewicz, J. (2014). The effects of strawberry, black currant, and chokeberry extracts in a grain dietary fiber matrix on intestinal fermentation in rats. *Food Research International*, 64, 752–761. https://doi.org/10.1016/j.foodres.2014.07.010.

Kroon, P. A., Clifford, M. N., Crozier, A., Day, A. J., Donovan, J. L., Manach, C., & Williamson, G. (2004). How should we assess the effects of exposure to dietary polyphenols *in vitro*?. *The American Journal of Clinical Nutrition*, 80(1), 15–21. https://doi.org/10.1093/ajcn/80.1.15.

Kutschera, M., Engst, W., Blaut, M., & Braune, A. (2011). Isolation of catechin-converting human intestinal bacteria. *Journal of Applied Microbiology*, 111, 165–175. https://doi.org/10.1111/j.1365-2672.2011.05025.x.

Labib, S., Hummel, S., Richling, E., Humpf, H. U., & Schreier, P. (2006). Use of the pig caecum model to mimic the human intestinal metabolism of hispidulin and related compounds. *Molecular Nutrition and Food Research*, 50(1), 78–86. https://doi.org/10.1002/mnfr.200500144.

Lafay, S., Gil-Izquierdo, A., Manach, C., Morand, C., Besson, C., & Scalbert, A. (2006). Chlorogenic acid is absorbed in its intact form in the stomach of rats. *The Journal of Nutrition*, 136(5), 1192–1197. https://doi.org/10.1093/jn/136.5.1192.

Lattanzio, V. (2013). Phenolic Compounds: Introduction. In K. G. Ramawat & J.-M. Mérillon (Eds.), Natural products: phytochemistry, botany and metabolism of alkaloids, phenolics and terpenes (pp. 1543–1580). https://doi.org/10.1007/978-3-642-22144-6_57.

Laurent, C., Besançon, P., & Caporiccio, B. (2007). Flavonoids from a grape seed extract interact with digestive secretions and intestinal cells as assessed in an *in vitro* digestion/Caco-2 cell culture model. *Food Chemistry*, 100, 1704–1712. https://doi.org/10.1016/j.foodchem.2005.10.016.

Leonard, F., Collnot, E., & Lehr, C. (2010). A three-dimensional coculture of enterocytes, monocytes and dendritic cells to model inflamed intestinal mucosa *in vitro*. *Molecular Pharmaceutics*, 7(6), 2103–2119. https://doi.org/10.1021/mp1000795.

León-González, A. J., Auger, C., & Schini-Kerth, V. B. (2015). Pro-oxidant activity of polyphenols and its implication on cancer chemoprevention and chemotherapy. *Biochemical Pharmacology*, 98(3), 371–380. https://doi.org/10.1016/j.bcp.2015.07.017.

Leyva-López, N., Gutierrez-Grijalva, E. P., Ambriz-Perez, D. L., & Heredia, J. B. (2016). Flavonoids as cytokine modulators: a possible therapy for inflammation-related diseases. *International Journal of Molecular Sciences*, 17, E921. https://doi.org/10.3390/ijms17060921.

Li, A. (2001). Adsorption of phenolic compounds on Amberlite XAD-4 and its acetylated derivative MX-4. *Reactive and Functional Polymers*, 49, 225–233. https://doi.org/10.1016/S1381-5148(01)00080-3.

Li, Q., Chen, J., Li, T., Liu, C., Wang, X., Dai, T., McClements, D. J., & Liu, J. (2015). Impact of *in vitro* simulated digestion on the potential health benefits of proanthocyanidins from *Choerospondias axillaris* peels. *Food Research International*, 78, 378–387. https://doi.org/10.1016/j.foodres.2015.09.004.

Lin, L., Sun, J., Chen, P., Monagas, M. J., & Harnly, J. M. (2014). UHPLC-PDA-ESI/HRMS^n profiling method to identify and quantify oligomeric proanthocyanidins in plant products. *Journal of Agricultural and Food Chemistry*, 62, 9387–9400. https://doi.org/10.1021/jf501011y.

Liu, X., Liu, Y., Huang, Y., Yu, H., Yuan, S., Tang, B., Wang, P. G., & He, Q. Q. (2017). Dietary total flavonoids intake and risk of mortality from all causes and cardiovascular disease in the general population: A systematic review and meta-analysis of cohort studies. *Molecular Nutrition and Food Research*, 61(6), 160100316. https://doi.org/10.1002/mnfr.20160100.

López-Alarcón, C., & Denicola, A. (2013). Evaluating the antioxidant capacity of natural products: A review on chemical and cellular-based assays. *Analytica Chimica Acta*, 763, 1–10. https://doi.org/10.1016/j.aca.2012.11.051.

Losada-Barreiro, S., & Bravo-Díaz, C. (2017). Free radicals and polyphenols: The redox chemistry of neurodegenerative diseases. *European Journal of Medicinal Chemistry*, 133, 379–402. https://doi.org/10.1016/j.ejmech.2017.03.061.

Lucas-Gonzalez, R., Navarro-Coves, S., Pérez-Álvarez, J. A., Fernández-López, J., Muñoz, L. A., & Viuda-Martos, M. (2016). Assessment of polyphenolic profile stability and changes in the antioxidant potential of maqui berry (*Aristotelia chilensis* (Molina) Stuntz) during *in vitro* gastrointestinal digestion. *Industrial Crops and Products*, 94, 774–782. https://doi.org/10.1016/j.indcrop.2016.09.057.

Ludwig, I. A., de Peña, M. P., Concepción, C., & Alan, C. (2013). Catabolism of coffee chlorogenic acids by human colonic microbiota. *BioFactors*, 39(6), 623–632. https://doi.org/10.1002/biof.1124.

Lyall, K. A., Hurst, S. M., Cooney, J., Jensen, D., Lo, K., Hurst, R. D., & Stevenson, L. M. (2009). Short-term blackcurrant extract consumption modulates exercise-induced oxidative stress and lipopolysaccharide-stimulated inflammatory responses. *American Journal of Physiology*, 297, R70–R81. https://doi.org/10.1152/ajpregu.90740.2008.

Lynch, S. V., & Pedersen, O. (2016). The human intestinal microbiome in health and disease. *The New England Journal of Medicine*, 375(24), 2369–2379. https://doi.org/10.1056/NEJMra1600266.

Macfarlane, G. T., & Macfarlane, S. (2007). Models for intestinal fermentation: association between food components, delivery systems, bioavailability and functional interactions in the gut. *Current Opinion in Biotechnology*, 18(2), 156–162. https://doi.org/10.1016/j.copbio.2007.01.011.

Magalhães, L. M., Segundo, M. A., Reis, S., & Lima, J. L. F. C. (2008). Methodological aspects about *in vitro* evaluation of antioxidant properties. *Analytica Chimica Acta*, 613(1), 1–19. https://doi.org/10.1016/j.aca.2008.02.047.

Manach, C., Scalbert, A., Morand, C., Rémésy, C., & Jiménez, L. (2004). Polyphenols: food sources and bioavailability. *American Journal of Clinical Nutrition*, 79, 727–747. https://doi.org/10.1093/ajcn/79.5.727.

Manach, C., Williamson, G., Morand, C., Scalbert, A., & Rémésy, C. (2005). Bioavailability and bioefficacy of polyphenols in humans. I. Review of 97 bioavailability studies. *American Journal of Clinical Nutrition*, 81, 230S-242S. https://doi.org/10.1093/ajcn/81.1.230S.

Marín, L., Miguélez, E. M., Villar, C. J., & Lombó, F. (2015). Bioavailability of dietary polyphenols and gut microbiota metabolism: antimicrobial properties. *BioMed Research International*, 2015, 905215. https://doi.org/10.1155/2015/905215.

Matsuki, T., Watanabe, K., Fujimoto, J., Miyamoto, Y., Takada, T., Matsumoto, K., Oyaizu, H., & Tanaka, R. (2002). Development of 16S rRNA-gene-targeted group-specific primers for the detection and identification of predominant bacteria in human feces. *Applied and Environmental Microbiology*, 68(11), 5445–5451. https://doi.org/10.1128/AEM.68.11.5445-5451.2002.

Mayta-Apaza, A. C., Pottgen, E., De Bodt, J., Papp, N., Marasini, D., Howard, L., Abranko, L., Van de Wiele, T., Lee, S. O., & Carbonero, F. (2018). Impact of tart cherries polyphenols on the human gut microbiota and phenolic metabolites *in vitro* and *in vivo*. *The Journal of Nutritional Biochemistry*, 59, 160-172. https://doi.org/10.1016/j.jnutbio.2018.04.001.

McLeod, C., Pino, M.T., Ojeda, A., Hirzel, J., Estay, P., Ferreyra, R., & Sellés Von Sch, G. (2014). Aspectos relevantes de la producción de Zarzaparrilla Roja (*Ribes rubrum*) bajo túnel. Boletín INIA N°286, 1–162.

McDougall, G. J., Dobson, P., Smith, P., Blake, A., & Stewart, D. (2005). Assessing potential bioavailability of raspberry anthocyanins using an *in vitro* digestion system. *Journal of Agricultural and Food Chemistry*, 53(15), 5896–5904. https://doi.org/10.1021/jf050131p.

McDougall, G. J., Kulkarni, N. N., & Stewart, D. (2009). Berry polyphenols inhibit pancreatic lipase activity *in vitro*. *Food Chemistry*, 115(1), 193–199. https://doi.org/10.1016/j.foodchem.2008.11.093.

Mezzetti, B. (2013). EUBerry: The sustainable improvement of European berry production, quality, and nutritional value in a changing environment. *International Journal of Fruit Science*, 13, 60–66. https://doi.org/10.1080/15538362.2012.696987.

Mills, C. E., Tzounis, X., Oruna-Concha, M.-J., Mottram, D. S., Gibson, G. R., & Spencer, J. P. E. (2015). *In vitro* colonic metabolism of coffee and chlorogenic acid results in selective changes in human faecal microbiota growth. *British Journal of Nutrition*, 113, 1220–1227. https://doi.org/10.1017/S0007114514003948.

Minekus, M., Alminger, M., Alvito, P., Ballance, S., Bohn, T., Bourlieu, C., et al. (2014). A standardised static *in vitro* digestion method suitable for food – An international consensus. *Food & Function*, 5(6), 1113–1124. https://doi.org/10.1039/c3fo60702j.

Molan, A. L., Liu, Z., & Plimmer, G. (2014). Evaluation of the effect of blackcurrant products on gut microbiota and on markers of risk for colon cancer in humans. *Phytotherapy Research*, 28(3), 416–422. https://doi.org/10.1002/ptr.5009.

Molinett, S., Nuñez, F., Moya-León, M. A., & Zúñiga-Hernández, J. (2015). Chilean strawberry consumption protects against LPS-induced liver injury by anti-inflammatory and antioxidant capability in sprague-dawley rats. *Evidence-Based Complementary and Alternative Medicine*, 2015, 320136. https://doi.org/10.1155/2015/320136.

Moon, J. S., Li, L., Bang, J., & Han, N. S. (2016). Application of *in vitro* gut fermentation models to food components: A review. *Food Science and Biotechnology*, 25(1), 1–7. https://doi.org/10.1007/s10068-016-0091-x.

Moreno-Pérez, D., Bressa, C., Bailén M., Hamed-Bousdar, S., Naclerio, F., Carmona, M., Pérez, M., González-Soltero., R., Montalvo-Lominchar, M. G., Carabaña, C., & Larrosa, M. (2018). Effect

of a protein supplement on the gut microbiota of endurance athletes: A randomized, controlled, double-blind pilot Study. *Nutrients*, 10, E337. https://doi.org/10.3390/nu10030337.

Mosele, J. I., Macià, A., Romero, M. P., Motilva, M. J., & Rubió, L. (2015). Application of *in vitro* gastrointestinal digestion and colonic fermentation models to pomegranate products (juice, pulp and peel extract) to study the stability and catabolism of phenolic compounds. *Journal of Functional Foods*, 14, 529–540. https://doi.org/10.1016/j.jff.2015.02.026.

Moyer, R. A., Hummer, K. E., Finn, C. E., Frei, B., & Wrolstad, R. E. (2002). Anthocyanins, phenolics, and antioxidant capacity in diverse small fruits: *Vaccinium*, *Rubus*, and *Ribes*. *Journal of Agricultural and Food Chemistry*, 50(3), 519–525. https://doi.org/10.1021/jf011062r.

Murakami, T., & Takano, M. (2008). Intestinal efflux transporters and drug absorption. *Expert Opinion on Drug Metabolism & Toxicology*, 4(7), 923–939. https://doi.org/10.1517/17425255.4.7.923.

Nderitu, A. M., Dykes, L., Awika, J. M., Minnaar, A., & Duodu, K. G. (2013). Phenolic composition and inhibitory effect against oxidative DNA damage of cooked cowpeas as affected by simulated *in vitro* gastrointestinal digestion. *Food Chemistry*, 141(3), 1763–1771. https://doi.org/10.1016/j.foodchem.2013.05.001.

Nielsen, I. L. F., Haren, G. R., Magnussen, E. L., Dragsted, L. O., & Rasmussen, S. E. (2003). Quantification of anthocyanins in commercial black currant juices by simple high-performance liquid chromatography. Investigation of their pH stability and antioxidative potency. *Journal of Agricultural and Food Chemistry*, 51(20), 5861–5866. https://doi.org/10.1021/jf034004+.

Ning, Y., Manegold, P. C., Hong, Y. K., Zhang, W., Pohl, A., Lurje, G., Winder, T., Yang, D., LaBonte, M. J., Wilson, P. M., Ladner, R. D., & Lenz, H. (2011). Interleukin-8 is associated with

proliferation, migration, angiogenesis and chemosensitivity *in vitro* and *in vivo* in colon cancer cell line models. *International Journal of Cancer*, 128, 2038–2049. https://doi.org/10.1002/ijc.25562.

Olejnik, A., Kowalska, K., Olkowicz, M., Juzwa, W., Dembczyński, R., & Schmidt, M. (2016). A gastrointestinally digested *Ribes nigrum* L. fruit extract inhibits inflammatory response in a co-culture model of intestinal Caco-2 cells and RAW264.7 macrophages. *Journal of Agricultural and Food Chemistry*, 64, 7710–7721. https://doi.org/10.1021/acs.jafc.6b02776.

Orqueda, M. E., Rivas, M., Zampini, I. C., Alberto, M. R., Torres, S., Cuello, S., Sayago, J., Thomas-Valdes, S., Jiménez-Aspee, F., Schmeda-Hirschmann, G., & Isla, M. I. (2017). Chemical and functional characterization of seed, pulp and skin powder from chilto (*Solanum betaceum*), an Argentine native fruit. Phenolic fractions affect key enzymes involved in metabolic syndrome and oxidative stress. *Food Chemistry*, 216, 70–79. https://doi.org/10.1016/j.foodchem.2016.08.015.

Ott, S. J., Musfeldt, M., Ullmann, U., Hampe, J., & Schreiber, S. (2004). Dispersion compensation in wavelength-division multiplexed optical fibre links. *Journal of Clinical Microbiology*, 42(6), 2566–2572. https://doi.org/10.1128/JCM.42.6.2566.

Ou, B., Hampsch-Woodill, M., & Prior, R. L. (2001). Development and validation of an improved oxygen radical absorbance capacity assay using fluorescein as the fluorescent probe. *Journal of Agricultural and Food Chemistry*, 49, 4619–4626. https://doi.org/10.1021/jf010586o.

Ozdal, T., Sela, D. A., Xiao, J., Boyacioglu, D., Chen, F., & Capanoglu, E. (2016). The reciprocal interactions between polyphenols and gut microbiota and effects on bioaccessibility. *Nutrients*, 8(2), 78. https://doi.org/10.3390/nu8020078.

Payne, A. N., Zihler, A., Chassard, C., & Lacroix, C. (2012). Advances and perspectives in *in vitro* human gut fermentation modeling. *Trends in Biotechnology*, 30(1), 17–25. https://doi.org/10.1016/j.tibtech.2011.06.011.

Peterson, M. D., & Mooseker, M. S. (1992). Characterization of the enterocyte-like brush border cytoskeleton of the C2BBe clones of the human intestinal cell line, Caco-2. *Journal of Cell Science*, 102, 581–600.

Prior, R. L., Wu, X., & Schaich, K. (2005). Standarized methods for the determination of antioxidant capacity and phenolics in foods and dietary supplements. *Journal of Agricultural and Food Chemistry*, 53(10), 4290-4302. https://doi.org/10.1021/jf0502698.

Procházková, D., Boušová, I., & Wilhelmová, N. (2011). Antioxidant and prooxidant properties of flavonoids. *Fitoterapia*, 82(4), 513–523. https://doi.org/10.1016/j.fitote.2011.01.018.

Quideau, S., Deffieux, D., Douat-Casassus, C., & Pouységu, L. (2011). Plant polyphenols: Chemical properties, biological activities, and synthesis. *Angewandte Chemie International Edition*, 50(3), 586–621. https://doi.org/10.1002/anie.201000044.

Reboul, E., Richelle, M., Perrot, E., Desmoulins-Malezet, C., Pirisi, V., & Borel, P. (2006). Bioaccessibility of carotenoids and vitamin E from their main dietary sources. *Journal of Agricultural and Food Chemistry*, 54(23), 8749–8755. https://doi.org/10.1021/jf061818s.

Rechner, A. R., Smith, M. A., Kuhnle, G., Gibson, G. R., Debnam, E. S., Srai, S. K. S., Moore, K. P., & Rice-Evans, C. A. (2004). Colonic metabolism of dietary polyphenols: Influence of structure on microbial fermentation products. *Free Radical Biology and Medicine*, 36(2), 212–225. https://doi.org/10.1016/j.freeradbiomed.2003.09.022.

Reyes-Farias, M., Vasquez, K., Ovalle-Marin, A., Fuentes, F., Parra, C., Quitral, V., Jimenez, P., & Garcia-Diaz, D. F. (2015). Chilean native fruit extracts inhibit inflammation linked to the pathogenic interaction between adipocytes and macrophages. *Journal of Medicinal Food*, 18(5), 601–608. https://doi.org/10.1089/jmf.2014.0031.

Ribeiro, D., Freitas, M., Lima, J. L. F. C., & Fernandes, E. (2015). Proinflammatory pathways: the modulation by flavonoids. *Medicinal Research Reviews*, 35(5), 877–936. https://doi.org/10.1002/med.21347.

Rodríguez-Morató, J., Matthan, N. R., Liu, J., de la Torre, R., & Chen, C. Y. O. (2018). Cranberries attenuate animal-based diet-induced changes in microbiota composition and functionality: a randomized crossover controlled feeding trial. *Journal of Nutritional Biochemistry*, 62, 76–86. https://doi.org/10.1016/j.jnutbio.2018.08.019.

Rojo, L. E., Ribnicky, D., Logendra, S., Poulev, A., Rojas-Silva, P., Kuhn, P., Dorn, R., Grace, M. H., Lila, M. A., & Raskin, I. (2012). *In vitro* and *in vivo* anti-diabetic effects of anthocyanins from Maqui Berry (*Aristotelia chilensis*). *Food Chemistry*, 131(2), 387-396. https://doi.org/10.1016/j.foodchem.2011.08.066.

Romier, B., Van De Walle, J., During, A., Larondelle, Y., & Schneider, Y. J. (2008). Modulation of signalling nuclear factor-kB activation pathway by polyphenols in human intestinal Caco-2 cells. *British Journal of Nutrition*, 100(3), 542–551. https://doi.org/10.1017/S0007114508966666.

Romier-Crouzet, B., Van De Walle, J., During, A., Joly, A., Rousseau, C., Henry, O., Larondelle, Y., & Schneider, Y. J. (2009). Inhibition of inflammatory mediators by polyphenolic plant extracts in human intestinal Caco-2 cells. *Food and Chemical Toxicology*, 47(6), 1221–1230. https://doi.org/10.1016/j.fct.2009.02.015.

Rubilar, M., Jara, C., Poo, Y., Acevedo, F., Gutierrez, C., Sineiro, J., & Shene, C. (2011). Extracts of maqui (*Aristotelia chilensis*) and murta (*Ugni molinae* Turcz.): sources of antioxidant compounds and α-glucosidase/α-amylase inhibitors. *Journal of Agricultural and Food Chemistry*, 59, 1630–1637. https://doi.org/10.1021/jf103461k.

Ruiz, A., Hermosín-Gutiérrez, I., Vergara, C., von Baer, D., Zapata, M., Hitschfeld, A., Obando, L., & Mardones, C. (2013). Anthocyanin profiles in south Patagonian wild berries by HPLC-DAD-ESI-MS/MS. *Food Research International*, 51(2), 706–713. https://doi.org/10.1016/j.foodres.2013.01.043.

Ruiz, A., Bustamante, L., Vergara, C., von Baer, D., Hermosín-Gutiérrez, I., Obando, L., & Mardones, C. (2015). Hydroxycinnamic acids and flavonols in native edible berries of South Patagonia. *Food Chemistry*, 167, 84–90. https://doi.org/10.1016/j.foodchem.2014.06.052.

Sánchez-Patán, F., Barroso, E., Van De Wiele, T., Jiménez-Girón, A., Martín-Alvarez, P. J., Moreno-Arribas, M. V., Martínez-Cuesta, M. C., Peláez, C., Requena, T., & Bartolomé, B. (2015). Comparative *in vitro* fermentations of cranberry and grape seed polyphenols with colonic microbiota. *Food Chemistry*, 183, 273–282. https://doi.org/10.1016/j.foodchem.2015.03.061.

Sánchez-Patán, F., Cueva, C., Monagas, M., Walton, G. E., Gibson M., G. R., Quintanilla López, J. E., Lebrón-Aguilar, R., Martín-Álvarez, P. J., Moreno-Arribas, M. V., & Bartolomé, B. (2012). *In vitro* fermentation of a red wine extract by human gut microbiota: changes in microbial groups and formation of phenolic metabolites. *Journal of Agricultural and Food Chemistry*, 60, 2136–2147. https://doi.org/10.1021/jf2040115.

Sangiovanni, E., Fumagalli, M., & Dell'Agli, M. (2017). Berries: gastrointestinal protection against oxidative stress and inflammation. In J. Gracia-Sancho & J. Salvadó (Eds.), Gastrointestinal Tissue: Oxidative Stress and Dietary Antioxidants. https://doi.org/10.1016/B978-0-12-805377-5.00018-7.

Sartor, R. B. (2006). Mechanisms of disease: pathogenesis of Crohn's disease and ulcerative colitis. *Gastroenterology & Hepatology*, 3(7), 390–407. https://doi.org/10.1038/ncpgasthep0528.

Sáyago-Ayerdi, S. G., Zamora-Gasga, V. M., & Venema, K. (2019). Prebiotic effect of predigested mango peel on gut microbiota assessed in a dynamic *in vitro* model of the human colon (TIM-2). *Food Research International*, 118, 89–95. https://doi.org/10.1016/j.foodres.2017.12.024.

Scalbert, A., & Williamson, G. (2000). Dietary intake and bioavailability of polyphenols. *The Journal of Nutrition*, 130(8), 2073S-2085S. https://doi.org/10.1093/jn/130.8.2073S.

Schmeda-Hirschmann, G., Jiménez-Aspee, F., Theoduloz, C., & Ladio, A. (2019). Patagonian berries as native food and medicine. *Journal of Ethnopharmacology*, 241, 111979. https://doi.org/10.1016/j.jep.2019.111979.

Schmidt, J. (2016). Negative ion electrospray high-resolution tandem mass spectrometry of polyphenols. *Journal of Mass Spectrometry*, 51, 33–43. https://doi.org/10.1002/jms.3712.

Schreckinger, M. E., Wang, J., Yousef, G., Lila, M. A., & Gonzalez de Mejia, E. (2010). Antioxidant capacity and *in vitro* inhibition of adipogenesis and inflammation by phenolic extracts of *Vaccinium floribundum* and *Aristotelia chilensis*. *Journal of Agricultural and Food Chemistry*, 58(16), 8966–8976. https://doi.org/10.1021/jf100975m.

Schulze, C., Bangert, A., Kottra, G., Geillinger, K. E., Schwanck, B., Vollert, H., Blaschek, W., & Daniel, H. (2014). Inhibition of the intestinal sodium-coupled glucose transporter 1 (SGLT1) by

extracts and polyphenols from apple reduces postprandial blood glucose levels in mice and humans. *Molecular Nutrition and Food Research*, 58(9), 1795–1808. https://doi.org/10.1002/mnfr.201400016.

Schulze, K. (2006). Imaging and modelling of digestion in the stomach and the duodenum. *Neurogastroenterology & Motility*, 18, 172–183. https://doi.org/10.1111/j.1365-2982.2006.00759.x.

Singh, R. K., Chang, H.-W., Yan, D., Lee, K. M., Ucmak, D., Wong, K., Abrouk, M., Farahnik, B., Nakamura, M., Zhu, T. H., Bhutani, T., & Liao, W. (2017). Influence of diet on the gut microbiome and implications for human health. *Journal of Translational Medicine*, 2017, 15, 73. https://doi.org/10.1186/s12967-017-1175-y.

Son, J.S., Zheng, L.J., Rowehl, L.M., Tian, X., Zhang, Y., Zhu, W., Litcher-Kelly, L., Gadow, K.D., Gathungu, G., Robertson, C.E., Ir, D., Frank, D. N. & Li, E. (2015). Comparison of fecal microbiota in children with autism spectrum disorders and neurotypical siblings in the Simons simplex collection. *PLoS ONE*, 10, e0137725. https://doi.org/ 10.1371/journal.pone.0137725.

Soriano Sancho, R. A., Pavan, V., & Pastore, G. M. (2015). Effect of *in vitro* digestion on bioactive compounds and antioxidant activity of common bean seed coats. *Food Research International*, 76(1), 74-78. https://doi.org/10.1016/j.foodres.2014.11.042.

Soufli, I., Toumi, R., Rafa, H., & Touil-Boukoffa, C. (2016). Overview of cytokines and nitric oxide involvement in immuno-pathogenesis of inflammatory bowel diseases. *World Journal of Gastrointestinal Pharmacology and Therapeutics*, 7(3), 353–360. https://doi.org/10.4292/wjgpt.v7.i3.353.

Stewart, M. L., Timm, D. A., & Slavin, J. L. (2008). Fructooligosaccharides exhibit more rapid fermentation than long-chain inulin in an *in vitro* fermentation system. *Nutrition Research*, 28, 329–334. https://doi.org/10.1016/j.nutres.2008.02.014.

Strugała, P., Gładkowski, W., Kucharska, A. Z., Sokół-Łętowska, A., & Gabrielska, J. (2016). Antioxidant activity and anti-inflammatory effect of fruit extracts from blackcurrant, chokeberry, hawthorn, and rosehip, and their mixture with linseed oil on a model lipid membrane. *European Journal of Lipid Science and Technology*, 118(3), 461–474. https://doi.org/10.1002/ejlt.201500001.

Surh, Y.-J., Chun, K.-S., Cha, H.-H., Han, S. S., Keum, Y.-S., Park, K.-K., & Lee, S. S. (2001). Molecular mechanisms underlying chemopreventive activities of anti-inflammatory phytochemicals: down-regulation of COX-2 and iNOS through suppression of NF-κB activation. *Mutation Research*, 480–481, 243–268. https://doi.org/10.1016/S0027-5107(01)00183-X.

Tabart, J., Franck, T., Kevers, C., Pincemail, J., Serteyn, D., Defraigne, J. O., & Dommes, J. (2012). Antioxidant and anti-inflammatory activities of *Ribes nigrum* extracts. *Food Chemistry*, 131(4), 1116–1122. https://doi.org/10.1016/j.foodchem.2011.09.076.

Tabart, J., Kevers, C., Pincemail, J., Defraigne, J. O., & Dommes, J. (2009). Comparative antioxidant capacities of phenolic compounds measured by various tests. *Food Chemistry*, 113(4), 1226–1233. https://doi.org/10.1016/j.foodchem.2008.08.013.

Tagliazucchi, D., Verzelloni, E., Bertolini, D., & Conte, A. (2010). *In vitro* bio-accessibility and antioxidant activity of grape polyphenols. *Food Chemistry*, 120(2), 599-606. https://doi.org/10.1016/j.foodchem.2009.10.030.

Tan, J., McKenzie, C., Potamitis, M., Thorburn, A. N., Mackay, C. R., & Macia, L. (2014). The role of short-chain fatty acids in health and disease. *Advances in Immunology*, 121, 91-119. https://doi.org/10.1016/B978-0-12-800100-4.00003-9.

Tan, Y., Chang, S. K. C., & Zhang, Y. (2017). Comparison of α-amylase, α-glucosidase and lipase inhibitory activity of the phenolic substances in two black legumes of different genera. *Food Chemistry*, 214, 259–268. https://doi.org/10.1016/j.foodchem.2016.06.100.

Tavares, L., Figueira, I., MacEdo, D., McDougall, G. J., Leitão, M. C., Vieira, H. L. A., Stewart, D., Alves, P. M., Ferreira, R. B., & Santos, C. N. (2012). Neuroprotective effect of blackberry (*Rubus* sp.) polyphenols is potentiated after simulated gastrointestinal digestion. *Food Chemistry*, 131(4), 1443–1452. https://doi.org/10.1016/j.foodchem.2011.10.025.

Theoduloz, C., Burgos-Edwards, A., Schmeda-Hirschmann, G., & Jiménez-Aspee, F. (2018). Effect of polyphenols from wild Chilean currants (*Ribes* spp.) on the activity of intracellular antioxidant enzymes in human gastric AGS cells. *Food Bioscience*, 24, 80–88. https://doi.org/10.1016/j.fbio.2018.06.003.

Thomas-Valdés, S., Theoduloz, C., Jiménez-Aspee, F., Burgos-Edwards, A., & Schmeda-Hirschmann, G. (2018). Changes in polyphenol composition and bioactivity of the native Chilean white strawberry (*Fragaria chiloensis* spp . *chiloensis f. chiloensis*) after *in vitro* gastrointestinal digestion. *Food Research International*, 105, 10–18. https://doi.org/10.1016/j.foodres.2017.10.074.

Tomas-Barberan, F., García-Villalba, R., Quartieri, A., Raimondi, S., Amaretti, A., Leonardi, A., & Rossi, M. (2014). *In vitro* transformation of chlorogenic acid by human gut microbiota. *Molecular Nutrition and Food Research*, 58(5), 1122–1131. https://doi.org/10.1002/mnfr.201300441.

Tuohy, K. M., Conterno, L., Gasperotti, M., & Viola, R. (2012). Up-regulating the human intestinal microbiome using whole plant foods, polyphenols, and/or fiber. *Journal of Agricultural and Food Chemistry*, 60, 8776-8782. https://doi.org/10.1021/jf2053959.

Tsimogiannis, D., & Oreopoulou, V. (2019). Classification of phenolic compounds in plants. In R. R. Watson (Ed.), Polyphenols in Plants (Second, pp. 263–284). https://doi.org/10.1016/B978-0-12-813768-0.00026-8.

Tudek, B., & Speina, E. (2012). Oxidatively damaged DNA and its repair in colon carcinogenesis. *Mutation Research*, 736, 82–92. https://doi.org/10.1016/j.mrfmmm.2012.04.003.

Tzounis, X., Vulevic, J., Kuhnle, G. G.,George, T., Leonczak, J., Gibson, G. R., Kwik-Uribe, C., & Spencer, J. P. (2008). Flavanol monomer-induced changes to the human faecal microflora. *British Journal of Nutrition, 99, 782–792.* https://doi.org/10.1017/S0007114507853384.

USP (1995). United States Pharmacopeia (USP 23), *the National Formulary (NF 18) United States Pharmacopeia Convention*.

Vacek, J., Ulrichová, J., Klejdus, B., & Šimánek, V. (2010). Analytical methods and strategies in the study of plant polyphenolics in clinical samples. *Analytical Methods*, 2, 604–613. https://doi.org/10.1039/c0ay00042f.

Valko, M., Leibfritz, D., Moncol, J., Cronin, M. T. D., Mazur, M., & Telser, J. (2007). Free radicals and antioxidants in normal physiological functions and human disease. *International Journal of Biochemistry and Cell Biology*, 39, 44–84. https://doi.org/10.1016/j.biocel.2006.07.001.

van Meerloo, J., Kaspers, G. J. L., & Cloos, J. (2011). Cell sensitivity assays: The MTT assay. In I. A. Cree (Ed.), Methods in Molecular Biology (Second, Vol. 731, pp. 237–245). https://doi.org/10.1385/1592594069.

Venditti, A., Serrilli, A. M., Rizza, L., Frasca, G., Cardile, V., Bonina, F. P., & Bianco, A. (2013). Aromadendrine, a new component of the flavonoid pattern of *Olea europaea* L. and its anti-inflammatory activity. *Natural Product Research*, 27(4–5), 340–349. https://doi.org/10.1080/14786419.2012.693924.

Vendrame, S., Guglielmetti, S., Riso, P., Arioli, S., Klimis-Zacas, D., & Porrini, M. (2011). Six-week consumption of a wild blueberry powder drink increases *Bifidobacteria* in the human gut. *Journal of Agricultural and Food Chemistry*, 59, 12815–12820. https://doi.org/10.1021/jf2028686.

Verbeke, K. A., Boobis, A. R., Chiodini, A., Edwards, C. A., Franck, A., Kleerebezem, M., Nauta, A., Raes, J., van Tol, E. A., & Tuohy, K. M. (2015). Towards microbial fermentation metabolites as markers for health benefits of prebiotics. *Nutrition Research Reviews*, 28, 42-66. https://doi.org/10.1017/S0954422415000037.

Vermerris, W., & Nicholson, R. (2008). Biosynthesis of phenolic compounds. In Phenolic Compound Biochemistry (pp. 63–149). https://doi.org/10.1007/978-1-4020-5164-7_3.

Vigsnæs, L. K., Holck, J., Meyer, A. S., & Licht, T. R. (2011). *In vitro* fermentation of sugar beet arabino-oligosaccharides by fecal microbiota obtained from patients with ulcerative colitis to selectively stimulate the growth of *Bifidobacterium* spp. and *Lactobacillus* spp. *Applied and Environmental Microbiology*, 77(23), 8336–8344. https://doi.org/10.1128/aem.05895-11.

Vukics, V., & Guttman, A. (2010). Structural characterization of flavonoid glycosides by multi-stage mass spectrometry. *Mass Spectrometry Reviews*, 29(1), 1–16. https://doi.org/10.1002/mas.20212.

WHO (World Health Organization). 2003. Fruit and vegetable promotion initiative –a meeting report, Geneva. <http://www.who.int/dietphysicalactivity/publications/f&v_promotion_ initiative_report.pdf>. (Accessed 07.03.2017).

Williamson, G. (2017). The role of polyphenols in modern nutrition. *Nutrition Bulletin*, 42, 226–235. https://doi.org/10.1111/nbu.12278.

Williamson, G. (2013). Possible effects of dietary polyphenols on sugar absorption and digestion. *Molecular Nutrition and Food Research*, 57(1), 48–57. https://doi.org/10.1002/mnfr.201200511.

Williamson, G., & Clifford, M. N. (2010). Colonic metabolites of berry polyphenols: the missing link to biological activity?. *British Journal of Nutrition*, 104(3), 48–66. https://doi.org/10.1017/S0007114510003946.

Windey, K., De Preter, V., & Verbeke, K. (2012). Relevance of protein fermentation to gut health. *Molecular Nutrition & Food Research*, 56, 184-196. doi: 10.1002/mnfr.201100542.

Wu, T., Grootaert, C., Pitart, J., Vidovic, N. K., Kamiloglu, S., Possemiers, S., Glibetic, M., Smagghe, G., Raes, K., Van de Wiele, T., & Van Camp, J. (2018). Aronia (*Aronia melanocarpa*) polyphenols modulate the microbial community in a simulator of the human intestinal microbial ecosystem (SHIME®) and decrease secretion of proinflammatory markers in a Caco-2/endothelial cell coculture model. *Molecular Nutrition and Food Research*, 62(22), e1800607. https://doi.org/10.1002/mnfr.201800607.

Yao, C. K., Muir, J. G., & Gibson, P. R. (2016). Review article: Insights into colonic protein fermentation, its modulation and potential health implications. *Alimentary Pharmacology and Therapeutics*, 43, 181–196. https://doi.org/10.1111/apt.13456.

Zhang, H., & Tsao, R. (2016). Dietary polyphenols, oxidative stress and antioxidant and anti-inflammatory effects. *Current Opinion in Food Science*, 8, 33–42. https://doi.org/10.1016/j.cofs.2016.02.002.

Zuo, L., Sypert, D. C., Clark, A. D., Xu, Z., Garrison, D. E., & He, F. (2017). Redox mechanism of reactive oxygen species in gastrointestinal tract diseases. In J. Gracia-Sancho & J. Salvadó (Eds.), *Gastrointestinal Tissue*. https://doi.org/10.1016/B978-0-12-805377-5.00002-3.

Annexes

1. Publications

1.1 Thesis-related publications

- Burgos-Edwards, A., Jiménez-Aspee, F., Thomas-Valdés, S., Schmeda-Hirschmann, G., & Theoduloz, C. (2017). Qualitative and quantitative changes in polyphenol composition and bioactivity of *Ribes magellanicum* and *R. punctatum* after *in vitro* gastrointestinal digestion. *Food Chemistry*, 237, 1073–1082.
- Burgos-Edwards, A., Jiménez-Aspee, F., Theoduloz, C., & Schmeda-Hirschmann, G. (2018). Colonic fermentation of polyphenols from Chilean currants (*Ribes spp.*) and its effect on antioxidant capacity and metabolic syndrome-associated enzymes. *Food Chemistry*, 258, 144–155.
- Burgos-Edwards, A., Martín-Pérez, L., Jiménez-Aspee, F., Theoduloz, C., Schmeda-Hirschmann, G., & Larrosa, M. (2019). Anti-inflammatory effect of polyphenols from Chilean currants (*Ribes magellanicum* and *R. punctatum*) after *in vitro* gastrointestinal digestion on Caco-2 cells. *Journal of Functional Foods*, 59, 329–336.
- Burgos-Edwards, A., Fernández-Romero, A., Carmona, M., Thuissard-Vasallo, I., Schmeda-Hirschmann, G., Larrosa, M. (2019). Prebiotic effect of *in vitro* gastrointestinal digested polyphenolic enriched extracts of Chilean currants (*Ribes magellanicum* and *Ribes punctatum*). Food Research International, (FOODRES-D-19-02005R1; under revision).

1.2 Other publications

- Schmeda-Hirschmann, G., Vega Gomez, C., Rojas de Arias, A., Burgos-Edwards, A., Alfonso, J., Rolon, M., Brusquetti, F., Netto, F., Urra, F. A., & Cárdenas, C. (2017). The Paraguayan *Rhinella* toad venom: Implications in the traditional medicine and proliferation of breast cancer cells. *Journal of Ethnopharmacology*, 199, 106–118.
- Moreno, M. A., Córdoba, S., Zampini, I. C., Mercado, M. I. Ponessa, G., Alberto, M. R., Nader-Macias, M.E. F., Sayago, J., Burgos-Edwards, A., Schmeda-Hirschmann, G., & Isla, M. I. (2018). *Tetraglochin andina* Ciald.: A medicinal plant from the Argentinean highlands with potential use in vaginal candidiasis. *Journal of Ethnopharmacology*, 216, 283–294.
- Thomas-Valdés, S., Theoduloz, C., Jiménez-Aspee, F., Burgos-Edwards, A., & Schmeda-Hirschmann, G. (2018). Changes in polyphenol composition and bioactivity of the native Chilean white strawberry (*Fragaria chiloensis* spp. *chiloensis f. chiloensis*) after *in vitro* gastrointestinal digestion. *Food Research International*, 105, 10–18.
- Theoduloz, C., Burgos-Edwards, A., Schmeda-Hirschmann, G., & Jiménez-Aspee, F. (2018). Effect of polyphenols from wild Chilean currants (*Ribes spp*.) on the activity of intracellular antioxidant enzymes in human gastric AGS cells. *Food Bioscience*, 24, 80–88.
- Schmeda-Hirschmanna, G., Burgos-Edwards, A., Theoduloz, C., Jiménez-Aspee, F., & Vargas-Arana, G. (2019). Male sexual enhancers from the Peruvian Amazon. *Journal of Ethnopharmacology*, 229, 167–179.
- Pino Ramos, L. L., Jiménez-Aspee, F., Theoduloz, C., Burgos-Edwards, A., Domínguez-Perles, R., Oger, C., Durand, T., Gil-Izquierdo, A., Bustamante, L., Mardones, C., Márquez, K., Contreras, D., & Schmeda-Hirschmann, G. (2019). Phenolic, oxylipin and fatty acid profiles of the Chilean hazelnut (*Gevuina avellana*): Antioxidant activity and inhibition of

pro-inflammatory and metabolic syndrome-associated enzymes. *Food Chemistry*, 298, 125026.

2. Conference presentations

- IX International symposium on natural products chemistry and applications, Chillán, Chile, November 22-25th, 2016. Qualitative and quantitative changes in polyphenol composition of *Ribes magellanicum* and *R. punctatum* after simulated gastric and intestinal digestion.
- 17th International Congress of the International Society of Ethnopharmacology, Beirut, Lebanon, April 24-28th, 2017. Effect of simulated gastrointestinal digestion of *Ribes magellanicum* and *R. punctatum* on metabolic syndrome-associated enzymes.
- 12th World Congress on Polyphenols Applications, Bonn, Germany, September 25-28th, 2018. Colonic fermentation of polyphenols from Chilean currants (*Ribes spp*.) and its effect on antioxidant capacity and metabolic syndrome-associated enzymes.

3. Negative controls of *in vitro* colonic fermentation

3.1. HPLC-DAD traces of fermented samples (Donor 1) without extracts at 280, 330 and 520 nm after 8 h (A) and 24 h (B) of incubation.

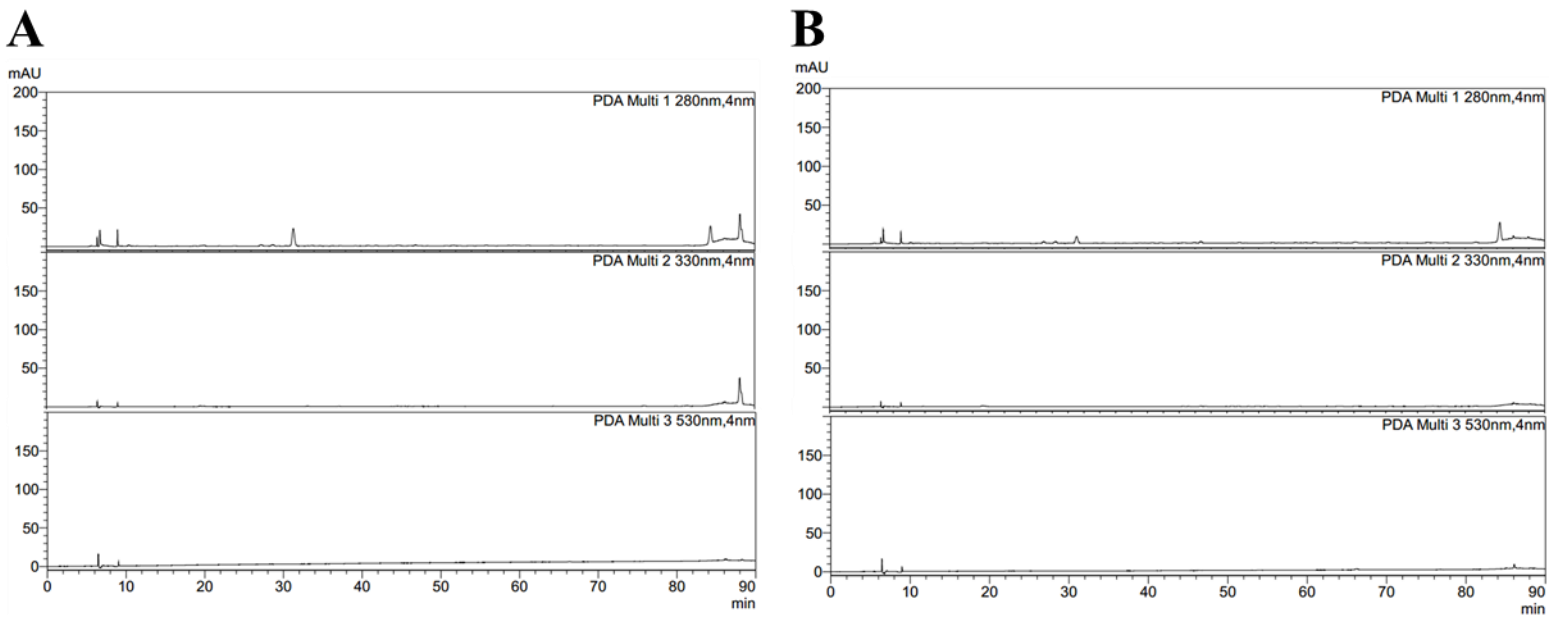

3.3. HPLC-DAD traces of fermented samples (Donor 2) without extracts at 280, 330 and 520 nm after 8 h (A) and 24 h (B) of incubation.

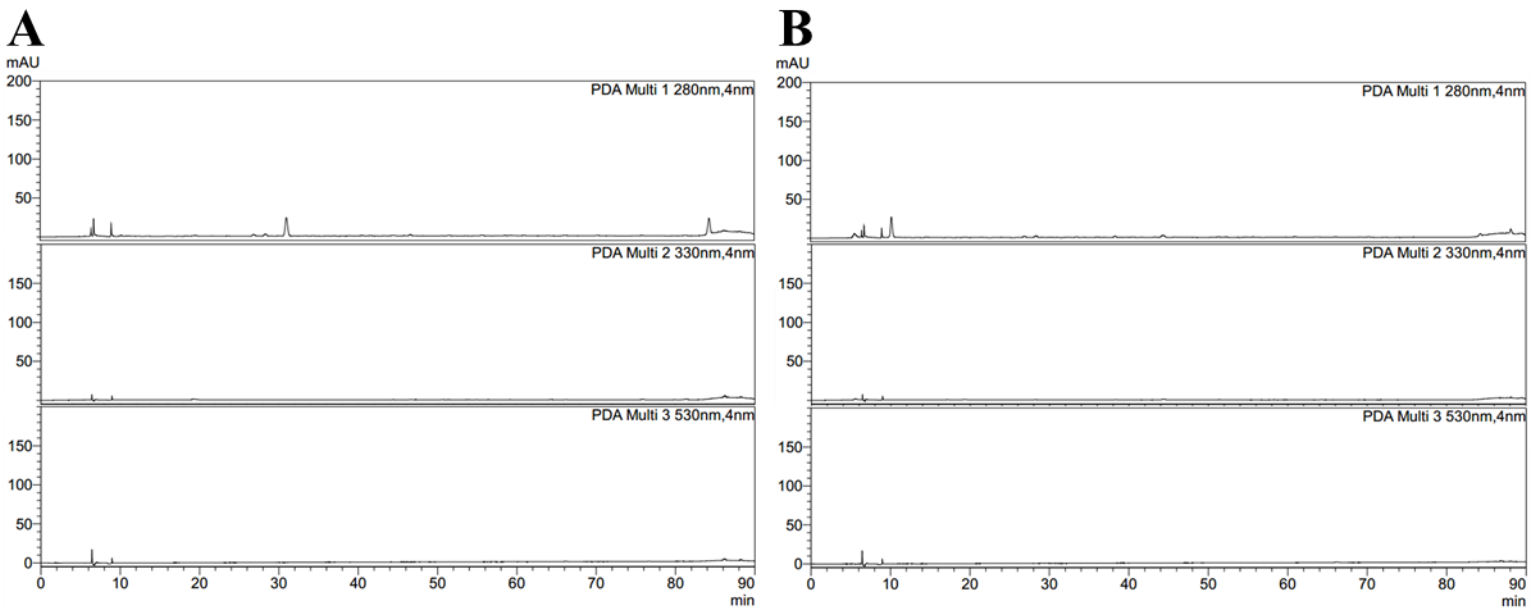

4. Citotoxicity of the extracts in cell-based assays

4.1. Cytotoxic effect of PEE (A), GD-PEE (B), and ID-PEE (C) of *R. magellanicum* and *R. punctatum* on gastric adenocarcinoma cell line (AGS). Data are shown as means ± SD (n = 5).

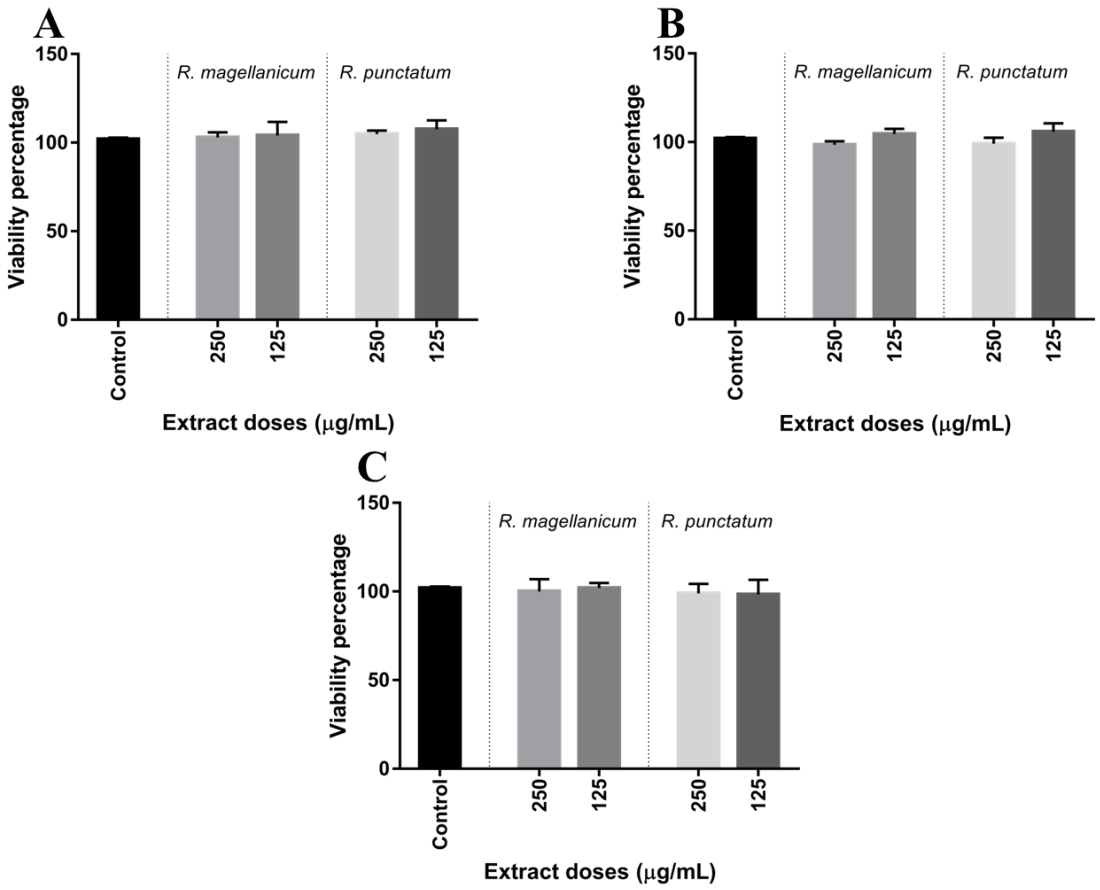

4.2. Cytotoxicity of *R. magellanicum* and *R. punctatum* ID-PEEs on Caco-2 clone C2BBe1 cells. Data are shown as means ± SD (n = 3).